

WAITE INSTITUTE

LIBRARY

10.5.65

THE MECHANISM OF PHOSPHATE ADSORPTION BY KAOLINITE,

GIBBSITE AND PSEUDOBOEHMITE

A Thesis Submitted

by

Djojmartono Muljadi B.Ag.Sc. (Hons.)

To the University of Adelaide

in fulfilment of the requirements

for the degree of

DOCTOR OF PHILOSOPHY

Department of Agricultural Chemistry

University of Adslaide

May, 1964.

TABLE OF CONTENTS

	Page
Table of Contents	i
Index to Figures	vii
List of important symbols	xii
Summary	xiv
Statement	xvi
Acknowledgement	xvii
<u>GENERAL INTRODUCTION</u>	1
<u>CHAPTER I</u>	
<u>REVIEW OF LITERATURE</u>	
1.1. <u>REACTION OF PHOSPHATE IN SOIL</u>	4
1.1. Introduction	4
1.2. Form of phosphorus in soils	4
1.2.1. Organic fraction	5
1.2.2. Inorganic fraction	5
1.2.2.1. Formation of discrete crystalline phase of aluminium and iron phosphates	6
1.2.2.2. Reactions with hydrated aluminium and iron oxides	11
1.2.2.3. Reaction with clay minerals	13
1.3. Soil solution concentration of phosphate	17
1.4. Solubility product of phosphate compounds	19
1.2. <u>STRUCTURE OF KAOLINITE, HALLOYSITE, GIBBSITE AND <u>PSEUDOBUEHMITE</u></u>	22

2.1.	Structure of kaolinite	22
2.2.	Structure of halloysite	24
2.3.	Structure of gibbsite	25
2.4.	Structure of pseudoboehmite	26
1.3.	<u>ELECTRIC CHARGES ON KAOLINITE</u>	28
3.1.	Origin of the permanent negative charges	28
3.2.	Origin of variable negative charges	29
3.3.	Origin of positive charges	30
1.4.	<u>ADSORPTION</u>	36
4.1.	Introduction	36
4.2.	Physical adsorption, chemisorption and ion-exchange	37
4.2.1.	Physical adsorption	37
4.2.2.	Chemisorption	38
4.2.3.	Ion-exchange	39
4.3.	Classification of adsorption isotherm	40
4.3.1.	S isotherm	41
4.3.2.	Ln (Linear) isotherm	41
4.3.3.	L isotherm or Localized model	43
4.3.4.	HA (High Affinity) type	45
4.4.	Equilibrium constant of linear isotherm	46
4.5.	Derivation of Langmuir adsorption isotherm	46
4.5.1.	Thermodynamic approach	47
4.5.1.1.	Thermodynamic equation for adsorption equilibria	47
4.5.1.2.	Localized monolayer model	49

4.5.2. Law of Mass Action approach	52
4.5.2.1. Adsorption	52
4.5.2.2. Ion-exchange	53
4.6. Effect of temperature	57
4.7. Reversibility of adsorption and Hysteresis	60
4.7.1. Phase change hypothesis	61
4.7.2. Swelling of the adsorbent	62
I.5. <u>SOLUBILITY PRODUCT PRINCIPLE</u>	62

CHAPTER II

<u>GENERAL EXPERIMENTAL METHODS</u>	65
II.1. <u>INTRODUCTION</u>	65
II.2. <u>CLAY MINERALS</u>	67
2.1. Kaolinite API-9	67
2.2. Kaolinite R.G.	68
II.3. <u>PREPARATION OF HOMOIONIC CLAY</u>	69
3.1. Potassium-kaolinite	69
3.2. Acid washed kaolinite API-9 (0.1 N HCl)	70
3.3. Acid washed gibbsite (0.1 N HCl)	71
3.4. Aluminium-kaolinite API-9	72
3.5. Sodium-kaolinite	72
3.6. Potassium-halloysite	73
II.4. <u>PREPARATION OF HYDRATED ALUMINIUM OXIDES</u>	73
4.1. Gibbsite	73
4.2. Pseudoboehmite	75

II.5.	<u>PREPARATION OF PHOSPHATE SOLUTIONS</u>	77
II.6.	<u>ADSORPTION EXPERIMENTS</u>	78
II.7.	<u>QUANTITATIVE ANALYSIS</u>	81
7.1.	Phosphate determination	81
7.2.	Potassium determination	84
7.3.	Silicon determination	84
7.4.	Aluminium determination	84
7.5.	Iron determination	84
7.6.	Chloride determination	84
7.7.	Electric charges determination	85
7.8.	X-ray diffraction	85
7.9.	I.R. absorption analysis	85

CHAPTER III

	<u>EXPERIMENTAL RESULTS AND DISCUSSION</u>	86
III.1.	<u>EFFECT OF pH ON ADSORPTION OF PHOSPHATE BY K-KAOLINITES AND HYDRATED ALUMINIUM OXIDES</u>	86
1.1.	Results	86
1.1.1.	Nature of isotherm.	86
1.1.2.	Effect of pH	89
1.1.3.	Effect of acid pretreatment	89
1.1.4.	Adsorption of potassium	90
1.2.	Discussion	91
1.2.1.	Region I : derivation of equation	91
1.2.2.	Region II : derivation of equation	98
1.2.3.	Effect of acid pretreatment	126
1.2.4.	Region III	130

III.2. <u>LOCATION OF THE SITES</u>	134
2.1. Results	134
2.1.1. Effect of aluminium associated with exchange sites and effect of neutral salt	134
2.1.2. Effect of cation (Na-kaolinite)	137
2.1.3. Adsorption of phosphate on K-halloysite	139
2.2. Discussion	142
2.2.1. Region I	142
2.2.2. Region II	145
2.2.3. Region III	148
III.3. <u>EFFECT OF TEMPERATURE ON ADSORPTION</u>	152
3.1. Results	152
3.2. Discussion	155
3.2.1. Region I	157
3.2.2. Region II	157
3.2.3. Region III	164
<u>CHAPTER IV</u>	
<u>GENERAL DISCUSSION</u>	
	170
<u>APPENDICES</u>	
	190
Appendix 1. Preparation of Potassium-kaolinite	190
Appendix 2. Aluminium and Silicon released in acid washing	191
Appendix 3. Determination of electric charges	192
Appendix 4. Kinetic adsorption data at different temperature	194
Appendix 5. Phosphorus determination	197
Appendix 6. Silicon determination	198

Appendix 7. Aluminium determination	199
Appendix 8. Chloride determination	200
Appendix 9. Typical example of the calculation of the results	201
Appendix 10. Regression analysis of region I	202
Appendix 11. Derivation of adsorption equation for region II if step 1 is dependent on step 2	205
Appendix 12. Regression analysis of region II	207
Appendix 13. Confidence limit for K_2^{II}	210
Appendix 14. Estimation of edge face area from the shadowed electron micrograph	211
Appendix 15. Calculation of K_{sp} of variscite	215

REFERENCES

217

INDEX TO FIGURES

<u>Figure No.</u>	<u>Title</u>	<u>Page</u>
1.	Mineralogical Structure of Kaolinite, (a) projection along a-axis and (b) projection along b-axis.	22a
2.	Mineralogical Structure of Gibbsite, (a) projection along a-axis and (b) projection on (001) plane.	22a
3.	Electric charges on the Edge Face of Kaolinite. (After Schofield and Samsom, 1953).	31
4.	Classification of Adsorption Isotherms occurring in solid-solution system.	41a
5.	X-ray Diffractometer Traces of Kaolinite API-9, Kaolinite R.G., Gibbsite and Pseudoboehmite. Infra-red Absorption Spectrograph traces of K-kaolinite API-9 and K-kaolinite R.G.	68a.
6a.	Shadowed Electron Micrograph of K-kaolinite API-9.	76a.
6b.	Shadowed Electron Micrograph of K-kaolinite R.G.	76b.
6c.	Shadowed Electron Micrograph of Gibbsite	76c.
7.	Effect of pH on Adsorption of Phosphate by K-kaolinite API-9 at 20°C.	87a
8.	Effect of pH on Adsorption of Phosphate by K-kaolinite R.G. at 20°C.	87b
9.	Effect of pH on Adsorption of Phosphate by Gibbsite at 20°C.	87c

10. Effect of pH on Adsorption of Phosphate by Pseudoboehmite at 20°C. 87d
11. Adsorption of Phosphate by Kaolinite, Gibbsite and Pseudoboehmite at pH 5, 20°C. 87e
12. Reversibility of Phosphate Adsorption with respect to pH for K-kaolinite API-9 at 20°C. 88a.
13. Reversibility of Phosphate Adsorption with respect to Concentration for K-kaolinite API-9 at pH 5, 20°C. 88b
14. Adsorption of Phosphate by Acid (0.1 N HCl) treated K-kaolinite at pH 5, 20°C. 89a
15. Adsorption of Phosphate by Acid (0.1 N HCl) treated Gibbsite at pH 5, 20°C. 89b
16. Effect of Acid treatment (0.1 N HCl) on Electric Charges on Kaolinite at different pH values. 89c
17. Relation between Potassium and Phosphate Adsorbed for K-kaolinite API-9 at pH 5 and 9, 20°C. 90a
18. Relation between Potassium and Phosphate Adsorbed for Gibbsite and Pseudoboehmite at pH 5, 20°C. 90b
19. Relation between Potassium Adsorbed and Phosphate Adsorbed in Region III for Gibbsite and Pseudoboehmite at pH 5, 20°C. 90c
20. Enlarged isotherms (Regions I and II) at different pH values for K-kaolinite API-9 at 20°C. 95a
21. Linear Regression Plots of Region I for K-kaolinite API-9 and K-kaolinite R.G. at 20°C. 96a

22. Linear Regression Plots of Region I for Gibbsite, and Pseudoboehmite at 20°C. 96b
23. Theoretical adsorption isotherms of region II at different values of $[\text{OH}^-]$: if Step 1 is dependent on Step 2. 101a
24. Relative Distribution of Phosphate Species at Different pH values. 101a
25. Adsorption Isotherms of Region II at different pH values for K-kaolinite API-9 at 20°C. 101b
26. Adsorption Isotherms of Region II at different pH values for K-kaolinite R.G. at 20°C. 101c
27. Adsorption Isotherms of Region II at different pH values for Gibbsite at 20°C. 101d
28. Adsorption Isotherms of Region II at different pH values for Pseudoboehmite at 20°C. 101e
29. Langmuir Plots (Region II) at different pH values for K-kaolinite API-9 at 20°C. 109a
30. Langmuir Plots (Region II) at different pH values for K-kaolinite R.G. at 20°C. 109b
31. Langmuir Plots (Region II) at different pH values for Gibbsite at 20°C. 109c
32. Langmuir Plots (Region II) at different pH values for Pseudoboehmite at 20°C. 109d
33. Linear Regression Plots of Region II for K-kaolinite API-9 and K-kaolinite R.G. at 20°C. 117a

34. Linear Regression Plots of Region II for Gibbsite and Pseudoboehmite at 20°C. 117b
35. Relation between V_o (Region I) and V_m (Region II) at different pH values for K-kaolinite API-9 at 20°C. 118a
- 36a. Electron Micrograph of Untreated K-kaolinite API-9 (control). 127a
- 36b. Electron Micrograph of Acid treated K-kaolinite API-9 127b
37. Adsorption of Phosphate by Al-kaolinite API-9 at pH 5, 20°C. 134a
38. Effect of Neutral Salt (0.1N KCl) and Initial treatments on Adsorption of Phosphate by K-kaolinite API-9 at pH 5, 20°C. 136a
39. Adsorption of Phosphate by Na-kaolinite API-9 and K-halloysite at pH 5, 20°C. 138a.
40. Langmuir Plots (Region II) of Na-kaolinite, K-kaolinite (in the absence and presence of salt), Al-kaolinite and K-halloysite at pH 5, 20°C. 139a
41. Effect of Temperature on Adsorption of Phosphate by K-kaolinite at pH 5. 152a
42. Effect of Temperature on Adsorption of Phosphate by Gibbsite at pH 5. 152b

43. Effect of Temperature on Adsorption of Phosphate
by Pseudoboehmite at pH 5. 152c
44. Langmuir Plots (Region II) at different
Temperatures for K-kaolinite API-9 at pH 5. 153a
45. Langmuir Plots (Region II) at different Temperatures
for Gibbsite and Pseudoboehmite at pH 5. 153b
46. Effect of Temperature on Adsorption of Phosphate
by Acid treated K-kaolinite API-9 at pH 5. 155a
47. Adsorption Isotherms of Region II as Function
of Surface Coverage Θ for K-kaolinite API-9
at pH 5. 157a
48. Relation between Log. K (Slope of Region III)
and $\frac{1}{T}$ for K-kaolinite API-9 at pH 5. 166a

LIST OF IMPORTANT SYMBOLS

a_i	activity of substance i .
C	concentration of an ion in solution.
e	base of natural logarithm.
f_A	activity coefficient of species A on the solid phase.
G	Gibbs free energy.
H	enthalpy or heat content.
K	thermodynamic equilibrium constant.
K_a	apparent equilibrium constant.
K_m	equilibrium quotient.
K'	dissociation constant or hydrolysis constant.
K_{sp}	ionic activity product or solubility product constant.
K_1^I	equilibrium constant for the uptake of a proton in region I.
K_1^{II}	equilibrium constant for the uptake of a proton in region II.
K_2^I	equilibrium constant for exchange reaction of the phosphate ion with the hydroxyl counter ion on positively charged aluminium in region I.
K_2^{II}	equilibrium constant for the corresponding exchange reaction in region II.
k	Boltzmann's constant = 1.3805×10^{-16} erg. deg. ⁻¹ .
\ln	natural logarithm.
$\log.$	decadic logarithm (to base 10).
N	Avogadro's number = 6.023×10^{23} mole ⁻¹ .

N_A	mole fraction of substance A on the solid phase.
$[P]$	equilibrium phosphate concentration ($\mu\text{g P/ml}$ or meq./ml).
pH	negative decadic logarithm of the H_3O^+ activity.
pK	negative decadic logarithm of constant K.
R	gas constant = $1.987 \text{ cal. deg.}^{-1} \text{ mole}^{-1}$.
S	entropy.
T	absolute temperature.
V_0	amount of phosphate adsorbed in region I at any particular pH (meq./100 g or meq. \%)
V_1	total number of sites in region I (meq. \%).
V_m	maximum amount of phosphate that can be adsorbed in region II at any particular pH (meq. \%).
V_2	total number of sites in region II (meq. \%).
Δ	change of a thermodynamic quantity.
γ_{\pm}	mean activity coefficient.
θ	fraction of surface covered.
Γ	surface concentration in moles per unit area.
μ	chemical potential.

SUMMARY

The adsorption isotherms of phosphate on K-kaolinite, gibbsite and pseudoboehmite are very similar in shape and differ only in the amounts adsorbed. The order pseudoboehmite > gibbsite > kaolinite was found to correlate better with estimates of the edge area rather than the total area of the adsorbent.

The isotherms have been divided by inspection into three distinct regions, designated as regions I, II and III, and it has been suggested that these are related to the affinity of phosphate for three energetically different types of reactive sites.

Region I. Region I occurs at very low concentrations $< 1 \times 10^{-4} \text{M}$, the isotherm rises steeply and remains close to the y-axis. This region represents sites with very high affinity for phosphate. The variation of this with pH value agrees with the postulate that the adsorption sites are formed by adsorption of H^+ from water, followed by exchange of the hydroxyl counter ions for phosphate. The exchange constant for the latter process is immeasurably large.

Region II. This region commences at $1 \times 10^{-4} \text{M}$ when the isotherm becomes convex to the y-axis. Region II behaves in a similar manner to region I, except that the exchange constant is no longer large.

It has been suggested that the adsorption sites of regions I and II are located on the first and second hydroxyl of an —Al(OH)_2 situated at the edge face of kaolinite and hydrated aluminium oxides, and on the exchange sites of kaolinite.

Region III. The third part of the isotherm is linear and occurs at medium to high concentration of phosphate (10^{-3} to 10^{-1} M). The slope for region III passed through a maximum at about neutrality.

Region III is thought to be associated with the occlusion of a phosphate ion pair, $(K^+H_2PO_4^-)$ into an amorphous or semi-crystalline region of the clay crystal.

The affinity constants of the various processes proposed to describe phosphate adsorption in regions I and II are very similar for all the adsorbents examined.

The adsorption isotherms of phosphate on kaolinite are reversible with respect to pH in all regions and with respect to concentration in regions II and III. The isotherms for the oxides are largely irreversible with respect to concentration, and hence it appears that a phase change occurred under the conditions of the desorption experiments.

Apart from increasing the number of adsorption sites in region II, increasing the temperature has little effect on regions I and II. Thus the driving force for phosphate adsorption was considered to be a positive entropy change ($+\Delta S_{1/2}$) associated with a desorption or rearrangement of perhaps two water molecules around the phosphate ion and at the adsorption site on the kaolinites and the oxides.

There was a small positive heat of adsorption ($+\Delta H$) in region III of the order of 3 to 5 k cal/mole, which probably arises from the need to break some hydrogen bonds before occlusion can occur.

STATEMENT

This thesis contains no material which has been accepted for the award of any other degree or diploma in any University, and, to the best of my knowledge and belief, the thesis contains no material previously published or written by another person, except when due reference is made in the text of the thesis.

~~_____~~
D. Muljadi

May, 1964.

ACKNOWLEDGEMENTS

I wish to express my sincere gratitude to Professor J.P. Quirk, Professor of Soil Science, and Dr. A.M. Posner, Reader in Soil Chemistry, University of Western Australia, formerly Reader in Soil Science and Senior Lecturer in Soil Science respectively, University of Adelaide, for their continued interest and guidance throughout this project.

I would also like to thank the other staff members of the Agricultural Chemistry Department, Soil Science Section, for their ready help and discussion; and to Dr. W.W. Forrest, C.S.I.R.O., Division of Biochemistry and General Nutrition, University of Adelaide, for the calorimetric measurements.

Thanks are also due to Mr. T. Sherwin for the measurements of the B.E.T. (Nitrogen) surface area of the samples, to Mr. B.A. Palk for the electron microscope work and also for the preparation of the photographic prints of the diagrams, and to Mrs. P. Coulls for typing the manuscript.

I am grateful to the late Professor R.K. Morton for his permission to undertake this study within the Department of Agricultural Chemistry, Waite Agricultural Research Institute, University of Adelaide.

The work described in this thesis was made possible by the award of a Colombo Plan Fellowship, and I gratefully acknowledge the Commonwealth Government of Australia for the award.

GENERAL INTRODUCTION

The chemistry of phosphorus in soil has been the subject of many investigations and discussions because of the important role of phosphate as a plant nutrient. The chemical processes occurring in soil have a very great influence on the utilization of soil phosphorus for plant production. Knowledge of the chemistry of phosphorus in soil is therefore a basic requirement for understanding of the partition of phosphate between the soil and plant systems.

From the agricultural point of view, the chemistry of phosphorus in soil is of great economic significance. The recovery of fertilizer phosphorus by field crops planted immediately after the application of fertilizer usually amounts to only 10 to 30 per cent of the total added to the soil. The remainder is said to be "fixed" in the soil, either being precipitated by soluble cations in the soil solution or adsorbed by the colloidal fraction of the soil complex.

The availability of the "fixed" fraction varies for different soils, depending on the nature and the form of the compounds produced by reaction with the soil components. In some circumstances the residual value of applied phosphate may be high (Woodroffe and Williams, 1953).

Phosphorus has long been recognized as an essential component of all living organisms. It is a constituent of the cell nucleus and is essential for cell division and the development of meristematic

tissue. It forms an integral part of enzymes and co-enzymes, and the high energy phosphate compound from which energy is derived for various cellular processes. Phosphorus is absorbed by plants chiefly as the ortho-phosphate ion H_2PO_4^- present in the soil solution. To ensure an adequate supply from the characteristically low concentration of the soil solution, repeated restoration of the water soluble phosphate is necessary. The water soluble phosphate in the soil is in equilibrium with the phosphate in the crystalline and adsorbed phases in the soil.

The adsorption of the phosphate ion from solution onto a solid surface will be determined by the atomic and molecular forces existing between the ion and the surface. The clay mineral kaolinite and the related mineral gibbsite are hexagonal plate-shaped particles of colloidal dimensions, which can carry both positive and negative charges. Both gibbsite and kaolinite are reputed to play an important role in phosphate "fixation" in the soil. Consequently, the elucidation of the mechanisms of the reaction between phosphate and these minerals would seem to be of fundamental importance.

Although the adsorption of phosphate from solution by clay minerals has been extensively studied, the mechanism of the adsorption reaction is not well understood.

The adsorption of phosphate depends on such factors as pH, concentration and temperature. To understand the adsorption process the effect of these variables has therefore to be separated. Most studies on the adsorption of phosphate have been carried out

either at an uncontrolled pH or in the presence of buffers. This is not altogether satisfactory because the buffer ions are likely to compete with the phosphate ion for the reactive sites, complicating the interpretation of the results.

In this thesis the reaction of dilute solutions of phosphate (10^{-5} to 10^{-1} M) with kaolinite and the related minerals gibbsite and pseudoboehmite has been studied as a function of pH value, temperature, exchangeable cation and electrolyte concentration. The reversibility of the adsorption process has also been examined.

The aim of this research was to obtain an appropriate model to describe the various features of the adsorption of phosphate on kaolinite and hydrated aluminium oxides.

This thesis is divided into four chapters. Chapter I contains a general review of the relevant literature. In Chapter II the general experimental methods are described and reference is made to the use of X-ray diffraction and Infra-Red spectroscopy which have been used to characterise the adsorbents. This chapter also deals with methods for the preparation of the clay minerals and the synthetic hydrated aluminium oxides (gibbsite and pseudoboehmite). The results and discussion are given in Chapter III, which is divided into three parts. Part III.1. contains the results and discussion of the adsorption of phosphate by several adsorbents as a function of pH values. Part III.2. discusses the location of the adsorption sites on the adsorbent surface, while III.3. describes the effect of temperature on the adsorption isotherms. Finally, Chapter IV contains the general discussion.

CHAPTER I.REVIEW OF LITERATUREI.1. THE REACTIONS OF PHOSPHATE IN SOIL1.1. Introduction

Soil is a very complex system which consists of a mixture of colloidal materials such as hydrated aluminium and iron oxides, and clay minerals (layer lattice alumino silicate). It also contains coarser fractions such as silt and sand. The colloidal fraction is the reactive component and is therefore largely responsible for the chemical and physical properties of soil. The colloidal fraction of the soil carries electric charges and has a very high specific surface area. Many of the soil properties can be accounted for in terms of these quantities.

The general feature of reaction of phosphate with the soil colloids has been recognized for a long time, however the mechanisms of the various reactions are still not fully understood.

Before considering these reactions some of the main features of the chemistry of phosphorus in soils will be considered.

1.2. The form of phosphorus in soils.

Soil usually contains a very low amount of total phosphorus, it varies very widely from a few ppm. for leached sandy soils to a few hundred ppm. for some soils derived from basalt. In general, more phosphate is present in the inorganic than the organic form, although

for some strongly leached tropical soils, organic phosphate is the principle source of available phosphate (Russell, 1961).

1.2.1. Organic fraction.

The principle form of organic compounds in soil are the phospholipids, nucleic acids, inositol phosphates and phosphoproteins. Usually these compounds come from plant and animal residues, which are slowly mineralized to orthophosphate by microorganisms.

The rate and extent of the mineralization of organic compounds depends largely on physical and climatic factors, particularly wetting and drying, and temperature (Birch, 1958-1960; Russell, 1961).

1.2.2. Inorganic fraction.

Generally the inorganic compounds in the soil constitute the most important fraction of the soil phosphorus. It is present in soil entirely as orthophosphate salts. The natural phosphate mineral occurring in massive deposits is rock phosphate. It is a composite of many minerals with fluoroapatite ($\text{Ca}_{10}(\text{PO}_4)_6\text{F}_2$) predominating. This material is used directly as a fertilizer, although it is usually processed into a more soluble form by treatment with sulphuric acid to give superphosphate (superphosphate : about 28 to 32 per cent of the monocalcium phosphate and 50 to 60 per cent of gypsum).

Considerable work has been done on the reactions of phosphate in soil. It has been reviewed by several authors in the Agronomy

Monograph (1953), and by Hemwall (1957).

The behaviour of phosphate in soil is conveniently divided into reactions under acid and alkaline (calcareous) conditions as follows:-

- (i) The reactions under acid conditions in which dissolution of the solid phase occurs followed by reaction with phosphate to give a precipitate of a discrete crystalline phase.
- (ii) Adsorption onto the solid surface occurs to give ill-defined surface complexes.
 - hydrated aluminium and iron oxides.
 - clay minerals.
- (iii) The reactions under calcareous conditions in which discrete crystalline phases of calcium phosphates are formed.

1.2.2.1. The formation of discrete crystalline phases of aluminium and iron phosphates under acid or neutral conditions.

In well drained soils, the principle crystalline compounds of aluminium and ferric phosphates are members of the variscite (aluminium phosphate, $Al(OH)_2 H_2PO_4 \cdot nH_2O$), barrandite (aluminium and ferric phosphate, $Al, Fe(OH)_2 H_2PO_4 \cdot nH_2O$) and strengite (ferric phosphate, $Fe(OH)_2 H_2PO_4 \cdot nH_2O$) groups (Wild, 1950; Hemwall, 1957; and Russell, 1961). Whereas in water logged soils, the only crystalline phosphate mineral which has been found (Koch, 1956) is vivianite ($Fe_3(PO_4)_2 \cdot 8H_2O$).

Norrish (1957) using X-ray diffraction has identified the crystalline phosphate of the gorceixite - florencite group, $(\text{Ba, Ce})\text{Al}_3(\text{PO}_4)_2(\text{OH})_2$, in a wide variety of Australian soils particularly in strongly weathered soil such as laterites or kraznozems. Recently Norrish and Sweatman (1962) showed that the gorceixite minerals were capable of incorporating a large range of elements, including trace elements, into the crystal lattice.

Haseman, Lehr and Smith (1950) using X-ray diffraction and optical techniques have identified the products, obtained from the reaction of aluminium and ferric chlorides with high concentrations of phosphate (1 M) in the presence of potassium and ammonium cations. The compounds formed were potassium or ammonium aluminium or iron phosphate minerals having the general formula $(\text{K})_3\text{AlPO}_4 \cdot n\text{H}_2\text{O}$, in which isomorphous substitution of ferric for aluminium or of ammonium for potassium was common. Using similar methods Cole and Jackson (1950a) showed that precipitates of variscite or strengite minerals were formed at room temperature when the pH of aluminium and ferric chloride solution containing excess phosphate were increased. These precipitates were initially microcrystalline and were the same as those precipitated at 90°C , except the latter were larger in size.

Kittrick and Jackson (1954, 1955a) showed that kaolinite and films of aluminium oxides will dissolve completely in a molar phosphate solution at 90°C within 30 days, forming a new crystalline phase the nature of which depends on the cation of the phosphate

solution. Subsequently (1956) they demonstrated that similar reactions occur at room temperature although at a greatly reduced rate. These experiments were carried out in the presence of a very high phosphate concentration which might not be found uniformly in soil.

Lindsay and Stephenson (1959a), however, have shown that the solution which diffuses out from a monocalcium phosphate granule ($\text{Ca}(\text{H}_2\text{PO}_4)_2$) under similar conditions to those occurring in soil, is very similar to the meta-stable triple point solution (MTPS) in which the concentration of phosphate is about 4 molar and the pH 1.5. With time, however, the meta-stable triple point solution shifts to a stable triple point solution (TPS) as the meta-stable dicalcium phosphate dihydrate disappears. The composition of the MTPS at 25°C is 22.0% P_2O_5 and 6.30% CaO , at a pH of 1.5 (Brown and Lehr, 1959), while that of the TPS at 25°C is 24.5% P_2O_5 , and 5.79% CaO , at a pH of 1.0 (Farr, 1950). The reaction of monocalcium phosphate in water can be written as follows:-



Further Lindsay and Stephenson (1959b) showed that this solution can dissolve appreciable amounts of both aluminium and iron compounds from the soil resulting in an increase of pH. They showed that under

these conditions of high local concentration and low acidity, crystalline aluminium and iron phosphate such as taranakite ($3K_2O, 5(Al, Fe)_2O_3, 8P_2O_5 \cdot 42H_2O$) were formed and could be isolated and identified.

Kukharenko and Nosouska (1953) have made chemical extractions of the soil surrounding placements of monocalcium phosphate granules. They found that phosphorus extractable in water, 0.5N acetic acid, and 0.5N HCl, all decreased very rapidly with time after placement. With increasing distances from the granule, the phosphorus concentration decreases to very low values and this phosphorus was extracted with greater difficulty and presumably at this stage surface complexes are formed with accessory oxides and clay minerals.

Cole and Jackson (1950b) have determined the solubility product (K_{sp}) of the variscite crystal ($Al(OH)_2H_2PO_4$) in 0.05N NaCl and found it to be 2.8×10^{-29} . They believed that K_{sp} of variscite describes the equilibrium concentration of phosphate in soil solution and the aluminium and iron activity in solutions. They suggest that variscite is sufficiently soluble to supply phosphate ion ($H_2PO_4^-$) for plant growth. However, in the presence of gibbsite, kaolinite or montmorillonite, the aluminium released from these compounds may decrease the concentration of phosphate in solution by the formation of a solid precipitate, so that the availability of phosphate becomes the limiting factor.

Similarly Kittrick and Jackson (1955b) have also studied the applicability of the solubility product principle to the variscite-

kaolinite system. Their results showed that addition of kaolinite to a 1% suspension of variscite increased the aluminium concentration from 2.3×10^{-5} to 4.8×10^{-5} M, and decreased the phosphate concentration from 2.5×10^{-4} M (7.5 $\mu\text{gP/ml}$) to 0.7×10^{-4} M (2 $\mu\text{gP/ml}$), the calculated value of pK_{sp} remaining constant.

They also studied (1955c) the common ion effect on phosphate solubility. They explained the discrepancy between the phosphate concentration supported by various precipitated compounds in pure water and the known phosphate concentration in soil solution, on the basis of the solubility product principle. They showed that addition of goethite (FeO(OH)) to an iron phosphate ($\text{Fe(OH)}_2\text{H}_2\text{PO}_4$) suspension decreased the phosphate concentration from 10 ppm to 1 ppm; similar results were obtained for the kaolinite - aluminium phosphate ($\text{Al(OH)}_2\text{H}_2\text{PO}_4$) system, and the kaolinite - strengite ($\text{Fe(OH)}_2\text{H}_2\text{PO}_4$) system. In all cases the solubility product of the phosphate remained constant. These workers concluded that precipitated crystalline phases such as variscite, strengite or barrandite was formed in these systems as the result of the dissolution of the kaolinite or the hydrated aluminium or iron oxides.

Another explanation can be offered to account for their results. It is very likely that at these low concentrations of phosphate (< 10 ppm), adsorption occurs onto the reactive sites of the colloid surface. This reaction will result in a decrease of H_2PO_4^- with the aluminium concentration increasing concomitantly at the

expense of the crystalline phosphate compound. This reaction will proceed until a new equilibrium has been attained in which the solubility product (K_{sp}) remains constant as long as there is a crystalline phosphate compound present in the system.

1.2.2.2. The reactions with hydrated aluminium and iron oxides.

The hydrated aluminium and iron oxides are thought by many workers to be the materials that react with phosphate under acid and neutral conditions.

This was first shown by indirect methods in which the free aluminium and iron oxides were removed by chemical extraction (Toth, 1937, 1942; Kelley and Midgley, 1943). The earliest method used for removing the oxides was the hydrogen sulphide reduction technique of Drosdoff and Truog (1935). The effectiveness of the method and its effect on the clay minerals have been questioned by many workers.

Mitchell and Mackenzie (1954) suggested a milder treatment using sodium dithionite ($\text{Na}_2\text{S}_2\text{O}_4$) at pH 5 to 6 for removing iron oxides. The dithionite method is more efficient and also does not affect the surface properties of the clays, since repeated treatments (Sumner, 1962) did not affect the electric charges distribution on the clay as measured by the method of Schofield (1949).

Using the dithionite method for removing iron oxides Muljadi (1961) has shown that the amount of phosphate or chloride adsorbed by the treated clay was not reduced significantly, although the total amount of iron removed was about 95% of the initial iron content (0.75%). It was suggested that the iron oxide in the kaolinite RG.

might be the unhydrated, Fe_2O_3 , such as haematite which did not react with phosphate.

More recently Bromfield (1964) using a biological reduction technique to remove iron oxides from the soil sample, has shown that the amount of phosphate adsorbed remains approximately constant with increasing amount of iron oxides removed. However, the corresponding amount of adsorbed phosphate decreased very markedly if the aluminium oxide was removed by extraction with 0.05N HCl. He concluded from the results that phosphate fixation in the soils used is dominated by aluminium and not by the readily reducible iron.

Further indirect evidence for the part played by the oxides of aluminium and iron has been given by the competition between phosphate and reagents that block the reaction sites on the oxides. A wide variety of blocking agents has been used e.g., 8-hydroxy quinoline (Ghani, 1943), fulvic acid (Leaver and Russell, 1957), fluoride (Swenson, Cole and Sieling, 1949) glucose and humic acid (De, 1961b).

Johansen and Buchanan (1957) have concluded from the measurement of the zeta potential of an unhydrated iron oxide (Fe_2O_3), that the unhydrated form of iron oxide does not adsorb phosphate. De (1961a) has suggested that the phosphate ion is adsorbed by several iron and aluminium hydroxides prepared at different pH values with formation of chemical compound-like products. More recently Hsu and Rennie (1962) have reached the conclusion that phosphate is primarily

adsorbed by the X-ray amorphous aluminium hydroxide. They also suggest that the adsorption mechanism is similar to the decomposition-precipitation reaction, except the latter requires the release of the aluminium ion into solution followed by the formation of discrete chemical compounds.

1.2.2.3. Reaction with clay minerals.

The mechanism by which phosphate is adsorbed by clay minerals was regarded by earlier workers as an exchange of the phosphate ion with the hydroxyl ions on the planar surface (Stout, 1939; Kelley and Midgley, 1943). But this theory has lost much of its support.

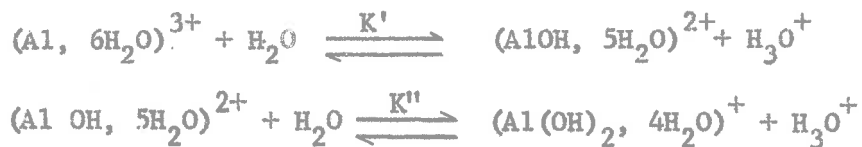
It is now generally accepted that the reactivity of the clay minerals for reaction with phosphate is due to aluminium atoms on the clay surface or in the crystal lattice (Coleman, 1944; Haseman, Brown and Whitt, 1950; Russell and Low, 1954; Hemwall, 1957).

Haseman, Brown and Whitt (1950) showed that clay minerals were similar to the hydrous oxides in that the fixation was characterized by two steps.

- (i) a rapid stage, due to reaction with the readily available aluminium and iron, which might be present on the exchange sites of the mineral (Harward and Coleman, 1954; Low 1955; Cashen, 1959).
- (ii) a slower stage, resulting from the reaction with the less readily available iron and aluminium released by the decomposition of the clay mineral (Schofield, 1946).

It has been shown by many workers that when aluminium occupies an exchange site either on a resin (Hsu and Rich, 1960) or clay mineral e.g. montmorillonite (Shen and Rich, 1962), it may undergo hydrolysis to give hydroxy aluminium compounds. This hydrolysis product is fixed by the exchange site and becomes non-exchangeable being in the form of a hydroxy aluminium compound with an average OH/Al molar ratio of 2 (Hsu and Rich, 1960; Thomas, 1960; Shen and Rich, 1962), which can be written as: Exchange site—Al(OH)₂. Recently Schwertmann and Jackson (1963) have also demonstrated from their potentiometric studies, the presence of this hydrolysis product on the surface of aged hydrogen - aluminium montmorillonite. They concluded that the first, the second and the third buffering range were due to exchangeable hydronium (H₃O⁺), the exchangeable aluminium (Al³⁺) and the weak basic group of the non-exchangeable hydroxy aluminium respectively.

The complete hydrolysis of an aluminium salt in aqueous solution can be written as follows:-



where $\text{pK}' = 4.98$ (Schofield and Taylor, 1954)

$\text{pK}'' = 10$ (Jackson, 1962)

It is suggested here that the chemical properties of the aluminium

atom associated with the exchange site on kaolinite (clay - $\text{Al}(\text{OH})_2$) may be very similar to that of the aluminium atom having the structure



Low and Black (1947) put forward the hypothesis that kaolinite dissociates into aluminium and silicate ions according to the following equation.



for which $K_{\text{sp}} \text{ kaolinite} = (C_{\text{Al}(\text{OH})_2^+} \cdot \gamma_+^2) (C_{\text{Si}_2\text{O}_5^{=}} \cdot \gamma_-)$.

where K_{sp} is the solubility product constant of kaolinite.

C is the concentration of the ion in solution.

γ_{\pm} is the mean activity coefficient.

In the presence of high concentration of phosphate (1M) the aluminium ion will be precipitated as aluminium phosphate, thereby disturbing the equilibrium and leading to the dissolution of kaolinite. However, the above reaction is unlikely to be a reversible process, since it is doubtful whether $\text{Al}(\text{OH})_2^+$ and $\text{Si}_2\text{O}_5^{=}$ ions can react to form kaolinite under room temperature at atmospheric pressure. The solubility product principle cannot therefore be applied to the kaolinite system as such.

Russell and Low (1954) using saturated aluminium clays showed that the adsorption of phosphate was markedly increased by the presence

of the aluminium and concluded that the adsorbed aluminium precipitated phosphate on the kaolinite surface.

Olsen and Watanabe (1957) showed that adsorption of dilute phosphate solution by three soils conformed to the Langmuir isotherm better than the Freundlich isotherm. They showed further that there is close relationship between the adsorption maximum obtained from the Langmuir plots and the surface area of the soil as measured by using ethylene glycol. Their results showed that the acid soil adsorbed more than an alkaline soil and similarly the "bonding energy" of the adsorbed phosphate is greater for the acid soil.

Muljadi (1961) using potassium kaolinite (Rocky Gully) after pretreatment with N KCl at pH 3, showed that in the presence of 0.1 N KCl the adsorption from dilute phosphate solution conformed closely to the Langmuir isotherm up to 5×10^{-3} M KH_2PO_4 . The adsorption maximum calculated from the Langmuir plot was found to be about 2.9 me%, which corresponds closely to the maximum chloride adsorption at pH 3 (Quirk, 1960). It was further suggested that the adsorption of phosphate from dilute solution is due to the reaction between phosphate ion and the positively charged aluminium atom situated on the edge of the crystal.

It can be concluded from this survey that the affinity of the clay mineral for phosphate is likely to be due to the aluminium atoms on the edge face of the crystal lattice, and on the degraded clay surface formed as a decomposition product of the crystal lattice. Hydrated aluminium oxides and iron oxides if present will also react

with phosphate.

The dissolution - precipitation reaction with the formation of a discrete crystalline phase with a definite chemical composition will be governed by the solubility product principle and is only important in the presence of high concentrations of phosphate ($>1M$), whereas at low phosphate concentration, adsorption onto the reactive adsorption sites may be predominant.

1.3. Soil solution concentration of phosphate.

The concentration of phosphorus in the soil solution or in water extracts of the soil is extremely low. It is seldom below 0.05 ppm. and rarely above 10 ppm. (Teakle, 1928). Arnon (1953) pointed out in his review that soils which had more than 1 ppm. P in the water extract invariably gave high relative yields, in both pot culture tests and field experiments and did not respond to phosphate fertilization.

The water-soluble phosphate in the soil is in dynamic equilibrium with all of that adsorbed onto colloidal surfaces and with any discrete phosphate mineral present.

Even where phosphate minerals may be the source of phosphate, the surface composition may be quite different from the bulk of the mineral. For example, the work of Weir and Soper (1963) showed that for the calcareous soils they used it appeared that the soil phosphates were more soluble than the expected values of hydroxy apatite. Presumably this is due to some surface composition on the phosphate compound which is more soluble than the bulk of the mineral.

Kurtz (1953) pointed out that, the idea that phosphate in the soil is in the form of a discrete crystalline phase sometimes leads to rather questionable conclusions. An ideal precipitation reaction is usually considered to lead to the formation of a definite solid compound of constant composition with stoichiometric proportion of the elements. The ideal precipitation is governed by the solubility product principle. Thus such precipitates will have a definite solubility constant (K_{sp}) and at equilibrium maintain a certain activity of the dissolved substance. Consequently if the phosphate in a given soil were present as a series of discrete crystalline phases, the theoretical consideration would require a stepwise decrease in solubility as the soil was extracted. The concentration of phosphate in the extract should be nearly constant until all of the most soluble compound dissolved. The concentration in solution would then drop markedly to a lower level characteristic of the compound of next solubility and so on.

The observed solubility of soil phosphate shows no such stepwise changes but decreases very gradually with repeated extraction or dilution (Aslyng, 1954; Fried and Shapiro, 1956). This gradual decrease is evidence, but not necessarily proof, that definite phosphate compounds are not present in soil. These results may be explained by the fact that in the soil system where the concentration of phosphate is low and there is an abundance of soil colloids of large surface area, adsorption processes will dominate the equilibrium.

The ease with which the adsorbed phosphate is released into solution will then be governed by the strength of binding or equilibrium constant between phosphate ion and the reactive sites on the soil colloid.

This view is supported by Fried and Shapiro (1960) who stated that in the plant-soil system, the plants respond to the soil solution phosphorus concentration and not to the mineralogical nature of the solid phase. From a knowledge of the adsorption constants, they believed that the phosphate concentration in the soil solution could be predicted both when phosphorus is removed from the system and when phosphorus is added to the system. However, the long term supply of phosphorus in soil is better described in terms of the mineralogical composition of the solid-phase of phosphate compounds.

1.4. The solubility product of phosphate compounds.

If phosphate in soil system is present as a definite chemical compound, it is possible to prove it by determining the solubility product of the soil phosphate and relating the calculated value to the solubilities of known pure phosphate compounds. To make this comparison a solubility diagram must be constructed. Variscite, $\text{Al}(\text{OH})_2\text{H}_2\text{PO}_4$, is given as an example.

For a variscite system having the chemical formula $\text{Al}(\text{OH})_2\text{H}_2\text{PO}_4$ in equilibrium with its solution the ionic activity product is

$$K_{sp} = a_{\text{Al}} \times a_{\text{OH}}^2 \times a_{\text{H}_2\text{PO}_4} \dots\dots\dots (1)$$

where a_{Al} is the activity of the Al^{3+} in solution.

K_{sp} is the solubility product constant of variscite.

Taking negative logarithms of the activities and using the dissociation constant of water, gives

$$pK_{sp} = pAl + pH_2PO_4 + 2pOH \quad \text{or}$$

$$3(pH - \frac{1}{3}pAl) - (pH + pH_2PO_4) = \text{constant}$$

$$= -2.48 \quad (25^\circ C) \quad (\text{Clark and Peech, 1955})$$

where $(pH - \frac{1}{3}pAl)$ is the potential of aluminium hydroxide.

$(pH + pH_2PO_4)$ is the phosphoric acid potential.

These potential terms are analogous to the phosphate potential, $(pH_2PO_4 + \frac{1}{2}pCa)$, which was first proposed by Schofield (1955). The solubility diagram for these systems can be obtained by plotting the potential of aluminium hydroxide on the x-axis, against the phosphoric acid potential on the y-axis.

Using this approach, therefore, it is possible to get some information about the existence of a crystalline solid phase in soil with respect to the known pure phosphate compounds.

Recently Bache (1963) has studied the reactions of variscite and strengite with dilute aqueous solutions and found that the thermodynamic solubility constants are maintained only at very low pH values.

For $Al(OH)_2H_2PO_4$ $pK_{sp} = 30.5$, at $pH < 3.1$

$Fe(OH)_2H_2PO_4$ $pK_{sp} = 34.3$, at $pH < 1.4$

This finding was explained by the fact that surface hydrolysis occurs at higher pH values thereby releasing phosphate ions into solution and forming a more basic insoluble metal phosphate. Thus he concluded that the solubility equilibria of these minerals are not likely to be relevant in soils at equilibrium.

In the light of these findings it is unreasonable to discuss soil systems in terms of the solubility equilibria of variscite and strengite minerals. It appears that surface reactions predominate in the soil-phosphate system.

I.2. THE STRUCTURE OF KAOLINITE, HALLOYSITE, GIBBSITE AND PSEUDO-BOEHMITE.

2.1. The structure of kaolinite.

The general structural feature of kaolinite was first described by Pauling (1930). Since then many refinements and detailed studies have been made (Gruner, 1932; Hendricks, 1936; Brindley and Robinson, 1946; Newnham, 1956; Brindley and Nakahira, 1958).

The fundamental unit consists of an extended sheet of two layers. The first layer is of $(\text{Si}_4\text{O}_{10})^{-4}$ formed by linkage of SiO_4 tetrahedra in hexagonal array, the bases of tetrahedra being approximately co-planar and their vertices all pointing in one direction. The second layer is of octahedrally co-ordinated aluminium which is arranged so that the apical oxygens of the tetrahedra, together with some additional OH^- ions located over the centre of the hexagons, form the base of the aluminium octahedral layer of composition $(\text{OH})_6^{-}\text{Al}_4^{+}(\text{OH})_2\text{O}_4$.

Brindley (1961) concluded that departure from ideal geometry of tetrahedral and octahedral networks is necessary to fit the Si and Al layers together in kaolinite.

The chemical composition of kaolinite is $2(\text{Al}_2\text{Si}_2\text{O}_5(\text{OH})_4)$ per unit cell, which agrees with the oxide formula $\text{Al}_2\text{O}_3 \cdot 2\text{SiO}_2 \cdot 2\text{H}_2\text{O}$.

The chemical structure of the kaolinite layer along the a and b axes is shown in Figure 1.

In the layer common to the octahedral and tetrahedral group $2/3$ of the atoms are shared by the silicon and aluminium, and then they become O instead of OH. Only two out of three possible positions for

MINERALOGICAL STRUCTURE

KAOLINITE

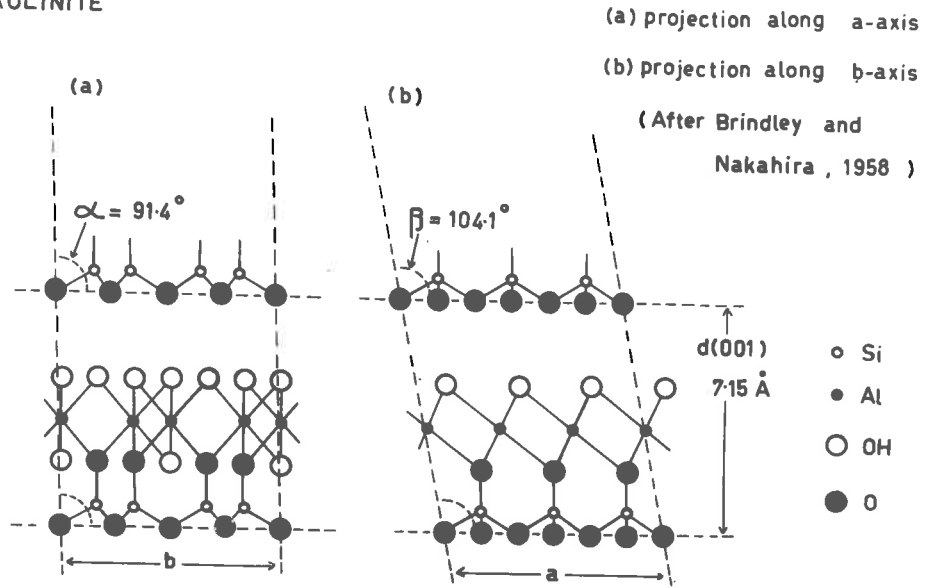


FIGURE 1

GIBBSITE

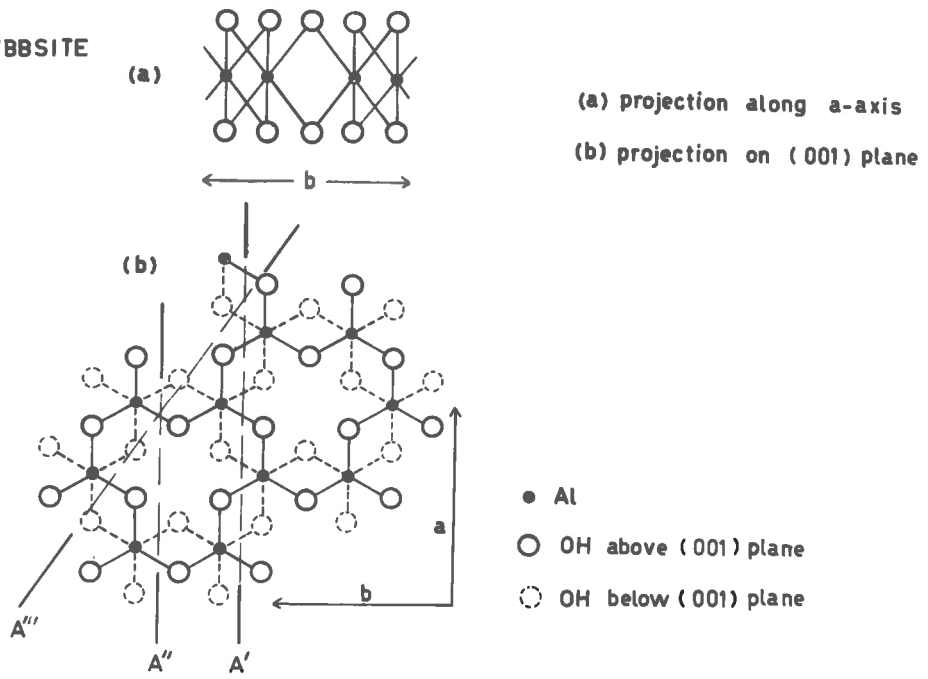


FIGURE 2

aluminium in the octahedral sheets are filled, thus there are three possible plans of regular populations of the octahedral layer with aluminium.

A complete structure determination must describe the mode of stacking of successive sheets. The analysis of the kaolinite structure was first attempted by Gruner (1932) who concluded that the crystal symmetry of kaolinite was monoclinic. Although some discrepancies remained between the observed X-ray intensities and those calculated from the monoclinic structure, Gruner's work was an important step in that it proved the correctness of the layer structure given schematically by Pauling (1930).

Brindley and Robinson (1946) undertook a more detailed study and found an additional reflection which could not be reconciled with the monoclinic cell. Their results suggest that the unit cell may be triclinic with the α angle making a small departure from 90° . Subsequently Newnham (1956) confirmed the triclinic structure of kaolinite.

The relation of adjacent layers to each other as proposed by Brindley and Nakahira (1958) in which oxygen of the Si-O network of one layer and hydroxyl ions of the octahedral sheet of the adjacent layer are grouped in pairs, suggests that the layers are bound together by hydrogen bonds. The strength of this bond is reflected by the fact that kaolinite shows only one characteristic $d(001)$ spacing of 7.15\AA . Thus it is expected that the layers will be stacked with respect to one another so that the O-OH distances are equal.

In an ideal kaolinite structure α and β would be 90° and 103.5° respectively as a result of layer displacements of $-\frac{a}{3}$ along x and zero along y. An explanation of the deviation of α and β angles from these ideal values has been put forward by Brindley and Nakahira (1958) who suggest, on the basis of their detailed studies on dickite, that the kaolinite structures involved are distorted tetrahedral and octahedral layers similar to those found for dickite. The distortion of the kaolinite layer modifies the displacements of one structural layer with respect to its neighbour which is required to make interlayer O-OH bonds all equal and results in α and β angles near to the observed values 91.6° and 104.8° (Figure 1).

2.2. The structure of halloysite.

Halloysite has the same chemical composition as that of kaolinite, but the water content is higher. The relation of halloysite to kaolinite based on the X-ray diffraction studies has been given by Brindley (1961). Halloysite dried at 110°C has a strong reflection at spacings of about 7.2 and 3.6 \AA , corresponding to the d(001) and d(002) reflections of kaolinite, and usually considerable broadening. The absence of sharp hkl reflections indicates an irregular stacking sequence.

Natural halloysite (hydrated form), before drying at 110°C , has a higher water content than kaolinite and shows a strong reflection at 10.1 \AA and a third order at about 3.4 \AA without a second order.

Simple re-hydration does not occur probably because of the strong hydrogen bonding between the sheets.

Halloysite dried at 200° to 300°C (dehydrated form) has a water content similar to that of kaolinite and its ideal composition is $\text{Al}_2\text{O}_3 \cdot 2\text{SiO}_2 \cdot 2\text{H}_2\text{O}$. The fully hydrated halloysite has a composition of $\text{Al}_2\text{O}_3 \cdot 2\text{SiO}_2 \cdot 4\text{H}_2\text{O}$. Ross and Kerr (1934) have shown that usually the less hydrous form of halloysites (metahalloysites) have a water content of about 2.2 to 2.3 H_2O . The excess water is lost very readily at temperature as low as 60°C and under vacuum conditions.

2.3. The structure of gibbsite.

There are two polymorphic forms of aluminium hydroxide, $\text{Al}(\text{OH})_3$, or alumina trihydrate, $\text{Al}_2\text{O}_3 \cdot 3\text{H}_2\text{O}$. The first crystalline form is gibbsite ($\gamma\text{-Al}_2\text{O}_3 \cdot 3\text{H}_2\text{O}$) which occurs naturally. Gibbsite is the stable form of crystalline aluminium hydroxide which can also be prepared synthetically (Weiser, 1935; Gastuche and Herbillon, 1962). The second crystalline form is metastable and is known as bayerite ($\alpha\text{-Al}_2\text{O}_3 \cdot 3\text{H}_2\text{O}$). It does not occur naturally but is readily prepared synthetically (Rooksby, 1961).

A highly gelatinous precipitate of aluminium hydroxide is formed upon the addition of alkali e.g. NaOH , KOH or NH_4OH , to an aluminium salt solution. The precipitate formed in the cold is usually amorphous and in a short time it transforms to $\gamma\text{-Al}_2\text{O}_3 \cdot \text{H}_2\text{O}$ (boehmite). Aging in cold water leads to the growth of crystals, and in addition a gradual transformation takes place from $\gamma\text{-Al}_2\text{O}_3 \cdot \text{H}_2\text{O} \longrightarrow$ metastable

$\alpha\text{-Al}_2\text{O}_3 \cdot 3\text{H}_2\text{O} \longrightarrow$ stable $\gamma\text{-Al}_2\text{O}_3 \cdot 3\text{H}_2\text{O}$. This transformation is more rapid in water containing alkali (Weiser, 1935).

Gibbsite has the same octahedral structure found in clay minerals. It is built up of double layers of hydroxyl groups bonded to aluminium atoms which occupy 2/3 of the octahedral holes between the two layers. An idealized plan of one such double layer is given in Figure 2. As a consequence of Pauling's electrostatic valence rules, where the sharing of octahedral edges within the layer shortens Al — O distances, the actual arrangement is a slightly distorted version of this. The stacking of octahedral layers one above another is governed by hydrogen bonds (Bernal and Megaw, 1935; Wells, 1950), where the OH groups on the underside of one layer rest on the oxygen groups of the layer below.

2.4. The structure of pseudoboehmite ($\gamma\text{-AlO(OH)}$)

Aluminium forms compounds of the type AlO(OH) , which is intermediate in composition between the trihydroxide Al(OH)_3 and the oxide Al_2O_3 . The oxy-hydroxide of aluminium has molecular formula AlO(OH) and has two crystalline forms which occur naturally.

$\alpha\text{-AlO(OH)}$ or $\alpha\text{-Al}_2\text{O}_3 \cdot \text{H}_2\text{O}$ diaspore.

$\gamma\text{-AlO(OH)}$ or $\gamma\text{-Al}_2\text{O}_3 \cdot \text{H}_2\text{O}$ boehmite.

Both forms have an octahedral structure, which consists essentially of close-packed oxygen atoms with an aluminium atom in certain of the octahedral holes. The crystal structure of diaspore (Ewing, 1935)

and boehmite (Reichertz and Yost, 1946) is orthorhombic, but it differs in the lattice parameters and the space group.

Rooksby (1961) pointed out that the principal constituent of gelatinous precipitates of aluminium hydroxide has a boehmite-like structure. The X-ray diffraction pattern consists of very diffuse bands. The spacings of the broad reflections correspond approximately with the spacings of the principal lines of the pattern of crystalline boehmite, but the first reflection indicates some displacement. Thus the diffuse X-ray diffraction bands can be used as an indication that the boehmite-like material is semi-crystalline or very poorly crystalline, having a less rigid structure. Papée, Tertian and Biaïis (1958) proposed that a precipitated alumina having diffuse X-ray diffraction bands of boehmite, should be described as pseudoboehmite. They suggest that although the structure resembles that of boehmite, the order is only very short range and of intramolecular nature.

The boehmite form of the monohydrate can also be produced on dehydration of most samples of gibbsite at temperatures just under 200°C .

I.3. THE ELECTRIC CHARGES ON KAOLINITE.

The electric charges on kaolinite and similar minerals are both negative and positive. The negative charge is composed of a constant and a pH dependent part. While the positive charge is pH dependent below pH 7 and above this, is pH independent. For this latter region, the positive charge on kaolinite depends on the concentration of chloride (Quirk, 1960).

3.1. The origin of the permanent negative charges.

Schofield (1948) has shown that at low pH values (pH 2.5 to 5) the negative charge on kaolinite is constant, and suggests that this charge is due to isomorphous substitutions in the tetrahedral layer.

Isomorphous substitutions within the lattice structure of the trimorphic clay minerals, consists of the substitution of trivalent aluminium for quadrivalent silicon in tetrahedral layers, or of ions of lower valence (e.g. Mg^{++}) for aluminium in the octahedral layer, resulting in a charge deficiency in the structural units of these clay minerals. This deficiency in charge, is balanced by exchangeable cations such as H^+ , Na^+ , K^+ , Ca^{++} or Al^{3+} . Exchangeable cations resulting from the isomorphous substitutions are mostly located on cleavage surfaces.

The presence of a permanent negative charge for kaolinite has led Schofield to postulate the existence of isomorphous replacement in this mineral. Isomorphous replacement for kaolinite is difficult to prove by chemical methods, since the degree of isomorphous

replacement is low. For instance, the replacement of one silicon in four hundred by an aluminium in kaolinite would give rise to deficiency of charge of 2 meq./100 g. At high pH values (> 7) Schofield suggests that dissociation of SiOH groups at the crystal edges increases (pK of silicic acid is about 9.5), and thus contributes to the cation exchange capacity (C.E.C.). Fripiat (1960a), using a different technique, obtained support for Schofield's suggestions, relating to the behaviour of SiOH. However, he believed that the permanent negative charge is caused by the presence of tetrahedral aluminium. This tetrahedral aluminium was possibly bound in an amorphous mixed gel, coating the particles, and perhaps preferentially located at the edges. It is obvious that no real agreement exists on the nature of the permanent negative charge of kaolinite type minerals.

3.2. The origin of variable negative charges.

Unsatisfied bonds arise at the edge face of a crystal, either by the cessation of crystal growth or by fracture of the crystal. The bonds then become satisfied by the uptake of an appropriate ion e.g. OH^- , H^+ . This type of edge face grouping will have identical properties and these will be independent of the mode of formation. The number of negative charges on these edge face groupings will vary with pH value (Schofield, 1948). In kaolinite and halloysite minerals dissociation of the H^+ of SiOH contributes to the exchange capacity at high pH values.

3.3. The origin of positive charges.

Positive charges on clay minerals are generally attributed to the aluminium atoms on the edge face of the crystal (van Olphen, 1951; Schofield and Samson, 1953, 1954; Cashen, 1959; Quirk, 1960).

By analogy with the positive charge of alumina sols, van Olphen (1951) has suggested that positive charges develop on the aluminium atoms on the edge-face of the alumino silicate layer.

Schofield and Samson (1953) have modified the concept of electric charges situated on the edge face of kaolinite as originally proposed by Hendricks (1945). They suggest that:-

- (i) all the oxygens at the edges of the silicon oxygen sheets could remain negatively charged only at very high pH values (pH 9).
- (ii) in neutral and slightly acid conditions, practically all these sites will combine with protons to form uncharged hydroxyls.
- (iii) under acid conditions there is a strong possibility that the oxygens at the edges of the gibbsite layers can each combine with a proton. Thus the balance of charge on each of these oxygens is one half positive, and these together make one positive charge per 33 \AA^2 .

The model proposed by Schofield and Samson is given in Figure 3.

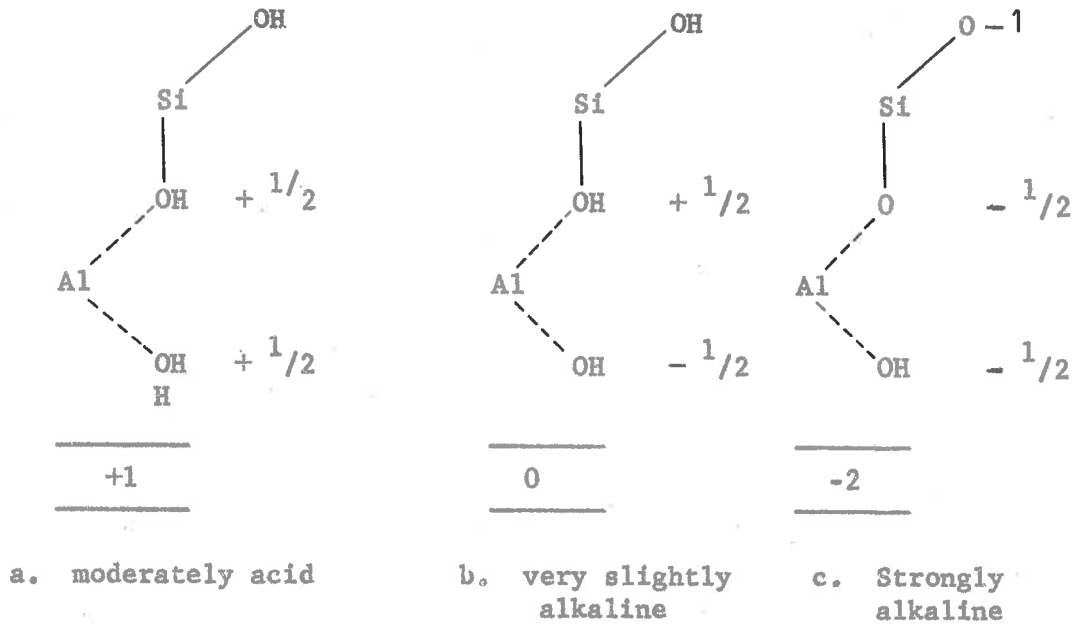


Figure 3. Proton attached to oxygens at the edge faces of kaolinite when the suspending solution is (a) acid, (b) slight alkaline, (c) strongly alkaline

Fieldes and Schofield (1960) have considered the nature of different types of sites which may be formed at the broken edge of a mineral structure containing aluminium. Fracture of these structures leads to the following terminal groups of aluminium and silicon.

(i) Gibbsite. In gibbsite aluminium exists in an octahedral structure.



(ii) Kaolinite. In well crystallized kaolinite, aluminium occupies octahedral positions and it appears that there is little isomorphous substitution in either the octahedral or tetrahedral layer.

There are four types of oxygens within a kaolinite layer, thus fracture of the structure gives rise to the following possibilities.



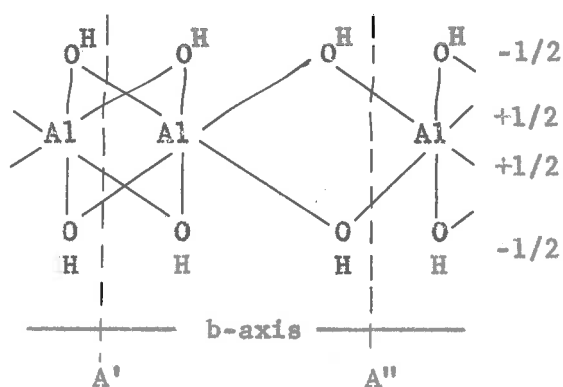
They consider that because of the disposition of the hydroxyls in kaolinite, there is the possibility that 1/3 of the sites due to type 1 fractures will not be neutralized by type 2 fracture as in gibbsite. Thus it can be expected that $\text{Al}^{+1/2}$ sites from type 1 and 3 fractures will accept OH and become $\text{AlOH}^{-1/2}$ sites. Combination of type 1 and 3 fractures will give $\text{Al} - \text{O}^{-1/2}$ and $\text{AlOH}^{-1/2}$ sites; under alkaline conditions both sites will be negatively charged. However, under slightly acid conditions both sites may accept a proton and each attains half a positive charge. They suggested that both broken bonds of Type 4 and 5 fractures may be reduced to neutrality by hydrolysis, resulting in uncharged SiOH and AlOH . As these are unlikely to dissociate in the pH range commonly encountered in soils, the sites are likely to be inactive. However, to be consistent with the model of Schofield and Samson discussed earlier, AlOH should take up a proton under acid conditions, and become a positively charged site, which is the site for the adsorption of chloride. SiOH will dissociate to

give SiO^- at high pH values.

It is concluded that there is general agreement between various workers that the origin of positive charges on clay mineral kaolinite is on the aluminium atoms on the edge face of the crystal. These positive sites are then likely to be the places at which anions will be adsorbed.

The suggestion of Fieldes and Schofield on the types of fracture or termination of crystal structures however, does not account for the relative distribution of aluminium groupings on the edge face. These have the following forms $>\text{AlOH}$ and $-\text{Al}(\text{OH})_2$.

It is suggested that the fracture of crystal surfaces or termination of crystal growth is simpler than the proposal of Fieldes and Schofield. There are three directions of fracture or termination of crystal growth across the crystal lattice, along the plane perpendicular to (001) plane. For simplicity the gibbsite structure will be used as an example, but these considerations apply also to the kaolinite crystal.

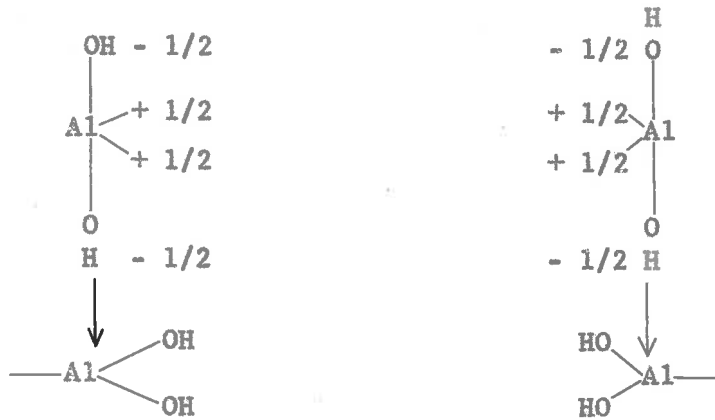


Bond termination at the edge face of the crystal.

(View of gibbsite structure along a-axis.)

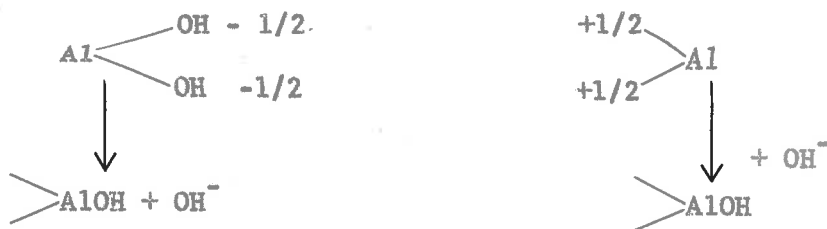
There are three possible positions at A', A'' and A''' planes, at which fracture or termination of growth of the crystal along any of these planes will give rise to different situations.

- (i) Fracture or termination of crystal growth along the A' plane will give the following forms of aluminium on the edge face.



This will give rise to two uncharged ---Al(OH)_2 situated on the edge face; however, under acid conditions this group takes up a proton (Schofield, 1949) and becomes a positively charged site $\text{---Al(H}_2\text{O)}^+$
 OH

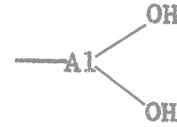
- (ii) Fracture or termination of crystal growth along the A'' plane.



This will give rise to two uncharged >AlOH groups situated on the edge face and under acid condition this group will accept a proton and become a positively charged site $\text{>Al(H}_2\text{O)}^+$.

(iii) Fracture or termination of crystal growth along the A'' plane (see Part I.2.3. Figure 2, projection of gibbsite layer on (001) plane). This would cause the breakage or termination of two or three half bonds for each aluminium. Breakage or termination of two half bonds will lead to the formation of

>AlOH group, whereas breakage or termination of three half bonds will give rise to the formation of —Al group.



It is not possible to decide 'a priori' the relative proportions of the groupings



I.4. ADSORPTION

4.1. Introduction

When a gas or solution is allowed to come to equilibrium with a solid or liquid surface, the concentration of gas molecules or solute is usually found to be greater in the immediate vicinity of the surface than in the bulk phase. The process by which this surface excess is formed is termed adsorption. The atoms at the surface of any solid or liquid are subject to unbalanced forces of attraction perpendicular to the surface plane, which are satisfied by the adsorption process.

Adsorption of a gas on a solid is a spontaneous process, it is accompanied therefore by a decrease in the free energy of the system. Because the process involves some loss of freedom of gas molecules, there is also a decrease in entropy. Therefore, from the equation

$$\Delta G = \Delta H - T\Delta S \quad \dots\dots\dots (2)$$

it can be seen that the adsorption process must always be exothermic, irrespective of the nature of the forces involved.

In the case of adsorption from solution, the driving force for the adsorption process may be attributed to the heat or entropy term, depending upon the relative importance of these terms in any particular system. Most of the adsorption studies and associated thermodynamic treatments have been carried out for solid-gas systems.

However, much additional information can be obtained by applying the same basic theories to adsorption of solutes at solid-liquid interfaces.

4.2. Physical adsorption, chemisorption and ion-exchange.

The classification of adsorption into physical and chemisorption is based on the nature of the forces involved. (Brunauer, 1943; Young and Crowell, 1962). The distinction between physical adsorption and chemisorption is usually clear cut. The characteristics of the two types of adsorption are outlined below.

4.2.1. Physical adsorption.

Physical adsorption or van der Waals adsorption is caused by molecular interaction forces; these are similar to those responsible for condensation of a vapour to form a liquid and similar to those responsible for crystallisation (Gregg, 1961).

This type of adsorption is non-specific and is characterised by a low energy of adsorption (up to 10 k.cal/mole). The heat of physical adsorption is of the same order of magnitude as the heat of liquefaction of a gas or crystallisation of a molecular lattice. A physically adsorbed layer may be removed simply by reducing the concentration at the temperature at which adsorption took place; the desorption may be slower than adsorption.

4.2.2. Chemisorption.

Chemisorption involves the formation of a chemical bond between the adsorbate and the outer most layer of adsorbent atoms.

For chemisorption the adsorption is specific and has a high energy (10-100 k.cal/mole). The heat of chemisorption is, therefore, of the same order of magnitude as that of the corresponding chemical reaction. Chemisorption will take place only if the adsorbate is capable of forming a chemical bond with the surface. Consequently, the removal of a chemisorbed layer is very difficult, if not impossible.

The chemisorption is characterised by monomolecular adsorption, whereas physical adsorption may involve the formation of either a monomolecular or multimolecular layers.

It can be concluded from the foregoing discussions that the two types of adsorptions are usually very different from each other. However, in some cases of chemisorption, exceptionally low heats of adsorption are found.

In both types of adsorption the heat of adsorption may vary considerably with surface coverage, because of surface heterogeneity and the effect of lateral interaction. This effect is particularly marked in chemisorption where the lateral interaction forces reinforce the effect of heterogeneity.

An important consequence of the dominant role played by solid - adsorbate forces, as opposed to adsorbate - adsorbate interactions, is that chemisorption tends to be localized. Therefore

adsorbate molecules tend to remain at specific sites, and in fact are chemically bonded to surface atoms. Hence the capacity of the solid for adsorption is determined primarily by the number of appropriate surface atoms of the solid, rather than the size of the adsorbate molecule (Adamson, 1960).

Thus, chemisorption conforms to the postulates of the Langmuir adsorption isotherm, which requires a localized adsorption in which the adsorbate molecules are distributed among a fixed number of sites and are held by a constant energy of adsorption.

4.2.3. Ion-Exchange.

Ion-exchange itself is not a chemical process (Helfferich, 1962), although the forces holding the ion to the surfaces are those involved in an ionic bond (Pauling, 1960). The process is probably best described as physico-chemical.

The heat or enthalpy of ion-exchange is usually small (Boyd, Schubert and Adamson, 1947; Helfferich, 1962), in contrast to the changes involved in physical and chemical adsorption. The driving force for ion-exchange is thus due to an entropy increase, which arises mainly from the entropy of mixing. In addition it will include a configurational entropy change of the matrix together with contributions from changes in the degree of ordering of solvent molecules resulting from the formation and degradation of solvation shells. Adsorption however usually involves a loss of entropy due to an ordering of the

surface region, whereas exchange reactions usually lead to an increase in disorder.

4.3. Classification of adsorption isotherm.

The general form of an adsorption isotherm is (Everett, 1950)

$$\ln \frac{a_1}{a_0} = \frac{\overline{\Delta H_\Gamma^0}}{RT} - \frac{\overline{\Delta S_\Gamma^0}}{R} \dots \dots \dots (3)$$

where a_1 is the activity of adsorbate in equilibrium with the adsorbed phase.

a_0 is the activity of adsorbate in the standard state.

$\overline{\Delta H_\Gamma^0}$ and $\overline{\Delta S_\Gamma^0}$ are the differential molar heat and entropy of

adsorption relative to the same standard state in the bulk when

the surface concentration is Γ .

If $\overline{\Delta H_\Gamma^0}$ and $\overline{\Delta S_\Gamma^0}$ can be expressed as functions of the surface concentration,

Γ , then equation (3) becomes the adsorption isotherm. This equation is quite general and involves no assumptions as to the nature of the adsorbed phase, hence it applies generally to physical and chemical adsorption.

Brunauer (1943) has classified adsorption isotherms for adsorption in the gas phase into five classes. Recently, Giles and MacEwan (1957), Giles, MacEwan, Nakhwa and Smith (1960), have discussed the significant features of adsorption of solutes from solution onto various solids and as a result have presented a classification involving four main classes of adsorption isotherms.

These classes are (Figure 4).

- (i) S type, the curve is concave to the y-axis.
- (ii) Ln type, the isotherm is linear.
- (iii) L (Langmuir) type, the isotherm is convex to the y-axis.
- (iv) HA. (High affinity) type, the isotherm coincides with the y-axis, until the sites are fully occupied.

The shape of the isotherm is considered to be determined by factors such as the relative affinity of the solute and solvent for the solid surface, the number of sites available for adsorption and the interaction of adsorbed molecules.

4.3.1. S isotherm.

The S type isotherm is very rare for solute adsorption. The shape of the isotherm indicates that the mechanism is governed by co-operative phenomena. A particular example of this type is the adsorption of phenol from water onto alumina (Giles et al., 1960)

4.3.2. Ln (Linear) isotherm.

This isotherm shows a linear relationship between amount adsorbed and bulk concentration.

Everett (1957) has proposed an ideal two-dimensional gas model, where the adsorbed molecules are constrained to move in a plane adjacent to the surface. Hence the motion of the molecules normal to the surface is completely restricted, while motion parallel to the surface is free. The behaviour of the adsorbed molecules can be represented by an

CLASSIFICATION OF ADSORPTION ISOTHERM

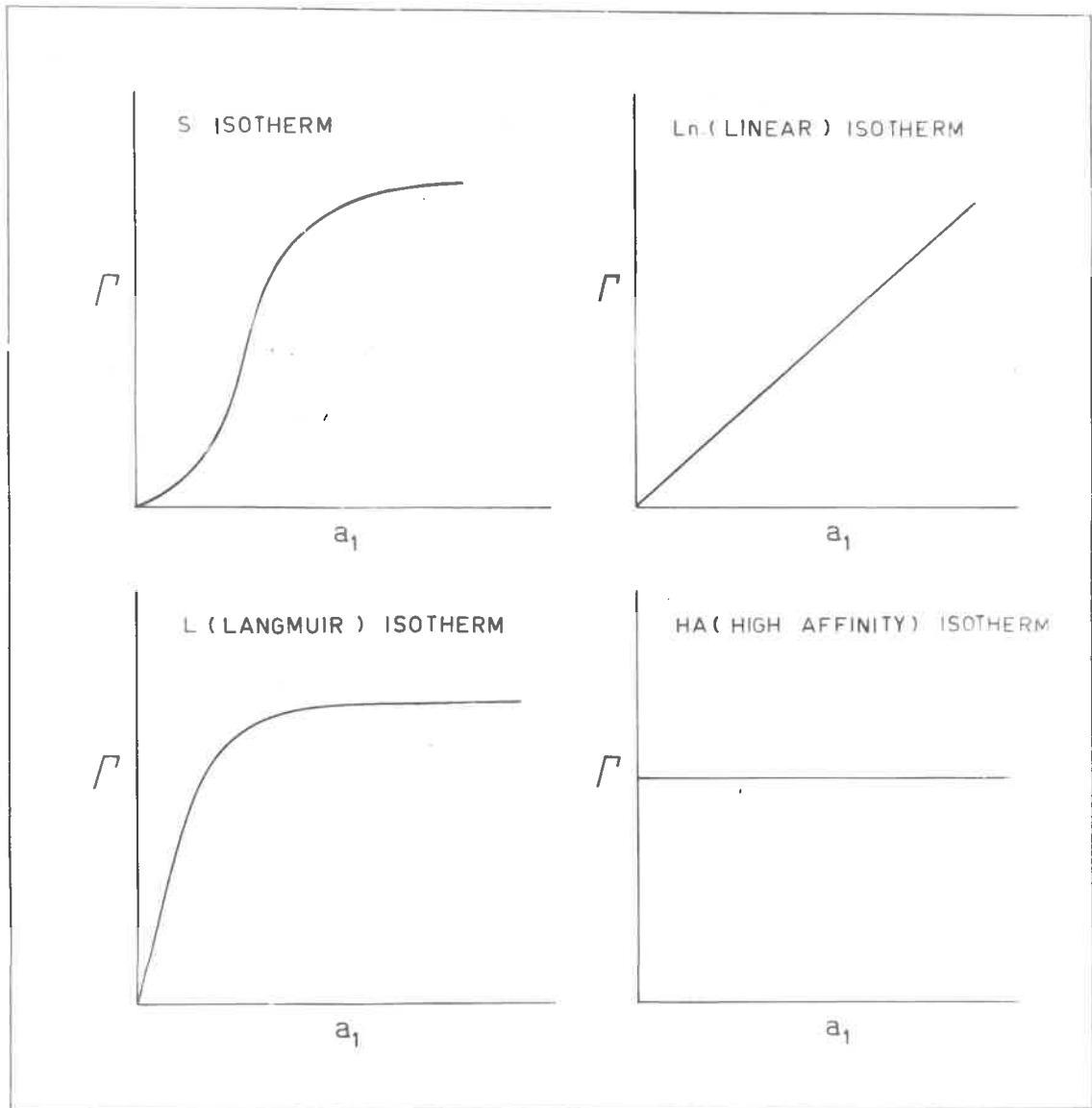


FIGURE 4

appropriate equation of state relating the spreading pressure (ϕ), and the surface concentration (Γ). The form of the adsorption isotherm, the energy and entropy of the surface phase can be derived by using the Gibbs adsorption equation.

In the simplest case, the adsorbed phase at temperature T, behaves as an ideal two-dimensional gas obeying the equation

$$\phi = \frac{mRT}{A^\sigma} = RT\Gamma = \frac{RT}{a^\sigma} \dots \dots \dots (4)$$

where A^σ is the area of the surface.

m is the number of moles adsorbed.

a^σ is the average area occupied per mole.

ϕ is the spreading pressure.

Γ is the surface concentration.

R is gas constant.

The work required to insert the adsorbing molecule into the adsorbed film will be a contributing factor to the entropy term. In the ideal case this will be given by the perfect gas law while in a slightly more complex case it will be given by a simple partition law so that

$$\overline{\Delta S_\Gamma^0} = \overline{\Delta S_\Gamma^*} - R \ln \Gamma \dots \dots \dots (5)$$

where $\overline{\Delta S_\Gamma^*}$ is the differential entropy of adsorption leaving out the localization term.

If $\overline{\Delta H_\Gamma^0}$ and $\overline{\Delta S_\Gamma^*}$ are constant, equation (3) will give a linear

isotherm. This may be the case if the number of adsorption sites remains constant even though the amount of solute adsorbed increases. This will occur when the solute can swell the substrate structure, where each solute molecule adsorbed exposes a fresh site on which the next molecule can be adsorbed. Giles et al (1960) have suggested that this process can take place only in the less readily ordered or amorphous regions of the substrate, the crystalline material being impenetrable. If the molecular dimensions are suitable the adsorbate could penetrate to regions in the substrate not already available to the solvent. The penetration stops abruptly when more highly crystalline regions of the substrate are reached, when a typical isotherm suddenly changes direction to give a horizontal plateau.

The above situations, for a linear isotherm, can be formulated as a simple partition phenomenon in which the solute effectively distributes itself between the bulk and surface phase.

In relation to the material presented in this thesis it is of some interest to note that linear isotherms have been reported for adsorption from solution. (see for example Greenland, Laby and Quirk, 1962).

4.3.3. L isotherm or Localized model.

This type of isotherm is generally referred to as the Langmuir isotherm. It is based on the idea that there are a fixed number of adsorption sites which are at first readily available. As the sites became filled the chance of a solute molecule finding a vacant site steadily decreases until at equilibrium, the rate of adsorption is equal to the rate of desorption.

The assumptions on which this approach is based are that

- (i) the adsorption sites are localized on the surface although adsorbed molecules can desorb;
- (ii) the surface is an array of active sites, all having the same adsorptive properties;
- (iii) there is no lateral interaction between adsorbed molecules;
- (iv) the adsorbed molecules retain a certain amount of translational kinetic energy, in the form of vibration both in a plane parallel to the surface and in a plane normal to the surface. Polyatomic molecules may also retain some rotational motion.

Since all adsorption sites are assumed to have the same properties, the molar heat of adsorption and the differential heat of adsorption are constant and independent of surface coverage.

The adsorption isotherm may be derived from the fact that under the above conditions the differential entropy of adsorption, $\overline{\Delta S_{\theta}^{\dagger}}$, is given by (Everett, 1950)

$$\overline{\Delta S_{\theta}^{\dagger}} = \overline{\Delta S_{\theta}^*} - R \ln \frac{\theta}{1-\theta} \dots\dots\dots (6)$$

where θ is the fraction of the surface covered, and $\overline{\Delta S_{\theta}^*}$ is the differential entropy of adsorption leaving out the localization terms since the sites are fixed.

The final form of the adsorption isotherm is obtained by substituting equation (6) into equation (3)

$$\frac{\theta}{1-\theta} = C \exp.\left(-\frac{\overline{\Delta H_{\theta}^{\dagger}}}{RT} + \frac{\overline{\Delta S_{\theta}^*}}{R}\right) \dots \dots \dots (7)$$

where C is the bulk concentration at coverage θ , (assuming the activity coefficient is unity).

If $\overline{\Delta H_{\theta}^{\dagger}}$ and $\overline{\Delta S_{\theta}^*}$ are constant and independent of T and θ , the familiar Langmuir isotherm is obtained. This can be expressed as

$$\Gamma = \frac{\Gamma_0 KC}{1 + KC} \dots \dots \dots (8)$$

where Γ is the surface concentration

Γ_0 is the surface concentration at saturation

K is constant.

Because the Langmuir adsorption isotherm has special importance in this thesis the detailed derivation of this isotherm form is set out in Part 4.5.

4.3.4. H A (High affinity) type.

The special feature of this isotherm form is that the solute has a high affinity for the surface and hence is almost completely adsorbed from dilute solutions. Therefore, the isotherm virtually coincides with the y-axis until the adsorption sites are fully occupied.

If the rate of desorption is small, then the desorption is negligible because of the very high affinity of solute for the surface.

In the most extreme form, that is in chemisorption, the isotherm is a horizontal line running into the y-axis.

For any given system, it is possible to have a single isotherm type or a combination of isotherm types occurring singly, consecutively or concomitantly depending on the distribution of energies amongst the adsorption sites.

4.4. The equilibrium constant of linear isotherms.

For the ideal gas model of the reaction



the equilibrium constant K can be written as

$$K = \frac{[B]}{[A]}$$

The Ln (linear) isotherm expresses a simple partition phenomenon in which the solute effectively distributes itself between the bulk and surface phase, therefore the isotherm can be written as

$$\Gamma = KC \quad \dots \dots \dots (10)$$

where Γ is the surface concentration.

K is the equilibrium constant.

C is the bulk concentration (activity coefficient assumed to be unity).

4.5. Derivation of Langmuir adsorption isotherm.

The Langmuir adsorption isotherm can be derived by using several different approaches, (i) kinetic, (ii) statistical-mechanical, (iii) thermodynamic or (iv) mass action.

The first adsorption isotherm for a localized model was derived from kinetic consideration by Langmuir in 1918. However, it suffers some disadvantages in that it is based on a very specific mechanism and unnecessary assumptions are involved. Subsequently, Fowler (1935) showed that the equation could be derived by applying statistical-mechanical considerations to the same model, without considering the kinetic mechanism of adsorption and desorption. The localized adsorption isotherm can also be derived on thermodynamic grounds without assuming the exact kinetic mechanism of adsorption and desorption. Thus the form of the adsorption isotherms derived statistically and thermodynamically are more general than the adsorption isotherm based on kinetic grounds. However, the statistically derived equation suffers from a disadvantage that no explicit account is taken of the possible variation of the entropy of adsorption with surface concentration of the adsorbed phase (Everett, 1950).

4.5.1. Thermodynamic approach.

A derivation (Everett 1950, 1957) of the localized adsorption isotherm will be given here following the thermodynamic approach to adsorption studies. In addition it is convenient to present the equivalent derivation based on the Law of Mass Action.

4.5.1.1. A thermodynamic equation for adsorption equilibria.

Consider a solid in equilibrium with a vapour at a partial pressure p_{Γ} , when m mols of the vapour are adsorbed. The surface concentration, Γ therefore is given by

$$\Gamma = \frac{m}{A^\sigma} \dots \dots \dots (11)$$

where A^σ is the surface area of the solid, cm^2/g , which is assumed independent of temperature.

The change in chemical potential due to the isothermal transfer of vapour from the standard gas state (unit pressure) to the surface is expressed by

$$\Delta\mu_\Gamma^\dagger = \mu_\Gamma^\sigma - \mu^{\dagger G} = RT \ln p_\Gamma \dots \dots \dots (12)$$

where μ_Γ^σ is the chemical potential of the adsorbate in the adsorbed phase at a surface concentration Γ .

$\mu^{\dagger G}$ is the chemical potential of the vapour at unit pressure.

The change in chemical potential in equation (12) can be expressed in terms of heat and entropy contributions.

$$\Delta\mu_\Gamma^\dagger = \overline{\Delta H_\Gamma^\dagger} - T \overline{\Delta S_\Gamma^\dagger} \dots \dots \dots (13)$$

$$\text{where } \overline{\Delta H_\Gamma^\dagger} = \overline{H_\Gamma^\sigma} - H^{\dagger G} \dots \dots \dots (14)$$

$$\overline{\Delta S_\Gamma^\dagger} = \overline{S_\Gamma^\sigma} - S^{\dagger G}$$

$\overline{H_\Gamma^\sigma}$ is the differential molar heat content of the adsorbed molecule.

$H^{\dagger G}$ is the molar heat content of the vapour in the standard gas state.

$\overline{\Delta H_\Gamma^\dagger}$ is the differential molar heat content of the adsorbed molecules relative to the standard gas state.

It is sometimes called the isosteric heat of adsorption. Similarly for the entropy terms, $\overline{\Delta S_\Gamma^\dagger}$ is the differential molar entropy of the adsorbed molecules relative to the standard gas state.

Combination of equations (12) and (13) gives the equilibrium vapour pressure of the adsorbed phase.

$$\ln p_{\Gamma} = \frac{\overline{\Delta H_{\Gamma}^{\dagger}}}{RT} - \frac{\overline{\Delta S_{\Gamma}^{\dagger}}}{R} \dots \dots \dots (15)$$

The corresponding form of equation (15) for solid-solution system can be written as

$$\ln \frac{a_1}{a_0} = \frac{\overline{\Delta H_{\Gamma}^{\circ}}}{RT} - \frac{\overline{\Delta S_{\Gamma}^{\circ}}}{R} \dots \dots \dots (15a)$$

where a_1 is the activity of adsorbate in equilibrium with the adsorbed phase.

a_0 is the activity of adsorbate at the standard state.

$\overline{\Delta H_{\Gamma}^{\circ}}$ and $\overline{\Delta S_{\Gamma}^{\circ}}$ are the differential molar heat and entropy of adsorption relative to the same standard state in the bulk, when the surface concentration is Γ . If $\overline{\Delta H_{\Gamma}^{\circ}}$ and $\overline{\Delta S_{\Gamma}^{\circ}}$ can be expressed as a function of the surface concentration, Γ , then equation (15a) becomes the adsorption isotherm.

It must be pointed out that the above equations are quite general and involve no assumptions as to the nature of the adsorbed phase. Therefore they apply generally to physical adsorption and to chemisorption.

4.5.1.2. Localized Monolayer model.

Using the assumption listed previously (Part I 4.3.3.) it is possible to calculate the configurational or localization entropy of

the surface phase.

The entropy of the surface phase is the sum of two contributions:

- (i) the thermal entropy, from the vibrations of the molecule in the neighbourhood of the adsorption site.
- (ii) the configurational entropy, from the number of ways of arranging the molecules among the sites.

$$\text{Therefore } S_{\theta}^{\sigma} = S_{\theta}^{\sigma} \text{ thermal} + S_{\theta}^{\sigma} \text{ config.} \quad \dots \dots \dots (16)$$

where S_{θ}^{σ} is the entropy of the surface phase at the fractional degree of coverage θ .

Because of the assumed independence of the adsorption sites, each molecule makes a constant contribution to the thermal entropy. However, the relationship of the configurational entropy and the number of adsorbed molecules is more complex.

The configurational entropy is a function of the number (Ω) of distinct arrangements of the m adsorbed molecules on the M adsorption sites, as given by the Boltzmann equation,

$$S_{\theta}^{\sigma} \text{ config.} = k \ln \Omega \quad \dots \dots \dots (17)$$

where the general form of Ω is $\frac{M!}{m! (M-m)!}$. With the use of

Sterling's approximation for factorials, it gives

$$S_{\theta}^{\sigma} \text{ config.} = k \left[m \ln \frac{m}{M} + (M-m) \ln \frac{M-m}{M} \right] \dots \dots \dots (18)$$

The differential molar entropy, $\overline{S_{\theta}^{\sigma} \text{ config.}}$, is obtained by differentiation

with respect to m and multiplication by Avogadro's number,

$$\overline{S_{\theta}^{\sigma}} \text{ config.} = -R \ln \frac{\theta}{1-\theta} \dots \dots \dots (19)$$

where $\theta = \frac{m}{M}$

therefore from equation (16)

$$\overline{S_{\theta}^{\sigma}} = \overline{S_{\theta}^{\sigma}} \text{ thermal} - R \ln \frac{\theta}{1-\theta} \dots \dots \dots (20)$$

The change of entropy on transferring one mole from gas at unit pressure to the surface (equation 14) is

$$\begin{aligned} \overline{\Delta S_{\theta}^{\dagger}} &= \overline{S_{\theta}^{\sigma}} - S^{\dagger G} \\ &= [\overline{S_{\theta}^{\sigma}} \text{ thermal} - S^{\dagger G}] - R \ln \frac{\theta}{1-\theta} \\ \overline{\Delta S_{\theta}^{\dagger}} &= \overline{\Delta S_{\theta}^*} - R \ln \frac{\theta}{1-\theta} \dots \dots \dots (21) \end{aligned}$$

where $\overline{\Delta S_{\theta}^{\dagger}}$ is the differential entropy of adsorption,

$\overline{\Delta S_{\theta}^*}$ is the differential entropy of adsorption leaving out the localization terms since the sites are fixed.

The standard state for the surface phase is taken to be that when the surface is half covered ($\theta = 0.5$).

The form of the adsorption isotherm is obtained by substituting equation (21) into (15a)

$$\frac{\theta}{1-\theta} = C \exp. \left(-\frac{\overline{\Delta H_{\theta}^{\dagger}}}{RT} + \frac{\overline{\Delta S_{\theta}^*}}{R} \right) \dots \dots \dots (22)$$

where C is the bulk concentration at coverage θ . (activity coefficient assumed to be unity). If $\overline{\Delta H_{\theta}^{\dagger}}$ and $\overline{\Delta S_{\theta}^*}$ are constant and independent of T and θ , equation (22) reduces to the familiar Langmuir equation.

$$\frac{\theta}{1-\theta} = K C \dots \dots \dots (23)$$

where $K = \exp. \left(\frac{-\overline{\Delta H_{\theta}^{\dagger}} + T \overline{\Delta S_{\theta}^*}}{RT} \right)$

Equation (23) can also be written as

$$\Gamma = \frac{\Gamma_0 K C}{1 + K C} \dots \dots \dots (24)$$

where Γ is surface concentration.

Γ_0 is surface concentration at saturation.

4.5.2. Law of Mass Action approach.

4.5.2.1. Adsorption.

Considering the situation in which the adsorption site A, combines with adsorbing solute C to form the adsorbed solute AC.



where K is the equilibrium constant of the reaction which can be written as

$$K = \frac{[AC]}{[A][C]} \longrightarrow K [A][C] = [AC] \dots \dots \dots (26)$$

in which the quantities in the square bracket are the concentration of the respective species, assuming that in dilute solution the activity coefficients are unity.

If the total adsorption sites is A_t , then the concentration of

$$[A] = [A_t] - [AC] \quad \dots \dots \dots (27)$$

Substituting equation (27) into (26), gives

$$K [C] ([A_t] - [AC]) = [AC]$$

$$K [C] [A_t] - K [C] [AC] = [AC]$$

By re-arranging $[AC] (1 + K [C]) = K [A_t] [C]$

therefore
$$[AC] = \frac{K [A_t] [C]}{1 + K [C]} \quad \dots \dots \dots (28)$$

Comparing equations (23), (24) and (28) it can be seen that the equilibrium constant K is identical to the thermodynamic constant

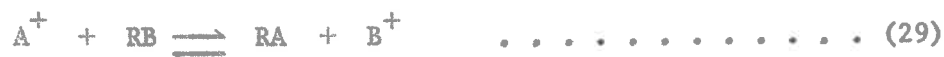
$$K = \exp. \left(- \frac{\overline{\Delta H_{\theta}^+} + \overline{\Delta S_{\theta}^*}}{RT} \right)$$

or
$$K = \exp. \left(- \frac{\Delta \mu_{\theta}^*}{RT} \right)$$

where $\Delta \mu_{\theta}^*$ is the differential molar free energy minus the localization term $RT \ln \frac{\theta}{1-\theta}$

4.5.2.2. Ion-exchange

Considering an exchange reaction involving two monovalent cations A^+ and B^+ which can be represented by equation



where R is the insoluble structurally bound anionic part of the exchanger.

At equilibrium, the Mass Law applies to the heterogeneous system : ion-exchanger and aqueous solution.

From a purely thermodynamic view point, the following equation should be applicable,

$$K = \frac{a_{B^+} \cdot a_{RA}}{a_{A^+} \cdot a_{RB}} \dots \dots \dots (30)$$

where a_{A^+} and a_{B^+} are the activities in aqueous solution of the ion A^+ B^+ respectively

a_{RA} and a_{RB} are the activity of species A and B on the solid phase.

K is the thermodynamic equilibrium constant.

The ionic activity is related to the mean activity coefficient of the electrolyte γ_{\pm} i.e. $a_{B^+} = C_{B^+} \times \gamma_{\pm}^2$ (where X is the anion in the solution).

The evaluation of the activities for the solid phase requires a special treatment. If reaction (29) is considered as a chemical reaction where RA and RB occur as independent solid phases, it would be permissible to assume their activities as constant and equal to unity. However, this is not so, since in ion exchange the ions freely substitute for one another in the exchanger. It is more appropriate (Vanselow, 1932; Boyd, Schubert and Adamson, 1947) to consider that the components of the solid phases form completely miscible solid solutions with one another. If the solid solutions are regarded as ideal, then the values

of a_{RA} and a_{RB} may be written as the mole fraction N_A and N_B . Thus equation (30) becomes

$$K_a = \frac{a_B^+ \cdot N_A}{a_A^+ \cdot N_B} \dots \dots \dots (31)$$

where K_a is the apparent equilibrium constant.

According to equation (31), $\log \frac{a_B^+}{a_A^+}$ is linear in $\log \frac{N_A}{N_B}$. This has been shown to be true by Boyd et al (1947) using system of sodium-hydrogen exchange on Amberlite IR-1.

The equilibrium quotient, K_m , for reaction (29) can be written as

$$K_m = \frac{m_B^+ \cdot N_A}{m_A^+ \cdot N_B} \dots \dots \dots (32)$$

where m is the concentration (molality) in the aqueous solution.

N_A and N_B are the mole fraction of species A and B on the solid phase.

The relation between the thermodynamic equilibrium constant K , the apparent equilibrium constant K_a and the equilibrium quotient K_m , is given by

$$K = K_a \frac{f_A}{f_B} = K_m \left(\frac{\gamma_{BX}}{\gamma_{AX}} \right)^2 \frac{f_A}{f_B} \dots \dots \dots (33)$$

where f_A and f_B are the activity coefficients of resin component A and B on a mole fraction basis, with pure resin as the standard state.

If the aqueous solution is sufficiently dilute so that the

ratio of the activity coefficient of the ions is approximately unity, equation (33) becomes

$$K = K_a \frac{f_A}{f_B} = K_m \frac{f_A}{f_B}$$

If the ratio of the activity coefficient of the solid phase is unity, then $K = K_a = K_m$.

The ion-exchange process can be expressed in a form equivalent to the Langmuir isotherm, which can be derived by using the Mass Law without assuming the kinetic mechanism of the adsorption and desorption; the derivation is as follows.

Exchange reaction given by equation (29) states



The apparent equilibrium constant K_a is given by

$$K_a = \frac{[RA][B^+]}{[RB][A^+]} \dots \dots \dots (34)$$

If the total anionic group available for adsorption is R^- , then

$$[RB] = [R^- - RA] \dots \dots \dots (35)$$

Substituting equation (35) into (34) and re-arranging, gives

$$RA = \frac{K_a R^- A^+}{B^+ + K_a A^+}$$

$$RA = \frac{K_a R^- (A^+/B^+)}{1 + K_a (A^+/B^+)} \dots \dots \dots (36)$$

If $[B^+]$ is constant equation (36) takes the form of the Langmuir isotherm, namely

$$\frac{[A^+]/[B^+]}{RA} = \frac{[A^+]/[R^+]}{R^-} + \frac{1}{K_a R^-} \dots \dots \dots (37)$$

where RA is the amount of species A^+ adsorbed per unit weight of adsorbent.

The quantity in the square bracket is the concentration of the respective species, assuming that in dilute solution the activity coefficients are unity.

Using equation (37) the values of K_a and R^- can be determined.

4.6. Effect of temperature.

The heat of adsorption can be determined by direct calorimetric measurements. This is called the integral heat of adsorption ΔE , which is the average heat of adsorption for that part of the surface occupied by adsorbate when equilibrium is established. The differential heat of adsorption, $\overline{\Delta E}$, is obtained by measuring the adsorption of small amounts of adsorbate at a time, and measuring the heat evolved calorimetrically, i.e. $\overline{\Delta E} = \Delta q / \Delta a$, where q is the heat evolved and a is the amount adsorbed. However, for some systems it is very difficult to determine the heat of adsorption by a direct calorimetric method. In this case the heat of adsorption is usually determined using an indirect method by carrying out the adsorption at several temperatures. The quantity obtained is the differential heat of adsorption $\overline{\Delta H}$. At a given surface concentration $\overline{\Delta H}$ is equal to the change in heat content, per mole transferred, when an infinitesimal

amount of material is transferred from the bulk phase to the surface, i.e. $\overline{\Delta H} = \frac{dq}{da}$. This is identical with "isosteric" heat of adsorption derived from the variation of the equilibrium concentration with temperature, when the surface concentration of the adsorbed molecule is constant according to the Clausius-Clapeyron equation.

The relation between the calorimetric differential heat of adsorption $\overline{\Delta E}$ and the isosteric heat of adsorption $\overline{\Delta H}$ (Everett, 1950; Young and Crowell, 1962) can be written as

$$\overline{\Delta E} = \overline{\Delta H} + RT \quad \dots \dots \dots (38)$$

where RT is the work done per mole of solute adsorbed.

It has been emphasized by many workers (Everett, 1950) that not only is it necessary for the experimental data to fit the equation of the proposed model but also the value of the constants derived from the equation must be reasonable. The heat and entropy of adsorption obtained from the adsorption isotherms may then be compared with the theoretical change to be expected from the proposed model, (Kemball, 1950). To do this it is usual to determine the integral heats and entropies since these are quantities most suitable for comparison with the results calculated from any proposed model using statistical mechanical methods (Kemball, 1950).

Adsorption is usually exothermic and the extent of adsorption therefore decreases with increasing temperature if the number of sites available for adsorption is independent of temperature. However, this is not always the case, since some experimental evidence has shown (Koral,

Ullman and Eirich, 1958) that the extent of adsorption increases with increasing temperature. According to equation (2)

$$\Delta G = \Delta H - T\Delta S$$

the positive effect of temperature could be explained by the fact that the driving force for adsorption is attributed to the increase of entropy. This may arise from a disordering of the solvent around both the sites and adsorbate. Alternatively, this may be due to an increase in the number of adsorption sites as the temperature is raised.

The isosteric heat of adsorption ($\overline{\Delta H}$) can be calculated using the Clausius-Clayperon equation:

$$\frac{\partial \ln c}{\partial \left(\frac{1}{T}\right)} = - \frac{\overline{\Delta H}}{R} \quad \dots \dots \dots (39)$$

A plot of $\ln c$ against $\frac{1}{T}$ for a constant amount of solute adsorbed should be a straight line, the slope of which gives the value of $\overline{\Delta H}$.

Alternatively, where the Langmuir isotherm is applicable $\overline{\Delta H}$ can be calculated using the following equation:

$$\overline{\Delta H} = 2.303 RTT' \left(\frac{\log.K' - \log.K}{T' - T} \right) \quad \dots \dots \dots (40)$$

where K' is the equilibrium constant at T'°

K is the equilibrium constant at T° for (T'° to T°)

The standard state in this instance would be half coverage of the surface.

The free energy and entropy of adsorption may be determined in the usual way from the following equations:

$$\Delta G = -RT \ln K \quad \dots \dots \dots (41a)$$

$$\Delta G = \overline{\Delta H} - T\overline{\Delta S} \quad \dots \dots \dots (41b)$$

$$\overline{\Delta S} = \frac{\overline{\Delta H} + RT \ln K}{T} \quad \dots \dots \dots (41c)$$

where K is the thermodynamic equilibrium constant.

For linear isotherms, the effect of temperature is manifested by a change in slope (distribution coefficient), between the adsorbed phase and the bulk phase. It is possible to use this change in K (i.e. slope) with temperatures to calculate the heat of adsorption from the above expressions.

4.7. Reversibility of adsorption and Hysteresis.

Thermodynamic considerations can only be applied to the interpretation of adsorption isotherms when the system is at equilibrium i.e. the adsorption process is independent of time. Desorption experiments in which the equilibrium concentration is lowered drastically, especially in solution, are not particularly good criteria of thermodynamic reversibility because this desorption is not necessarily the thermodynamic reverse process of the adsorption. Such treatment could induce a phase change or orientation of the adsorbed phase.

It is suggested that true irreversibility would be indicated by the isotherm laying on the y-axis. If the limb of the isotherm is

independent of time and it does not lie on the y-axis, then each point on the isotherm should be microscopically reversible and thermodynamic arguments can be applied to each limb.

For different solute-adsorption isotherms the following explanations for hysteresis have been advanced.

4.7.1. Phase change hypothesis

In a series of papers Everett and his co-workers (1952, 1954, 1955) have devoted considerable attention to the nature of hysteresis.

Adsorption hysteresis can be regarded as being analogous to the delayed phase change in physical chemistry. This is shown for instance in the phase diagram for the conversion of rhombic into monoclinic sulphur which occurs at a very slow rate, so that the transition temperature shows hysteresis.

Hysteresis in adsorption can be ascribed to a kind of saturation effect, in which the rearrangement and reorientation of the adsorbed molecules is delayed as in the phase change just discussed.

Everett and his co-workers have further refined and developed this concept to give a general theory of hysteresis based on thermodynamic concepts and molecular domains. They consider that for a system to exhibit hysteresis, it must consist of a large number of more or less independent domains and each domain must be able to exist in at least two physical states or microphases. Conversion of state I to state II must take place irreversibly with an increase in entropy.

4.7.2. Swelling of the adsorbent.

Swelling may be regarded as a special case of hysteresis.

This phenomenon may bring about a distortion of the adsorbent in such a way as to cause an increase in accessible area for adsorption (Hirst, 1948). The increase in surface area may be regarded as a delayed phase change of the solid surface, where the adsorption occurs.

I.5. SOLUBILITY PRODUCT PRINCIPLE

The condition for two phases to be in equilibrium is that the chemical potential, μ , of each component, should be the same in both phases, i.e.

$$\mu_1' = \mu_1'' \quad \dots \dots \dots (42)$$

where μ_1' is the chemical potential of substance i in one phase.

μ_1'' is the chemical potential of substance i in other phase.

Considering the situation in which a pure solid phase of substance A is in equilibrium with its saturated solution ,

$$\text{therefore } \mu_{O,A}' = \mu_A'' \quad \dots \dots \dots (43)$$

$$\mu_A'' = \mu_{O,A}'' + RT \ln a_A \quad \dots \dots \dots (44)$$

where $\mu_{O,A}'$ is the standard chemical potential of pure solid phase A.

μ_A'' is the chemical potential of saturated solution A.

$\mu_{O,A}''$ is the standard chemical potential of saturated solution A.

a_A is the activity of dissolved A.

Substituting equation (44) into (43), gives

$$\mu'_{O,A} = \mu''_{O,A} + RT \ln a_A \quad \dots \dots \dots (45)$$

$$\text{therefore } a_A = \exp. \left(\frac{\mu'_{O,A} - \mu''_{O,A}}{RT} \right) = \text{constant} \quad \dots \dots \dots (46)$$

$$= K_{sp}$$

Since $(\mu'_{O,A} - \mu''_{O,A})$ is constant at given value of T and P, K_{sp} is the ionic activity product or the solubility product constant.

The solubility product principle is only applicable to a system if the dissolved substance which is in equilibrium with the solid phase has a constant activity. Adsorption equilibria express the fact that a series of solution activities can exist in equilibrium with the solid phase. Both of these situations are governed by the same basic equilibrium relationship, namely



$$K = \frac{[C]}{[A][B]} \quad \dots \dots \dots (48)$$

where A is the reactant in solution phase.

B is the reactant in solid phase.

C is the product.

K is the thermodynamic equilibrium constant.

The quantity in the square bracket is the concentration of the respective species, assuming that for dilute solutions the activity coefficients are unity.

For dissolution and precipitation reactions, the system requires that C be a discrete crystalline phase which is in equilibrium with its solution of constant activity. Therefore, equation (48) becomes

$$[A][B] = \frac{C}{K} = \text{constant} \quad \dots \dots \dots (48a)$$

For adsorption equilibrium, C is not a discrete solid phase, but can be regarded as a two-dimensional solution. Thus the activity of the adsorbed phase and the bulk phase is not constant; the equilibrium equation (48) then becomes

$$K_{\text{adsorption}} = \frac{[\text{Adsorbed phase}]}{[A][B]} \quad \dots \dots \dots (48b)$$

CHAPTER II.GENERAL EXPERIMENTAL METHODSII.1. INTRODUCTION

Earlier workers have recognised that factors such as pH, concentration and temperature are very important in determining the adsorption of phosphate by clay minerals. However, no satisfactory attempt has yet been made to separate these variables in order to understand the adsorption process.

Most studies of the adsorption of phosphate have been carried out either at uncontrolled pH values or in the presence of buffers (Low and Black, 1950; Hsu and Rennie, 1962). This is not altogether satisfactory because the buffer ions are likely to compete with the phosphate ion for the reactive sites, complicating the interpretation of the results.

Adsorption is the predominant phenomenon at low to medium concentration of phosphate (Low and Black, 1950; Johansen and Buchanan, 1957; Hsu and Rennie, 1962). Whereas at high concentration (> 1 M phosphate solution), dissolution and precipitation reactions with the formation of new crystalline phase are important (Kittrick and Jackson, 1954, 1955a, 1956). It is very difficult to determine at which concentration the change from adsorption to dissolution-precipitation reactions occurs. The criteria which have been used by many workers to determine the dissolution and precipitation processes are the solubility product principle, electron microscopic examination

for new crystalline forms, and X-ray diffraction analysis of the reaction products.

Adsorption is usually exothermic and hence the extent of adsorption decreases with increasing temperature, if the number of sites on which adsorption can occur remains constant. However, Low and Black (1950) have shown that the amount of phosphate adsorbed by kaolinite increases as the temperature is raised, suggesting that in solid-solution systems the situation is more complex as a result of solvent-adsorbent interaction.

These considerations have determined the approach in the present work. To differentiate the nature of the reactive sites, adsorption isotherms at constant pH have been determined on the following systems, which for convenience are discussed under the following three categories:

- A.1. Kaolinites and hydrated aluminium oxides at various pH values and at temperature of 20°C. This series of experiments has been carried out on four adsorbents: (1) K-kaolinite API-9 (2) K-kaolinite R.G. (3) Gibbsite and (4) Pseudoboehmite.
2. Acid (pH 1) treated kaolinite API-9 and gibbsite, at pH 5 and 20°C.
3. Some desorption experiments were carried out with respect to pH and concentration.
4. Determination of potassium adsorption by kaolinite and hydrated aluminium oxides.

- B. Aluminium-kaolinite API-9, unwashed K-kaolinite and K-kaolinite in the presence of 0.1 N KCl, Sodium-kaolinite API-9 and potassium-halloysite at pH 5 and 20°C.
- C.1. Kaolinite and hydrated aluminium oxides, at pH 5 and at temperatures of 2°, 20° and 40°C.
- This series of experiments has been carried out on three adsorbents:
- (1) K-kaolinite API-9, (2) Gibbsite and (3) Pseudoboehmite.
2. Some reversibility experiments were carried out with respect to temperature.

More experimental details of the treatments are given in Table 2.

II.2. THE CLAY MINERALS

2.1. Kaolinite API-9

The kaolinite was obtained from Ward's Natural Science Establishment Incorporated, U.S.A. It originated from Canada del Camino, Mesa Alta, New Mexico, U.S.A., and was a sample of the standard clay mineral number 9 of the American Petroleum Institute, project number 49.

The unground clay, as received, was in a large aggregate as in its natural state. The aggregate was broken down into smaller size, and was immersed in distilled water for 12 hours at 2°C. The clay material was wet ground very mildly using an agate mortar at 2°C for 5 minutes. This procedure was adopted to eliminate the heat evolved due to interface friction of the clay particle. The slurry suspension was dispersed by adding KOH solution to increase the pH value to 8.5. The dispersed clay suspension was passed through a 300 mesh (53 micron) sieve and was finally diluted to obtain a 2% suspension. The pH of the clay suspension was re-adjusted to 8.5.

2.2. Kaolinite R.G. (Rocky Gully kaolinite).

Kaolinite R.G. was obtained from the pallid zone of a laterite, Rocky Gully, Western Australia. The original soil sample contained about 50 per cent sand. The sample was suspended in distilled water and dispersed at pH 8.5. The suspension was passed through a 70 mesh (228 micron) sieve to remove the sand. The clay suspension was then diluted to about 2% concentration and the pH of the clay suspension was re-adjusted to 8.5.

The fraction less than 2 microns equivalent spherical diameter of both kaolinites was separated by dispersion in distilled water at pH 8.5, followed by repeated sedimentation and decantation after an appropriate time.

An X-ray powder photograph of the kaolinite API-9 ($< 2\mu$) obtained from the suspension showed that the kaolinite API-9 was homogeneous, no extraneous lines being observed. X-ray diffraction (Brindley, 1961) and Infra-red absorption spectra (Fripiat, 1960b) confirmed the homogeneity of the clay, being free from gibbsite (aluminium oxides) and iron oxides. The X-ray diffractometer trace and I-R absorption spectrograph trace for kaolinite API-9 are given in Figure 5. Iron determination of the acid (HCl) digest of kaolinite API-9 showed that the iron content was not detectable.

X-ray diffraction analysis on kaolinite R.G. ($< 2\mu$) showed that the kaolinite was homogeneous (Brindley, 1961), except that a small quantity of gibbsite was detected as a distinct peak on the tracing. However, the iron oxide peak did not show clearly because

Figure 5.

X-ray diffractometer trace.

(Kaolinite API-9 and Kaolinite R.G.)

The unlabelled peaks are the general diffraction lines of kaolinite (Brindley, 1961).

I-R absorption spectrograph trace

stretching region.

X-RAY DIFFRACTOMETER TRACE

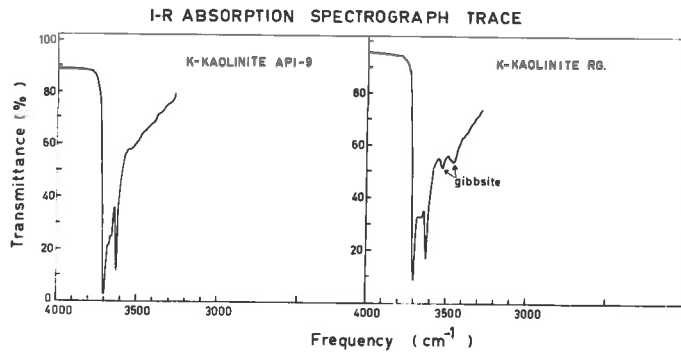
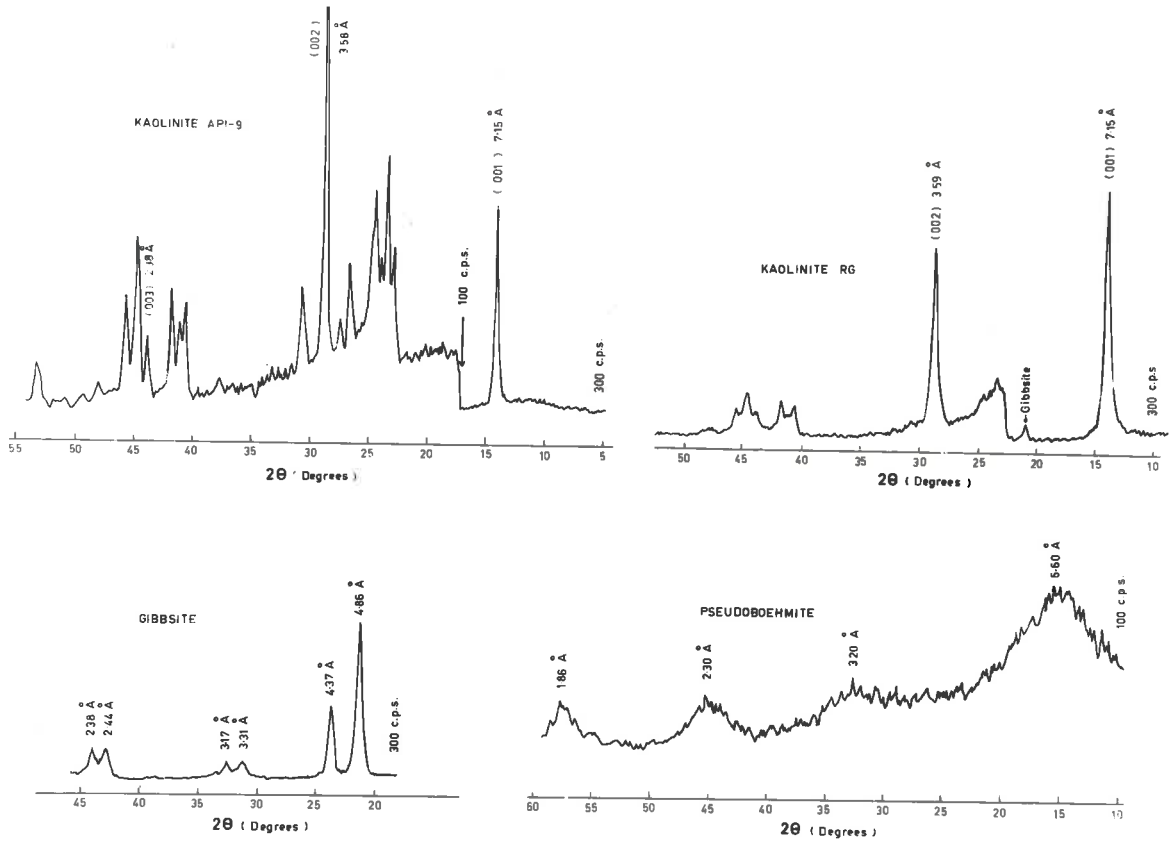


FIGURE 5

the position of its strong reflection coincided with the general kaolinite lines (Figure 5).

Infra-red absorption spectra confirmed the homogeneity of the clay, and the presence of gibbsite (Frederickson, 1954; Fripiat, 1960b), whereas the absorption spectra of iron oxide were not recorded. The X-ray diffractometer trace and I-R absorption spectrograph trace for kaolinite R.G. are given in Figure 5. The analysis of the original sample showed that the iron content was 0.70%.

Chemical analysis of the clay sample showed that the initial phosphorus content was extremely low (25 ppm = 0.08 meq.% for kaolinite API-9, and 50 ppm = 0.16 meq.% for kaolinite R.G.)

II.3. PREPARATION OF HOMOIONIC CLAY

It is very difficult to obtain clean surface for studying adsorption phenomena. The problem is particularly troublesome for clay minerals because of the instability of the clean clay surface (Martin, 1960), and the difficulty of removing the various forms of aluminium likely to be present as contaminants.

Nevertheless an attempt was made to prepare a reproducible surface by the procedure described below.

3.1. Potassium-kaolinite

To avoid interference from reactive cations, such as Al^{3+} , it was necessary to treat the clay with a normal potassium chloride solution at pH 3, using a method similar to that used by Posner and Quirk (1964). The $10^{-3}N$ HCl was used to assist in releasing aluminium

compounds from the surface of kaolinite, by converting these to the ionic form, which can then be easily replaced by K^+ . The normal salt solution was also used to decrease the risk of decomposition of the clay by preventing the H^+ concentration rising to too high a value near the crystal surface, i.e. it reduced the potential gradient across the surface regions.

The method involved the following steps:-

- a. equilibration of the clay with a normal potassium chloride solution at pH 3. This was repeated fourteen times until the pH value of the supernatant approached 3 and the amount of aluminium ion released reached approximately a constant value (see Appendix 1). Several equilibrations were continued overnight.
- b. re-equilibration four times with neutral potassium chloride solution (1.0 N).
- c. washing the excess salt away with distilled water until the supernatant approached the resistance of the distilled water.

Full details of the method are given in Appendix 1.

3.2. Acid washed kaolinite API-9 at pH 1 (0.1 N HCl).

The method employed was similar to that used by Deshpande, Greenland and Quirk (private communication). It consisted of the following steps:-

- a. Potassium-kaolinite API-9 was washed with 0.1 N HCl followed by centrifugation. This procedure was repeated seven times, the first washing was equilibrated overnight, the others usually about 30 minutes.
- b. the clay suspension was then equilibrated with 1.0 N KCl at pH 3 overnight.
- c. the clay suspension was then shaken with 1.0 N KCl and then centrifuged. This saturation procedure was repeated seven times, one of the later treatments was equilibrated overnight while the others were only for about 30 minutes.
- d. the excess salt was removed with distilled water until the salt concentration dropped to about 0.1 N KCl. The prepared clay was kept in suspension for a few days before use.

Aluminium and silicon in the acid washing was determined and the results are given in Appendix 2.

The electric charge on the untreated and acid treated K-kaolinite was measured using the method of Schofield (1949) (Appendix 3).

3.3. Acid washed gibbsite at pH 1 (0.1 N HCl).

The gibbsite was washed once with 0.1 N HCl and then centrifuged. This equilibration was carried out overnight. The acid treated gibbsite was then washed with distilled water followed by centrifugation, until the supernatant approached the resistance of distilled water. The gibbsite was dried at 60°C overnight and was ground very lightly. Aluminium was not determined in the acid washing.

3.4. Aluminium-kaolinite API-9.

Aluminium-kaolinite was prepared by a method similar to that used by Lin and Coleman (1960). The K-clay ($< 2\mu$) was shaken in 0.1 N AlCl_3 (pH 4) and the clay was separated by centrifugation. This treatment was repeated eight times, one of the later ones being continued overnight, the others usually lasting for about 30 minutes. The excess salt was removed by washing with distilled water followed by centrifugation, until the supernatant approached the resistance of distilled water. In the final stages of washing there was a definite dispersion of the Al-clay suspension*. The clay suspension was finally dried at 60°C for 48 hours, and the dried clay then ground very lightly to pass through a 0.25 mm sieve. Infra-red analysis of the Al-clay was carried out and showed no detectable difference between Al-clay and K-clay.

3.5. Sodium-kaolinite API-9

The sodium-clay was prepared using two methods.

- (i) Potassium-kaolinite (API-9) was converted into sodium form by washing with 1.0 N NaCl at pH 3, followed by four washes with 1.0 N NaCl. One of the later treatments being continued overnight, the others were equilibrated for about 30 minutes. The excess salt was removed by washing with distilled water followed by repeated centrifugation, until the supernatant approached the resistance of the distilled water.

* It is of interest to note that Samson (1953) has observed that Al-kaolinite requires more NaOH solution to get a complete dispersion. However, this may be due to the fact that some of the NaOH is consumed by Al hydroxide on the clay surface.

The clay suspension was dried at 60°C for 48 hours. The dried clay was then ground very lightly to pass through a 0.25 mm sieve.

- (ii) The second method of preparation was exactly the same as the first one except that washing with 1.0 N NaCl at pH 3 was omitted.

No dispersion was observed during the washing of the sodium-clays with distilled water.

3.6. Potassium-halloysite.

The halloysite from Nairne in the South East of South Australia, was always kept in distilled water to prevent dehydration. It was wet ground very lightly for 5 minutes in 2°C cold room and fractionated by a method similar to that used for kaolinite API-9.

Potassium-halloysite ($< 2\mu$) was prepared by treatment with 1.0 N KCl at pH 3 and re-saturation with 1.0 N KCl in exactly the same way that potassium-kaolinite was prepared.

The prepared potassium-halloysite was kept in suspension for a few days before use.

II.4. PREPARATION OF HYDRATED ALUMINIUM OXIDES.

4.1. Gibbsite.

The gibbsite was prepared by the modified methods of Weiser (1935) and Gastuche and Herbillon (1962). To one litre solution of 1 molar aluminium chloride (A.R.) 4 N sodium hydroxide solution was

gradually added at a constant temperature of 20°C, with continuous stirring, until the pH reached 8.4. The gelatinous precipitate was transferred to four one litre centrifuge bottles, to remove the excess salt with distilled water by centrifugation. This procedure was repeated five times. The suspension was then transferred to a "visking" cellulose casing, which had been refluxed for three hours to remove impurities, and dialyzed against double distilled water for 25 days at 20°C in a constant temperature room.

The purpose of the aging was to induce the gradual transformation from γ - $\text{Al}_2\text{O}_3 \cdot \text{H}_2\text{O}$ (pseudoboehmite) through metastable α - $\text{Al}_2\text{O}_3 \cdot 3\text{H}_2\text{O}$ (bayerite) to stable γ - $\text{Al}_2\text{O}_3 \cdot 3\text{H}_2\text{O}$ (gibbsite). This process was more rapid in water containing alkali (Weiser, 1935).

It was found from the preliminary preparation that the electrolyte content of the suspension was a very important factor in the aging process. If the electrolyte concentration was reduced very rapidly in the first 7 days, by changing the dialysis water daily, X-ray diffraction techniques revealed a mixture of gibbsite and a small amount of bayerite, even when the aging was continued for 60 days.

Therefore, the dialysis water was changed only five times during 25 days aging (4th, 8th, 15th, 24th and 25th day). During the aging process a small sample was taken for X-ray analysis. It was found that at the end of the 7th day, the sample was pure gibbsite, although the peak of the diffraction lines was not very sharp. With increasing time the diffraction lines became sharper indicating that the gibbsite

sample was well crystallized. At the end of the period the suspension was dried in an oven at 105°C for 24 hours, and was ground very lightly and passed through a 70 mesh sieve. An X-ray diffraction analysis of the samples showed that the material was pure gibbsite (Figure 5).

4.2. Pseudoboehmite (γ -Al₂O₃·H₂O).

The aluminium hydroxide was precipitated in exactly the same way as for gibbsite, except that instead of dialysing, the precipitate was repeatedly washed (seven times) with distilled water by centrifugation until the supernatant was free from chloride. The gelatinous precipitate was then dried in the oven at 105°C for 24 hours, and was ground very lightly and passed through a 70 mesh sieve. The X-ray diffraction pattern of the sample showed very diffuse bands. The spacings of the broad reflections corresponded approximately with the spacings of the principal lines of the pattern of crystalline boehmite, but the first reflection indicated some displacement to a value 6.6 Å compared with 6.11 Å for the (020) line of boehmite (Figure 5). Pseudoboehmite was therefore a semi-crystalline material, having a less rigid structure than boehmite.

The cation exchange capacity and the surface area as measured using low temperature N₂ adsorption for the various adsorbents used are given in Table 1.

TABLE 1CATION EXCHANGE CAPACITY AND SURFACE AREA OF THE
ADSORBENTS USED

Adsorbent	C.E.C. (meq.%)	Total Surface Area m ² /g
K-kaolinite API-9	2.2	12
K-kaolinite RG	3.9	40
Gibbsite	0	48
Pseudoboehmite	0	176

Figure 6a

Shadowed electron micrograph K-kaolinite API-9

Magnification : 20,000 x

Scale : 1 μ 

Direction of shadowing



Angle of shadowing i.e. cotangent = 5

Shadowed using Platinum (Pt.)

(Siemens Elmiskop 1)

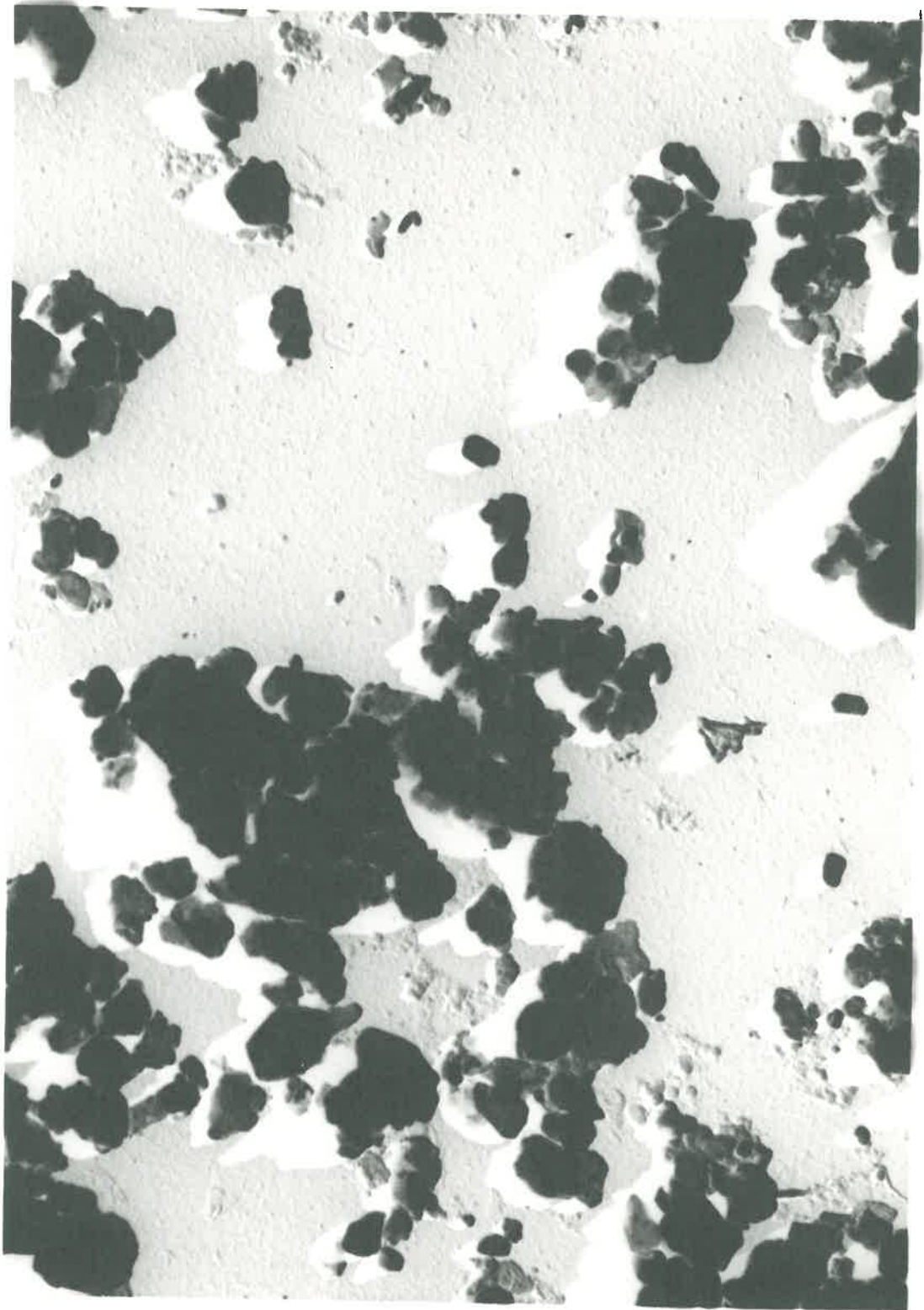


Figure 6b

Shadowed electron micrograph K-kaolinite R.G.

Magnification : 20,000 x

Scale : 1 μ 

Direction of shadowing 

Angle of shadowing i.e. cotangent = 5

Shadowed using Platinum (Pt.)

(Siemens Elmiskop 1)

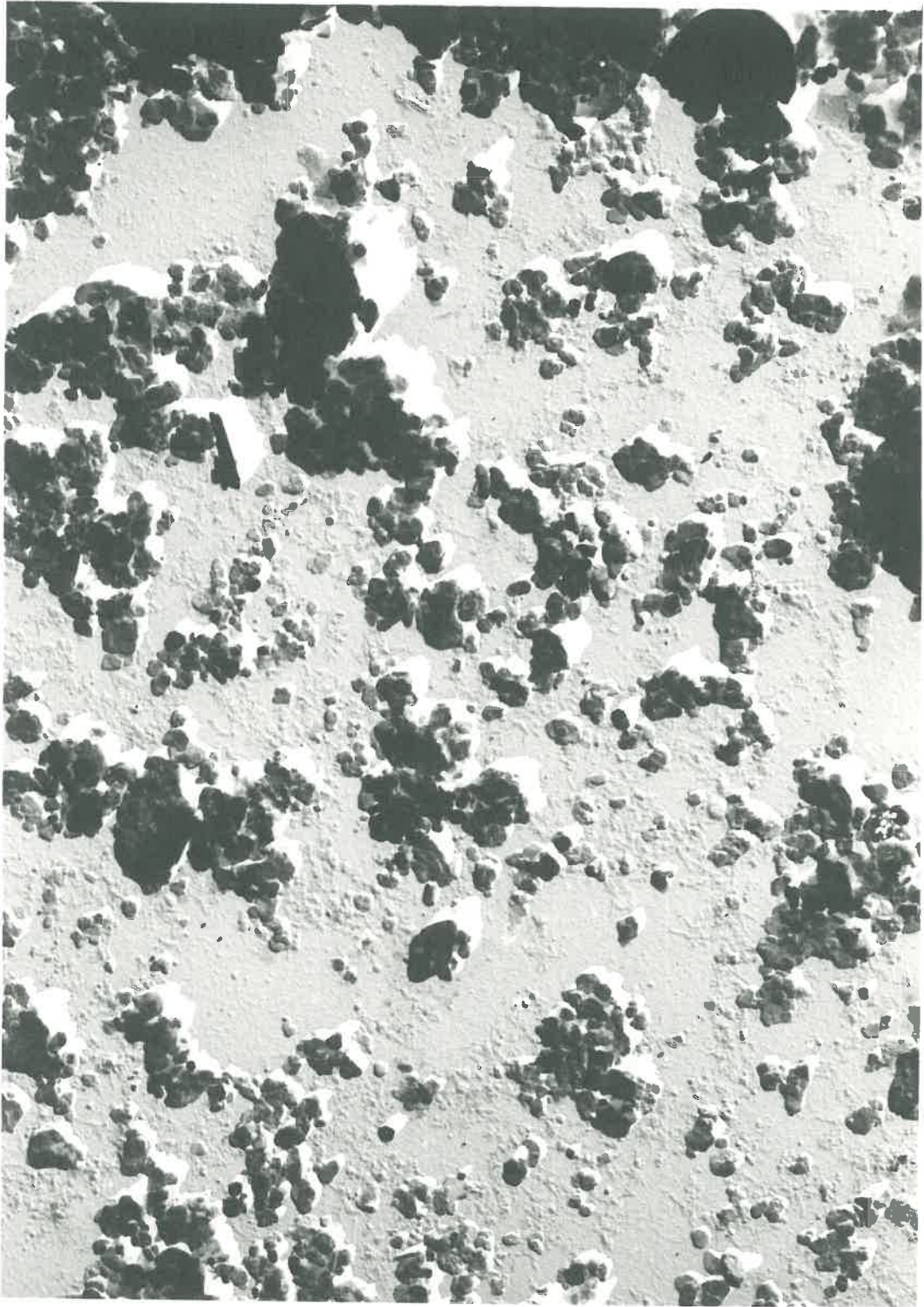


Figure 6c

Shadowed electron micrograph

Synthetic Gibbsite

Magnification : 40,000 x

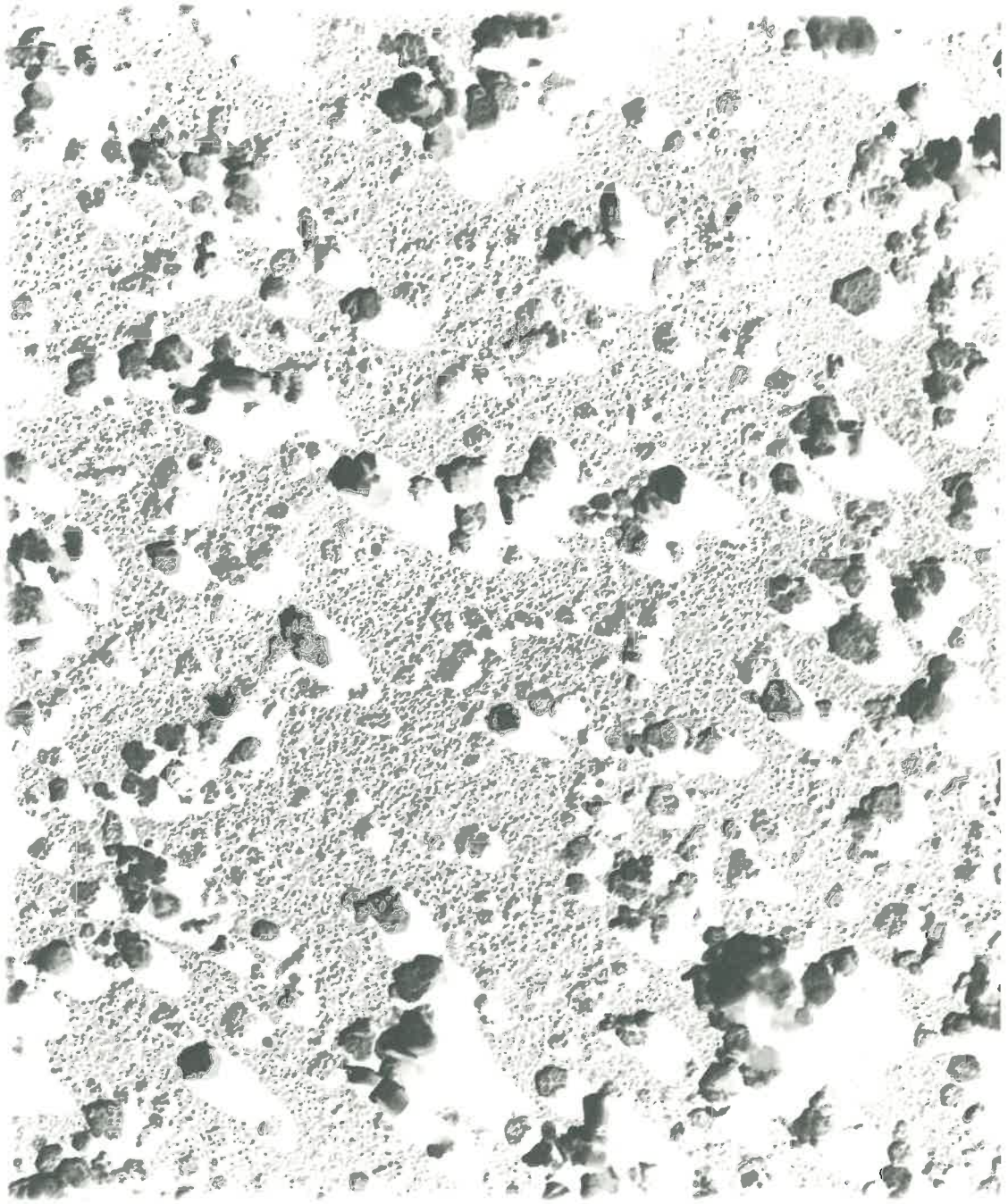
Scale : 1 μ 

Direction of shadowing 

Angle of shadowing i.e. cotangent = 4

Shadowed using Platinum (Pt.)

(Phillips EM 75)



The shadowed electron micrograph of K-kaolinite API-9, K-kaolinite R.G. and synthetic gibbsite are given in Figures 6a, 6b and 6c respectively.

II.5. PREPARATION OF PHOSPHATE SOLUTIONS

- The reagents used were
1. KH_2PO_4 (A.R.)
 2. K_2HPO_4 (A.R.)
 3. NaH_2PO_4 (A.R.)
 4. NaOH (A.R.)
 5. KOH (A.R.)
 6. 80% H_3PO_4

Bulk phosphate solutions of the required strength (ranging from 1×10^{-5} to 10^{-1} M) was prepared using doubly distilled water. The pH of potassium phosphate solution was adjusted to the desired value by adding H_3PO_4 or KOH solution (or using NaOH in the case of sodium system). The solution was then stored in a half gallon polythene bottle at least overnight to obtain equilibrium. The pH of the solution was checked, and if necessary was re-adjusted to the desired value, before use. All pH determinations were carried out using a "Cambridge Bench type pH meter", fitted with glass and calomel electrodes. Two reference standard solutions were used (phthalate buffer pH 4.0 and sodium borate buffer pH 9.27).

One litre of each prepared solution was transferred from a litre volumetric flask to a litre screwtop polythene centrifuge bottle. These bottles were then kept at the required temperature, i.e. 2^o, 20^o or 40^oC, overnight to reach equilibrium, before the adsorbent was added.

II.6. ADSORPTION EXPERIMENTS

By the use of a large volume of phosphate solution and a small amount of adsorbent, it was possible to achieve a virtually constant pH value without using buffers. This technique was based on the fact that

- a. the phosphate solution itself can act as a buffer over certain concentration ranges, although it would have a lower buffering capacity in dilute solution.
- b. if the liquid/solid ratio is sufficiently high, the pH of the solution and phosphate concentration will be practically unchanged since the amount of phosphate, H⁺ and OH⁻ ions taken up by the adsorbent is very small.

Consequently, the amount of phosphate adsorbed was determined by analyzing the solid material.

The liquid/solid ratio used was 5,000 for clay minerals and 10,000 for hydrated aluminium oxides. Approximately 0.200 g kaolinite (or 0.100 g hydrated aluminium oxide) was weighed and transferred into a litre screwtop polythene centrifuge bottle containing a litre of prepared phosphate solution.

The suspension was equilibrated on an end-over-end mechanical shaker at constant temperature. Three temperatures were used, 2°, 20° and 40° C. For the 2° C and 20°C isotherms, the experiments were carried out in a 2°C and a 20°C constant temperature room. The 40°C isotherm was obtained by equilibration on a mechanical shaker placed in a large thermostatically controlled oven (Colwell, private communication).

Preliminary kinetic experiments (Appendix 4) indicated that the standard equilibration time for kaolinite was 24 hours for 2°, 20° and 40° C isotherms, while for the hydrated aluminium oxides at 20° and 40°C, the equilibration time was 48 hours. The results in Appendix 4 have shown that the extent of adsorption increases as the temperature is raised.

Hunter and Alexander (1963) have suggested that the increase in phosphate adsorption with temperature reported by Low and Black (1950) is an experimental artefact due to lack of equilibrium. However, this criticism cannot be applied to the present results, since the systems have reached an equilibrium condition (Appendix 4).

After the equilibration period the suspension was centrifuged at 1800 r.p.m. for 30 minutes, using a centrifuge MSE Major controlled at the appropriate temperature. For kaolinite systems at high pH values ($>$ pH 5), the suspension was centrifuged for 1¹/₂ hours, since the clay suspension was deflocculated. The centrifuge was fitted with heating elements and thermostatic control (Honeywell), so that any

desired temperature from 20° to 60°C could be obtained. The centrifuge was placed in the cold room at 2°C to enable the desired control to be achieved. Temperature control was $\pm 0.5^\circ\text{C}$ for 2° and 20°C and $\pm 1^\circ\text{C}$ for 40°C.

A sample of clear supernatant of about 200 ml was pipetted for pH and equilibrium phosphate concentration determinations. The remainder of the supernatant was removed very carefully using a water pump. About 5 to 10 ml of supernatant was left with the solid material, which was then resuspended by adding small quantities of the equilibrium solution so that the solid material could be transferred by pipetting into a weighed polypropylene centrifuge tube of 40 ml capacity.

To obtain the solid material for analysis the suspension was centrifuged for half an hour at 4000 r.p.m. at the required temperature. The clear supernatant was then decanted as completely as possible.

A preliminary experiment was carried out to determine the phosphate concentration in both supernatant of first and second centrifugations, and it was found that no detectable difference was observed. Therefore, the equilibrium concentration was determined from the supernatant of the first centrifugation. The tube with the moist solid was weighed before drying at 70°C for 40 hours. The tube with the dry solid was again weighed, therefore the weight of the dry solid and the entrained liquid could be calculated.

The adsorbent was then transferred quantitatively into a 150 ml

pyrex conical flask using 25 ml of 5.5 N HCl and 10 ml of distilled water. This was digested for 4 hours. The rate of evaporation of water during the digestion was controlled using an inverted pyrex glass bulb which was used as a lid.

The warm digest of the clay was filtered and then washed with 50 ml of hot 2% HCl on a Buchner funnel fitted with a Whatman filter paper No. 50. For the aluminium oxide systems the solid material was completely dissolved, hence no filtration procedure was necessary. The filtrate was made up to 100 ml in a volumetric flask.

In some of the systems, duplicate runs were carried out in order to test the reproducibility of the results. It was found (Appendix 9) the results were reproducible to within 1.5%. In the subsequent experiments, some of the isotherms were based only on single determination of 12 to 20 points depending on the precision required.

II.7. QUANTITATIVE ANALYSIS

All quantitative volumetric apparatus was of A grade quality.

7.1. Phosphate determination.

The phosphate in the acid digest and equilibrium solution was determined using the heteropoly blue method of Boltz and Mellon (1947).

For the acid digest after pipetting into 100 ml volumetric flask for analysis, the sample was titrated using KOH solution to neutrality using paranitrophenol as an indicator. The detailed procedure is given in Appendix 5.

TABLE 2

DETAILS OF THE ADSORPTION EXPERIMENTS

Adsorbent	System	Temperature	Equilibrium pH	Determination	
				K ⁺	Al ³⁺
I. K-kaolinite API-9	pH 3 isotherm	20° ± 0.5°C	3 ± 0.05	-	Yes
"	pH 4 "	"	4 ± 0.05	-	-
"	pH 5 "	"	5 ± 0.02	Yes	Yes
"	pH 7 "	"	7 ± 0.02	-	-
"	pH 9 "	"	9 ± 0.06	Yes	-
"	pH 10 "	"	10 ± 0.10	-	-
K-kaolinite R.G.	pH 3 isotherm	20° ± 0.5°C	3 ± 0.05	-	-
"	pH 5 "	"	5 ± 0.03	-	-
"	pH 8 "	"	8 ± 0.04	-	-
"	pH 9 "	"	9 ± 0.06	-	-
"	pH 10 "	"	10 ± 0.10	-	-
Gibbsite	pH 3 isotherm	20° ± 0.05°C	3 ± 0.06	-	-
"	pH 5 "	"	5 ± 0.03	Yes	Yes
"	pH 9 "	"	9 ± 0.08	-	-
"	pH 10 "	"	10 ± 0.12	-	-
Pseudoboehmite	pH 3 isotherm	20° ± 0.5°C	3 ± 0.09	-	Yes
"	pH 5 "	"	5 ± 0.03	Yes	-
"	pH 9 "	"	9 ± 0.09	-	-
"	pH 10 "	"	10 ± 0.12	-	-
Acid treated K- Kaolinite API-9	pH 5 isotherm	20° ± 0.5°C	5 ± 0.02	-	-
K-kaolinite API-9	Reversibility from pH 5 to pH 9	20° ± 0.5°C	9 ± 0.05	-	-
K-kaolinite API-9	Desorption at pH 5	20° ± 0.5°C	5 ± 0.02	-	Yes

Table 2 (cont.)

	Adsorbent	System	Temperature	Equilibrium pH	Determination	
					K ⁺	Al ³⁺
II.	Al-kaolinite API-9	pH 5 isotherm	20° ± 0.5°C	5 ± 0.02	-	-
	Unwashed K- kaolinite API-9	pH 5 isotherm in 0.1 N KCl	20° ± 0.5°C	5 ± 0.02	-	-
	K-kaolinite API-9	pH 5 isotherm in 0.1 N KCl	20° ± 0.5°C	5 ± 0.02	-	-
	Na-kaolinite API-9	pH 5 isotherm	20° ± 0.5°C	5 ± 0.02	-	-
	K-halloysite	pH 5 isotherm	20° ± 0.5°C	5 ± 0.02	-	-
III.	K-kaolinite API-9	pH 5 isotherm	20° ± 0.5°C	5 ± 0.02	-	-
	"	"	20° ± 0.5°C	5 ± 0.02	-	-
	"	"	40° ± 1.0°C	5 ± 0.02	-	-
	K-kaolinite API-9	pH 5 isotherm reversibility with respect to temp.	40° to 2°C	5 ± 0.02	-	-
	K-kaolinite API-9	pH 5 isotherm reversibility	20° to 2°C	5 ± 0.02	-	-
	Gibbsite	pH 5 isotherm	20° ± 0.5°C	5 ± 0.03	-	-
	"	"	40° ± 1.0°C	5 ± 0.03	-	-
	Gibbsite	pH 5 isotherm reversibility	40° to 20°	5 ± 0.03	-	-
	Pseudoboehmite	pH 5 isotherm	20° ± 0.5°C	5 ± 0.03	-	-
	"	pH 5 "	40° ± 1.0°C	5 ± 0.03	-	-
	Pseudoboehmite	pH 5 isotherm reversibility	40° to 20°	5 ± 0.03	-	-

7.2. Potassium determination.

Potassium in the HCl digest and in the equilibrium solution was determined using "EEL" flame photometer. In the determination of K^+ in the HCl digests, a blank correction was made by adding equal strength of HCl to the standard potassium solution.

7.3. Silicon determination.

Silicon in the solution was analysed using the method of Mullin and Riley (1955). For details see Appendix 6.

7.4. Aluminium determination.

Aluminium in solution was determined using Alizarin red-S method (a modified method as suggested by Bond (1957)). For details see Appendix 7.

7.5. Iron determination.

Iron in solution was determined using O-phenanthroline method (a modified method as suggested by Bond (1957)).

7.6. Chloride determination.

Chloride in solution was determined using potentiometric titration techniques. This method was a modification of the technique proposed by Best (1929) and combined with the method of Kolthoff and Kuroda (1951). The detailed procedure is given in Appendix 8.

7.7. Electric charges determination.

Electric charges on the clays or oxides were determined using the method of Schofield (1949). (Appendix 3).

7.8. X-ray diffraction.

Iron-filtered Co radiation obtained from a Phillip PW 1010 X-ray generator was used with a model PW 1005 diffractometer. The diffraction patterns were obtained from powder specimens.

7.9. Infra-red absorption analysis.

A Perkin-Elmer model 237, double beam grating spectrophotometer was used to determine the spectra of kaolinite. The infra-red absorption spectra were obtained from a sample dispersed in a KCl disc.

CHAPTER IIIEXPERIMENTAL RESULTS AND DISCUSSIONIII.1. EFFECT OF pH ON THE ADSORPTION OF PHOSPHATE BY K-KAOLINITES
AND HYDRATED ALUMINIUM OXIDES.1.1. Results.

The amount of phosphate adsorbed, expressed as milli-equivalent of phosphorus per 100 g. of oven dry clay (meq.%) is plotted against the equilibrium concentration of the bulk solution (microgram phosphorus per ml., $\mu\text{gP/ml.}$), to give the adsorption isotherm. A typical example of the calculation of the results is given in Appendix 9.

1.1.1. The nature of isotherm.

In Part I.4.3. four types of isotherms found for solid-solution systems have been discussed in detail. The shape of an isotherm is determined by such factors as the relative affinity of the solute and solvent for the solid surface, the number of sites available for adsorption, and the interaction between the adsorbed molecules. However, for any given system it is possible to have one or more of the types occurring singly, consecutively or concomitantly depending on the distribution of energies amongst the adsorption sites.

Several workers (Low and Black, 1950; Olsen and Watanabe, 1957; De, 1961a; Hsu and Rennie, 1962) have attempted to represent phosphate adsorption by kaolinite or aluminium oxides or soil either by a Langmuir or Freundlich isotherm. It seems that a single isotherm

type cannot describe the whole curve. In most instances the concentration range covered is not as great as the range covered in the present work.

The adsorption isotherm shown in Figures 7, 8, 9, 10 and 11 can be divided by inspection into three distinct regions, designated as regions I, II and III, and it is suggested that these are related to the affinity of phosphate for three energetically different types of reactive sites. Depending on the experimental conditions the three regions can be shown to behave independently of one another. The regions may be described as follows:-

Region I. At low phosphate concentration ($< 1 \times 10^{-4}$ M) the adsorption isotherm rises steeply and remain close to the y-axis. This region represents sites with very high affinity for phosphate.

Region II. The second region commences approximately at 10^{-4} M when the isotherm becomes convex to the y-axis.

Region III. The third part of the isotherm is linear and occurs at medium to high concentrations (10^{-3} to 10^{-1} M).

Experiments were carried out to examine the reversibility of the isotherm with respect to pH value and phosphate concentration. From Figure 12 it may be seen that in all three regions the adsorbed phosphate is reversible with respect to pH value for K-kaolinite API-9 at 20° C. This experiment was carried out by changing the solution pH of the system equilibrated at pH 5 to pH 9 by adding KOH dropwise until the pH reached the desired value. The system was then re-equilibrated.

The reversibility with respect to phosphate concentration was

EFFECT OF pH ON ADSORPTION

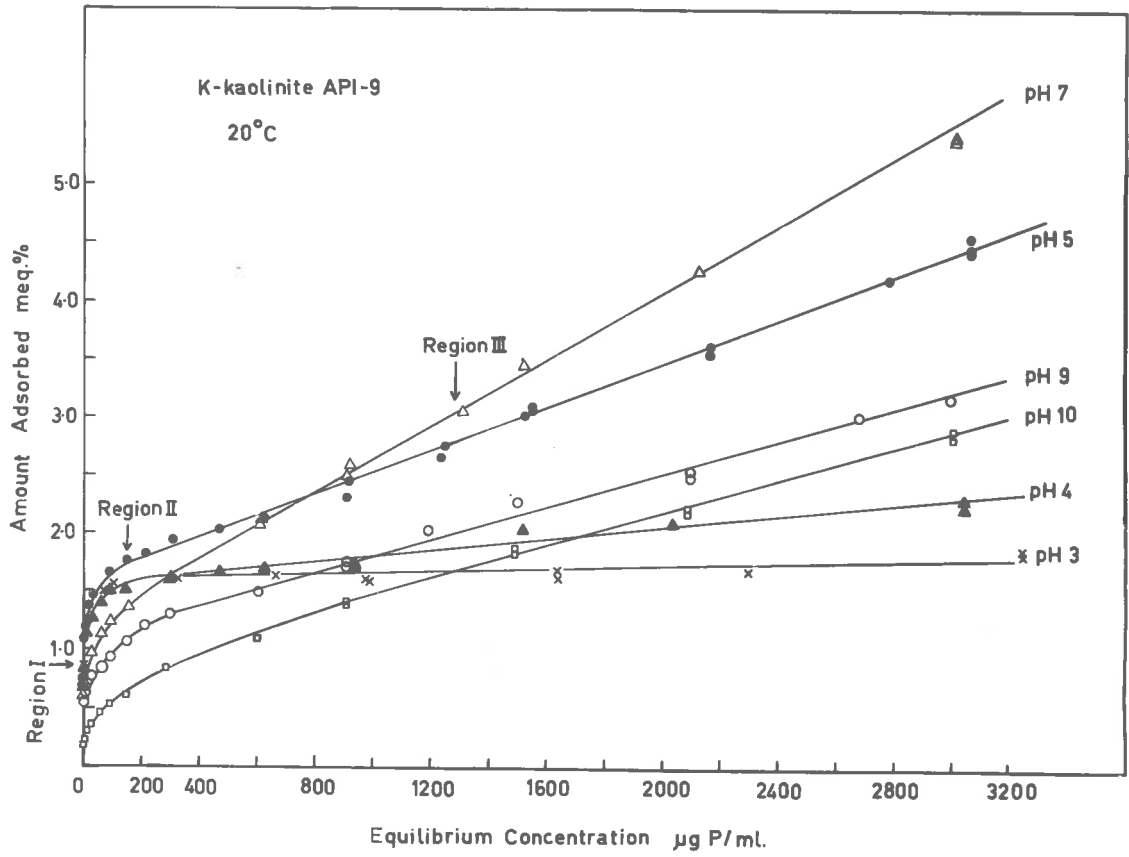


FIGURE 7

EFFECT OF pH ON ADSORPTION

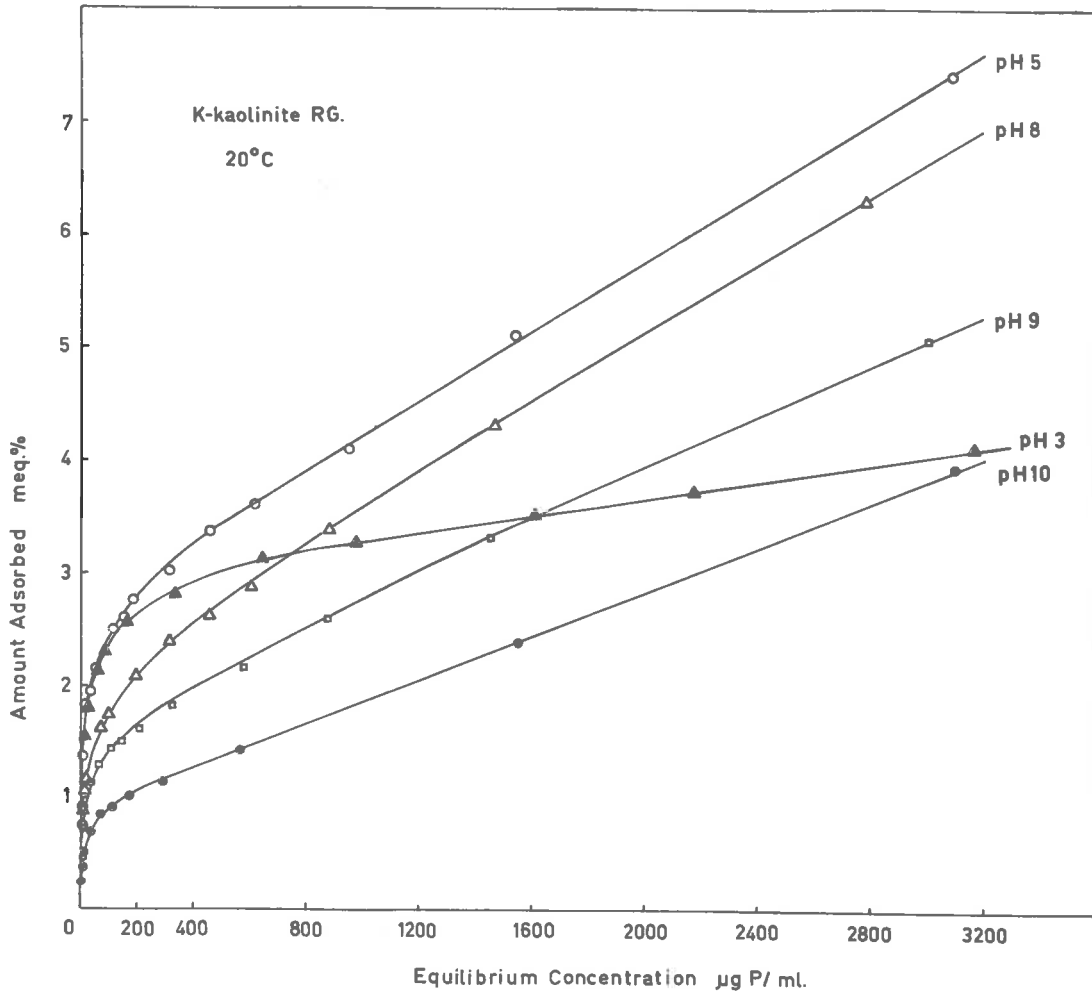


FIGURE 8

EFFECT OF pH ON ADSORPTION

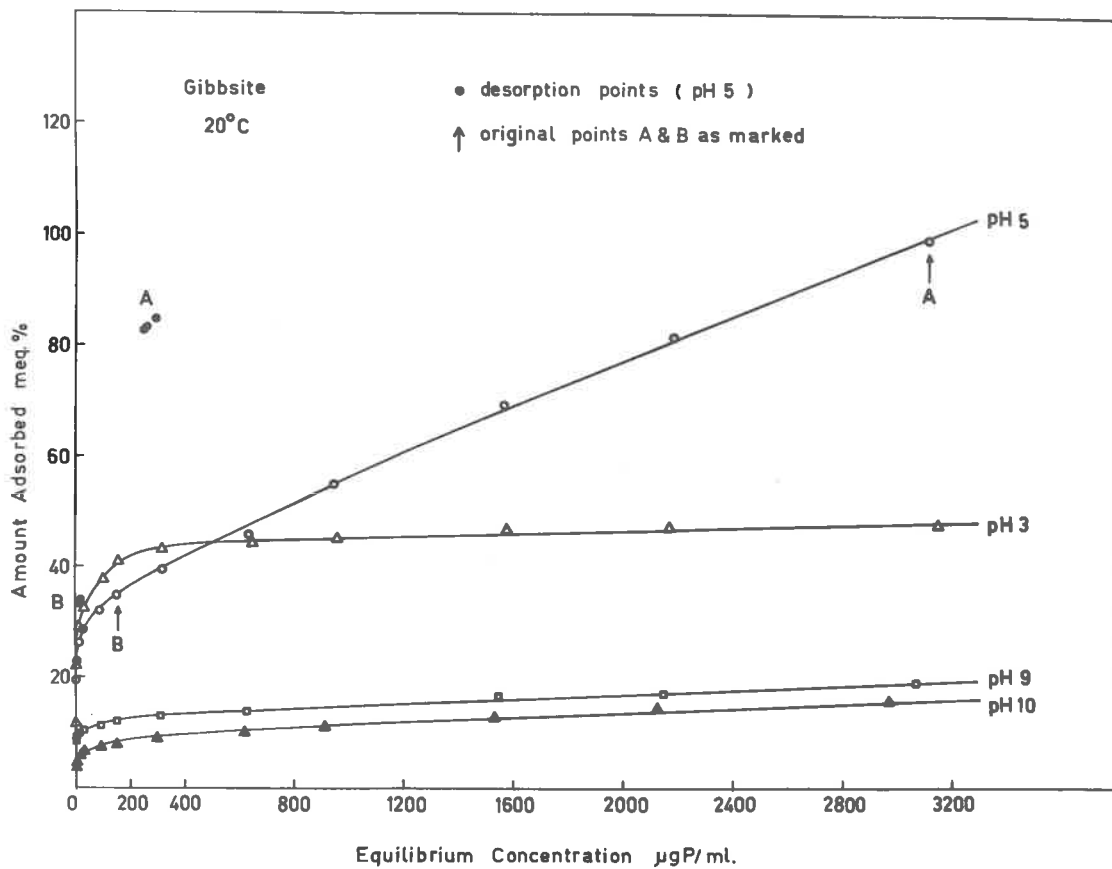


FIGURE 9

EFFECT OF pH ON ADSORPTION

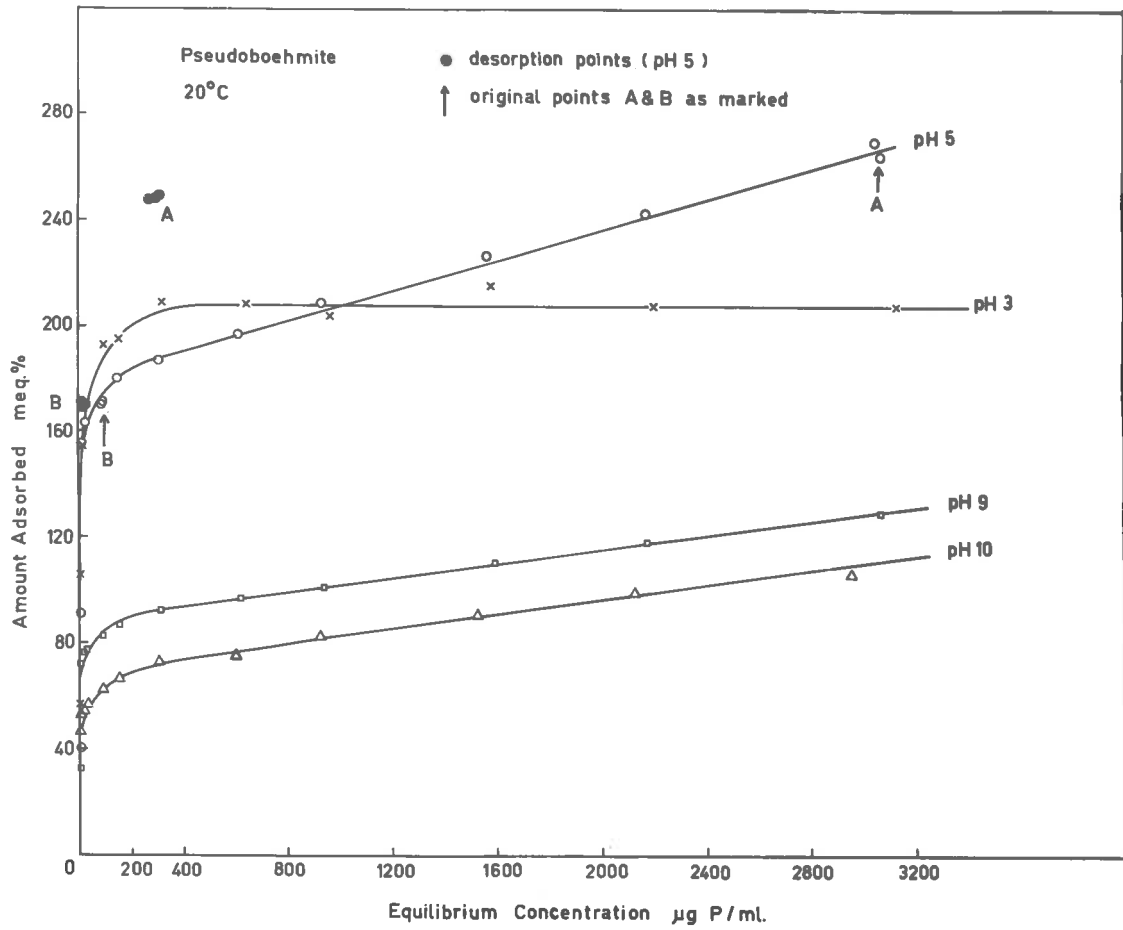


FIGURE 10

PHOSPHATE ADSORPTION BY PSEUDOBOEHMITE, GIBBSITE AND KAOLINITE

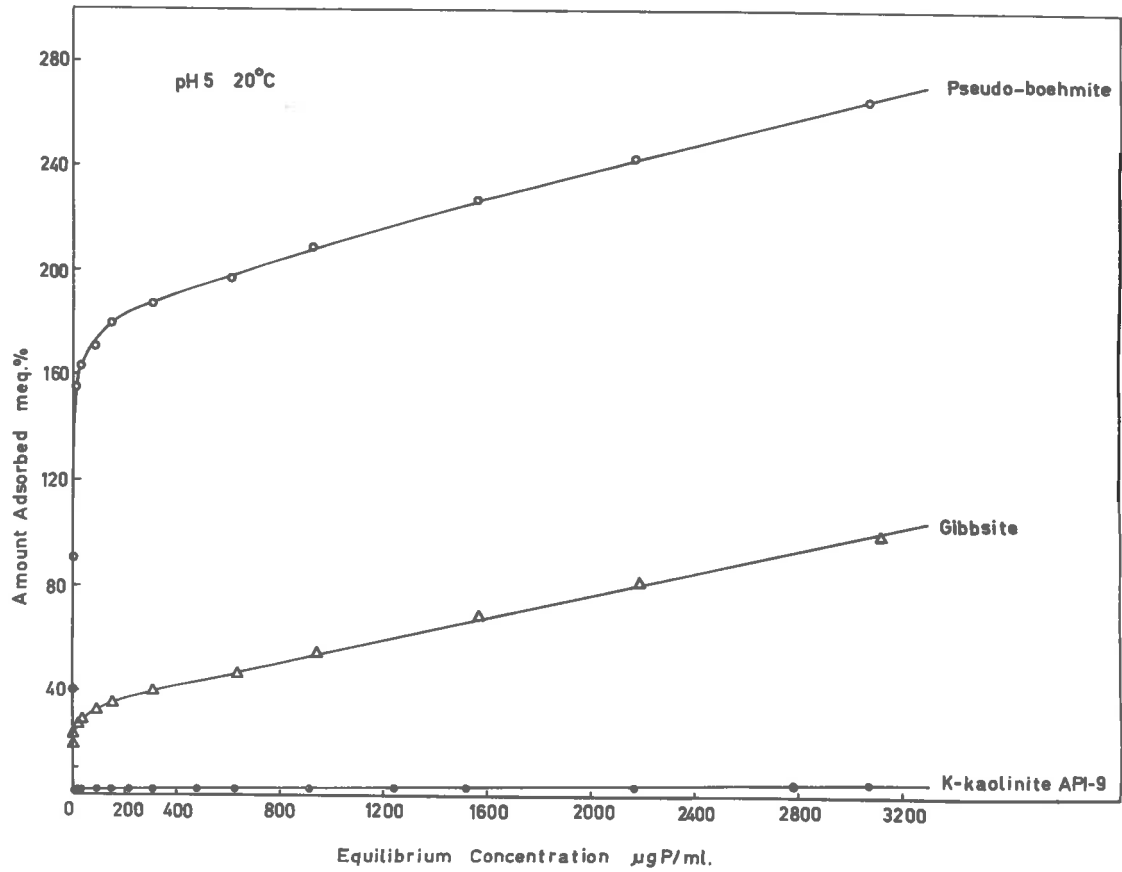


FIGURE 11

investigated by decreasing the bulk concentration. This was achieved by replacing the equilibrium solution with distilled water at the same pH and temperature. The system was then re-equilibrated for 2, 4 and 7 days. The results for K-kaolinite API-9 at 2°C are given in Figure 13, which shows that the adsorption in regions II and III is largely reversible with respect to concentration, while the steep part of the isotherm (region I) is not reversible even after seven days. This observation is in agreement with the early results of Muljadi (1961) which showed that in K-kaolinite RG system after several desorption cycles the points reached a region very close to the y-axis at which the adsorbed phosphate could not be removed except by increasing the pH of the system.

The results for gibbsite and pseudoboehmite (Figures 9 and 10) show that the phosphate adsorbed in regions II and III is much less reversible with respect to concentration than that for kaolinite. It is suggested that under the conditions of these desorption experiments where the concentration of phosphate was reduced drastically, the adsorbed phosphate undergoes a phase change. True irreversibility is considered to exist only if the isotherm lies on the y-axis. If the isotherm is independent of time and does not lie on the y-axis, then each point in regions II and III of the isotherm should be microscopically reversible with respect to concentration. Arguments based on thermodynamic reversibility should therefore be applicable to both adsorption limbs when considered separately.

REVERSIBILITY WITH RESPECT TO pH

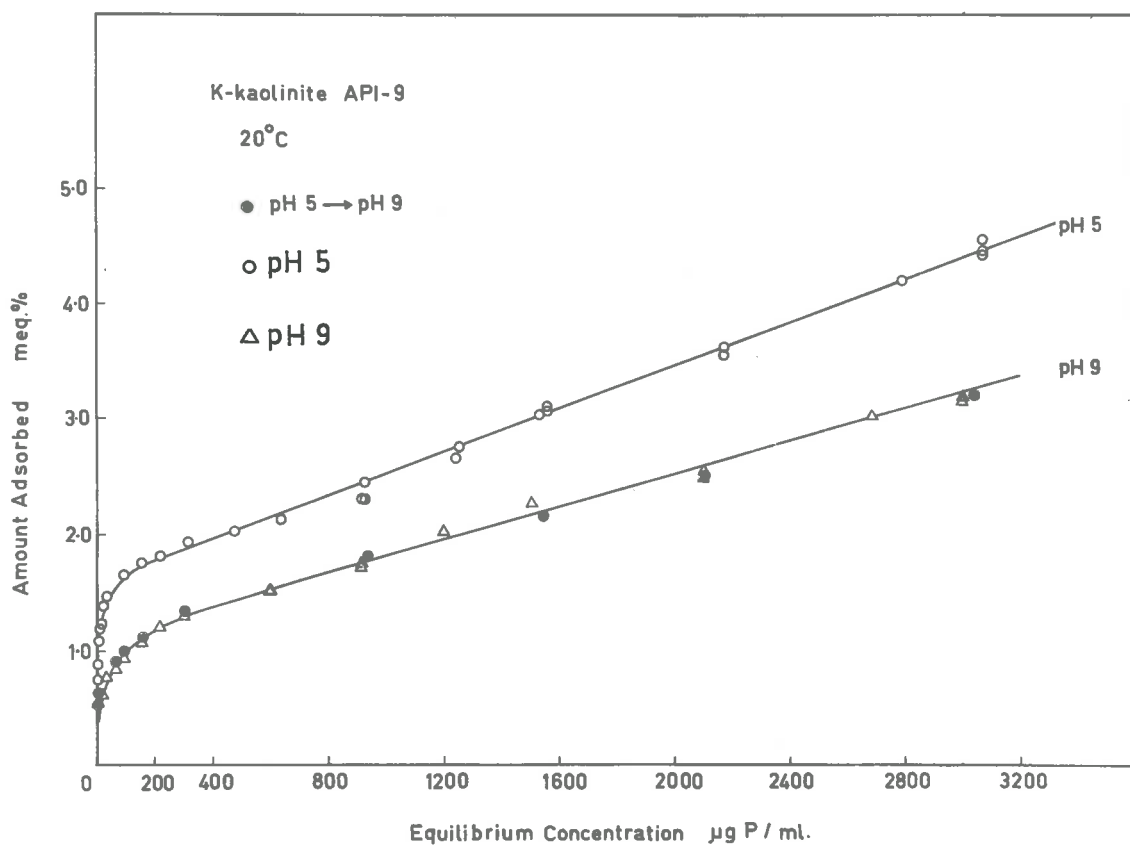


FIGURE 12

Figure 13.

Reversibility with respect to concentration.

A	region	III
B	region	II
C	region	I

REVERSIBILITY WITH RESPECT TO CONCENTRATION

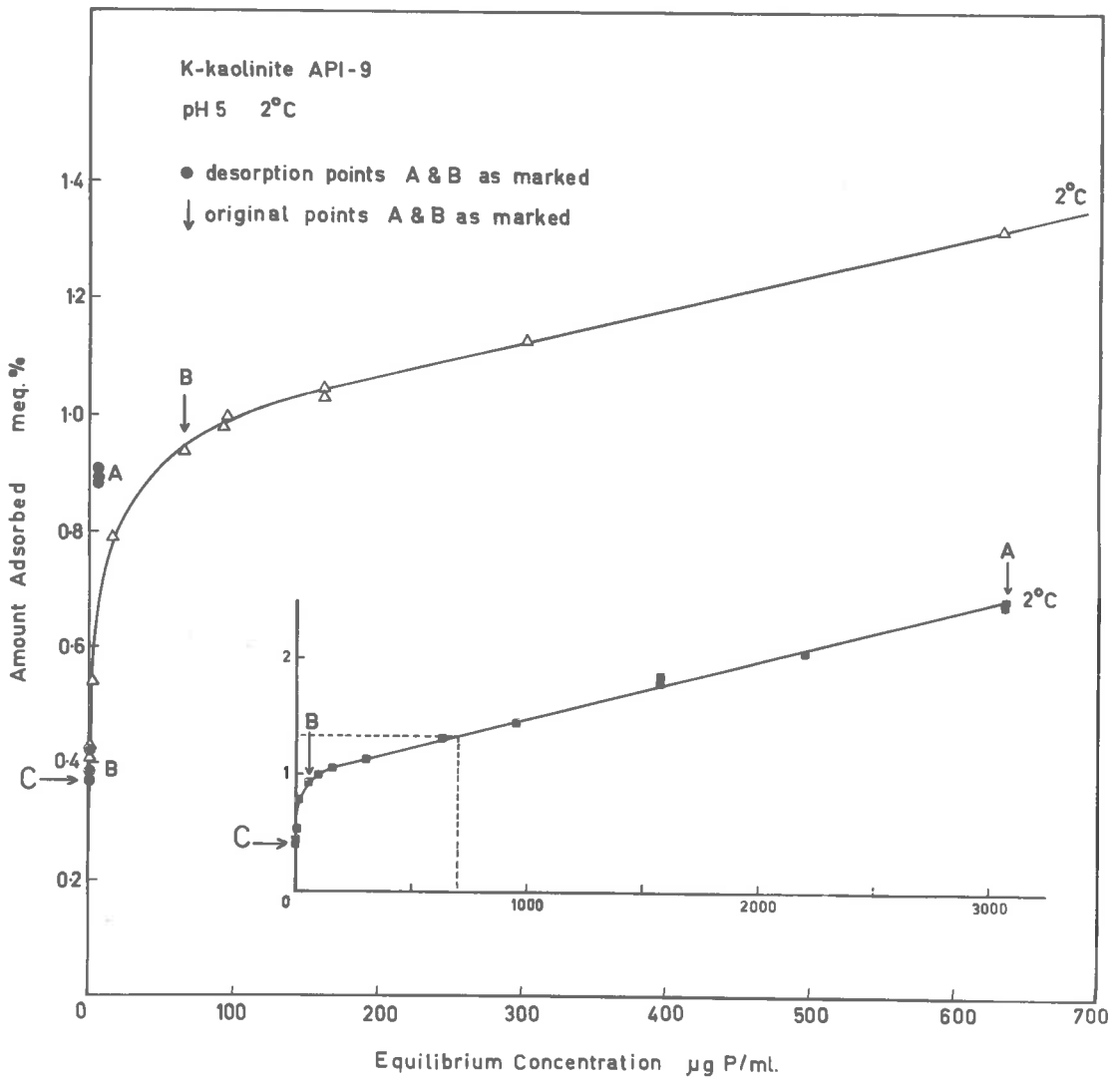


FIGURE 13

1.1.2. The effect of pH.

The effect of pH on the shape of adsorption isotherms at 20°C for K-kaolinite API-9, K-kaolinite R.G., gibbsite and pseudoboehmite is shown in Figures 7, 8, 9 and 10. It may be clearly seen that region I increases to a constant value at pH 5 as the pH is lowered. Region II behaves similarly to region I, while for region III the slope passes through a maximum at about neutrality (pH 7).

1.1.3. The effect of acid pretreatment (0.1 N HCl).

The adsorption isotherm (Figure 14) for the acid washed kaolinite API-9 (K-clay) in the presence of 0.1 N HCl, shows that acid washing has only slightly modified regions I and II but has almost eliminated region III.

Deshpande, Greenland and Quirk (private communication) have suggested that acid pretreatment (0.1 N HCl) will remove some form of alumina or some part of the clay having a reasonable reactivity, greater than ^{the} crystalline region. Thus the adsorption of phosphate in region III may be due to less crystalline material on the clay surface and this is probably at the edge faces of the crystals.

The adsorption of phosphate by acid treated gibbsite (Figure 15) shows that there is some reduction in regions I and II, while region III is only slightly reduced. The different effect of acid pretreatment on kaolinite and gibbsite in regions I and II may be due to the fact that the synthetic gibbsite is not as resistant to acid attack as the kaolinite.

EFFECT OF ACID (0.1N HCl) TREATMENT ON ADSORPTION

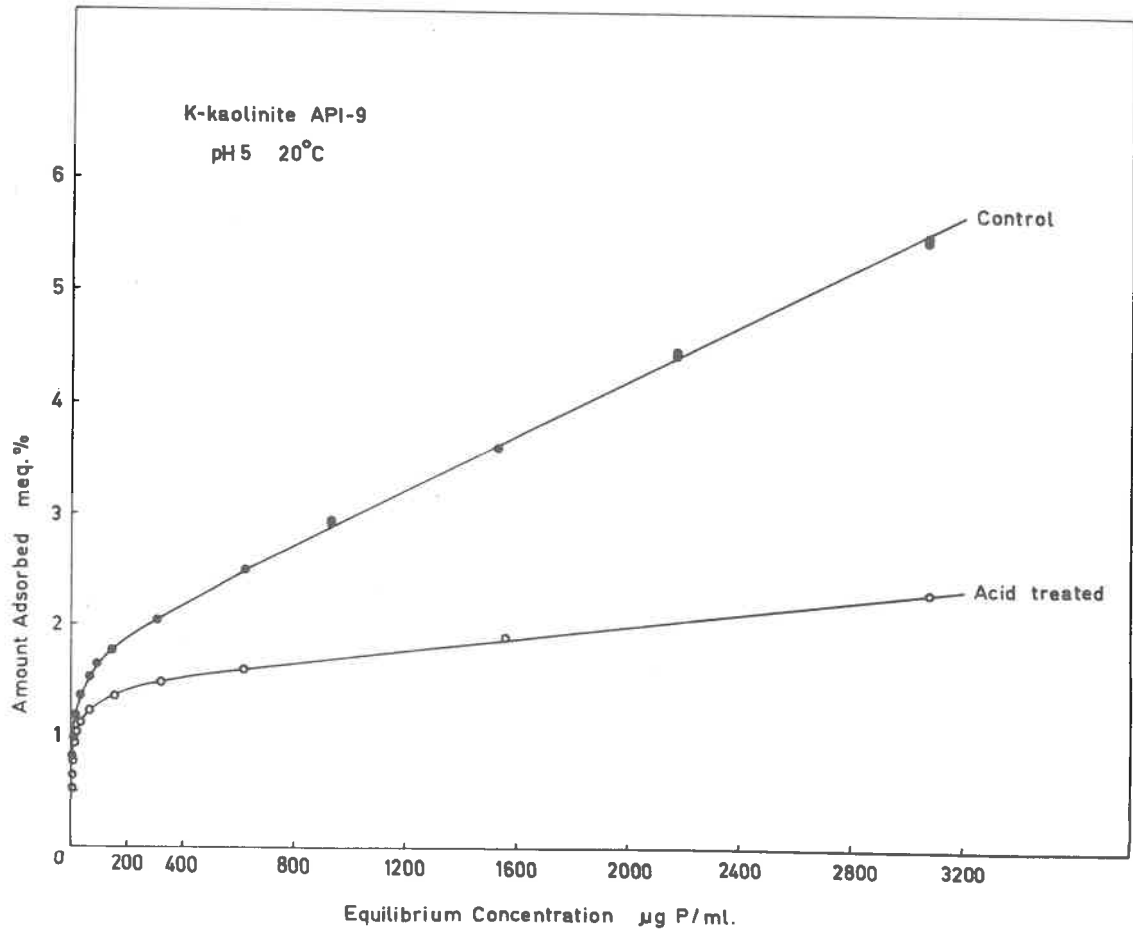


FIGURE 14

EFFECT OF ACID TREATMENT (0.1N HCl) ON ADSORPTION

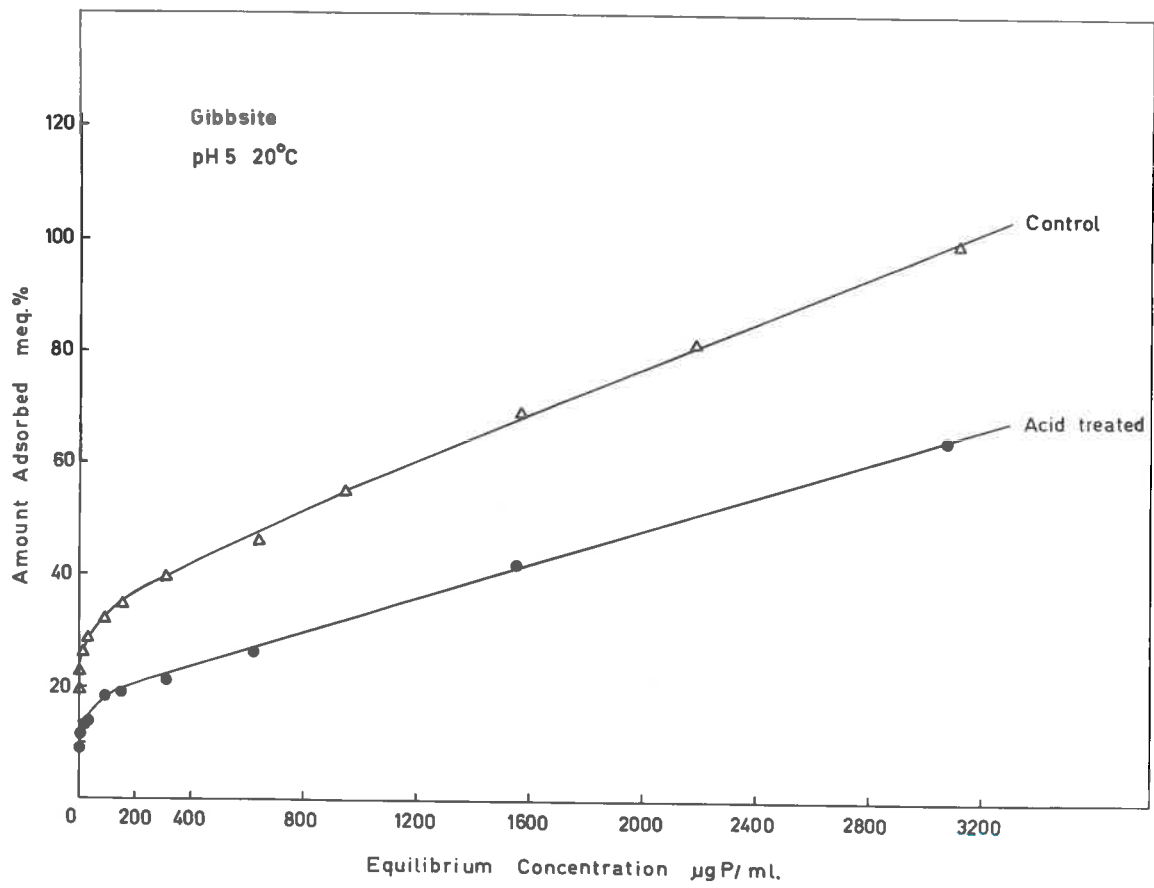


FIGURE 15

EFFECT OF ACID TREATMENT (0.1N HCl) ON ELECTRIC CHARGES ON KAOLINITE AT DIFFERENT pH VALUES

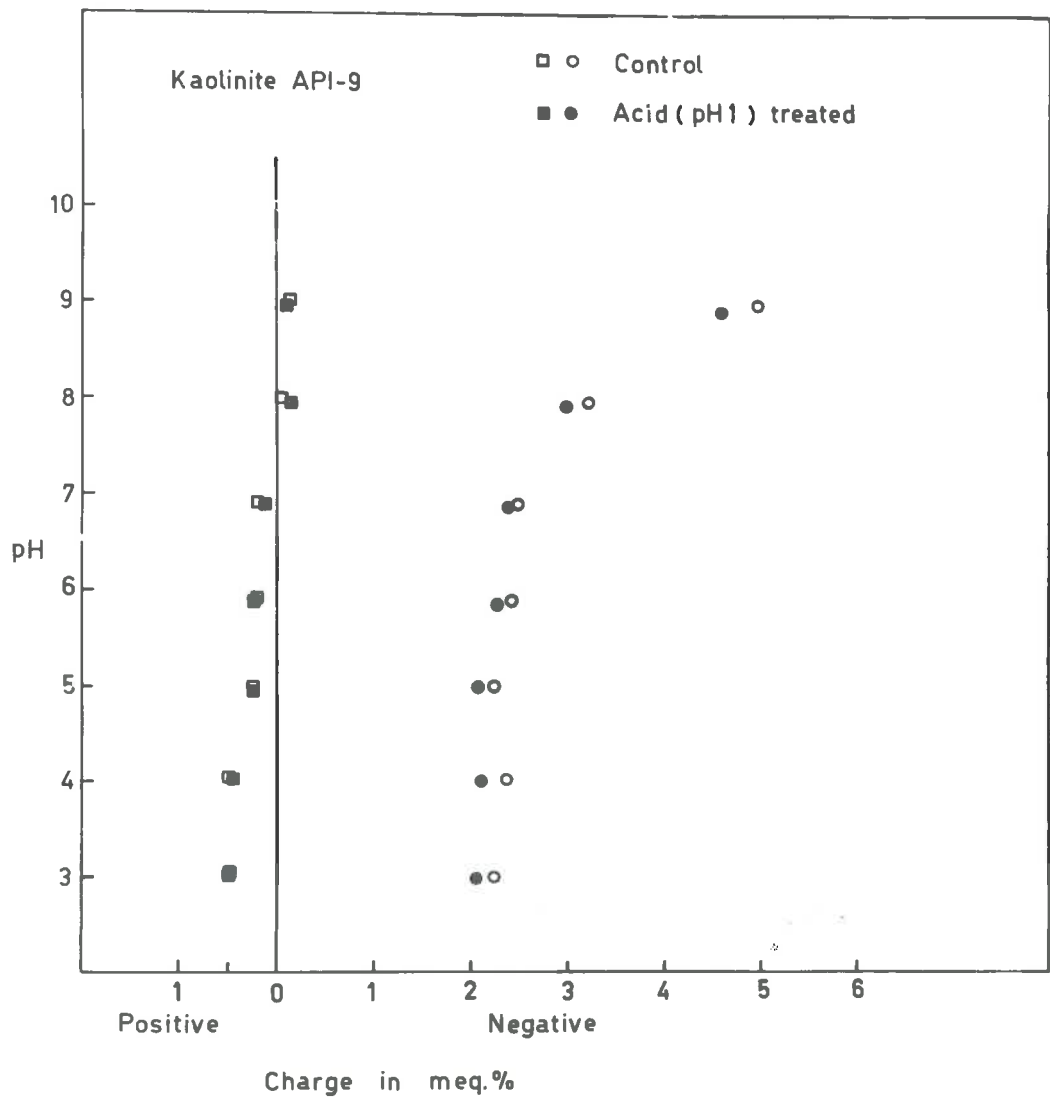


FIGURE 16

The small effect of acid treatment on region III may be due to the re-formation of the amorphous material on the gibbsite surface during the washing of the excess acid with distilled water, where the pH increases from 3.5 to 5.6.

The electric charges at different pH values on the acid treated kaolinite and untreated kaolinite API-9 (Figure 16) shows no significant difference between these two kaolinites. This indicates (Sumner, 1962) that the surface properties of the kaolinite has not been altered significantly by the acid pretreatment.

The electric charges on the acid treated gibbsite was not determined, and hence the extent of the alteration of the surface properties by acid treatment cannot be compared to the untreated sample (control).

1.1.4. Adsorption of potassium.

In addition to measuring phosphate adsorption from KH_2PO_4 and K_2HPO_4 solutions the corresponding potassium adsorption was also determined. The results relating adsorbed potassium and phosphate for K-kaolinite API-9 are shown in Figure 17. At pH 5 where the species involved is H_2PO_4^- there is an almost 1:1 ratio between potassium and phosphate adsorption, while at pH 9 where the species involved is HPO_4^{2-} this ratio is almost 2:1.

The adsorption of potassium by gibbsite and pseudoboehmite at pH 5 are shown in Figure 18. A significant feature is that no potassium uptake occurs until adsorption into region III takes place. For gibbsite and pseudoboehmite at pH 5 the ratio between potassium

RELATION BETWEEN POTASSIUM AND PHOSPHATE
ADSORBED

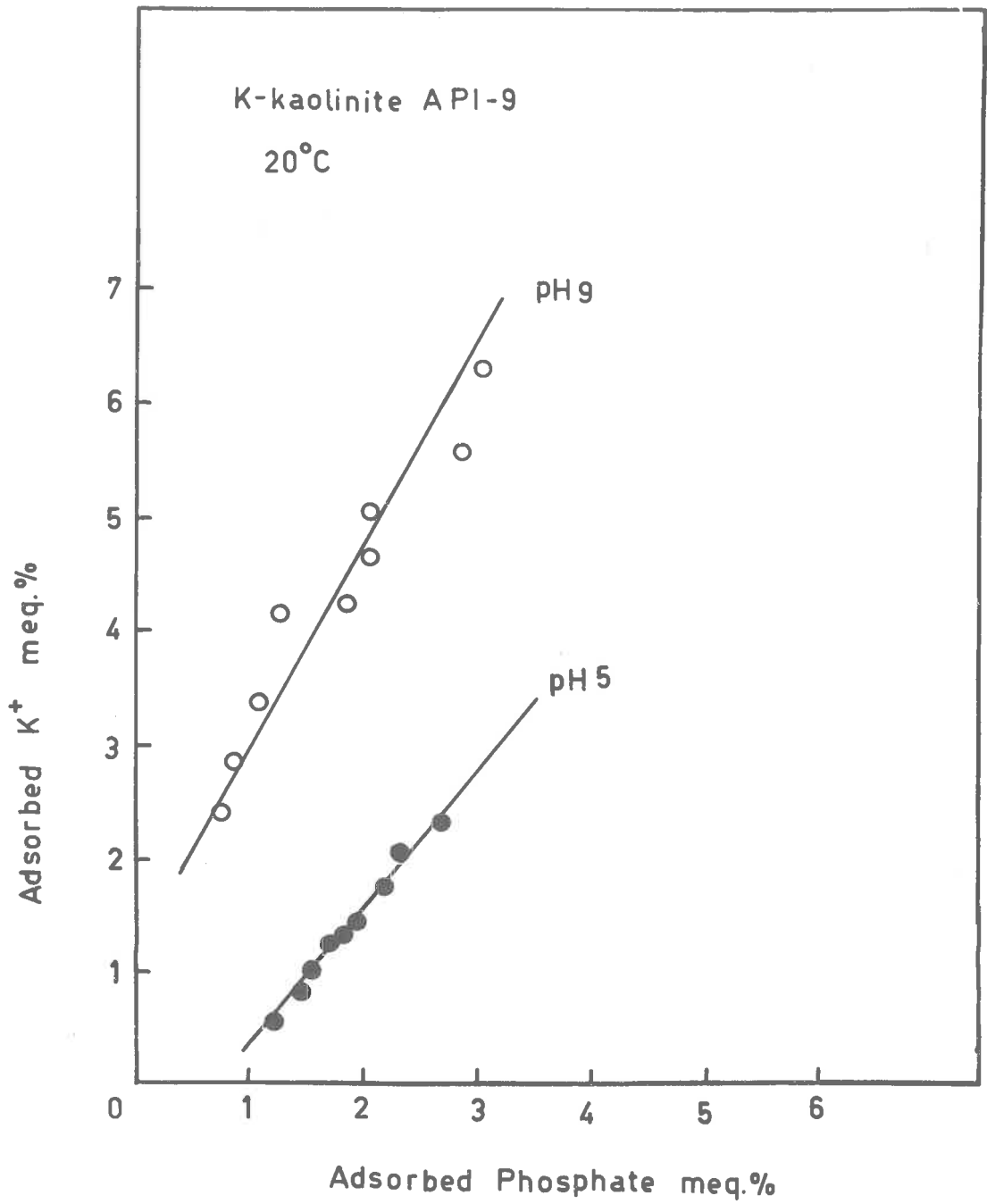


FIGURE 17

RELATION BETWEEN POTASSIUM AND PHOSPHATE ADSORBED

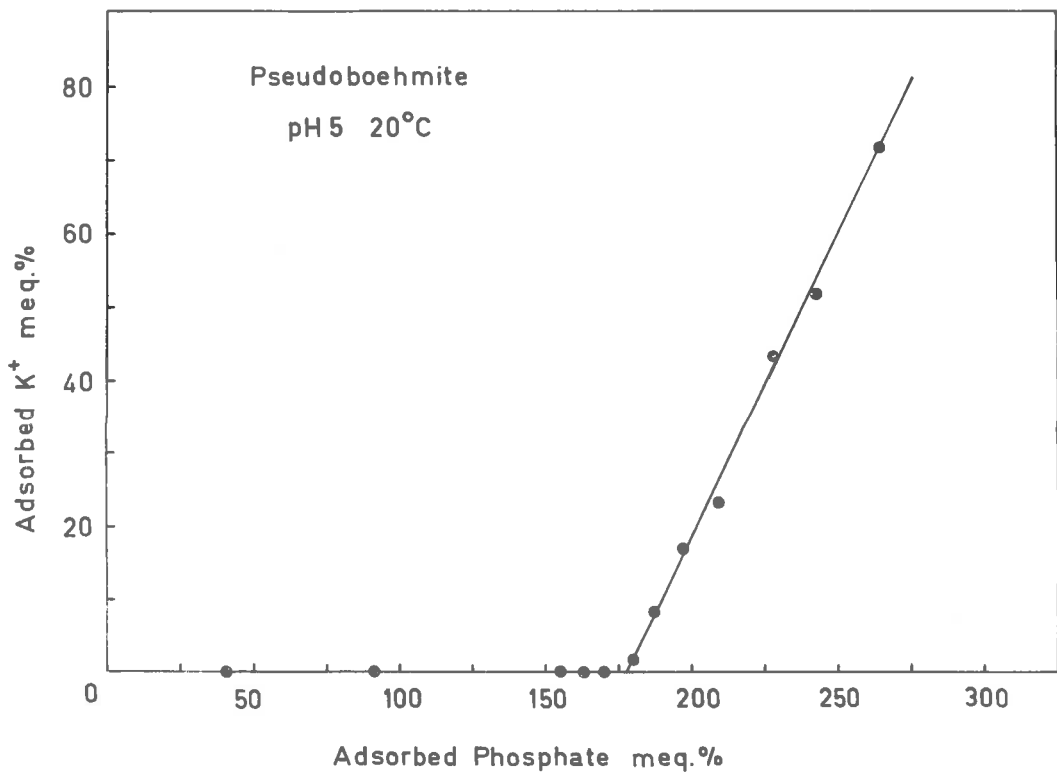
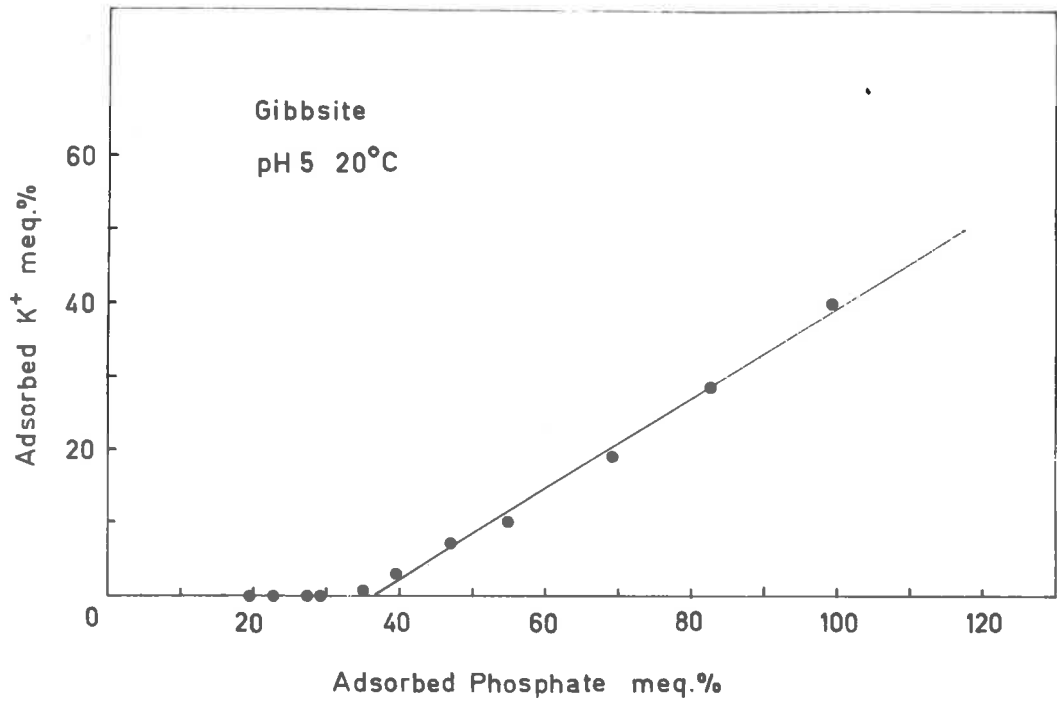


FIGURE 18

RELATION BETWEEN POTASSIUM AND PHOSPHATE ADSORBED

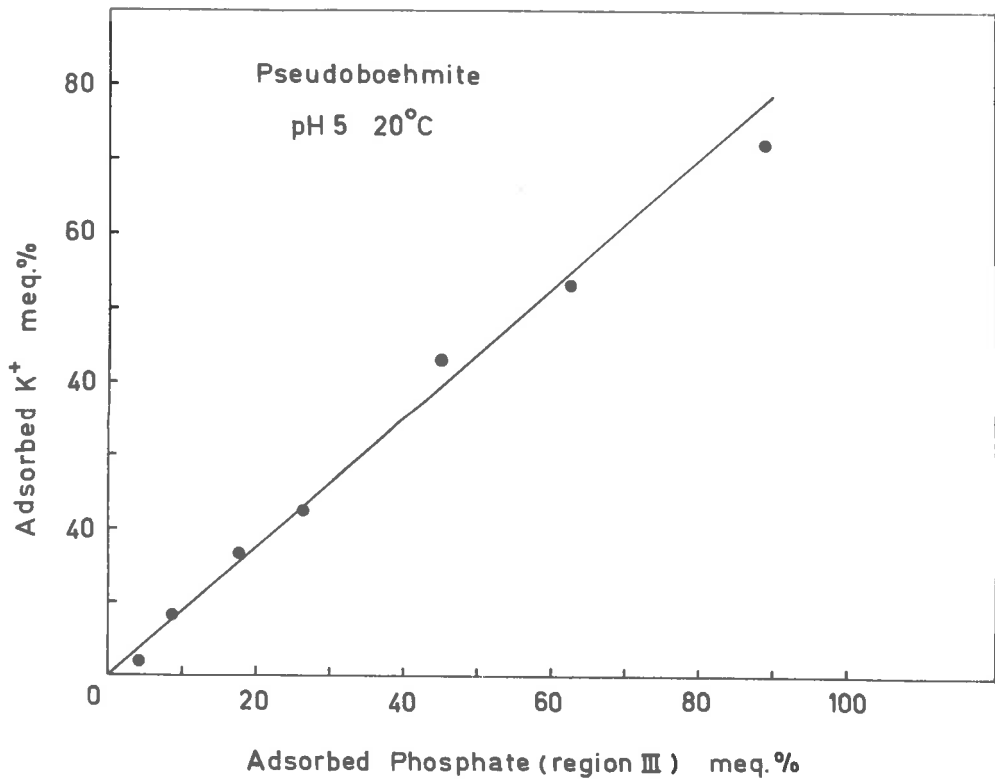
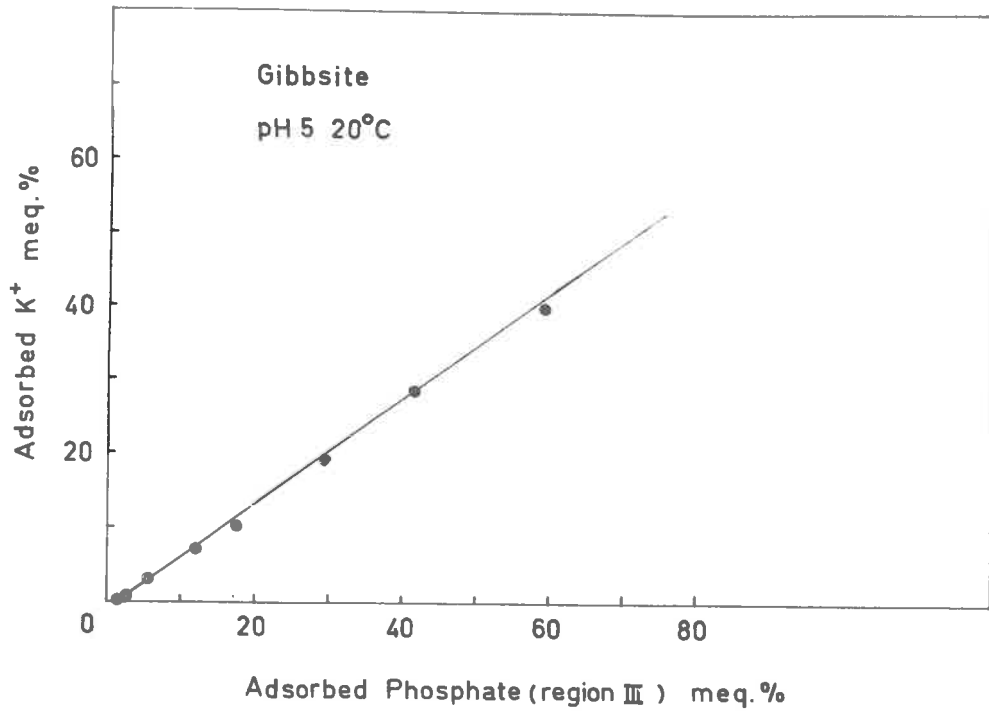


FIGURE 19

uptake and phosphate adsorption in this region is almost 1:1 (Figure 19).

1.2. Discussion.

de Boer (1950) points out that the most reactive sites on a surface will be associated with corners, edges, cavities and lattice disturbances. Schofield and Samson (1953, 1954) have shown that positive edge charges are probably an important factor in determining the edge to face flocculation mechanism in a salt free system of kaolinite. Furthermore, the positively charged sites which are responsible for chloride adsorption have been attributed to exposed aluminium atoms on the edge face of the crystal (Schofield and Samson, 1953; Quirk, 1960).

It has been suggested earlier that there are three energetically dissimilar regions on kaolinite and hydrated aluminium oxides surfaces responsible for phosphate adsorption. These have been designated as regions I, II and III. These sites are most probably located on the edge face of the crystal.

1.2.1. Region I.

Several workers (Kolthoff, 1936; Hsu and Rennie, 1962) have suggested that phosphate ions can exchange with the OH^- on an edge $> \text{Al-OH}$, as one of the simplest mechanisms of reaction. This may be represented thus,



sites maintain their identity after exchange with phosphate and retain their role in determining the uptake of H^+ . This would be expected for an ion-exchange reaction. If this were not so then provided sufficient phosphate is present, the number of sites available for adsorption in region I would not depend on the pH value. However, the results (Figure 20, Table 3) show that the amount of phosphate adsorbed in region I does depend on the pH value of the system.

Region I is clearly represented by a high affinity (HA) type isotherm and therefore K_2^I is very large. Consequently reaction 1 will determine the extent of the reaction in region I. The effect of the phosphate species is negligible because reaction 1 is the determining factor at all pH values examined, the values of K_2^I for both species thus appears to be very large.

Therefore K_1^I can be written as

$$K_1^I = \frac{[>Al(H_2O)^+ \text{---} OH^-]}{[>AlOH] [H^+]} \dots \dots \dots (51)$$

If the total sites available for adsorption of phosphate in region I is V_1 , then

$$[>AlOH] = [V_1 - >Al(H_2O)^+ \text{---} OH^-] \dots \dots \dots (52)$$

substituting equation (52) into (51), gives

$$K_1^I = \frac{[>Al(H_2O)^+ \cdots OH^-]}{[V_1 - >Al(H_2O)^+ \cdots OH^-][H^+]}$$

$$[>Al(H_2O)^+ \cdots OH^-][1 + K_1^I H^+] = K_1^I V_1 [H^+]$$

$$[>Al(H_2O)^+ \cdots OH^-] = \frac{K_1^I V_1 [H^+]}{1 + K_1^I [H^+]} \quad \dots \dots \dots (53)$$

Since the value of K_2^I for reaction 2 is very large, equation (53) can be written,

$$V_o = \frac{K_1^I V_1 [H^+]}{1 + K_1^I [H^+]} \quad \dots \dots \dots (54)$$

where V_o is the amount of adsorbed phosphate in region I at any particular pH.

V_1 is the total number of sites in region I.

Since region I occurs at very low concentrations ($< 10^{-4} M$), it is assumed that activity coefficients are unity. The square bracket thus indicates the concentration of the reacting species.

The above equation describes the fact that the pH value determines number of adsorption sites and that all available phosphate will react with these sites until they are fully occupied.

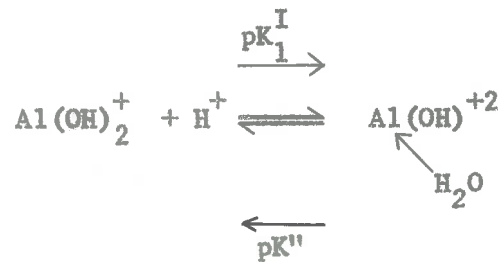
Equation (54) can be written in the linear form

$$\frac{1}{V_o} = \frac{1}{K_1^I V_1} \frac{1}{[H^+]} + \frac{1}{V_1} \quad \dots \dots \dots (55)$$

This is used to test the experimental data, V_0 being obtained from the enlarged isotherms (Figure 20); the values of V_0 are given in Table 3. These results have been shown by linear regression analysis to fit the above equation (Appendix 10). When the results are plotted in the form of $\frac{1}{V_0}$ against $\frac{1}{[H^+]}$ only three points can be accommodated because of the extended x-axis scale (Figures 21, 22). The values of the constant K_1^I and V_1 and the regression coefficients are given in Table 4.

A significant feature of the results is that the value of K_1^I (Table 4) of region I for different adsorbents is relatively constant. However, their adsorption capacities (V_1) differ widely.

The value of pK_1^I ($-\log. K_1^I$) for the uptake of proton is about -10. This is similar in magnitude to the value of $pK''=10$ (Jackson, 1962) for the second stage hydrolysis, which is the reverse process of the uptake of proton, thus $pK_1^I = -pK''$.



The relative constancy of K_1^I for the different adsorbents supports the suggestion that the adsorption sites in region I for kaolinite, gibbsite and pseudoboehmite are essentially the same, that is the aluminium atom situated on the edge of the crystal, $>AlOH$.

ENLARGED ISOTHERMS (REGIONS I & II) AT DIFFERENT pH VALUES

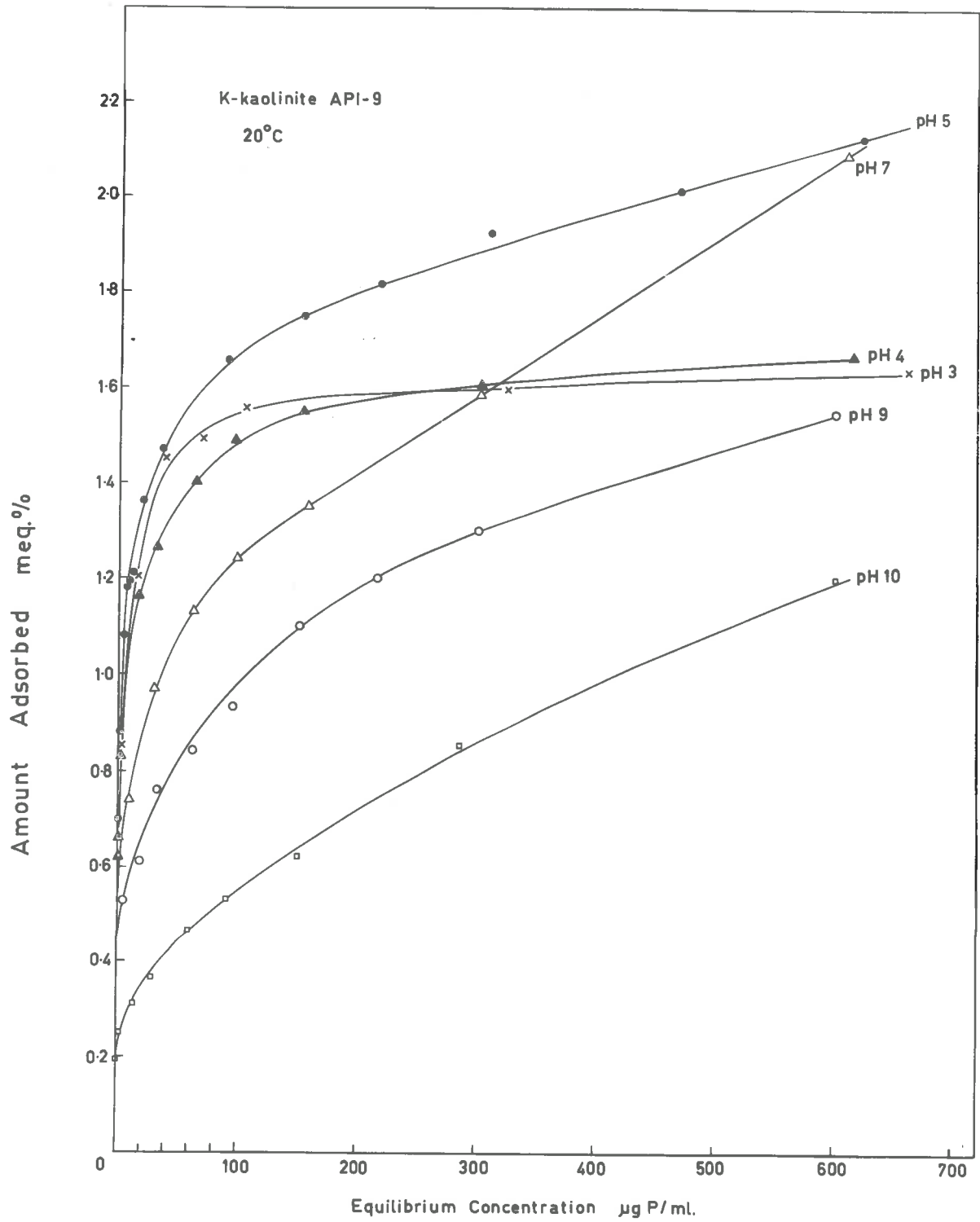


FIGURE 20

TABLE 3

ADSORPTION OF PHOSPHATE IN REGION I (V_o) AT DIFFERENT pH VALUES
(20°C)

pH	V_o (meq.%)			
	K-kaolinite API-9	K-kaolinite R.G.	Gibbsite	Pseudoboehmite
3	0.85	1.0	22	120
4	0.85	-	-	-
5	0.85	1.0	22	120
7	0.60	-	-	-
8	-	0.80	-	-
9	0.45	0.65	8.5	60
10	0.15	0.40	4.5	45

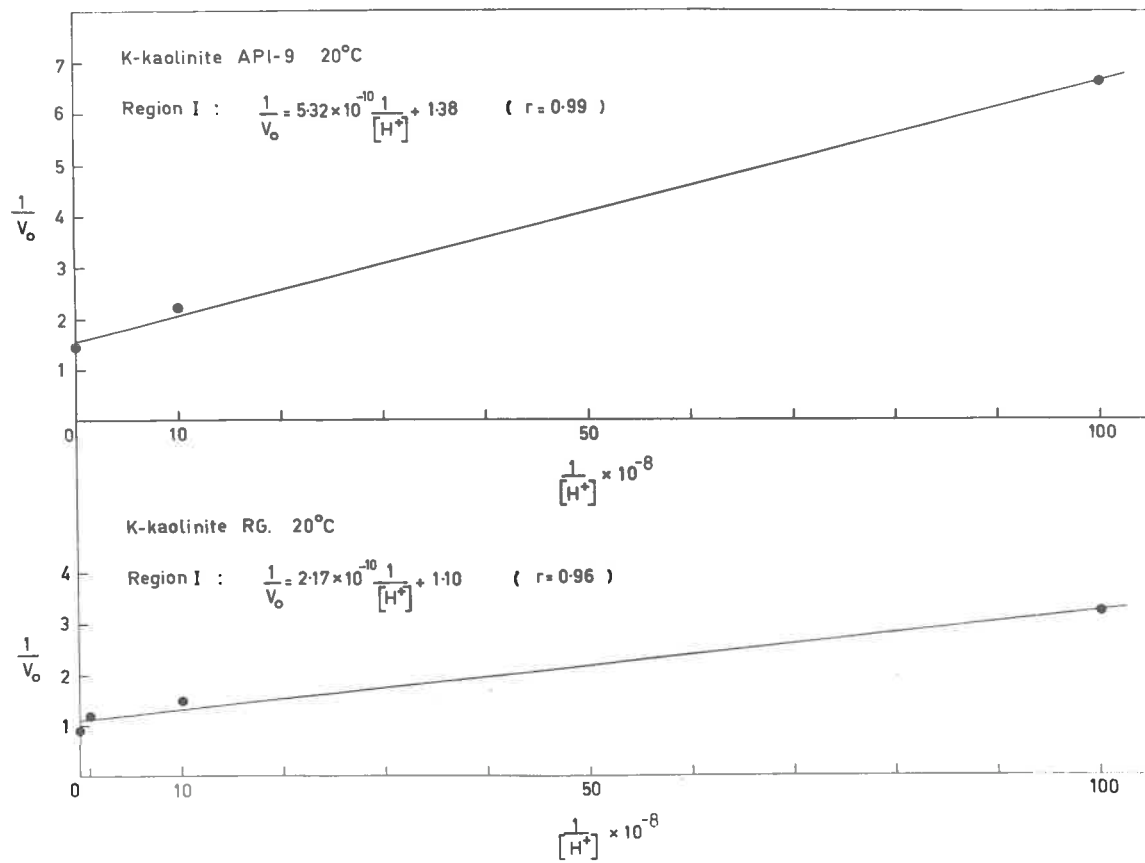


FIGURE 21

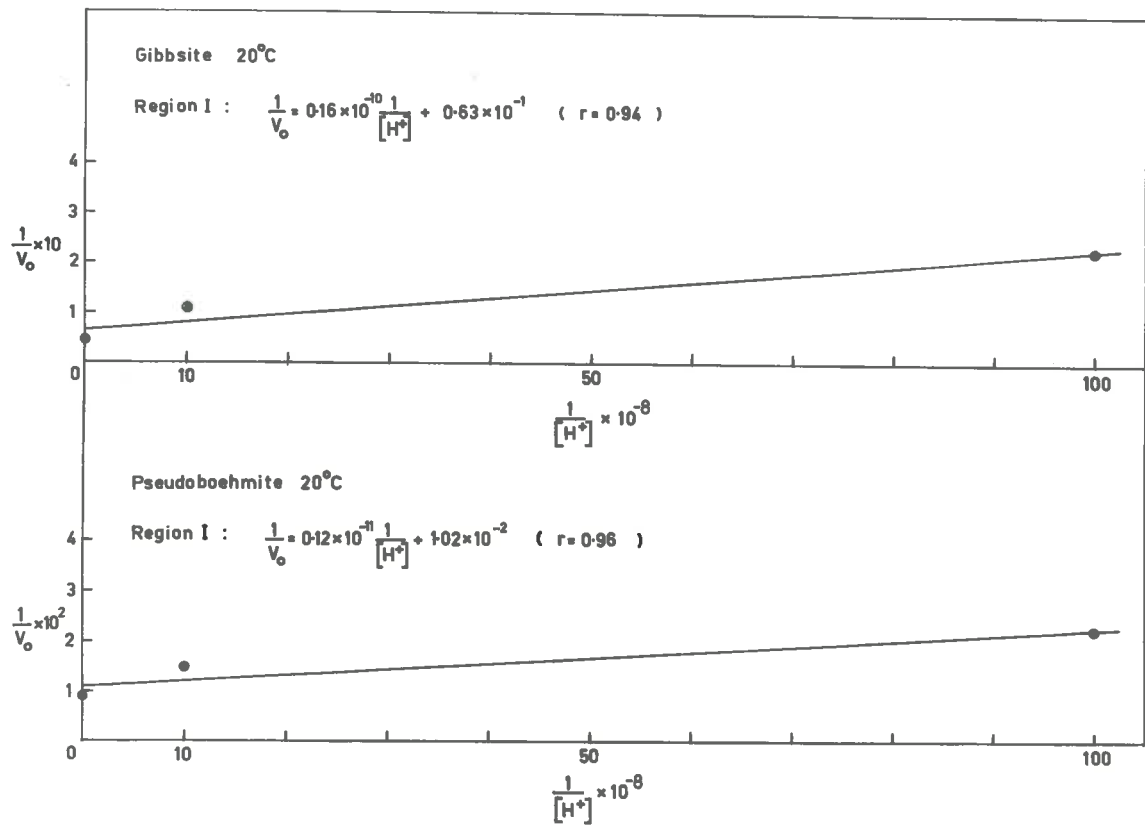


FIGURE 22

TABLE 4

K_1^I and V_1 for region I determined from the equation

$$\frac{1}{V_0} = \frac{1}{K_1^I V_1 [H^+]} + \frac{1}{V_1} \text{ at } 20^\circ\text{C.}$$

Adsorbent	Regr. coeff.	$K_1^I \times 10^{-10}$ (ml/meq.)	V_1 (meq.%)
K-kaolinite API-9	0.99	(0.26 \pm 0.03)	0.72 \pm 0.08
K-kaolinite R.G.	0.96	(0.54 \pm 0.16)	0.86 \pm 0.06
Gibbsite	0.94	(0.38 \pm 0.2)	15.87 \pm 5.2
Pseudoboehmite	0.96	(0.85 \pm 0.3)	98.0 \pm 13.3

The adsorption sites of region I of kaolinite were originally thought to be aluminium atoms associated with exchangeable cation sites, the aluminium ions being derived from the edge face of the crystals when the clay was washed with distilled water following the treatment (1.0 N KCl pH 3, Cashen, 1959) given to ensure that all the cation exchange sites were occupied by potassium.

While this idea could be relevant, the existence of region I for gibbsite and pseudoboehmite, which do not have any negative charges at these pH values, supports the argument that the phosphate sites of region I are associated with the edge face of the crystal. Furthermore, the maximum positive charges of these two oxides and the clays as measured by chloride adsorption, is approximately equal to region I for phosphate adsorption (Table 5). Thus the same sites responsible for the positive adsorption of chloride seem to be responsible for the adsorption of phosphate in region I. Quirk (1960) has also suggested that the sites responsible for chloride and phosphate adsorption may be the same.

The simplest suggestion is that region I corresponds to the uptake of phosphate at one of the hydroxyl groups $>AlOH$ situated on the edge face of the crystal. This grouping would be common to both oxides and kaolinites and is likely to be the most reactive.

1.2.2. Region II

The reaction sites responsible for adsorption in region II are considered to be similar to those of region I, that is aluminium atoms located on the edge face of the crystal lattice.

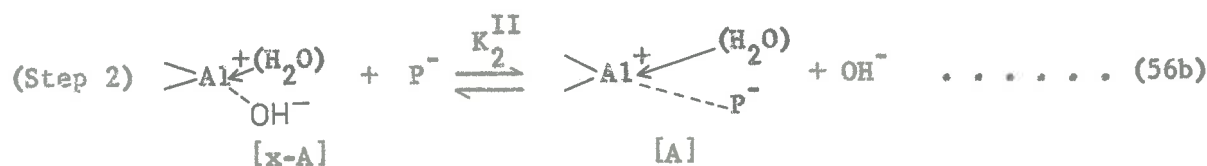
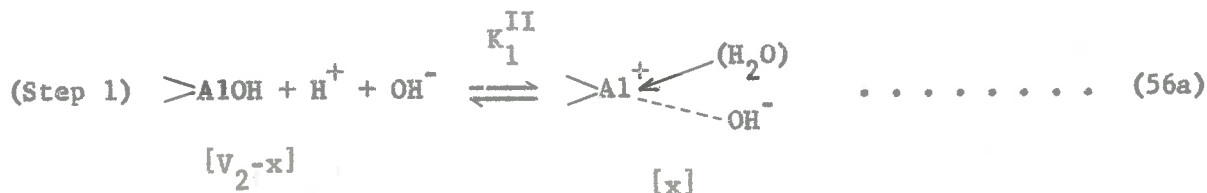
TABLE 5

COMPARISON OF PHOSPHATE ADSORPTION IN REGION I AND
 POSITIVE CHLORIDE ADSORPTION MEASURED AT pH 3, 20°C.

Adsorbent	Cl ⁻ adsorption (meq. %)	Phosphate adsorption (meq. %)	Surface Area (N ₂) m ² /g.
Kaolinite API-9	0.55	0.85	12
Kaolinite R.G.	0.95	1.0	40
Gibbsite	20	22	48
Pseudoboehmite	120	120	176

The fact that the isotherm in region II does not lie on the y-axis suggests that the equilibrium constant for the reaction between the adsorption site and the phosphate ion is no longer large.

To simplify the derivation of the adsorption equation, edge face aluminium atoms forming region II are initially written as >AlOH . The reactions may be represented in a similar manner to those of region I, thus



where V_2 is the total number of sites in region II (meq. %)

x is the number of positively charged aluminium atoms on the crystal edge (meq. %)

P^- is the equilibrium phosphate concentration ($\mu\text{gP/ml}$)

A is the amount of phosphate adsorbed in region II (meq. %)

K_1^{II} and K_2^{II} are the equilibria constants for region II.

Again it is considered that step 1 is independent of step 2 to the extent that the uptake of phosphate in step 2 does not promote the formation of further positively charged adsorption sites. If this were not so, then provided sufficient phosphate were present, the number

of sites available for adsorption in region II would not depend on pH value. Figure 23 shows the way in which the isotherms would be expected to vary with pH as compared with the observed variation (Figures 25, 26, 27 and 28). The theoretical curves (Figure 23) have been calculated from the relationship derived in Appendix 11.

Derivation of equation for region II.

Phosphoric acid dissociates into three species as follows:



The relative amounts of each phosphate species in solution is governed by the pH of the medium as shown in Figure 24. These curves were calculated using the equilibrium constants (Vogel, 1951) of phosphoric acid,

$$K' = 7.50 \times 10^{-3}$$

$$K'' = 6.20 \times 10^{-8}$$

$$K''' = 5.00 \times 10^{-13}$$

It is obvious from Figure 24 that between pH 3 and 11 only the first and second species of phosphate ions are present in the solution to any significant extent. It is therefore necessary to include the two species of phosphate ion in the derivation of the adsorption

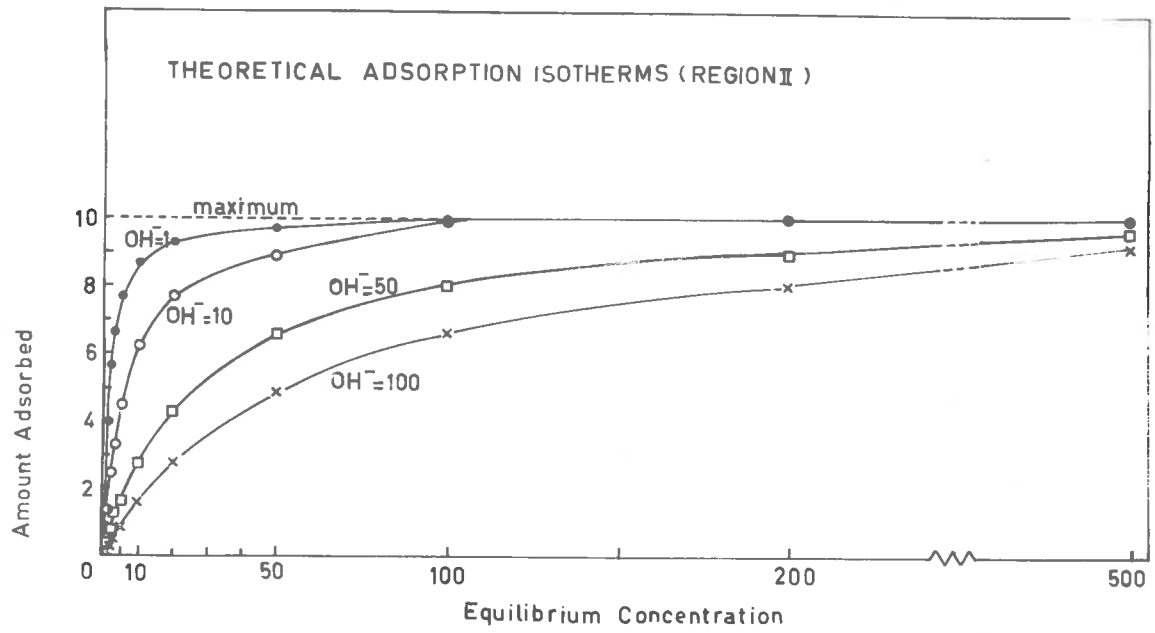


FIGURE 23

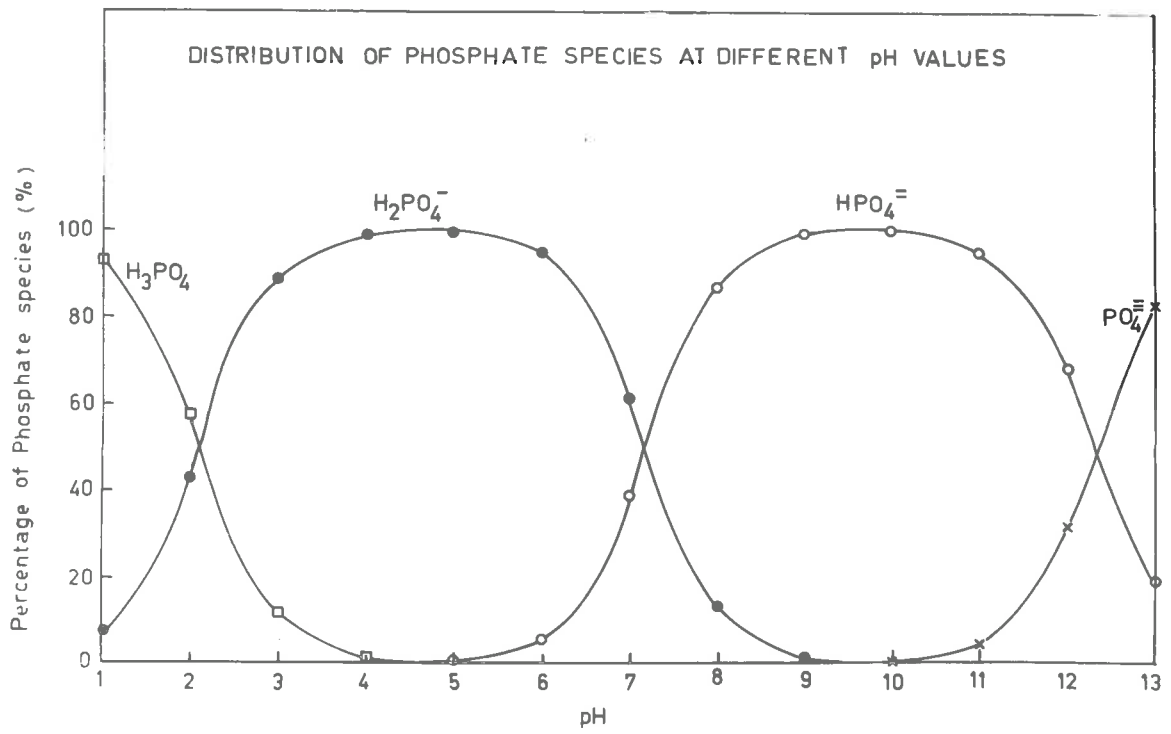


FIGURE 24

ADSORPTION ISOTHERMS (REGION II) AT DIFFERENT pH VALUES

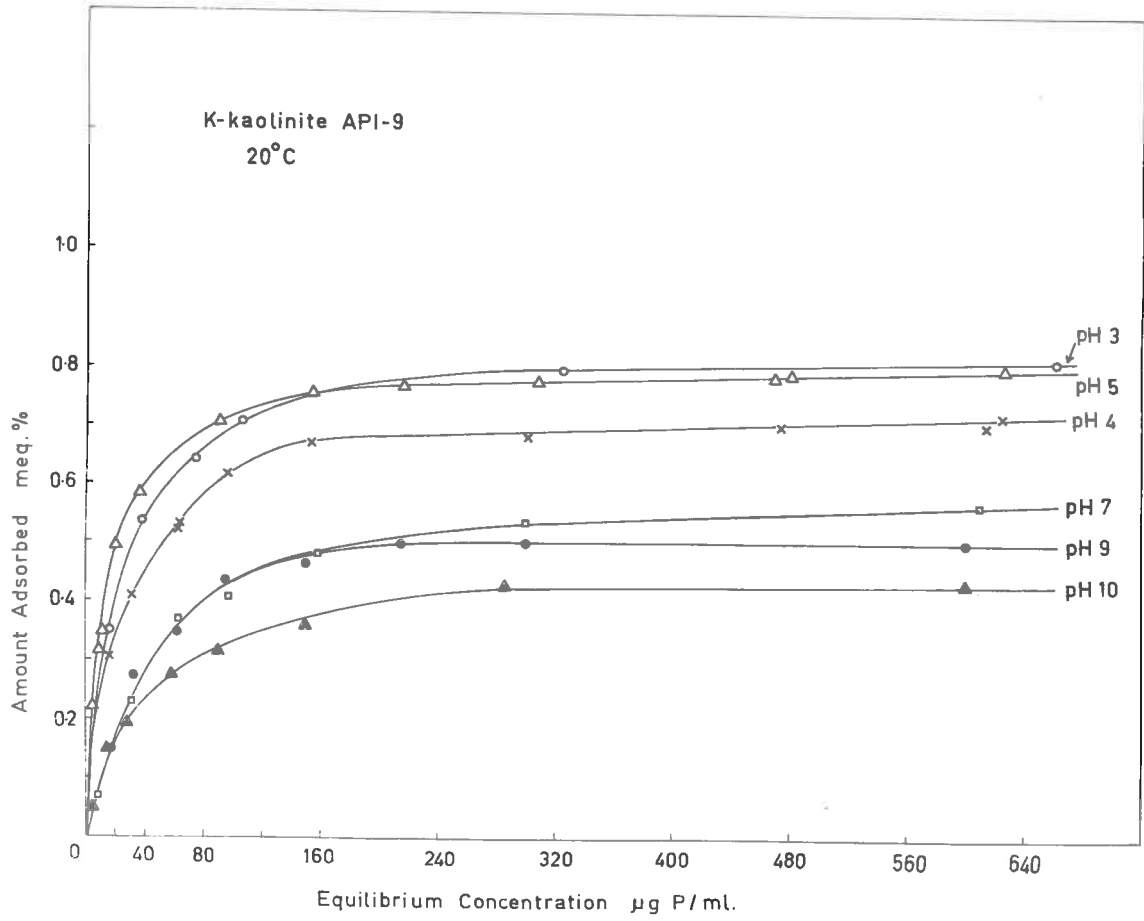


FIGURE 25

ADSORPTION ISOTHERMS (REGION II) AT DIFFERENT pH VALUES

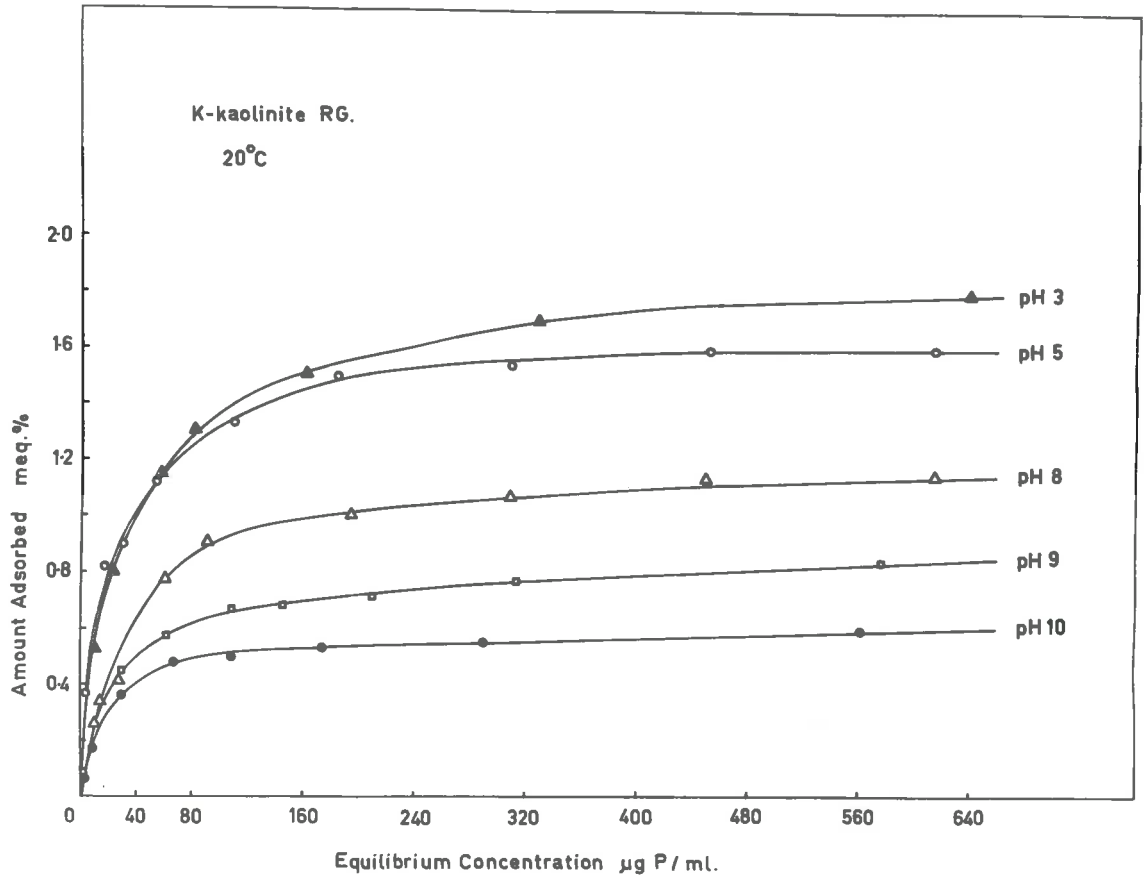


FIGURE 26

ADSORPTION ISOTHERMS (REGION II) AT DIFFERENT pH VALUES

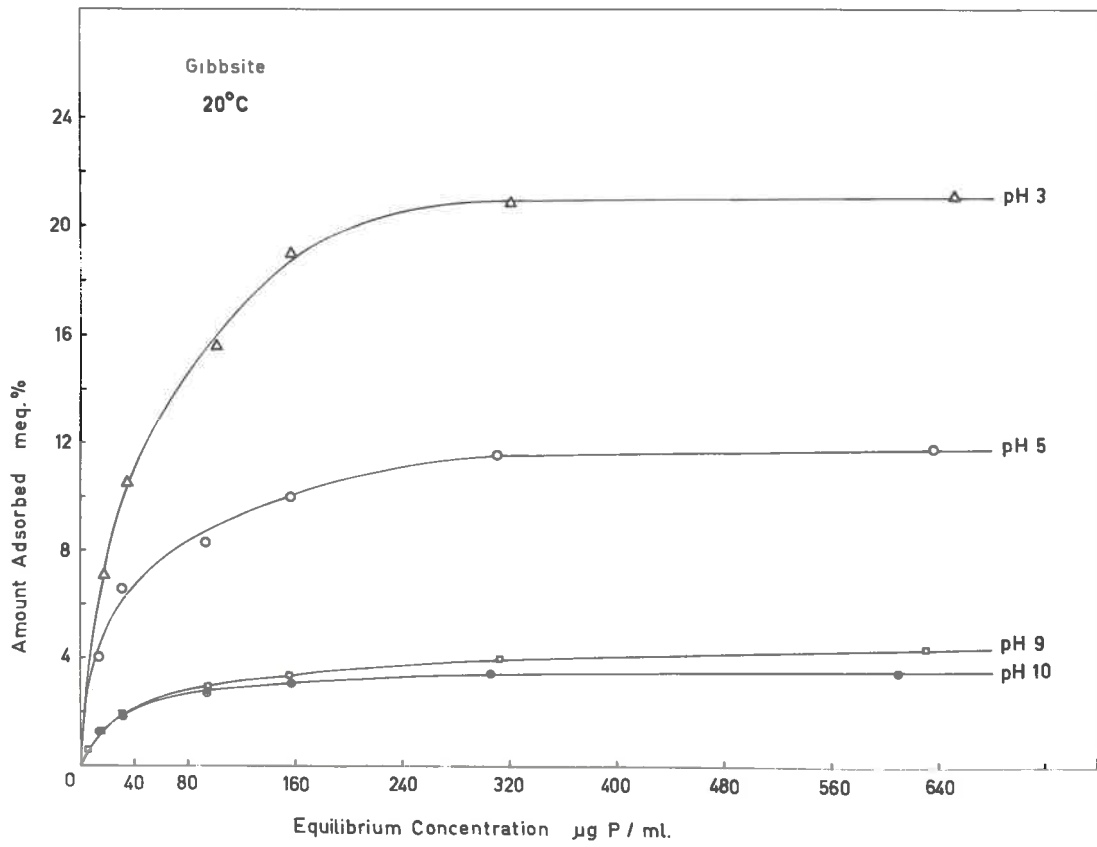


FIGURE 27

ADSORPTION ISOTHERMS (REGION II) AT DIFFERENT pH VALUES

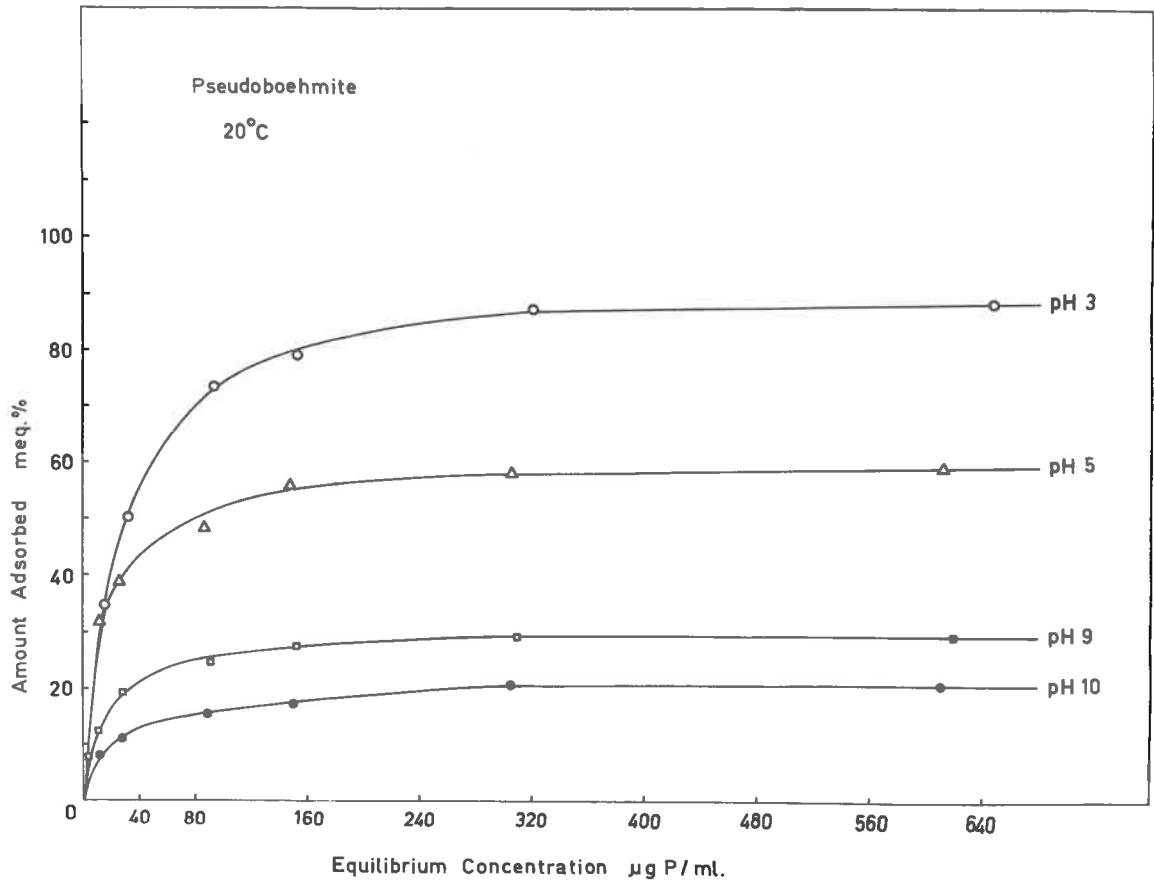
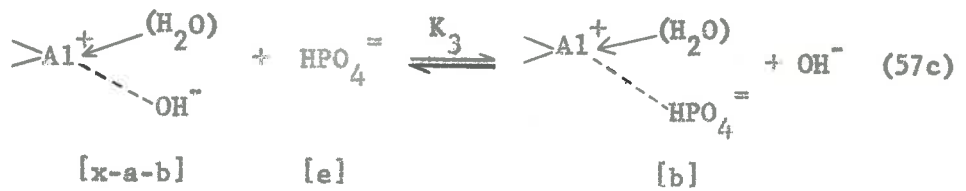
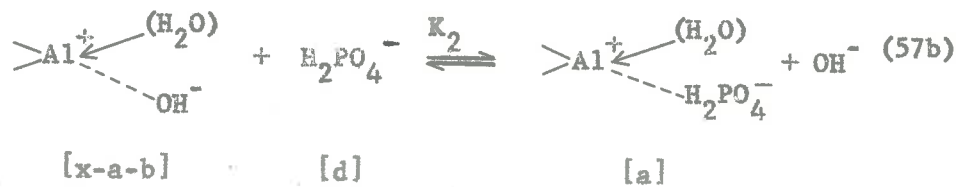
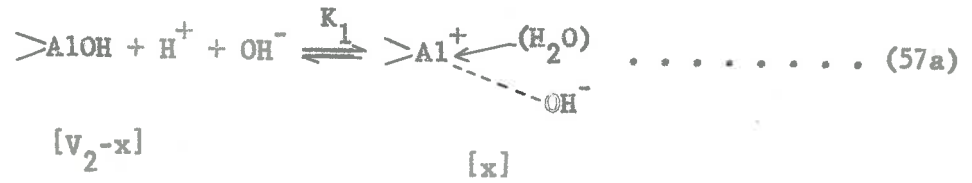


FIGURE 28

equation for region II.

The complete reactions can be represented as follows:-



where K_1 is the equilibrium constant of the uptake of H^+ by the edge aluminium atom.

K_2 is the equilibrium constant of the reaction between adsorption site and $H_2PO_4^-$.

K_3 is the equilibrium constant of the reaction between adsorption site and $HPO_4^{=}$.

K_4 is the equilibrium constant of the distribution of $H_2PO_4^-$ and $HPO_4^{=}$, i.e. K''

V_2 is the total number of potentially reactive (charged) sites.

x is the number of active sites available at any particular pH value.

$(a+b)$ is the total amount of adsorbed phosphate.

Since this region occurs at concentration of $< 10^{-2}M$, it is assumed that activity coefficients are unity. The square bracket thus indicates the concentration of the reacting species. Because OH^- appears on both sides of reactions (57a), (57b) and (57c), it does not appear in the final equations.

The equilibrium constants of the above reactions can be written as follows:-

$$K_1 = \frac{[x]}{[V_2-x][H^+]}$$

$$[x] = \frac{K_1 V_2 [H^+]}{1 + K_1 [H^+]} \dots \dots \dots (58a)$$

$$K_2 = \frac{[a]}{[x-a-b][d]}$$

$$[a] = K_2 [x][d] - K_2 [d](a+b) \dots \dots \dots (58b)$$

$$K_3 = \frac{[b]}{[x-a-b][e]}$$

$$[b] = K_3 [x][e] - K_3 [e](a+b) \dots \dots \dots (58c)$$

Combining equations (58b) + (58c), gives

$$(a+b) = K_2[x][d] + K_3[x][e] - K_2[d](a+b) - K_3[e](a+b) \dots \dots \dots (59a)$$

Rearranging equation (59a), gives

$$(a+b) = \frac{[x] (K_2[d] + K_3[e])}{(1+K_2[d] + K_3[e])} \dots \dots \dots (59b)$$

$$K_4 = \frac{[d]}{[e][H^+]} \quad [d] = K_4[e][H^+]$$

Substituting [d] into $([d] + [e]) = [P]$, where [P] is the total equilibrium concentration of phosphate, gives

$$K_4[e][H^+] + [e] = [P] \quad [e] = \frac{[P]}{1+K_4[H^+]}$$

Substituting the expression for [d] and [e] into equation (59b), produces

$$\begin{aligned} (a+b) &= \frac{[x] (K_2 K_4 [e][H^+] + K_3 [e])}{1 + K_2 K_4 [e][H^+] + K_3 [e]} \\ &= \frac{[x][e] (K_2 K_4 [H^+] + K_3)}{1 + [e] (K_2 K_4 [H^+] + K_3)} \\ (a+b) &= \frac{[x][P] \left(\frac{K_2 K_4 [H^+] + K_3}{1 + K_4 [H^+]} \right)}{1 + [P] \left(\frac{K_2 K_4 [H^+] + K_3}{1 + K_4 [H^+]} \right)} \dots \dots \dots (59c) \end{aligned}$$

Finally [x] from equation (58a) is substituted into equation (59c) to give

$$A = \frac{\left(\frac{K_1 V_2 [H^+] [P]}{1 + K_1 [H^+]} \right) \left(\frac{K_2 K_4 [H^+] + K_3}{1 + K_4 [H^+]} \right)}{1 + [P] \left(\frac{K_2 K_4 [H^+] + K_3}{1 + K_4 [H^+]} \right)} \dots \dots \dots (60a)$$

where $A = (a+b)$ is the total amount of phosphate adsorbed in region II.

Equation (60a) may be written in the form

$$A = \frac{V_m [P] C}{1 + [P] C} \dots \dots \dots (60b)$$

where $V_m = \frac{V_2 K_1 [H^+]}{1 + K_1 [H^+]}$ is the maximum amount of phosphate that can be adsorbed at any particular pH.

C is constant at any pH and equal to $\frac{K_2 K_4 [H^+] + K_3}{1 + K_4 [H^+]}$

Equation (60a) or (60b) is the equation describing the adsorption in region II. It has the familiar form of the Langmuir adsorption isotherm.

Equation (60a) can be written in the linear form as follows:-

$$A + A[P] \left(\frac{K_2 K_4 [H^+] + K_3}{1 + K_4 [H^+]} \right) = \left(\frac{K_1 V_2 [H^+] [P]}{1 + K_1 [H^+]} \right) \left(\frac{K_2 K_4 [H^+] + K_3}{1 + K_4 [H^+]} \right)$$

dividing by A , and rearranging, gives

$$1 + [P] \left(\frac{K_2 K_4 [H^+] + K_3}{1 + K_4 [H^+]} \right) = \frac{[P]}{A} \left(\frac{K_1 V_2 [H^+]}{1 + K_1 [H^+]} \right) \left(\frac{K_2 K_4 [H^+] + K_3}{1 + K_4 [H^+]} \right)$$

$$\frac{[P]}{A} = [P] \left(\frac{1 + K_1 [H^+]}{K_1 v_2 [H^+]} \right) + \left(\frac{1 + K_1 [H^+]}{K_1 v_2 [H^+]} \right) \left(\frac{1 + K_4 [H^+]}{K_2 K_4 [H^+] + K_3} \right) \dots \dots (60c)$$

If $\frac{[P]}{A}$ is plotted against $[P]$, it should give a straight line plot with

$$\text{Slope } S = \frac{1 + K_1 [H^+]}{K_1 v_2 [H^+]} = \frac{1}{v_m}$$

$$\text{intercept } I = \left(\frac{1 + K_1 [H^+]}{K_1 v_2 [H^+]} \right) \left(\frac{1 + K_4 [H^+]}{K_2 K_4 [H^+] + K_3} \right)$$

$$\text{and } \frac{S}{I} = \frac{K_2 K_4 [H^+] + K_3}{1 + K_4 [H^+]} = C$$

The behaviour of the slope S.

The slope S is given by $\frac{1 + K_1 [H^+]}{K_1 v_2 [H^+]}$ or $S = \frac{1}{K_1 v_2 [H^+]} + \frac{1}{v_2}$,

S should not be affected by the species of phosphate ion. If it is plotted against $\frac{1}{[H^+]}$, it should give a straight line with intercept =

$\frac{1}{v_2}$ and Slope = $\frac{1}{K_1 v_2}$. K_1 can be obtained from ratio of intercept and slope where $\frac{\text{intercept}}{\text{slope}} = K_1$.

The behaviour of the ratio $\frac{S}{I} = C$

$$C = \frac{K_2 K_4 [H^+] + K_3}{1 + K_4 [H^+]}$$

- (i) if $K_2 = K_3$, i.e. the affinity of the two species of phosphate ions is the same, C reduces to K_2 . Therefore the ratio $\frac{S}{I}$ would be a constant and independent of pH.
- (ii) if $K_3 \gg K_2$, the ratio becomes

$$C \approx \frac{K_3}{1 + K_4[H^+]}$$
, i.e. C decreases as $[H^+]$ increases
 and $C[H^+]$ will vary linearly with C .
- (iii) if $K_4[H^+] \ll 1$, C becomes

$$C \approx K_2K_4[H^+] + K_3$$

 and C will vary linearly with $[H^+]$.
- (iv) if $K_2K_4[H^+] \gg K_3$, the ratio $\frac{S}{I}$ becomes

$$\frac{1}{C} \approx \frac{1}{K_2K_4[H^+]} + \frac{1}{K_2}$$

 and $\frac{1}{C}$ will vary linearly with $\frac{1}{[H^+]}$.

If the various constants have values intermediate between the limits given above there will be corresponding trends in the values of C .

Treatment of the adsorption data for region II.

To determine the extent of adsorption of phosphate in region II, allowance must be made for the adsorption in region III overlapping into region II.

A correction is obtained by multiplying the slope of the linear isotherm representing region III by the corresponding equilibrium

concentration. This value together with the adsorption for region I, is subtracted from the total adsorption to give region II adsorption values. A typical example of the calculation is given in Table 6 for the adsorption onto K-kaolinite API-9 at pH 5 and 20°C.

The adsorption data derived in the above manner are then used to test equation (60a) or (60c) by plotting $\frac{[P]}{A}$ against [P]. The results for K-kaolinite API-9, K-kaolinite R.G., gibbsite and pseudoboehmite are shown in Figures 29, 30, 31 and 32. As required by equation (60c) the graphs are good straight lines with regression coefficients of about 0.99 for kaolinite API-9, kaolinite R.G., gibbsite and pseudoboehmite (Appendix 12).

The values of the constants in equation (60c) can be determined from the straight line plots and these values are given in Tables 7, 8, 9 and 10.

Equation (60c) shows that if $K_2 = K_3$, i.e. $H_2PO_4^-$ and HPO_4^- ions have equal affinity for the reaction site, the ratio of $\frac{S}{I}$ should be constant and independent of pH value.

The calculated values of the ratio $\frac{S}{I}$ in Tables 7, 8, 9 and 10 show some non-systematic variation with pH, although a statistical analysis shows that the values of $\frac{S}{I}$ at different pH values are not significantly different from the mean value (Appendix 13). Thus it is concluded that the ratio $\frac{S}{I}$ is sufficiently constant to assume that there is no difference in the affinity of the phosphate species for the adsorption sites.

TABLE 6

TREATMENT OF THE ADSORPTION DATA FOR REGION II.

K-KAOLINITE API-9 (pH 5, 20°C).

Equilibrium Concentration		Adsorbed phosphate meq. %	s.c. meq. % $s = \frac{0.95}{1000}$	C.F. ($V_0 + s.c.$) meq. % $V_0 = 0.85$	A (Ads.P-C.F.) meq. %	$\frac{[P]}{A}$ $\times 10^3$
$\mu\text{gP/ml}$ c	meq./ml. [P] $\times 10^3$					
0.74	0.024	0.70	-	0.850	-	-
1.88	0.060	0.88	0.0017	0.852	-	-
5.86	0.189	1.08	0.0055	0.855	0.225	0.84
7.90	0.255	1.16	0.0075	0.857	0.303	0.84
9.16	0.295	1.18	0.0090	0.859	0.320	0.92
12.20	0.394	1.21	0.0116	0.862	0.348	1.13
20.8	0.671	1.36	0.0197	0.869	0.491	1.37
36.6	1.181	1.47	0.0348	0.885	0.585	2.02
91.8	2.96	1.64	0.0872	0.937	0.703	4.20
154.5	4.98	1.75	0.1468	0.997	0.754	6.58
217.0	7.00	1.82	0.2061	1.056	0.766	9.06
311.0	10.04	1.92	0.296	1.145	0.775	12.75
470.0	-	2.07	0.447	1.297	0.783	-
481.0	-	2.09	0.457	1.307	0.79	-
627.5	-	2.24	0.596	1.44	0.80	-

s.c. = slope of region III x equilibrium concentration (meq.%)

s = slope of region III (meq.%/ $\mu\text{gP/ml}$)c = equilibrium concentration ($\mu\text{gP/ml.}$)C.F. = correction factor ($V_0 + s.c.$).

A = phosphate adsorbed in region II. (i.e. Ads.P-C.F.).

LANGMUIR PLOTS (REGION II) AT DIFFERENT pH VALUES

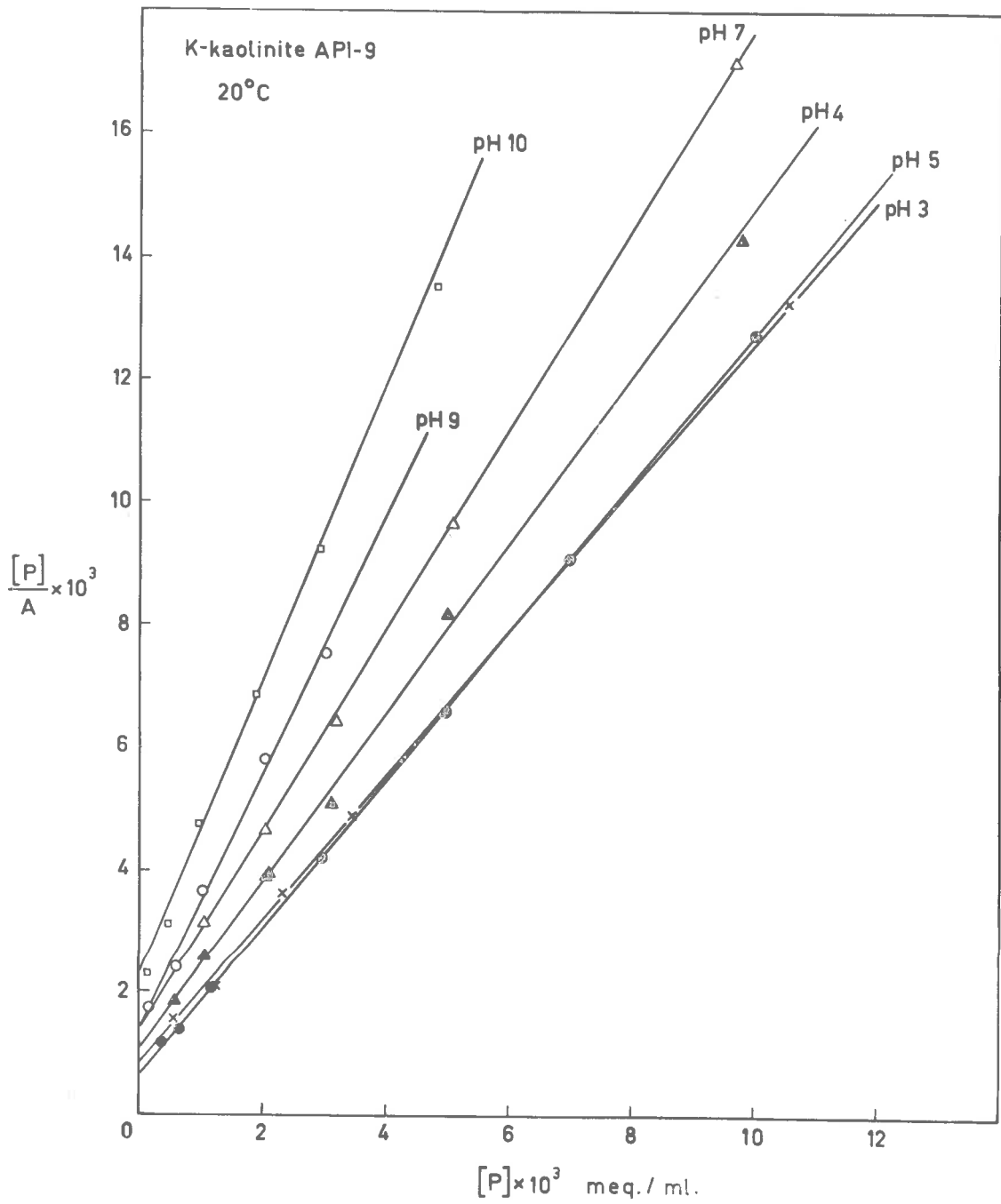


FIGURE 29

LANGMUIR PLOTS (REGION II) AT DIFFERENT pH VALUES

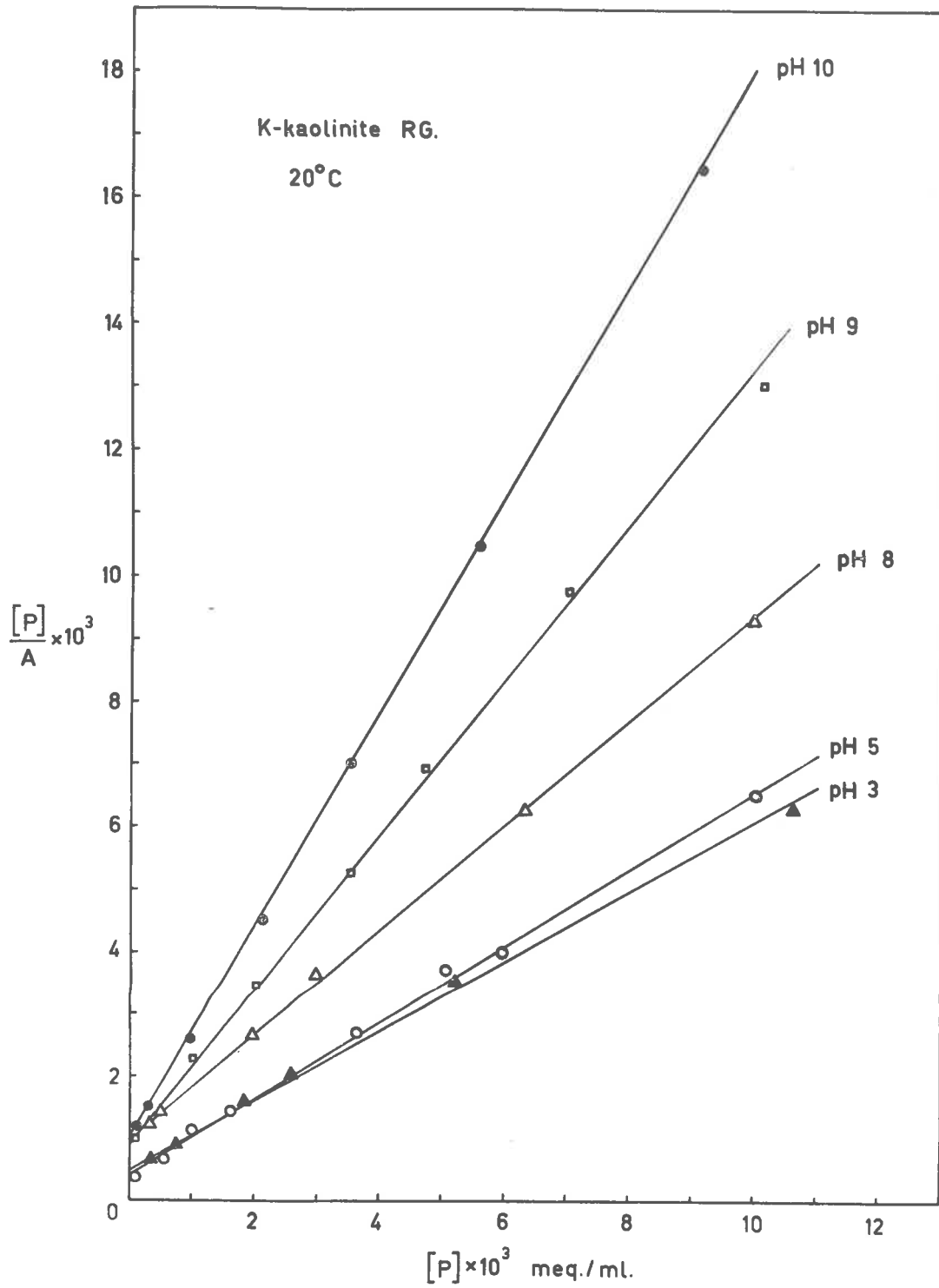


FIGURE 30

LANGMUIR PLOTS (REGION II) AT DIFFERENT pH VALUES

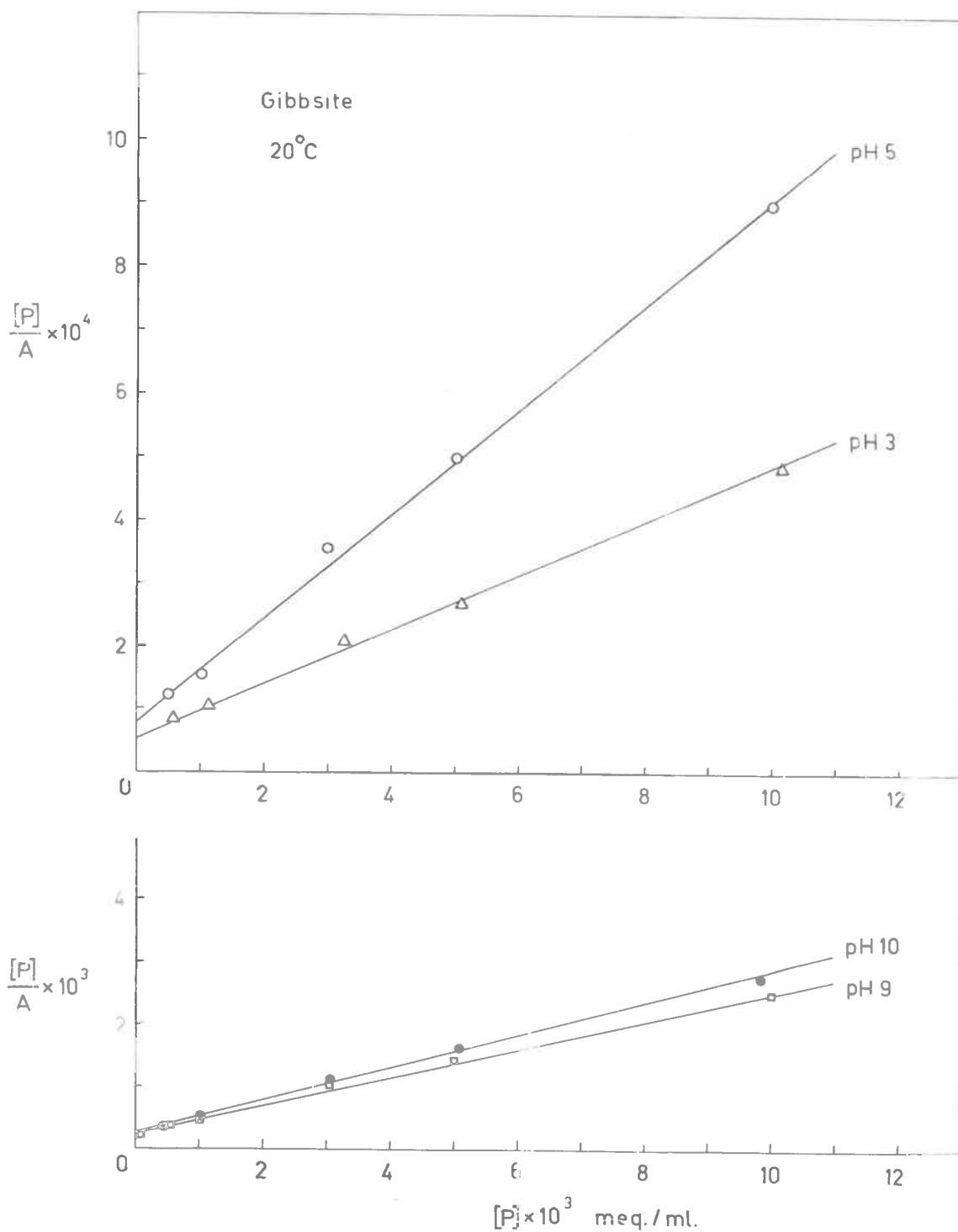


FIGURE 31

LANGMUIR PLOTS (REGION II) AT DIFFERENT pH VALUES

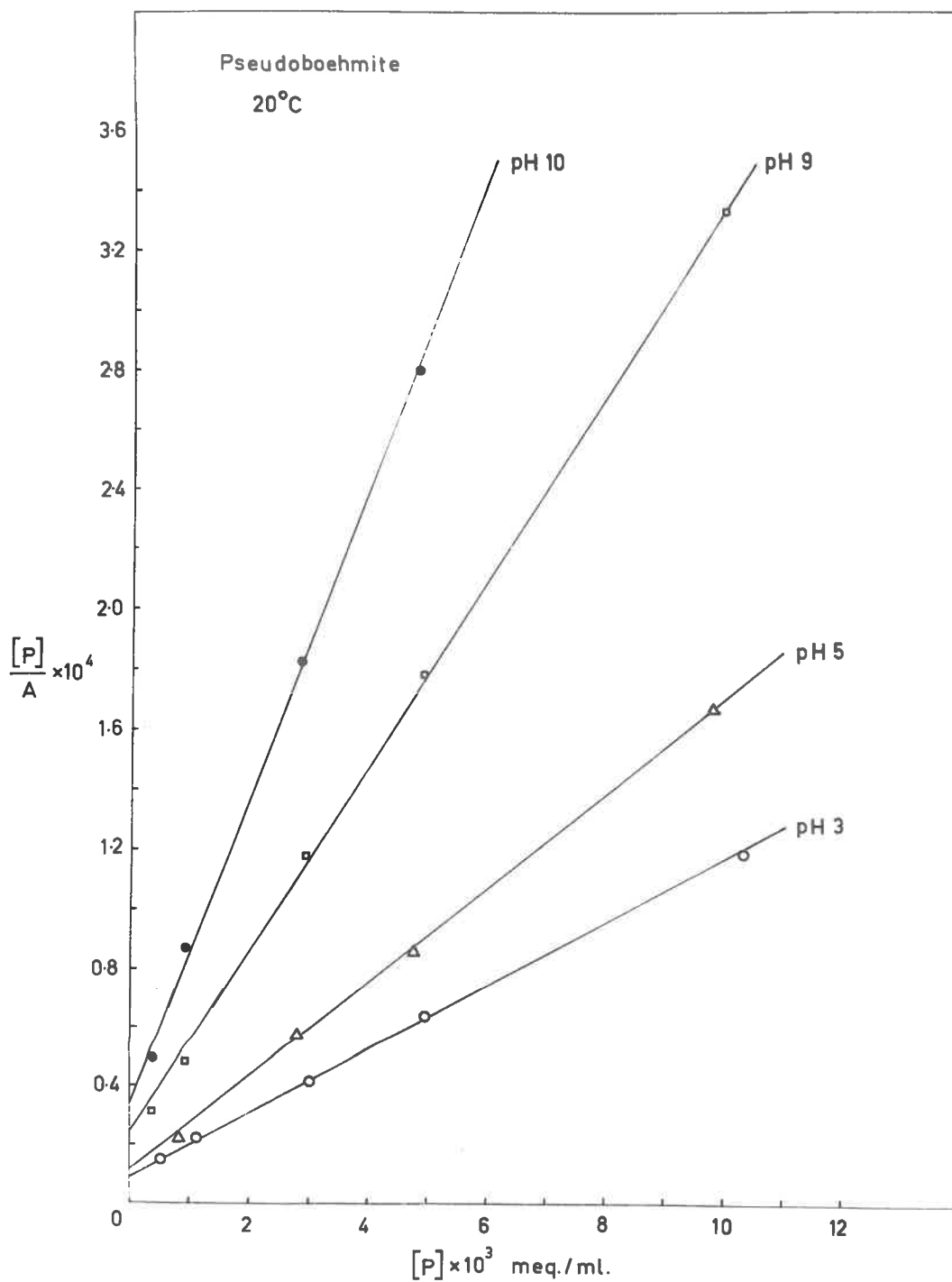


FIGURE 32

TABLE 7

THE CONSTANTS OF EQUATION (50C), DETERMINED FOR K-KAOLINITE API-9 AT 20°C.

pH	Slope S	Intercept I x 10 ³	$V_m = \frac{1}{S}$ (meq.%)	$\frac{S}{I} \times 10^{-3}$ (ml/meq.)
3	1.18	0.81	0.85	1.46
4	1.36	1.10	0.74	1.23
5	1.21	0.62	0.82	1.95
7	1.63	1.32	0.61	1.23
9	2.06	1.37	0.49	1.49
10	2.38	2.20	0.42	1.08
				Average (1.40 ± 0.14)

TABLE 8

THE CONSTANTS OF EQUATION (60c), DETERMINED FOR K-KAOLINITE R.G. AT 20°C

pH	Slope S	Intercept I x 10 ³	$V_m = \frac{1}{S}$ (meq. %)	$\frac{S}{I} \times 10^{-3}$ (ml/meq.)
3	0.55	0.46	1.82	1.19
5	0.62	0.40	1.61	1.55
8	0.90	0.95	1.11	0.95
9	1.25	0.90	0.80	1.39
10	1.60	1.0	0.62	1.60
Average				1.33

TABLE 9

THE CONSTANTS OF EQUATION (60c), DETERMINED FOR GIBBSITE AT 20°C

pH	Slope S x 10	Intercept I x 10 ⁴	$V_m = \frac{1}{S}$ (meq. %)	$\frac{S}{I} \times 10^{-3}$ (ml/meq.)
3	0.48	0.50	20.8	0.96
5	0.80	0.80	12.5	1.00
9	2.25	2.20	4.4	1.02
10	3.00	2.40	3.4	1.25
Average				1.03

TABLE 10

THE CONSTANTS OF EQUATION (60c), DETERMINED FOR PSEUDOBOEHMITE AT 20°C.

pH	Slope S x 10	Intercept I x 10 ⁴	$V_m = \frac{1}{S}$ (meq. %)	$\frac{S}{I} \times 10^{-3}$ (ml/meq.)
3	0.11	0.09	90.2	1.22
5	0.16	0.12	60.6	1.38
9	0.30	0.24	33.3	1.25
10	0.51	0.34	19.6	1.50
Average				1.34

A very significant feature is that the mean values of $\frac{S}{I}$ for different adsorbents is relatively constant. This strongly suggests that the adsorption reaction between phosphate ion and adsorption site in region II is very similar for kaolinites and hydrated aluminium oxides, although the number of adsorption sites (V_m) has very different value.

In Table 11 V_m values together with the edge areas estimated from shadowed electron micrographs (See Appendix 14) and total area determined by low temperature nitrogen adsorption, are given. There is no simple correlation between V_m and total surface area, however there is a slightly better correlation between V_m and the edge area when it is assumed that there are twice as many aluminium atoms per unit edge face area of the gibbsite, as there are for kaolinite.

The value of edge face area for gibbsite of $18.6 \text{ m}^2/\text{g}$. is the minimum estimated area, because it is based on the measurement of the large particles on the shadowed electron micrograph.

It may be appropriate to give some discussion here to the area occupied by a phosphate ion adsorbed on the edge surface. There is no problem with regard to the edge face of kaolinite where the area for each positive charge is 33 \AA^2 (Samson, 1953; Schofield and Samson, 1953). This is determined by the aluminium distances in the crystal and because 33 \AA^2 is considerably greater than the area occupied by a phosphate ion even by the most generous assumption i.e. a sphere of radius 2.9 \AA ($= 27 \text{ \AA}^2$).

For gibbsite, however, the position is very different since

TABLE 11

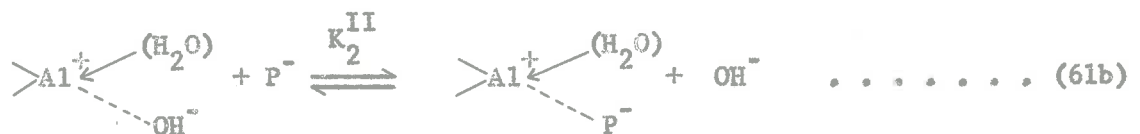
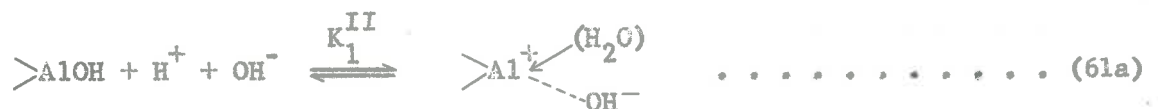
THE VALUES OF V_m (pH 3), K_2^{II} , EDGE FACE AREA AND TOTAL SURFACE AREA AT 20°C

Adsorbent	V_m (pH 3) (meq. %)	Edge face area (m ² /g.)	Total S.A. (m ² /g.)	Mean value $K_2^{II} \times 10^{-3}$ (ml/meq.)
K-kaolinite API-9	0.85	4	12	1.40 \pm 0.14
K-kaolinite R.G.	1.82	5.2	40	1.33
Gibbsite	20.8	18.6	48	1.08
Pseudoboehmite	90.2	-	176	1.34

there would be twice the number of aluminium atoms on the edge, so that the area for one aluminium atom is 16.5 \AA^2 . The best estimate for the area of a phosphate ion is 21 \AA^2 (Olson, 1952), this is the area in an apatite crystal and for adsorption on a surface it is possible that the value may be lower than 21 \AA^2 . With an area of 16.5 \AA^2 per aluminium atom in the edge per adsorbed ion, the edge surface area would be calculated as $20.6 \text{ m}^2/\text{g}$. This is the same order of magnitude as the estimated edge face area from the shadowed electron micrograph.

The adsorption of H_2PO_4^- and HPO_4^{2-} in region II has been found to have the same affinity constant (K_2^{II}) and therefore the reactions in region II can be simplified by replacing H_2PO_4^- and HPO_4^{2-} by P^- . The similarity in the affinity constants is surprising since it might have been expected that the doubly charged ion would have been adsorbed more strongly. However, from results already presented on the concomitant phosphate and potassium adsorption, it appears that at high pH the exchanging species may be $(\text{K}^+\text{HPO}_4^{2-})^-$, sufficient potassium always being present to form the ion pair.

Thus the reactions in region II can be represented by the following equations.



where K_1^{II} and K_2^{II} are the equilibria constants for region II. Similarly the derived adsorption equation for region II (equation 60a) becomes

$$A = \frac{\left(\frac{K_1^{II} v_2 [H^+]}{1 + K_1^{II} [H^+]} \right) K_2^{II} [P]}{1 + K_2^{II} [P]} \dots \dots \dots (62a)$$

or

$$A = \frac{v_m K_2^{II} [P]}{1 + K_2^{II} [P]}$$

where $v_m = \frac{v_2 K_1^{II} [H^+]}{1 + K_1^{II} [H^+]}$

and equation (60c) becomes

$$\frac{[P]}{A} = [P] \left(\frac{1 + K_1^{II} [H^+]}{K_1^{II} v_2 [H^+]} \right) + \left(\frac{1 + K_1^{II} [H^+]}{K_1^{II} K_2^{II} v_2 [H^+]} \right) \dots \dots \dots (62b)$$

Determination of constants v_2 and K_1^{II} from the slope S of equation (62b).

$$\text{The slope } S = \frac{1}{v_m} = \frac{1 + K_1^{II} [H^+]}{K_1^{II} v_2 [H^+]}$$

or

$$S = \frac{1}{v_2 K_1^{II} [H^+]} + \frac{1}{v_2} \dots \dots \dots (63)$$

The slopes of the Langmuir plots fit the above equation as shown by the regression analysis with a regression coefficient of 0.8 to 0.9. When the results are plotted (Figures 33, 34) in the form of

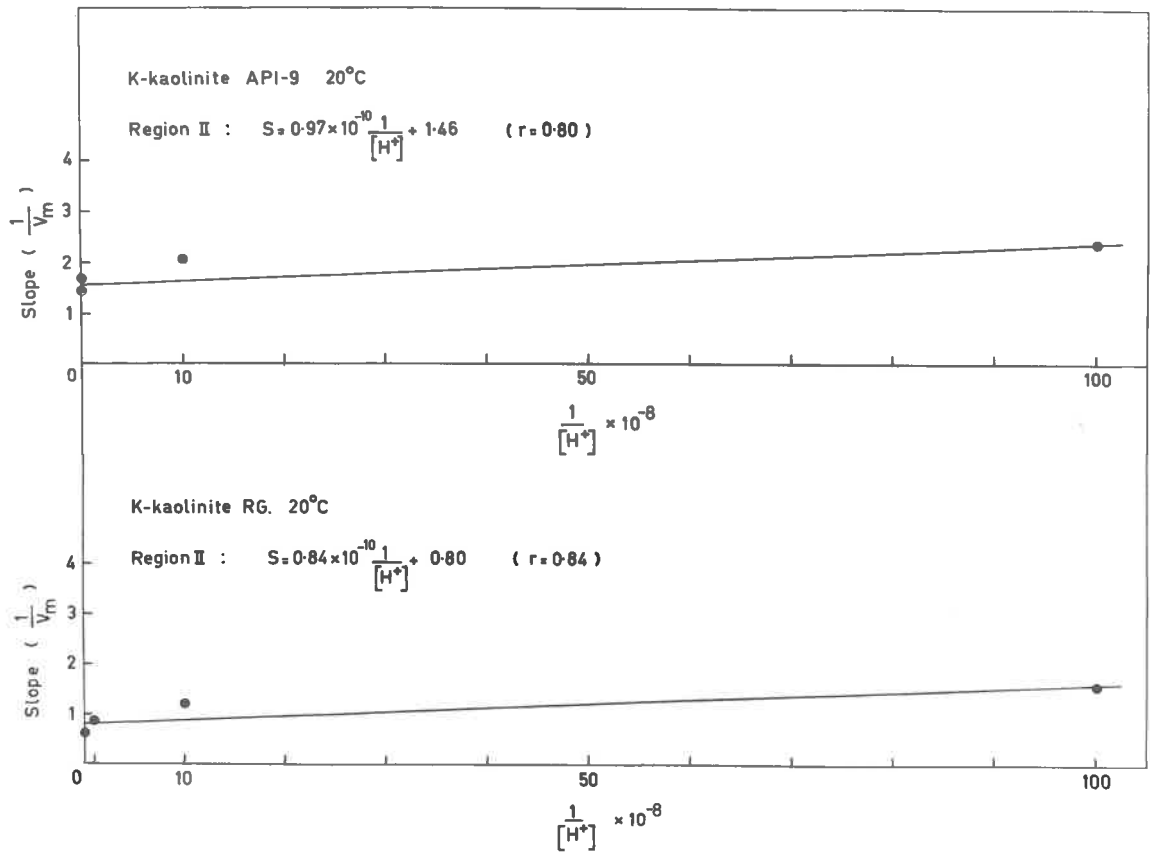


FIGURE 33

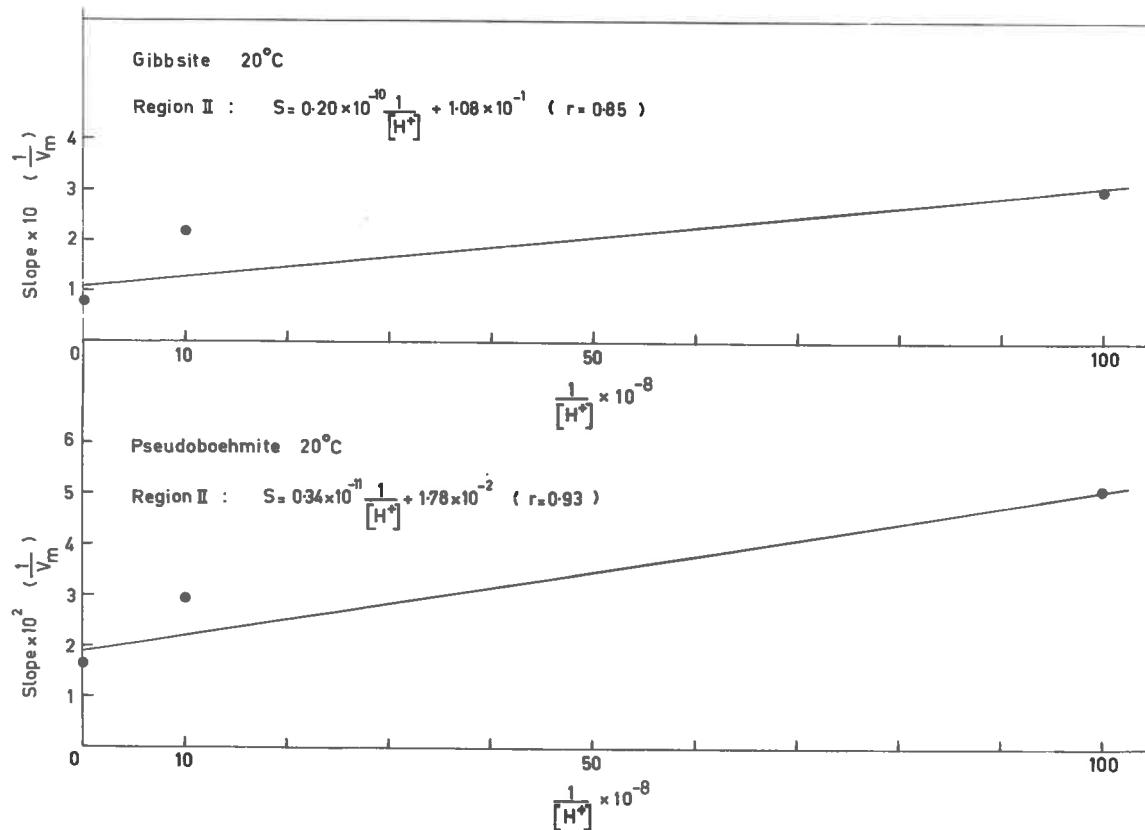


FIGURE 34

RELATION BETWEEN V_o (REGION I) AND V_m (REGION II)

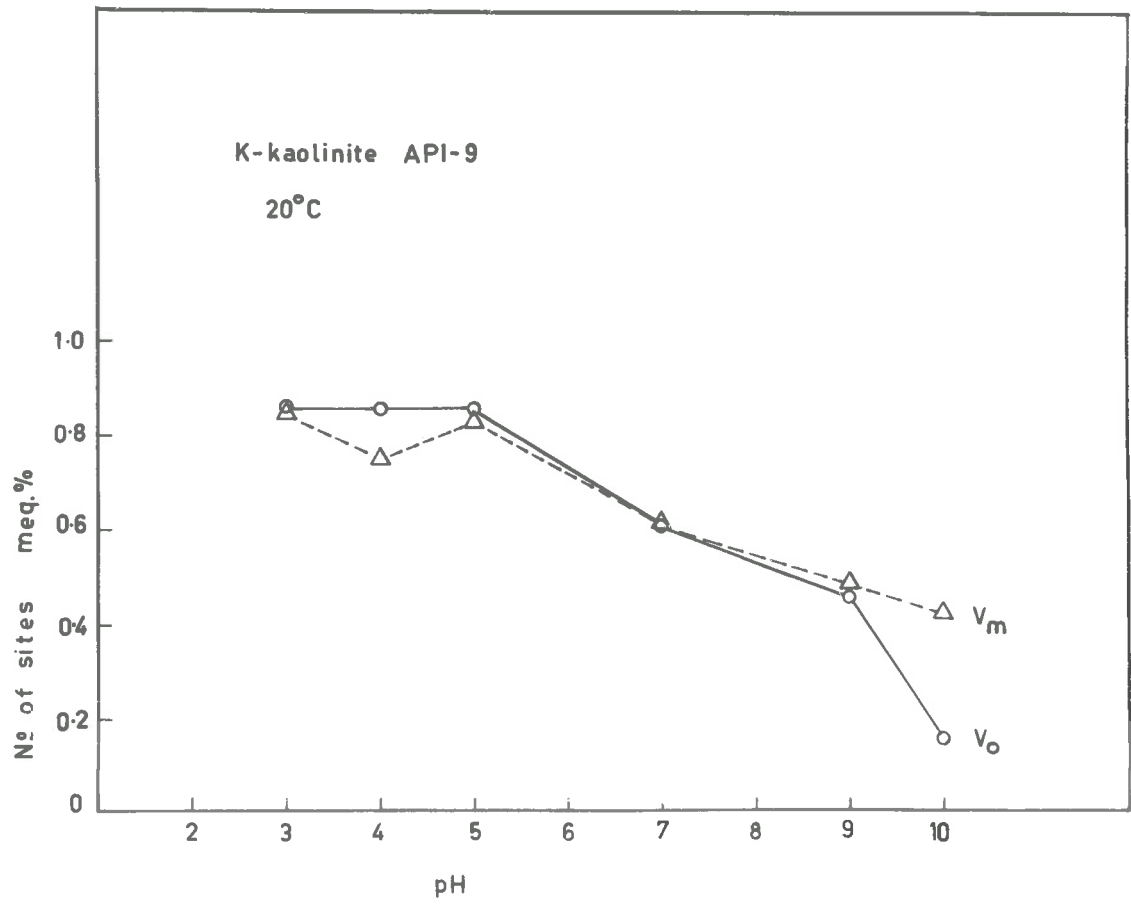


FIGURE 35

TABLE 12

K_1^{II} , V_2 and the regression coefficient of equation (63), for K-kaolinite
API-9, at 20°C.

pH	Slope S	$\frac{1}{[H^+]}$	Reg. coeff.	V_2 (meq. %)	$K_1^{II} \times 10^{-10}$ (ml/meq.)
3	1.18	10^3			
4	1.36	10^4			
5	1.21	10^5			
7	1.63	10^7			
9	2.06	10^9			
10	2.38	10^{10}			
			0.80	0.68 ± 0.06	1.50 ± 0.58

TABLE 13

K_1^{II} , V_2 and the regression coefficient of equation (63), for K-kaolinite
R.G. at 20°C.

pH	Slope S	$\frac{1}{[H^+]}$	Reg. coeff.	V_2 (meq. %)	$K_1^{II} \times 10^{-10}$ (ml/meq.)
3	0.55	10^3			
5	0.62	10^5			
8	0.90	10^8			
9	1.25	10^9			
10	1.60	10^{10}			
			0.84	1.25 ± 0.14	0.96 ± 0.37

TABLE 14

K_1^{II} , V_2 and the regression coefficient of equation (63) for gibbsite at 20°C.

pH	Slope S x 10	$\frac{1}{[H^+]}$	Reg. coeff.	V_2 (meq. %)	$K_1^{II} \times 10^{-10}$ (ml/meq.)
3	0.48	10^3			
5	0.80	10^5			
9	2.25	10^9			
10	3.00	10^{10}			
			0.85	9.3 ± 4.3	0.6 ± 0.4

TABLE 15

K_1^{II} , V_2 and the regression coefficient of equation (63) for pseudoboehmite
at 20°C

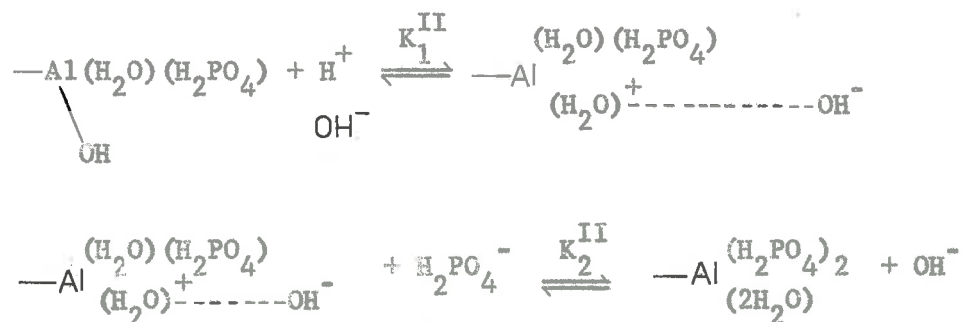
pH	Slope S x 10	$\frac{1}{[H^+]}$	Reg. coeff.	V_2 (meq. %)	$K_1^{II} \times 10^{-10}$ (ml/meq.)
3	0.11	10^3			
5	0.16	10^5			
9	0.30	10^9			
10	0.51	10^{10}			
			0.90	56 ± 15.6	0.55 ± 0.25

TABLE 16

The constants V_1 and K_1^I for region I, and V_2 , K_1^{II} and K_2^{II} for region II at 20°C.

Adsorbent	Region I		Region II		
	V_1 (meq. %)	$K_1^I \times 10^{-10}$ (ml/meq.)	V_2 (meq. %)	$K_1^{II} \times 10^{-10}$ (ml/meq.)	$K_2^{II} \times 10^{-3}$ (ml/meq.)
K-kaolinite API-9	0.72 \pm 0.08	(0.26 \pm 0.03)	0.68 \pm 0.06	(1.50 \pm 0.58)	(1.40 \pm 0.14)
K-kaolinite R.G.	0.86 \pm 0.06	(0.54 \pm 0.16)	1.25 \pm 0.14	(0.96 \pm 0.37)	1.33
Gibbsite	15.9 \pm 5.2	(0.38 \pm 0.2)	9.3 \pm 4.3	(0.60 \pm 0.4)	1.08
Pseudoboehmite	98.0 \pm 13.5	(0.85 \pm 0.3)	56.0 \pm 15.6	(0.55 \pm 0.25)	1.34

Region II.



It is not possible to say with certainty what type of phosphorus compounds exist in regions I, II and III. However, it may be that these phosphate species exist only as surface complexes having no three dimensional counterpart.

The free energy change (ΔG) of phosphate adsorption (Table 16a) was calculated from the equilibria constants, K_1^{I} , K_1^{II} and K_2^{II} , using equation (41a):

$$\Delta G = -RT \ln K$$

where K_1^{I} is the equilibrium constant defined by equation (54).

K_1^{II} and K_2^{II} are the equilibria constants defined by equation (62a).

For adsorption to take place, it must be accompanied by a decrease in the free energy of the system, thus ΔG is negative (Table 16a).

It should be noted from Table 16a that the value of ΔG of regions I and II for different adsorbents is relatively constant, indicating that the adsorption of phosphate for different adsorbents consists of the same basic mechanism.

TABLE 16a

FREE ENERGY CHANGE (ΔG) OF PHOSPHATE ADSORPTION FOR
DIFFERENT ADSORBENTS AT 20°C

Adsorbent	Region I	Region II	
	ΔG (Step 1) Kcal./mole	ΔG (Step 1) Kcal./mole	ΔG (Step 2) Kcal./mole
K-kaolinite API-9	-12.60	-13.60	-4.20
K-kaolinite R.G.	-13.0	-13.35	-4.17
Gibbsite	-12.80	-13.10	-4.06
Pseudoboehmite	-13.30	-13.0	-4.18

1.2.3. The effect of pretreatment at pH₁ (0.1 N HCl).

It was suggested earlier that the adsorption of phosphate in the linear part of the isotherm (region III) might be due to a penetration into some amorphous or semi-crystalline region of the clay which was not removed during the preparation of the potassium-clay.

Deshpande, Greenland and Quirk (private communication) have shown that repeated acid washing of clay mineral kaolinites at pH 1 (0.1 N HCl) dissolves only a small amount of aluminium and silicon in the ratio of about 1. Most of this silicon and aluminium was released in the first wash with little more being liberated in subsequent washings. They believe that this is due to the removal of some form of aluminium hydroxide, alumina or some part of the clay which is less crystalline than the bulk mineral.

The ratio of the aluminium and silicon released into solution, on acid washing of kaolinite API-9, was also found to be approximately 1 (see Appendix 2).

The effect of pretreatment at pH 1 on the clay mineral has been examined by determining the positive and negative charge distribution of the acid treated and untreated kaolinite using the method of Schofield (1949). The electric charge distribution (Figure 16) clearly shows that the positive and negative charges of the acid treated and untreated kaolinite are exactly the same over the entire range of pH values from 3 to 9. This result indicates that the kaolinite API-9 is free from any large amount of contamination with amorphous material carrying a high charge such as allophane (Fieldes and Schofield, 1960). The

unchanged charge distribution also indicates that the acid treatment could not have decomposed the kaolinite crystal (Sumner, 1962) and thus the surface properties of the kaolinite is not altered by the treatment. Further examination of the clay in the electron microscope showed no detectable difference between the acid treated and the untreated samples (Figures 36a, 36b).

The phosphate adsorption isotherm on acid treated kaolinite in the presence of 0.1 N KCl has shown that acid washing has had little effect in reducing regions I and II, but has almost eliminated region III (Figure 14). It is concluded from this result that the adsorption of phosphate in region III is associated with the less crystalline material of the clay surface. The main difference between various parameters of untreated and acid treated kaolinite (Table 17) lies in the slope of region III.

It is of interest to note the effect of acid pretreatment on the parameters describing regions I, II and III of acid treated gibbsite and untreated gibbsite (Table 18).

The pronounced effect of acid pretreatment on regions I and II (Table 18) has been attributed to the nature of the surface of the synthetic gibbsite (hydrated aluminium oxide) which is more sensitive to acid attack than kaolinite. Thus it is suggested that the surface properties of the gibbsite have been significantly altered by the acid treatment.

The small effect of acid treatment on region III may be due to the ability of Al^{3+} to form an amorphous $Al(OH)_3$ precipitate on the

Figure 36a

Electron micrograph

Untreated K-kaolinite API-9 (control)

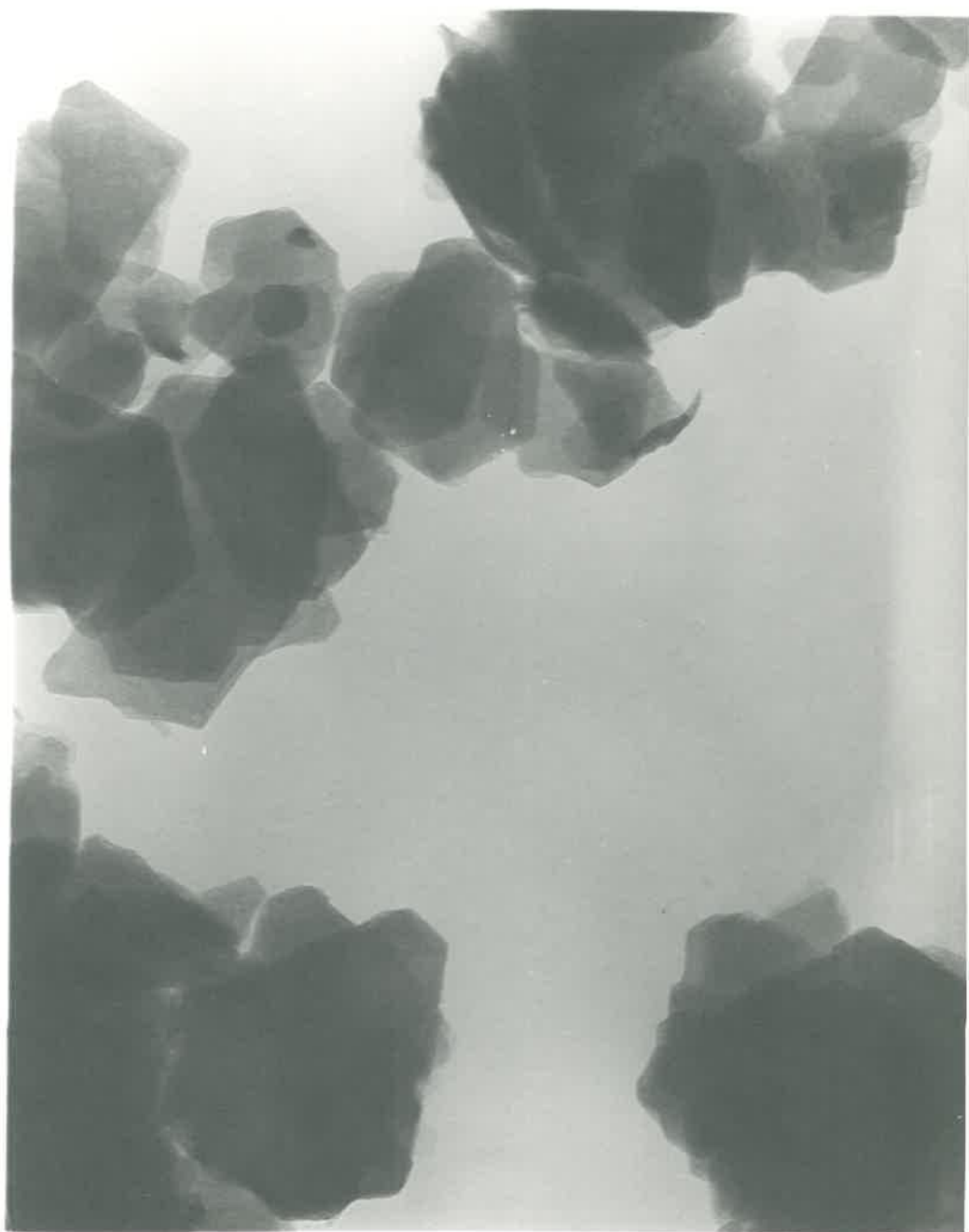
Magnification : 90,000 x

Scale : 1 μ



Shadowed using Au/Pd (Gold-Palladium)

(Siemens Elmiskop 1)



100

100

100

100

100

Figure 36b

Electron micrograph

Acid treated (0.1N HCl) K-kaolinite API-9

Magnification : 90,000 x

Scale : 1 μ



Shadowed using Au/Pd (Gold-Palladium)

(Siemens Elmiskop 1)

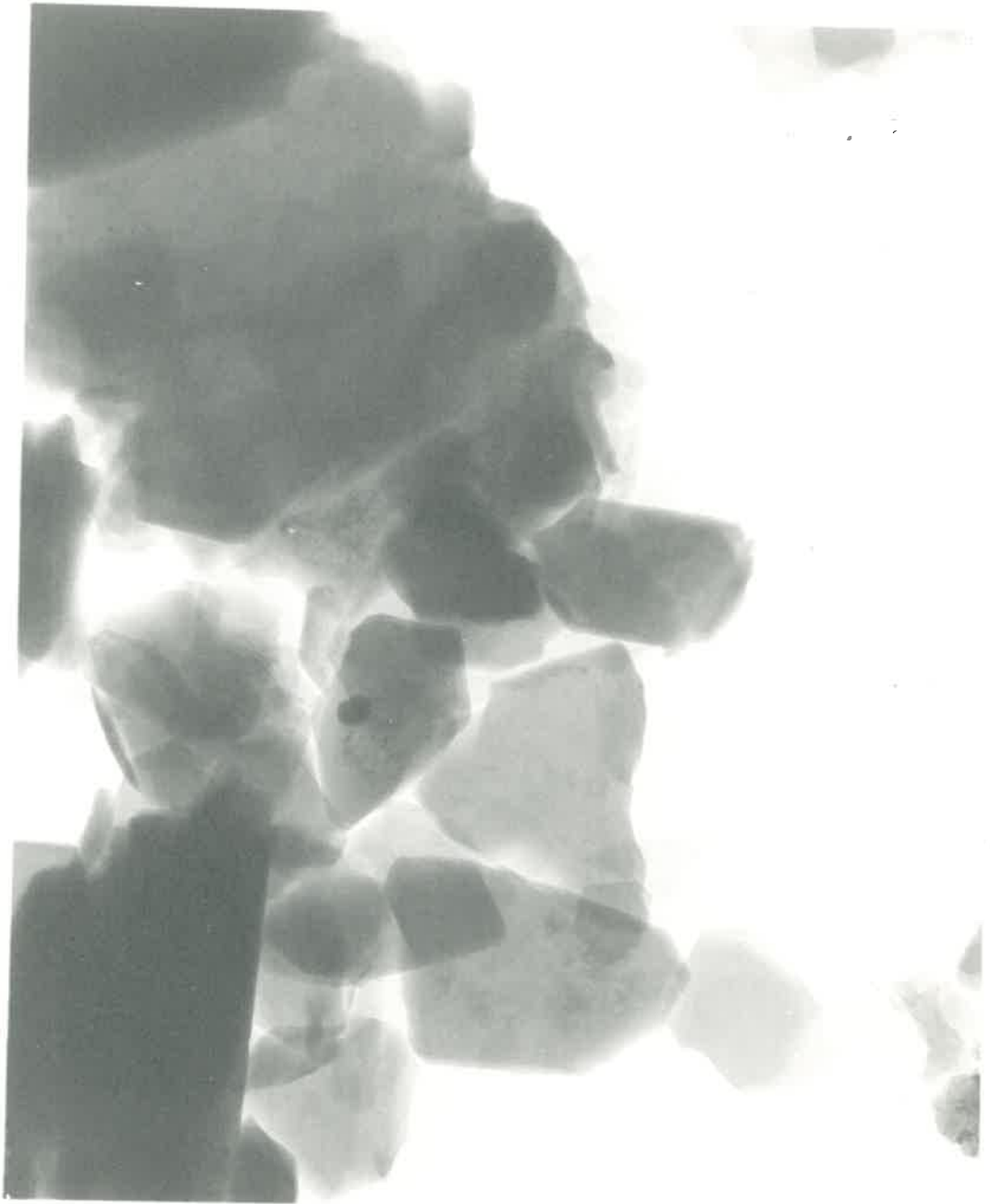


TABLE 17

THE PARAMETERS DESCRIBING REGIONS I, II AND III OF UNTREATED AND ACID TREATED K-KAOLINITE API-9 IN 0.1 N KCl (pH 5, 20°C).

System	Region I	Region II		Region III
	V_o (meq. %)	V_m (meq. %)	$K_2^{II} \times 10^{-3}$ (ml/meq.)	Slope (ml/100g.)
Untreated K-kaolinite	0.85	0.3	1.08	38.1
Acid treated K-kaolinite	0.75	0.7	1.0	6.2

TABLE 18

THE PARAMETERS DESCRIBING REGIONS I, II AND III OF UNTREATED AND ACID
TREATED GIBBSITE (pH 5, 20°C)

System	Region I	Region II		Region III
	V_o (meq. %)	V_m (meq. %)	$K_2^{II} \times 10^{-3}$ (ml/meq.)	Slope (ml/100 g.)
Untreated Gibbsite	22	12.5	1.08	550
Acid treated Gibbsite	10	7.7	1.80	484

gibbsite surface as the pH increases, during the washing of the excess acid with distilled water.

1.2.4. Region III.

The adsorption isotherms of phosphate in region III on all the material examined are linear, their slopes passing through a maximum at neutrality (pH 7). The linearity of the isotherm indicates that either the number of adsorption sites remains constant even though the amount of solute adsorbed increases or that the number of sites is large compared with the amount adsorbed. If the former is the case it suggests that the solute can swell the substrate structure exposing a fresh site on which the next molecule can be adsorbed. Giles et al (1960) have suggested that this process takes place most readily in the less ordered or amorphous regions of the adsorbent, the crystalline material being impenetrable. If the molecular dimensions are suitable, the adsorbate could penetrate to a region in the substrate not already available to the solvent.

The effect of pH on the slope of region III may be due to some reduction in the number of sites occurring at the lower pH value, while the hydroxyl ions compete for the sites at the higher pH value. It is likely that an aluminium compound is implicated, since region III exists for gibbsite and pseudoboehmite.

It has been shown that adsorption of phosphate in region III on acid treated K-kaolinite (0.1 N HCl) is almost eliminated, whereas the adsorption in regions I and II is hardly affected. This result supports the suggestion that the adsorption of phosphate in region III

is connected with some less crystalline material, associated with the clay surface, which is readily removed by washing at pH 1.

Surface areas calculation from phosphate adsorption.

From considerations of the crystal structure of kaolinite, Samson (1953), Schofield and Samson (1953) have suggested that there is one positively charged aluminium per 33 \AA^2 of edge face. The area of 33 \AA^2 for each site is considerably greater than the area occupied by a phosphate ion. Using this value, therefore, the area required to accommodate one milliequivalent of phosphate as monolayer is about 198 m^2 .

The maximum amount of phosphate adsorbed onto K-kaolinite API-9 in the present experiments is 5.5 meq. % at pH 7, 20°C , at a bulk concentration of 0.1 M. The total area occupied by this phosphate would be about $10.8 \text{ m}^2/\text{g}$.

The surface area of K-kaolinite API-9 measured using low temperature N_2 adsorption was $12 \text{ m}^2/\text{g}$. The edge face area of the clay particle as estimated from a shadowed electron micrograph was $4 \text{ m}^2/\text{g}$. (for details of the calculation see Appendix 14). If the edge face is the only surface capable of adsorbing phosphate, then the maximum available area for adsorption is only about $4 \text{ m}^2/\text{g}$. The maximum amount of phosphate adsorbed in regions I and II corresponds to an area of $3.1 \text{ m}^2/\text{g}$, which is well within the limit of edge face area of $4 \text{ m}^2/\text{g}$. However, the amount of phosphate adsorbed in region III calculated from the phosphate isotherm would correspond to an area of $7.7 \text{ m}^2/\text{g}$, which is more than the value of edge face area of $4 \text{ m}^2/\text{g}$. It may be seen from

the isotherm that adsorption of phosphate in region III (linear isotherm) has not reached the limit and therefore adsorption in region III is most likely to be associated with some penetration into less crystalline region of the clay crystal.

Similar calculations have also been made for K-kaolinite R.G., which has a surface area of $40 \text{ m}^2/\text{g}$, as measured using low temperature N_2 adsorption. The estimated edge face area calculated from the shadowed electron micrograph was about $5 \text{ m}^2/\text{g}$. The amount of phosphate adsorbed at pH 5, 20°C , on K-kaolinite R.G. is about 8 meq.%, and this would occupy an area of $15.8 \text{ m}^2/\text{g}$.

The maximum amount of phosphate adsorbed in regions I and II for K-kaolinite R.G. would correspond to an area of $5.1 \text{ m}^2/\text{g}$, which agrees well with the edge area of $5 \text{ m}^2/\text{g}$. However, the amount of phosphate adsorbed in region III corresponds to an area of $10.6 \text{ m}^2/\text{g}$, which is more than the available edge face area of $5 \text{ m}^2/\text{g}$.

Therefore these calculations suggest that the linear part of the isotherm (region III) is most likely due to penetration into some less ordered or amorphous region of the clay crystal.

Potassium uptake.

A significant feature in the results for kaolinite API-9 at pH 5 where the species of phosphate in solution is H_2PO_4^- , is that an almost 1:1 correspondence is found for potassium and phosphate adsorption, while at pH 9, where the species is HPO_4^{2-} the ratio is almost 2:1 (Figure 17). Furthermore, the results (Figure 18) for the

hydrated aluminium oxides show that there is no adsorption of potassium until adsorption into region III takes place. Adsorption of potassium then occurs in stoichiometric amounts with the phosphate adsorbed in region III (Figure 19).

Any direct dependency on the potassium ion for phosphate adsorption in regions I and II would lead to a Langmuir expression involving the product of $[K][P]$ or $[P]^2$. This is not the case, in agreement with the concept of an ion exchange process involving OH^- and a phosphate ion. It is suggested that the KOH produced by the exchange process is taken up by the clay, since it was found in preliminary experiments that the clay will readily take up KOH, acting as a buffer.

Alternatively potassium may replace one of the hydrogen ions of the adsorbed phosphate. However, the adsorption of potassium by gibbsite and pseudoboehmite does not occur until there is adsorption of phosphate into region III, suggesting that potassium adsorption is not a necessity until region III is reached. Thus the KOH produced as a result of the exchange in regions I and II could well be reacting with the clay. The coupled adsorption of potassium and phosphate in region III may be due to penetration of $K^+H_2PO_4^-$ into some less crystalline region on the clay surface.

It is concluded from the measurement of potassium adsorption that the reaction of phosphate in region III is distinct from those in regions I and II.

III.2. LOCATION OF THE SITES

It has been suggested earlier that the site most likely to be responsible for phosphate adsorption in regions I and II is the aluminium atom, in the form of $\text{—Al} \begin{matrix} \text{OH} \\ \text{OH} \end{matrix}$, situated on the edge of the crystal, while the adsorption in region III might be due to some penetration into a less ordered region of the crystal surface.

One of the important problems requiring further clarification is the nature and location of the adsorption sites of the various regions. With this in mind experiments were carried out on the following kaolinite API-9 preparations:

- (i) Aluminium-kaolinite.
- (ii) Sodium-kaolinite.
- (iii) Potassium-halloysite.

In addition some experiments were carried out at different temperatures, which will be presented in Part III.3.

2.1. Results

2.1.1. The effect of aluminium associated with the exchange sites.

It was pointed out earlier that aluminium on the exchange sites may play an important role in the adsorption of phosphate in region I. It was therefore decided to examine the adsorption of phosphate on Al-kaolinite.

The adsorption isotherm of phosphate at pH 5, 20°C on Al-kaolinite was determined, and shown in Figure 37. Comparing this with

PHOSPHATE ADSORPTION BY POTASSIUM AND ALUMINIUM KAOLINITES

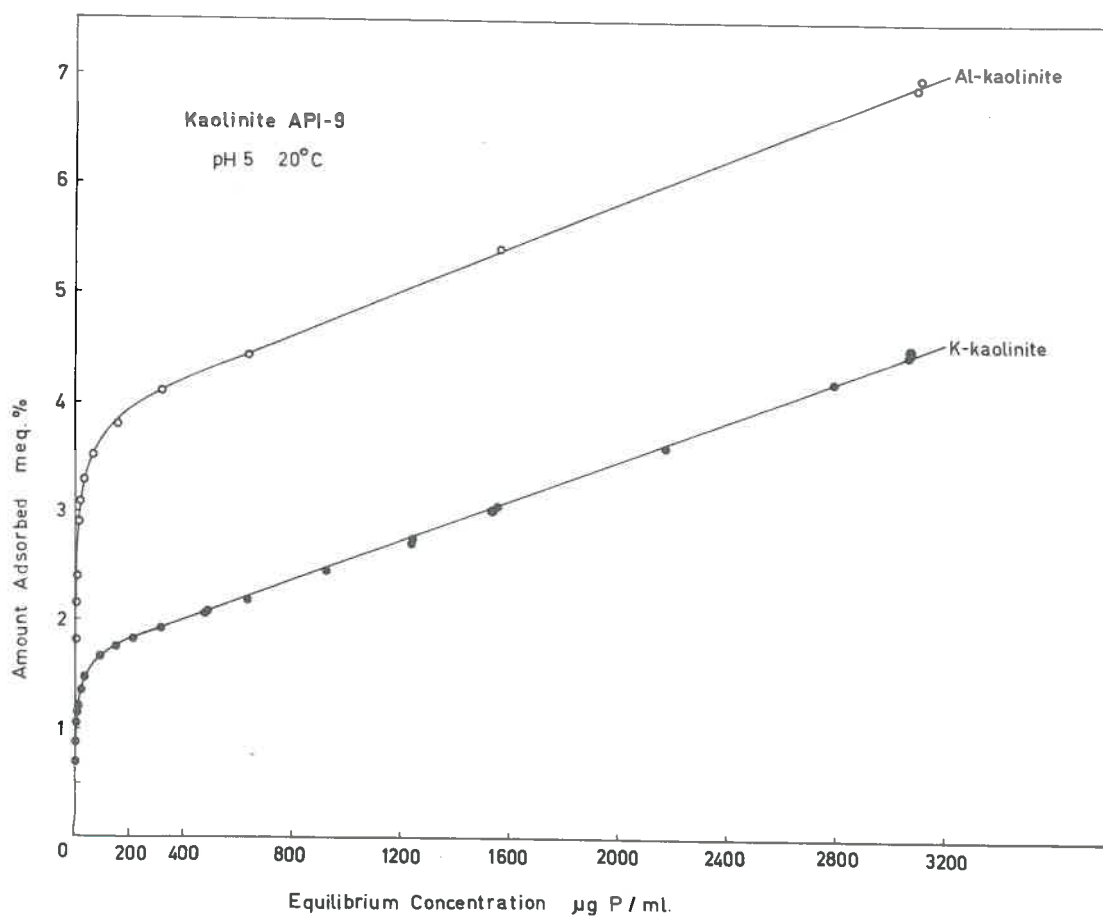


FIGURE 37

TABLE 19

THE PARAMETERS DESCRIBING REGIONS I, II and III OF K-KAOLINITE

API-9 AND Al-KAOLINITE API-9. (pH 5, 20°C)

System	Region I	Region II		Region III
	V_o (meq. %)	V_m (meq. %)	$K_2^{II} \times 10^{-3}$ (ml/meq.)	Slope (ml/100 g.)
K-kaolinite	0.85	0.82	(1.40 \pm 0.14)	29.4
Al-kaolinite	2.10	1.80	1.90	29.4

the isotherm on K-kaolinite (pH 5, 20°C), it is obvious that the extent of region I is increased considerably i.e. from 0.85 meq. % to 2.10 meq. %. Region II is also increased while adsorption in region III is not affected since its slope is unchanged. Table 19 gives the value of the parameters describing regions I, II and III. The values of V_m and K_2^{II} were determined from the Langmuir plots (Figure 40).

The value of K_2^{II} is not significantly changed while V_m is increased to almost the same extent as region I.

Cashen (1959) considered that aluminium was introduced onto the exchange sites from the lattice as the excess salt is removed when washing the clay suspension with distilled water. He believed that this is caused by an increase in potential difference across the clay interface as the salt concentration is lowered. It was thought that if the electrolyte concentration was not reduced too much during the preparation of the clay, aluminium release from the lattice would be reduced and the amount of aluminium on the exchange sites minimized.

An adsorption isotherm on K-kaolinite API-9 which had never been washed below 0.1 N KCl was compared with the standard preparation of K-kaolinite API-9 (washed in distilled water), in the presence of 0.1 N KCl. The results in Figure 38 show only minor differences for the two kaolinites. Both regions I and II are practically unchanged, suggesting that region I is not due to aluminium released in this way.

Acid washing at pH 1 might be expected to make a considerable reduction in any aluminium on the exchange sites of kaolinite. The actual reduction is only very small (V_0 in Table 17).

EFFECT OF SALT AND INITIAL TREATMENTS ON ADSORPTION

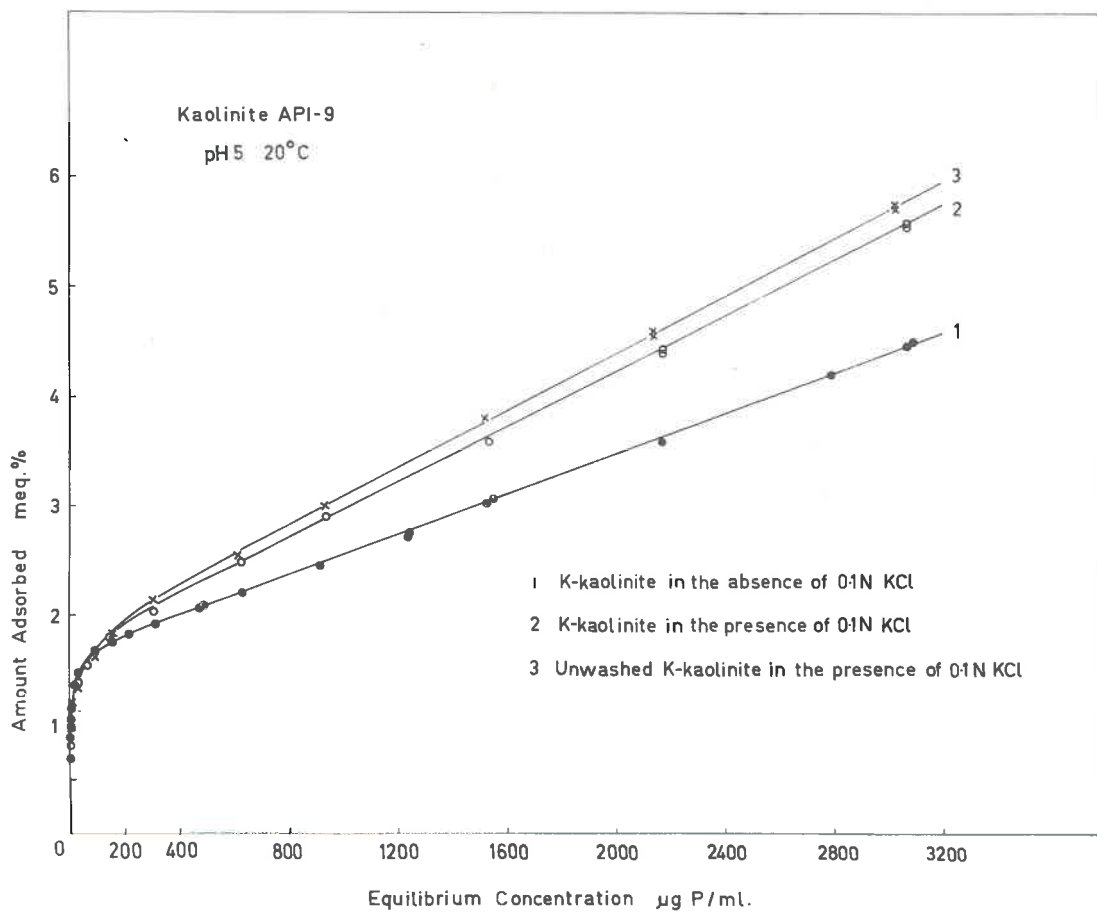


FIGURE 38

The fact that the increase in phosphate adsorption on the Al-kaolinite did not correspond to the cation exchange capacity indicates that aluminium on the exchange is probably not all present as reactive sites.

Further, comparing the results in the presence and absence of KCl (Figure 38; Table 20) shows that KCl produces its biggest effect in region III, whereas the adsorption in regions I and II are hardly affected. The value of parameters describing region II given in Table 20 have been determined from the Langmuir plots (Figure 40).

2.1.2. Effect of cation (Sodium-kaolinite)

The discussion on the available area for adsorption supports the idea that in region III (the linear isotherm), the phosphate ions are able to penetrate into some less crystalline region of the clay edge which can be removed by treatment with acid at pH 1.

It is known that at certain concentrations phosphate will penetrate between the lamellae of halloysite expanding the crystal (Wada, 1959). However, penetration between the lamellae is absent in the case of sodium phosphate.

While no X-ray evidence of interlamellar expansion was observed for the kaolinite, there was a marked difference in the results for region III between sodium and potassium phosphate as shown in Figure 39. There is an almost complete absence of region III for the sodium phosphate, whereas regions I and II are hardly affected. The result suggests that penetration occurs into some less crystalline region of the

TABLE 20

THE PARAMETERS DESCRIBING REGIONS I, II AND III OF K-KAOLINITE
API-9 IN THE ABSENCE AND PRESENCE OF 0.1 N KCl (pH 5, 20°C)

System	Region I	Region II		Region III
	V_o (meq. %)	V_m (meq. %)	$K_2^{II} \times 10^{-3}$ (ml/meq.)	Slope (ml/100 g.)
K-kaolinite	0.85	0.82	1.40 ± 0.14	29.4
K-kaolinite in 0.1 N KCl	0.85	0.89	1.08	38.1

PHOSPHATE ADSORPTION BY HOMOIONIC SYSTEMS

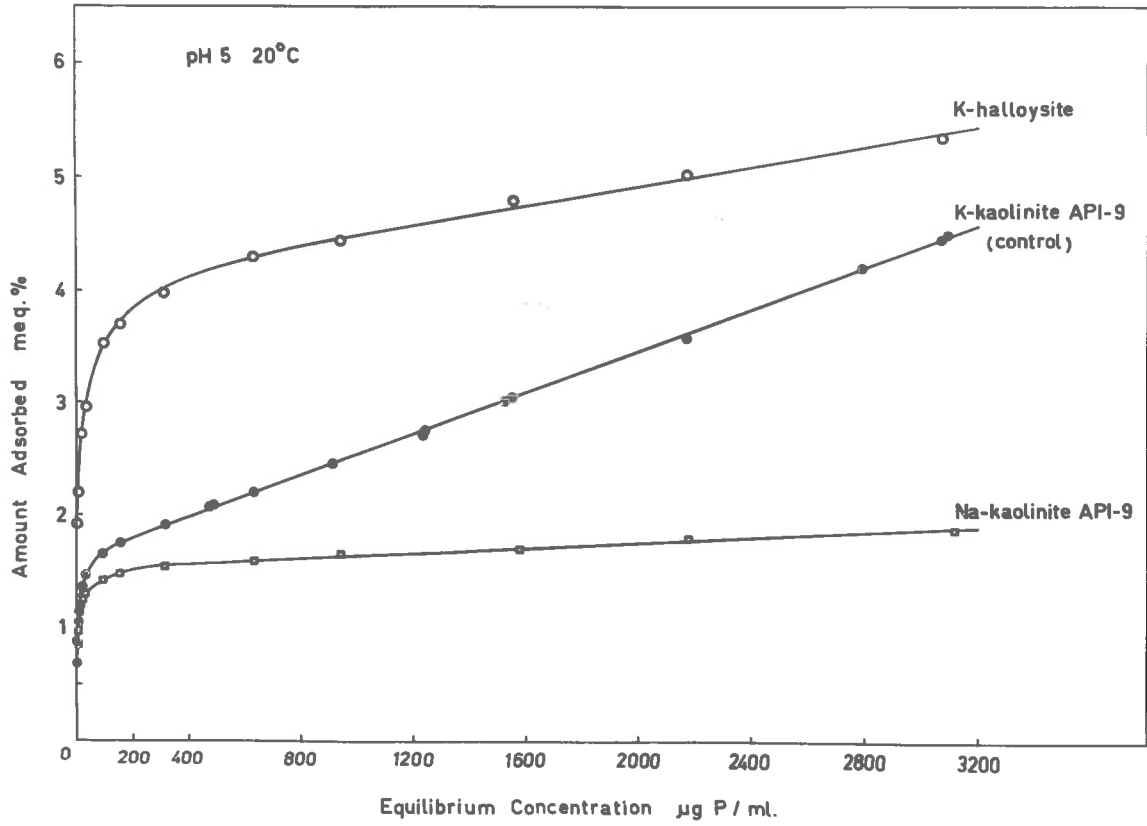


FIGURE 39

kaolinite surface when there is uptake of phosphate in region III.

The penetration is limited by the greater size of the more highly hydrated sodium ion that would have to accompany the phosphate. Table 21 gives the value of V_0 for region I, and the values of V_m and K_2^{II} for region II obtained from the Langmuir plots (Figure 40). These values are very similar for both potassium-clay and sodium-clay.

2.1.3. Adsorption of phosphate on K-halloysite at pH 5, 20°C.

It was thought that if region III involved interlamellar penetration of the kaolinite crystal, then region III for halloysite would have a very steep slope. Accordingly the adsorption isotherm of phosphate on K-halloysite at pH 5 and 20°C was determined.

The results in Figure 39 show that the shape of the isotherm is very similar to that of K-kaolinite API-9. The extent of the adsorption in regions I and II is increased, but the slope of region III is slightly reduced (Table 22). The increase in adsorption in regions I and II could be expected since the surface area of K-halloysite, as measured using low temperature N_2 adsorption, is $47.5 \text{ m}^2/\text{g}$. Thus the number of the adsorption sites in regions I and II are higher. The magnitude of the slope in region III suggests that penetration into the interlayer region does not occur at low concentration (i.e. up to 0.1 M). Therefore the adsorption of phosphate in region III is most likely due to occlusion by a less crystalline region of the clay surface rather than interlayer penetration between the kaolinite sheets.

LANGMUIR PLOTS (REGION II) OF DIFFERENT SYSTEMS

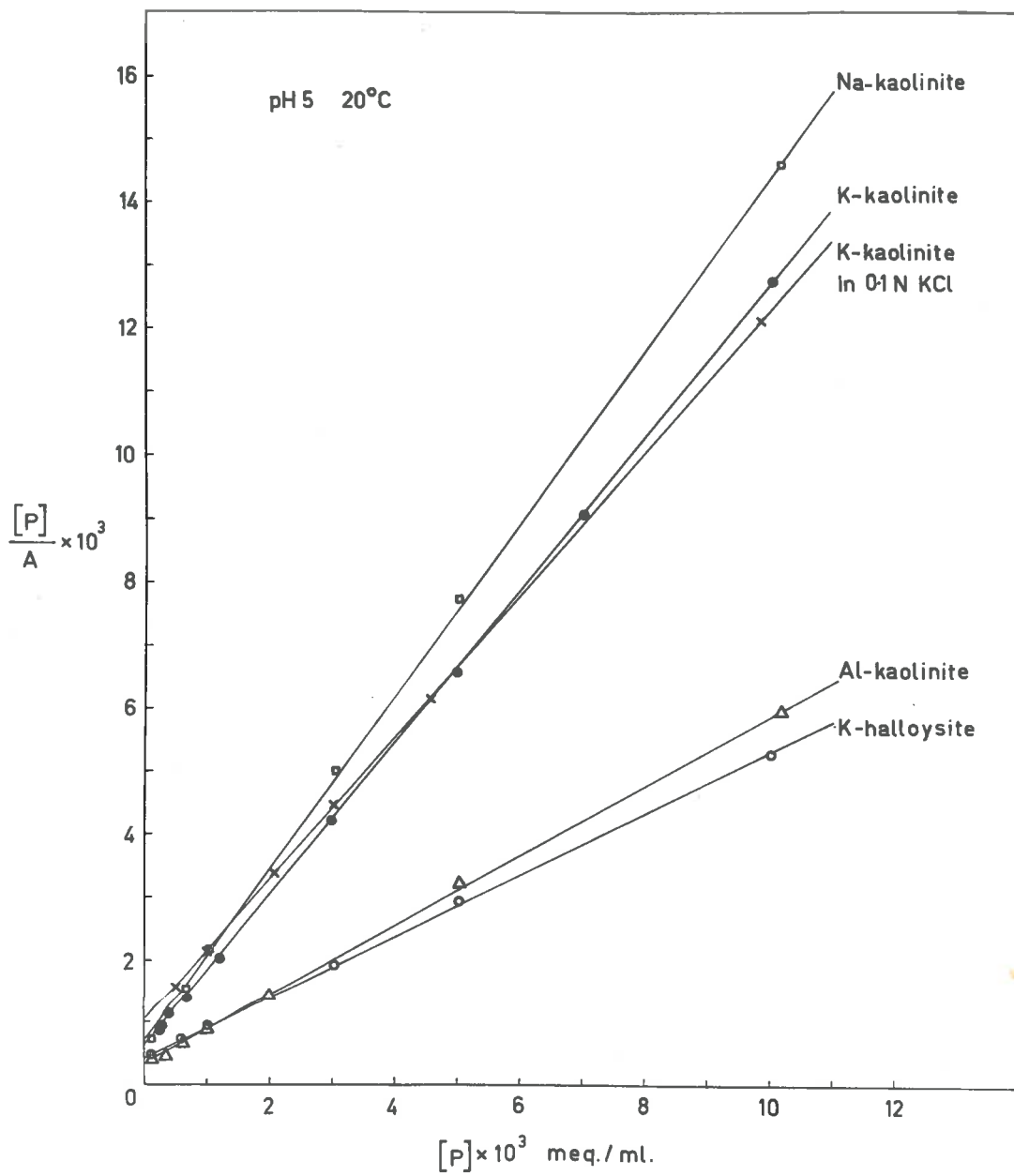


FIGURE 40

TABLE 21

THE PARAMETERS DESCRIBING REGIONS I, II AND III OF K-KAOLINITE
 API-9 AND Na-KAOLINITE API-9 (pH 5, 20°C).

System	Region I	Region II		Region III
	V_o (meq. %)	V_m (meq. %)	$K_2^{II} \times 10^{-3}$ (ml/meq.)	Slope (ml/100 g.)
K-kaolinite	0.85	0.82	(1.40 \pm 0.14)	29.4
Na-kaolinite	0.80	0.77	1.86	4.6

TABLE 22

THE PARAMETERS DESCRIBING REGIONS I, II AND III OF K-KAOLINITE
API-9 AND K-HALLOYSITE (pH 5, 20°C)

Adsorbent	Surface Area (N ₂) m ² /g.	Region I	Region II		Region III
		V ₀ (meq.%)	V _m (meq. %)	K ₂ ^{II} x 10 ⁻³ (ml/meq.)	Slope (ml/100 g.)
K-kaolinite API-9	12	0.85	0.82	(1.40 ± 0.14)	29.4
K-halloysite	47.5	1.95	2.0	1.25	13.0

Table 22 gives the value of V_0 (region I), and the values of V_m and K_2^{II} (region II) obtained from the Langmuir plots (Figure 40).

2.2. Discussion

2.2.1. Region I.

The isotherm expressing the adsorption of phosphate in region I has been derived in Part III.1.2.1. (equation 54) and is written as

$$V_0 = \frac{K_1^I V_1 [H^+]}{1 + K_1^I [H^+]}$$

where V_0 is the amount of adsorbed phosphate in region I at any particular pH value.

V_1 is the total number of sites in region I.

K_1^I is the equilibrium constant governing the formation of the positively charged aluminium.

Adsorption of phosphate on the hydrated aluminium oxides (i.e. gibbsite and pseudoboehmite) shows that there is a corresponding region I having the same K_1^I as kaolinite. These hydrated aluminium oxides do not have any negative charges at these pH values; the results therefore strongly suggest that similar sites for region I may be located not only on any aluminium on the exchange sites, but also on the edge face of the clay crystals. The simplest suggestion which can be offered to account for these results is that region I corresponds to the uptake of phosphate at one of the hydroxyl groups on the hydroxy

aluminium atom, $\text{—Al} \begin{array}{l} \text{OH}^{\text{I}} \\ \text{OH} \end{array}$ situated on the edge of the crystal and on the exchange sites. This grouping would be common to both hydrated aluminium oxides and kaolinites and is likely to be the most reactive.

The fact that the extent of phosphate adsorption in regions I and II for an Al-kaolinite system was increased considerably to similar value (Table 19), whereas region III was unchanged, supports the idea that the aluminium on the exchange site of the clay might have the form or grouping of regions I and II. However, the increase in phosphate adsorption on the Al-kaolinite did not correspond to the cation exchange capacity, indicating that aluminium on the exchange site is probably not all present as reactive sites.

It has been shown by many workers that when aluminium occupies an exchange site either on a resin (Hsu and Rich, 1960) or clay mineral e.g. montmorillonite (Shen and Rich, 1962), it may undergo hydrolysis to give a hydroxy aluminium compound. This hydrolysis product is fixed by the exchange site becoming non-exchangeable and has been shown to have the form of a hydroxy aluminium compound with an average OH/Al molar ratio of 2 (Hsu and Rich, 1960; Thomas, 1960), which can be written as



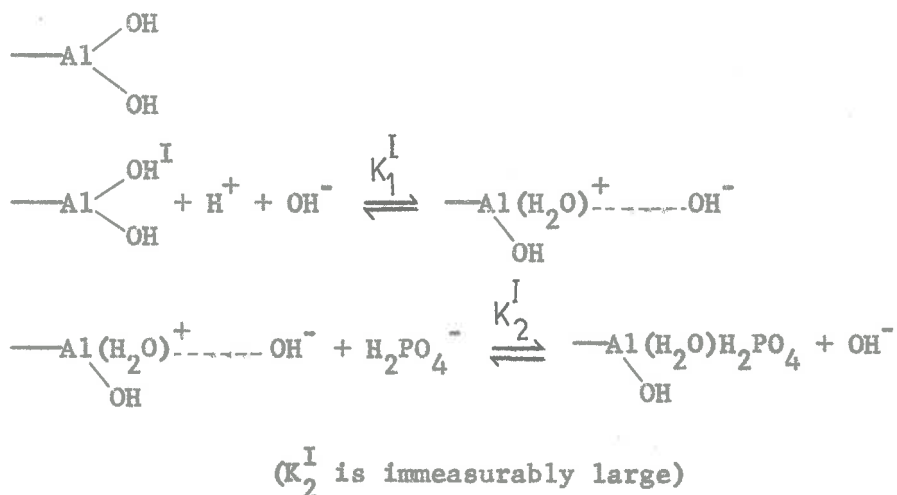
Because Al(OH)_2^+ on the exchange site of the clay is held by Coulombic forces, it would be expected that most of these sites would be removed by treatment at pH 1, whereas the —Al(OH)_2 grouping on the edge, being part of the crystal lattice of the clay, is partly covalent, and hence will not be affected to the same extent by acid treatment. It has been shown (Figure 14; Table 17) that acid treatment only reduced

region I of K-kaolinite by a small amount suggesting that the number of aluminium atoms associated with the exchange sites of the K-kaolinite may be small in the present case.

Recently Schwertmann and Jackson (1963) have also demonstrated from their potentiometric studies, the presence of this hydrolysis product on the surface of aged hydrogen-aluminium montmorillonite.

It is thus suggested that the adsorption sites of region I of kaolinite or oxides are located on one of the hydroxyl groups of an —Al(OH)_2 situated either on the exchange site of kaolinite or on an edge face. In this regard it is of significance that K_2^{II} for the Al-kaolinite is similar to that for K-kaolinite and the hydrated aluminium oxides (Table 24).

The adsorption of phosphate in region I can be re-written as follows, by writing the adsorption site as



It is noteworthy that K_1^{I} of region I (Table 23) for different

adsorbents is relatively constant.

The value of K_1 (or pK_1) is similar in magnitude to the expected value from the second hydrolysis constant (K'') of aluminium salt (Jackson, 1962).

The evidence presented so far suggests that the reactive sites may be located on —Al(OH)_2 situated on the exchange site of the clay or, by analogy with the hydrated aluminium oxides, on the edge face of the crystal.

2.2.2. Region II.

The derived isotherm expressing the adsorption of phosphate (equation 62a) is written as

$$A = \frac{\left(\frac{K_1^{\text{II}} v_2 [\text{H}^+]}{1 + K_1^{\text{II}} [\text{H}^+]} \right) K_2^{\text{II}} [\text{P}]}{1 + K_2^{\text{II}} [\text{P}]} \quad \text{or}$$

$$\frac{[\text{P}]}{A} = [\text{P}] \left(\frac{1 + K_1^{\text{II}} [\text{H}^+]}{K_1^{\text{II}} v_2 [\text{H}^+]} \right) + \left(\frac{1 + K_1^{\text{II}} [\text{H}^+]}{K_1^{\text{II}} K_2^{\text{II}} v_2 [\text{H}^+]} \right)$$

where A is the total amount of phosphate adsorbed in region II at any particular pH value.

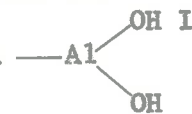
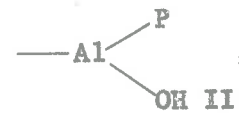
K_1^{II} is the equilibrium constant of the uptake of proton by the edge aluminium atom.

K_2^{II} is the equilibrium constant of the reaction between adsorption site and phosphate ion.

V_2 is the total number of potentially reactive (charged) sites.

[P] is the equilibrium concentration of phosphate, assuming the activity coefficient is unity, because region II occurs at low concentration ($< 10^{-2}$ M).

It has been postulated that the adsorption sites of region II are also associated with an aluminium atom located on the edge face. The basic difference between the reactions in regions I and II is that the reaction takes place at the second OH on the —Al(OH)_2 to which the first phosphate is already attached. Thus the exchange constant K_2^{II} for the reaction between the adsorption site and the phosphate in region II would not be so large.

It is therefore suggested that the potential sites for adsorption on regions I and II are the hydroxyl groups on —Al  and —Al , which will be common to the edge faces and aluminium on the exchange site of kaolinite, and the edge faces of the oxides. The apparent 1:1 correlation between the extent of regions I and II (Table 16; Figure 35) would tend to rule out >AlOH as the reactive sites. Furthermore this grouping (>AlOH) is unlikely to be present on the exchange site of the clay, as an intermediate hydrolysis product of the exchangeable aluminium (Hsu and Rich, 1960; Thomas, 1960; Shen and Rich, 1962).

The value of K_I for regions I and II is of the same order of magnitude for the aluminium oxides and kaolinites (Table 23), indicating that the formation of the positively charged site is very similar for these materials.

TABLE 23.

THE VALUES OF CONSTANT K_1 OF REGIONS I AND II FOR VARIOUS ADSORBENTS
AT 20°C.

Adsorbent	Region I $K_1^I \times 10^{-10}$ (ml/meq.)	Region II $K_1^{II} \times 10^{-10}$ (ml/meq.)
K-kaolinite (API-9)	(0.26 \pm 0.03)	(1.50 \pm 0.58)
K-kaolinite (R.G.)	(0.54 \pm 0.16)	(0.97 \pm 0.37)
Gibbsite	(0.38 \pm 0.20)	(0.60 \pm 0.40)
Pseudoboehmite	(0.85 \pm 0.30)	(0.55 \pm 0.25)

The value of K_2^{II} .

It should be noted that the values of K_2^{II} are relatively constant for the adsorbents studied even though they have very different adsorption capacities (V_m) (Table 24). K_2^{II} is also much the same for the derived systems such as aluminium-kaolinite, sodium-kaolinite, acid treated potassium-kaolinite and potassium-halloysite. (Table 24). These results give a further support to the idea that the adsorption of phosphate on these adsorbents consists of the same basic mechanism, involving the aluminium atom associated with edge face of the crystal.

2.2.3. Region III

The linear isotherm can be formulated as a simple partition phenomenon in which the solute effectively distributes itself between the bulk and surface phase. Thus the adsorption of phosphate in region III can be represented by the simple equation

$$\text{Adsorbed-P} = K[P] \dots \dots \dots (64)$$

where Adsorbed-P is the amount of phosphate adsorbed in region III.

K is the equilibrium constant.

[P] is the equilibrium phosphate concentration.

The results previously described suggest that some form of penetration into the less crystalline region of the clay might be responsible for this process. These poorly crystallized regions situated on the crystal surface are readily removed by acid pretreatment at pH 1 (0.1N HCl).

TABLE 24

THE VALUES OF CONSTANTS V_m AND K_2^{II} FOR DIFFERENT ADSORBENTS AT pH 5, 20°C

Adsorbent	V_m (meq. %)	$K_2^{II} \times 10^{-3}$ (ml/meq.)
K-kaolinite API-9	0.82	(1.40 ± 0.14)
Al-kaolinite API-9	1.80	1.90
Na-kaolinite API-9	0.77	1.86
Acid treated K-kaolinite API-9 in 0.1N KCl	0.70	1.0
K-kaolinite API-9 in 0.1N KCl	0.89	1.08
K-kaolinite R.G.	1.60	1.33
K-halloysite	2.0	1.25
Gibbsite	12.5	1.08
Pseudoboehmite	60.6	1.34

Limited entry of phosphate ion pair, i.e. $\text{K}^+\text{H}_2\text{PO}_4^-$, might be possible into the crystal lattice itself or between crystal lamellae through the steps on the crystal edges. If interlamellar penetration was an important factor, the adsorption isotherm in region III for K-halloysite would have very steep slope. However, this is not the case (Figure 39), and it is concluded that region III is not associated with an entry between crystal lamellae.

The linearity of the isotherm in region III offers further support for some penetration into an amorphous region of the surface where the phosphate adsorption opens up the structure (Giles *et al.*, 1960). The slope of region III for kaolinite and hydrated aluminium oxides passes through a maximum at about neutrality (pH 7). Increasing the ionic strength had its greatest effect in increasing the slope of region III (Figure 38), indicating that part of the barrier preventing entry may be electrostatic.

The effect of pH on the slope of region III may also be due to some dissolution or destruction of this region occurring at the lower pH values, while the OH^- ions compete for the sites at the higher pH values. Aluminium might again be implicated, because region III also exists for gibbsite and pseudoboehmite. It is of interest to note that acid treatment has only a small effect on region III of gibbsite (Figure 15). This may be due to the ability of Al^{3+} to form amorphous $\text{Al}(\text{OH})_3$ precipitates on the gibbsite surface as the pH increases during the washing of the excess acid with distilled water.

The studies on potassium uptake by gibbsite and pseudoboehmite

(Figures 18, 19) have shown that only in region III is potassium uptake necessary for phosphate adsorption. This supports the idea that the adsorption mechanism in region III is distinct from that of regions I and II.

Consideration of the area available for adsorption of phosphate in regions I, II and III also supports the idea that in region III penetration of the adsorbate occurs into some less crystalline region of the clay surfaces. This suggestion is further supported by the results of phosphate adsorption in sodium system (Figure 39), which have clearly shown that there was a marked difference for region III between sodium and potassium phosphates. The complete absence of region III for the sodium phosphate, while regions I and II are hardly affected, suggests that the penetration into some less crystalline region of kaolinite surface is limited by the greater size of the more highly hydrated sodium ion that would have to accompany the phosphate ion.

It may be argued that the adsorption of phosphate in region III is due to the formation of a new crystalline phase, such as variscite ($\text{Al}(\text{OH})_2\text{H}_2\text{PO}_4$) or potassium taranakite (potassium aluminium phosphate) or brazilianite (sodium taranakite, $\text{NaAl}_3(\text{PO}_4)_4(\text{OH})_4$). However, this argument can be dismissed because the observed results (for details see Chapter IV) are not in agreement with expectation if the solubility product principle is obeyed.

III.3. EFFECT OF TEMPERATURE ON ADSORPTION

3.1. Results

The effect of temperature (2° , 20° and 40°C) on the adsorption of phosphate has been determined on potassium-kaolinite (API-9) at pH 5 (Figure 41). For gibbsite and pseudoboehmite the effect of temperature on adsorption was only determined at 20° and 40°C (Figures 42, 43).

An increase in temperature affects the adsorption regions of potassium-kaolinite in different ways. Region I (V_o) increases to a maximum at 20°C ; region II (V_m) is increased both from $2^{\circ} \rightarrow 20^{\circ}\text{C}$ and $20^{\circ} \rightarrow 40^{\circ}\text{C}$, the increase remains when the temperature is lowered from $40^{\circ} \rightarrow 2^{\circ}\text{C}$, although for the change of $20^{\circ} \rightarrow 2^{\circ}\text{C}$, the increase is partly reversible (Figure 41). The increase of adsorption in region III is very marked, but is reversible with respect to temperature.

Table 25 shows the effect of temperature on the value of the parameters describing regions I, II and III of K-kaolinite API-9. The constants for region II were determined from the Langmuir plots (Figure 44). The values of K_2^{II} are very similar.

For the hydrated aluminium oxides, the effect of temperature is very similar to that on kaolinite. As shown in Figures 42, 43, the extent of region I (V_o) for gibbsite and pseudoboehmite is maximum at 20°C . Region II (V_m) is increased on raising the temperature from 20° to 40°C , the increase remaining when the temperature is lowered from 40° to 20°C (Figures 42, 43; Table 26). Increasing temperature produces

EFFECT OF TEMPERATURE ON ADSORPTION

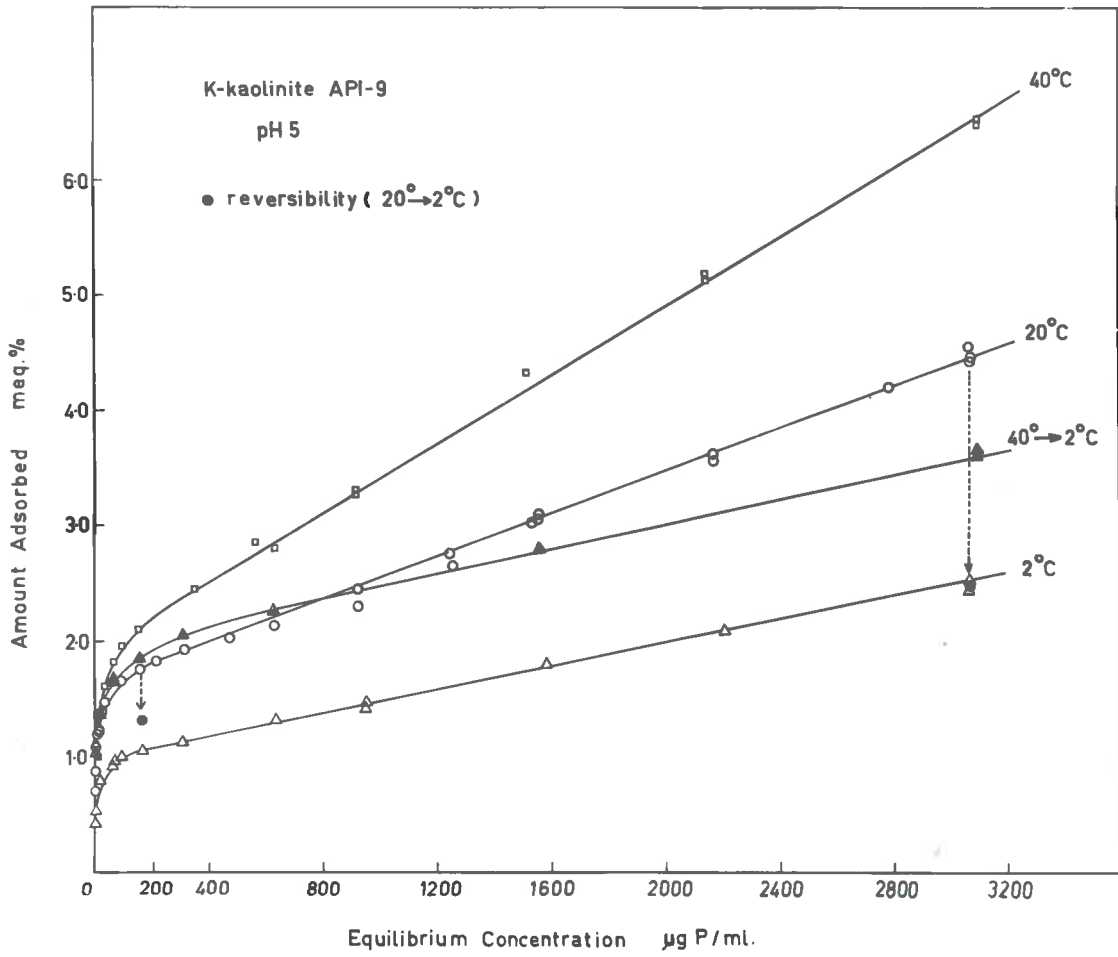


FIGURE 41

EFFECT OF TEMPERATURE ON ADSORPTION

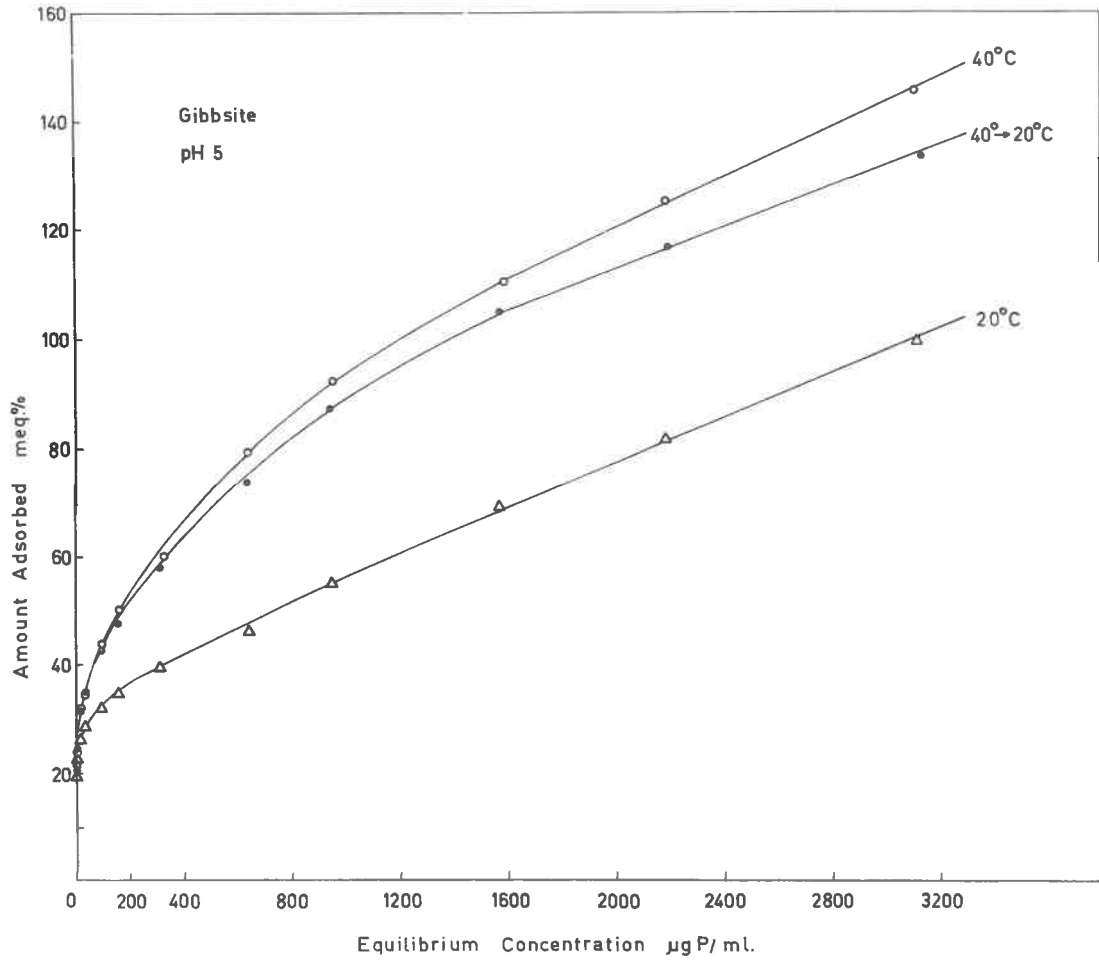


FIGURE 42

EFFECT OF TEMPERATURE ON ADSORPTION

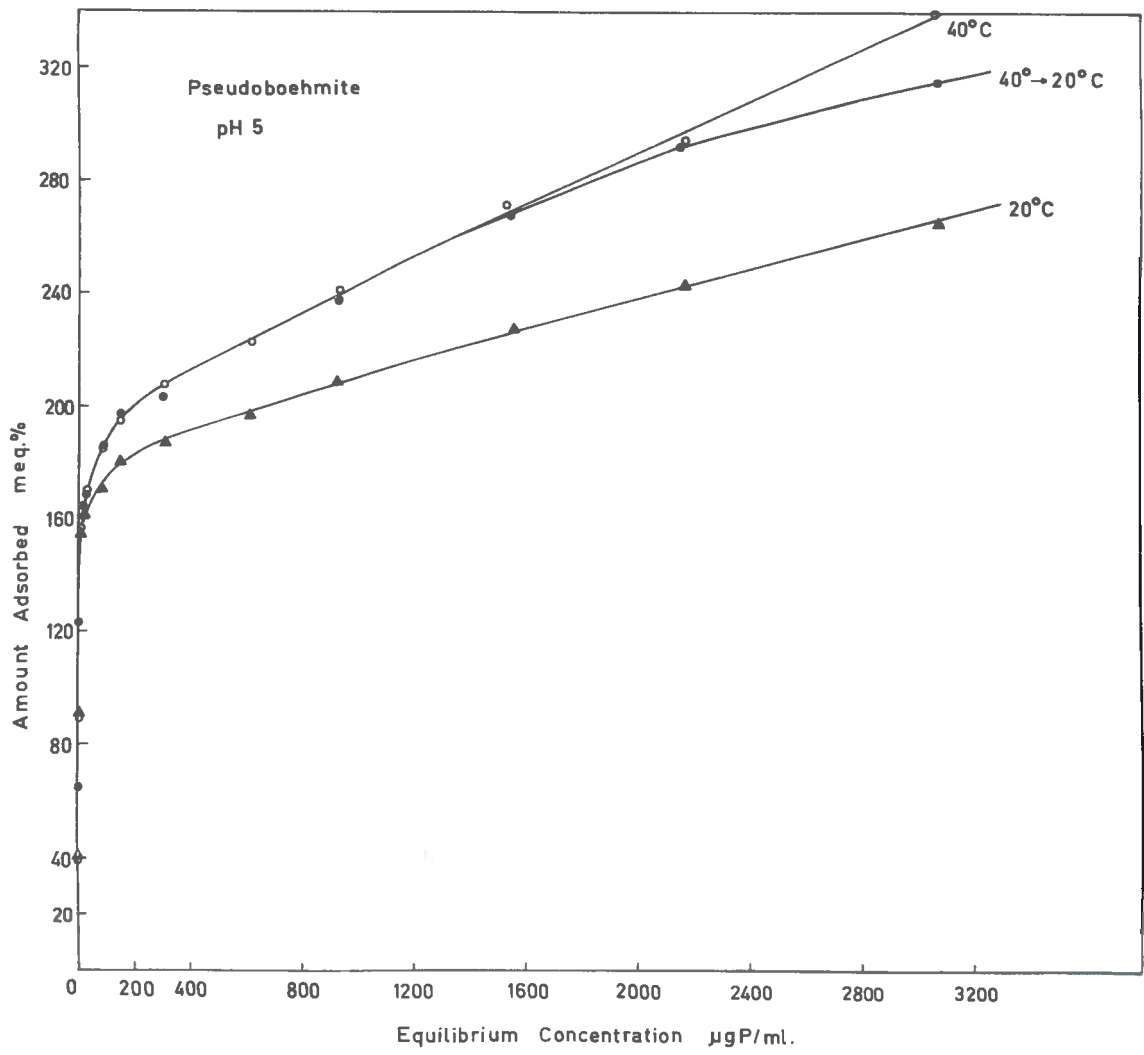


FIGURE 43

TABLE 25

THE PARAMETERS DESCRIBING REGIONS I, II AND III OF K-KAOLINITE API-9
AT DIFFERENT TEMPERATURES (pH 5).

System	Temp. °C	Region I (V _o) (ineq. %)	Region II		Region III Slope (ml/100 g.)
			V _m (ineq. %)	K ₂ ^{II} x 10 ⁻³ (ml/meq.)	
K-kaolinite	2°	0.40	0.63	1.89	14.7
"	20°	0.85	0.82	(1.40 ± 0.14)	29.5
"	40°	0.85	1.11	1.80	48.0
"	(40° → 2°)	0.85	1.11	1.80	14.7

LANGMUIR PLOTS (REGION II) AT DIFFERENT TEMPERATURES

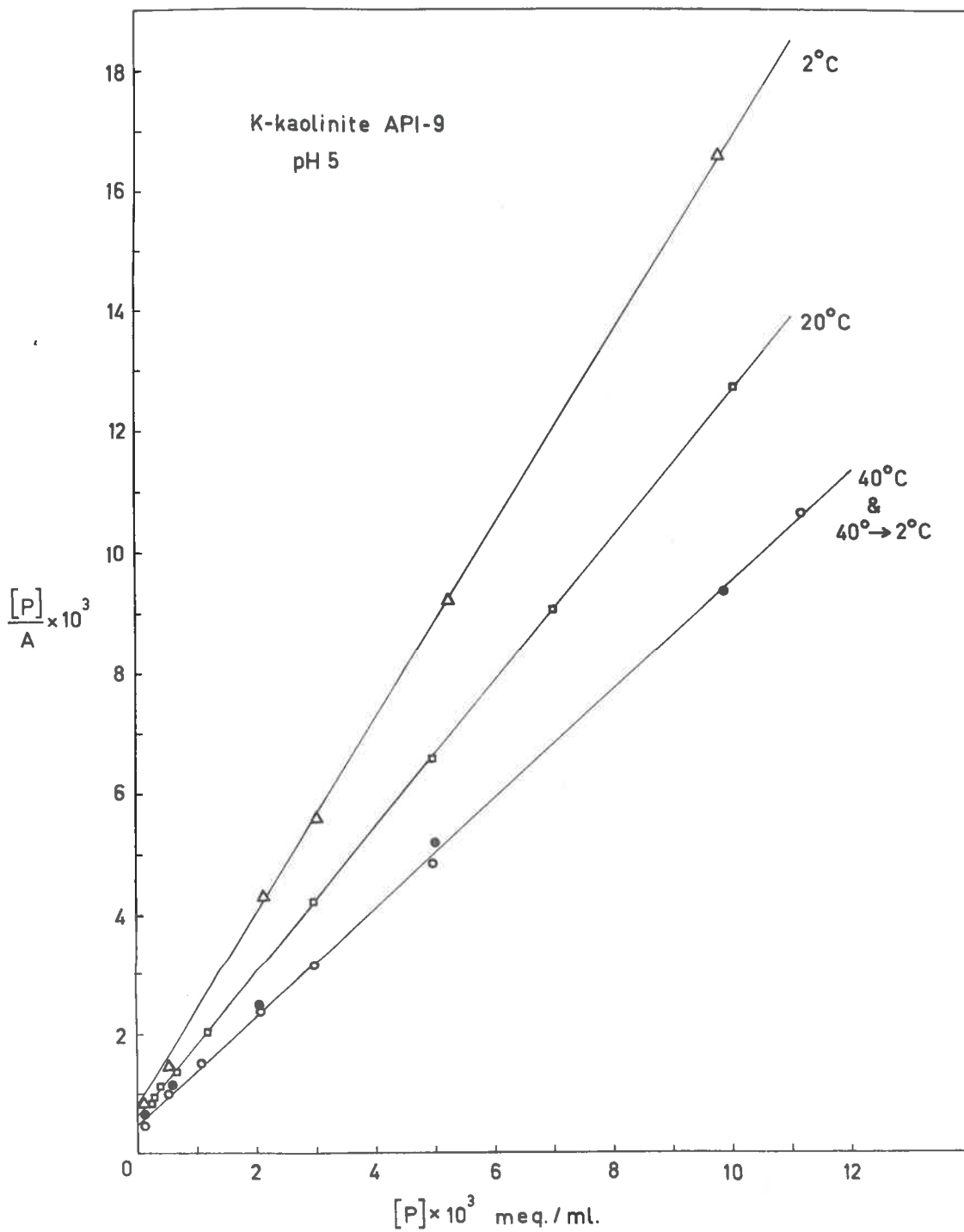


FIGURE 44

LANGMUIR PLOTS (REGION II) AT DIFFERENT TEMPERATURES

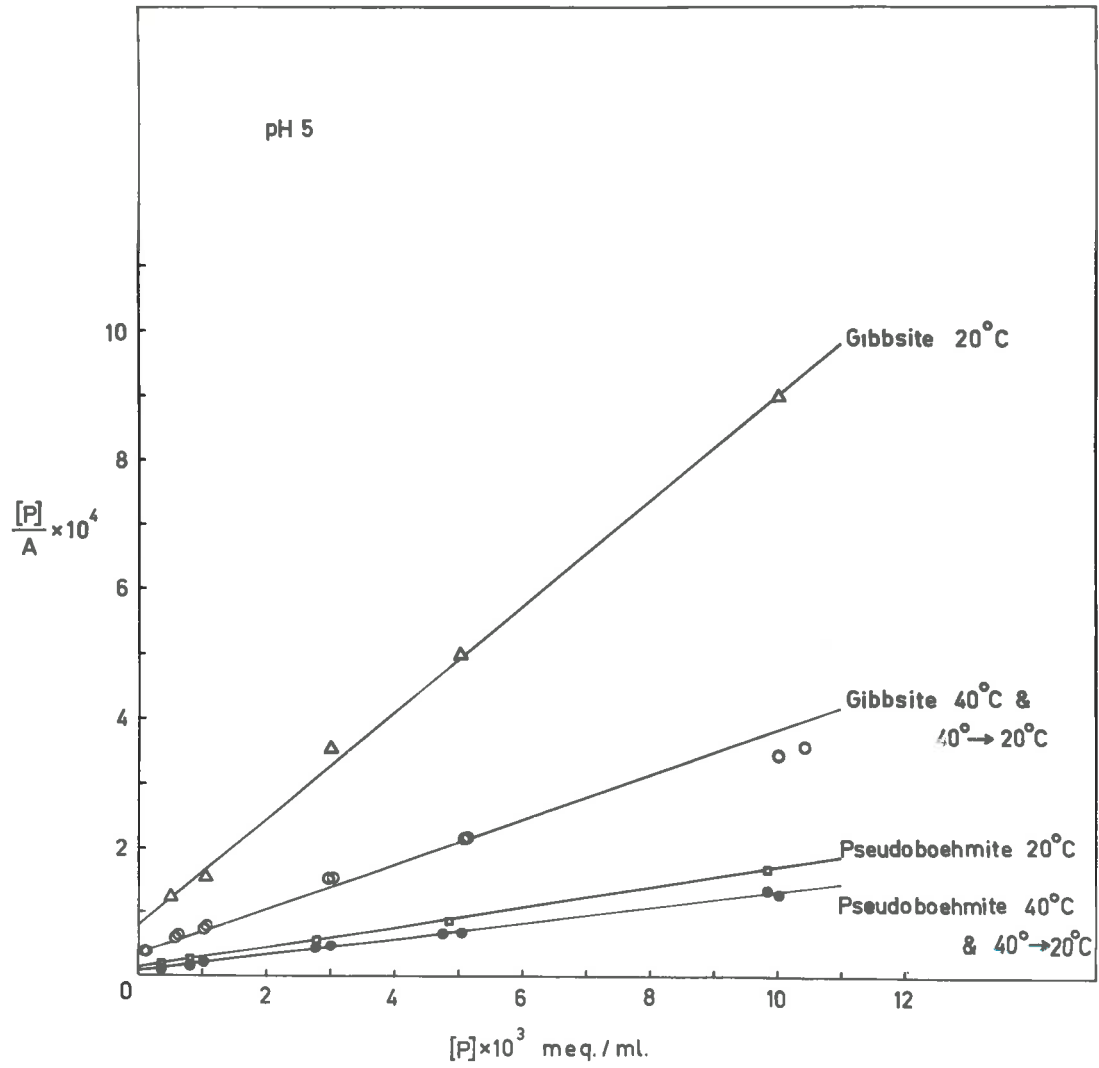


FIGURE 45

TABLE 26

THE PARAMETERS DESCRIBING REGIONS I, II AND III OF GIBBSITE AND
PSEUDOBOEHMITE AT DIFFERENT TEMPERATURES (pH 5)

System	Temp. °C	Region I	Region II		Region III
		V _o (meq. %)	V _m (meq. %)	K ₂ ^{II} x 10 ⁻³ (ml/meq.)	Slope (ml/100 g.)
Gibbsite	20°	22	12.5	1.08	550
"	40°	22	28.5	1.0	744
"	(40° → 20°)	22	28.5	1.0	500
Pseudo-boehmite	20°	120	60.6	1.34	899
"	40°	120	80.0	1.40	1395
"	(40° → 20°)	120	80.0	1.40	930

a reversible increase in the adsorption in region III for gibbsite; however, the increase for pseudoboehmite is only partly reversible. (Figure 43). Table 26 shows the effect of increasing the temperature from 20° to 40°C on the value of the parameters describing regions I, II and III of gibbsite and pseudoboehmite. The constants for region II have been determined from the Langmuir plots (Figure 45). V_m increases markedly with temperature, but the values of K_2^{II} remain approximately unchanged.

The results for acid pretreated K-kaolinite (0.1 N HCl), in 0.1N KCl, are given in Figure 46. This shows that at 40°C there are some definite increases in phosphate adsorption in regions II, and III, whereas region I is hardly affected. The parameters describing regions I, II and III are given in Table 27. The value of V_m increases with temperature, but K_2^{II} is relatively constant. New region III sites may be formed by raising the temperature.

It would be noted that the values of K_2^{II} are very similar for kaolinite, gibbsite and pseudoboehmite and also for the acid treated K-kaolinite. These indicate that the reaction of phosphate ion and the reactive site in region II involves basically the same mechanism.

3.2. Discussion.

An increase in temperature affects the three regions in different ways. However, the effect of temperature on adsorption of phosphate on K-kaolinite, gibbsite and pseudoboehmite in general is essentially the same.

EFFECT OF TEMPERATURE ON ADSORPTION

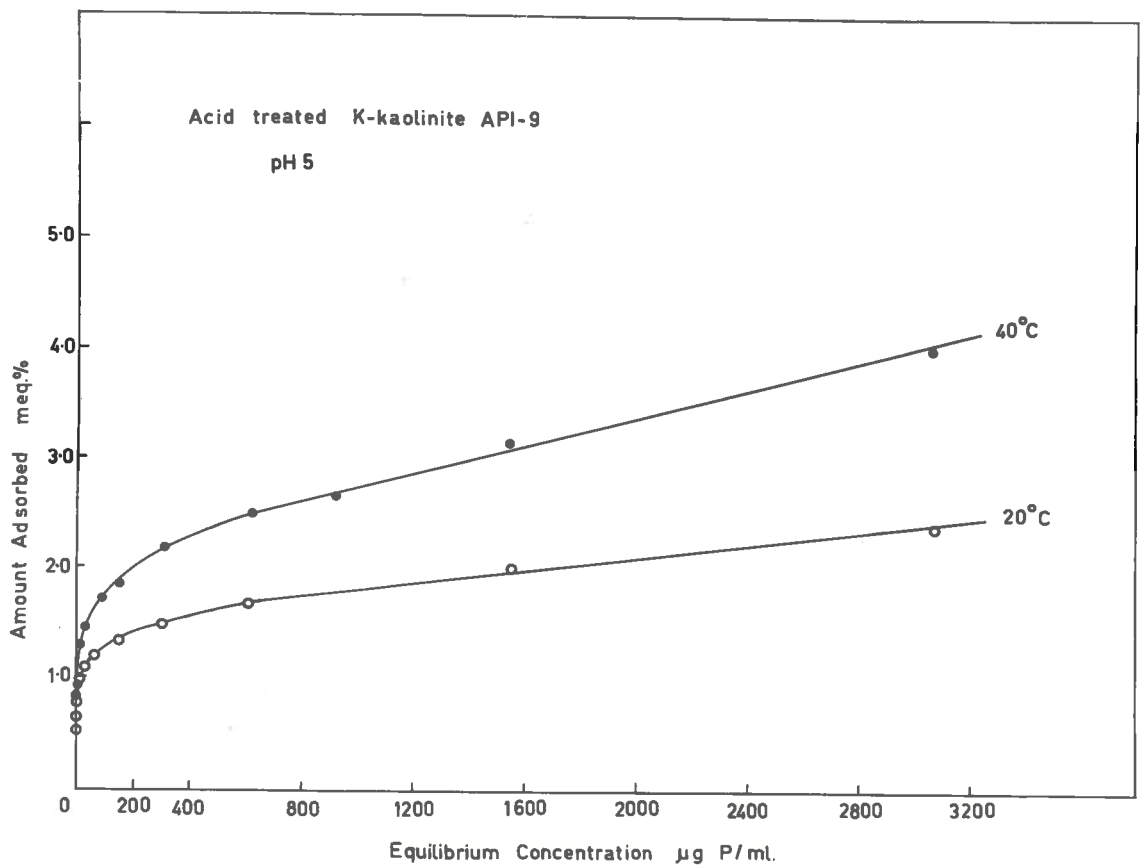


FIGURE 46

TABLE 27

THE PARAMETERS DESCRIBING REGIONS I, II AND III OF ACID TREATED
K-KAOLINITE API-9 , AT DIFFERENT TEMPERATURES (pH 5)

System	Temp. °C	Region I V_o (meq.%)	Region II		Region III Slope (ml/100 g.)
			V_m (meq.%)	$K_2^{II} \times 10^{-3}$ (ml/meq.)	
Acid treated					
K-kaolinite	20°	0.75	0.70	1.0	9.3
Acid treated					
K-kaolinite	40°	0.80	1.11	1.11	19.8

3.2.1. Region I

The extent of region I for K-kaolinite reaches a maximum at about 20°C, presumably because of the large value of K_2^I and the fact that the experiment was carried out at pH 5, where the number of sites available was maximum. This is also true for gibbsite and pseudoboehmite (Tables 25, 26). The increase in the number of sites (V_o) is not reversible if the system is cooled from 40° to 2°C for kaolinite. A similar comparison cannot be made for gibbsite and pseudoboehmite because only 20° and 40°C isotherms were determined for these systems.

It is interesting to note that V_o for the acid treated K-kaolinite is relatively constant at 20° and 40°C, indicating that the extent of adsorption has also reached a maximum level at 20°C. This is in agreement with the results for the other adsorbents.

3.2.2. Region II

In region II there is a definite increase in the number of sites (V_m) available for adsorption of phosphate on K-kaolinite, gibbsite and pseudoboehmite (Tables 25, 26). Furthermore, if the systems are subsequently cooled from 40° to 2°C for kaolinite (API-9) or from 40° to 20°C for gibbsite and pseudoboehmite, there is hardly any decrease in the amount adsorbed (V_m) (Tables 25, 26), the isotherms of region II tending to maintain their original shape. This is shown in Figure 47 for kaolinite, where the results are expressed in terms of surface coverage. Comparison with the 2°C isotherm indicates that some of the new sites may not be as reactive as the original since the 40° or (40° to 2°C) isotherms are slightly displaced downwards. These

ADSORPTION ISOTHERMS (REGION II) AS FUNCTION OF SURFACE COVERAGE θ

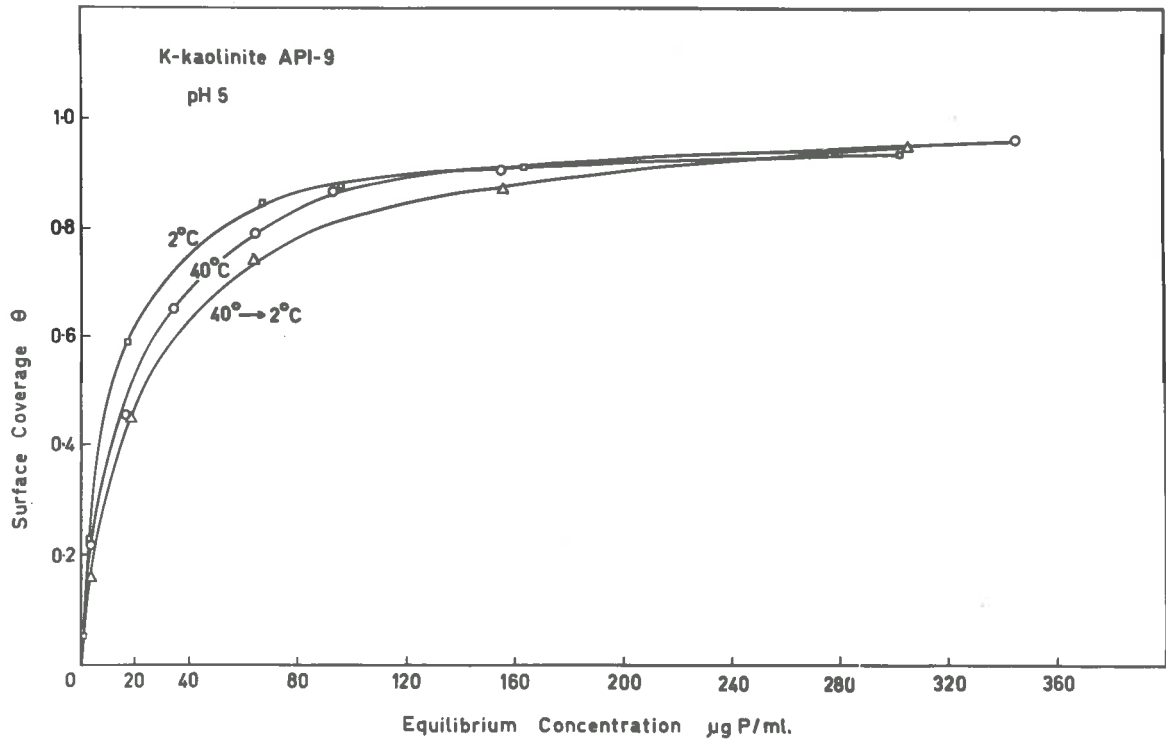


FIGURE 47

new sites were presumably formed at 40°C by breaking some bonds with the same energy as region II. Cooling from 20° to 2°C does appear to reverse some of the adsorption (Figure 41) suggesting that bond re-formation might be able to occur if the system is not subjected to too a high temperature.

The heat of adsorption may be divided into two parts:

- (i) due to the irreversible increase in the number of sites, i.e. an endothermic process, and
- (ii) due to the effect of temperature on the exchange process represented by K_2^{II} .

The free energy of adsorption must be negative (i.e. Table 16a) for adsorption to take place, and since ΔH is apparently positive $T \Delta S$ should be positive and greater than ΔH in accordance with $\Delta G = \Delta H - T \Delta S$. This is reasonable in solid-solution system, since the adsorption of one adsorbate molecule on the adsorption site might release several solvent molecules into the solution with a net heat change of zero. Consequently, the net number of translational degrees of freedom is increased when the adsorption occurs, and the entropy change is positive.

Calculation of entropy of adsorption for region II.

Kaolinite API-9

Heat of adsorption $\overline{\Delta H}_{1/2}$ is calculated using the relationship (equation 40)

$$\overline{\Delta H}_{1/2} = 2.303 RTT' \frac{(\log K' - \log K)}{T' - T}$$

where K' is the equilibrium constant at 40°C ($K_2^{\text{II}} = 1.80 \times 10^3$)

K is the equilibrium constant at 2°C for (40° to 2°C) ($K_2^{\text{II}} = 1.80 \times 10^3$) (Table 25).

$$\overline{\Delta H}_{1/2} = \underline{\underline{\text{zero}}}$$

The integral molar entropy $\Delta S_{1/2}$ at half coverage ($\theta = 1/2$) is calculated using the following equation (Heath and Culver, 1955).

$$\Delta S_{1/2} = \overline{\Delta S}_{1/2} + 2 R \ln 2 \quad \dots \dots \dots (65)$$

where $\overline{\Delta S}_{1/2}$ is the differential molar entropy at half coverage ($\theta = 1/2$).

The differential molar entropy at half coverage $\overline{\Delta S}_{1/2}$ can be calculated as follows:

$$\begin{aligned} \Delta G_\theta &= \overline{\Delta H}_\theta - T \overline{\Delta S}_\theta \\ &= -RT \ln K_2^{\text{II}} \end{aligned}$$

where K_2^{II} is the equilibrium constant defined by equation (62a).

since $\overline{\Delta H}_\theta = \text{zero}$, thus

$$\begin{aligned} T \overline{\Delta S}_\theta &= RT \ln K_2^{\text{II}} \\ \overline{\Delta S}_\theta &= R \ln K_2^{\text{II}} \end{aligned}$$

$$\text{At } \theta = 1/2, \overline{\Delta S}_{1/2} = 1.987 \times 2.303 \times \log (1.4 \times 10^3)$$

where K_2^{II} is the equilibrium constant at $20^\circ\text{C} = 1.4 \times 10^3$ (Table 25)

$$\overline{\Delta S}_{1/2} = \underline{\underline{14.4 \text{ e.u.}}}$$

Substituting $\overline{\Delta S}_{1/2}$ into equation (65), gives

$$\begin{aligned} \Delta S_{1/2} &= 14.4 + 2 R \ln 2 \\ &= 14.4 + 2.75 \end{aligned}$$

$$\Delta S_{1/2} = \underline{\underline{17.15 \text{ e.u.}}}$$

The integral molar entropy at half coverage, $\Delta S_{1/2}$, can be converted to the unitary quantity by following equation (Gurney, 1953; Rossotti, 1960):

$$\begin{aligned}\Delta S_{\text{unitary}} &= \Delta S_{1/2} + Z R \ln 55.5 \dots \dots \dots (66) \\ &= \Delta S_{1/2} + Z \times 7.9 \\ &= \underline{\underline{(17.15 + 7.9Z) \text{ e.u.}}}\end{aligned}$$

where Z is the number of moles of water.

Similar calculation can be made for gibbsite and pseudoboehmite.

Gibbsite

$$\overline{\Delta H}_{1/2} = 2.303 RT'T \frac{(\log K' - \log K)}{(T' - T)}$$

$$\overline{\Delta H}_{1/2} = \underline{\underline{\text{zero}}}$$

Since K' (40°C) is equal to K (at 20°C for (40° to 20°C)) ($K_2^{\text{II}} = 1.0 \times 10^3$) (Table 26).

$$\overline{\Delta S}_{1/2} = R \ln K_2^{\text{II}}$$

where K_2^{II} is the equilibrium constant at $20^\circ = 1.08 \times 10^3$. (Table 26).

$$\begin{aligned}\overline{\Delta S}_{1/2} &= 1.987 \times 2.303 \times \log (1.08 \times 10^3) \\ &= \underline{\underline{13.9 \text{ e.u.}}}\end{aligned}$$

$$\begin{aligned}\Delta S_{1/2} &= \overline{\Delta S}_{1/2} + 2 R \ln 2 \\ &= 13.9 + 2.75 \\ &= \underline{\underline{16.65 \text{ e.u.}}}\end{aligned}$$

$$\begin{aligned}\Delta S_{\text{unitary}} &= \Delta S_{1/2} + Z R \ln 55.5 \\ &= \underline{\underline{(16.65 + 7.9 Z) \text{ e.u.}}}\end{aligned}$$

Pseudoboehmite

$$\left. \begin{aligned}K_2^{\text{II}} (40^\circ\text{C}) &= 1.40 \times 10^3 \\ K_2^{\text{II}} (\text{at } 20^\circ\text{C for} \\ & (40^\circ \text{ to } 20^\circ\text{C})) = 1.40 \times 10^3\end{aligned} \right\} \text{Table 26.}$$

$$\overline{\Delta H}_{1/2} = 2.303 RT'T \frac{(\log K' - \log K)}{(T' - T)}$$

$$\overline{\Delta H}_{1/2} = \underline{\underline{\text{zero.}}}$$

$$\overline{\Delta S}_{1/2} = R \ln K_2^{\text{II}}$$

where K_2^{II} is the equilibrium constant at $20^\circ\text{C} = 1.28 \times 10^3$ (Table 26).

$$\overline{\Delta S}_{1/2} = \underline{\underline{14.2 \text{ e.u.}}}$$

$$\begin{aligned}\Delta S_{1/2} &= \overline{\Delta S}_{1/2} + 2 R \ln 2 \\ &= 14.2 + 2.75 \\ &= \underline{\underline{16.75 \text{ e.u.}}}\end{aligned}$$

$$\begin{aligned}\Delta S_{\text{unitary}} &= \Delta S_{1/2} + Z \ln 55.5 \\ &= \underline{\underline{(16.75 + 7.9 Z) \text{ e.u.}}}\end{aligned}$$

TABLE 28

THE VALUES OF HEAT AND ENTROPY OF PHOSPHATE ADSORPTION IN REGION II
ON KAOLINITE, GIBBSITE AND PSEUDOBOEHMITE.

Adsorbent	$\overline{\Delta H}_{1/2}$ kcal/mole	Integral entropy change $\Delta S_{1/2}$ e.u.	Unitary entropy $\Delta S_{\text{unitary}}$ e.u.
K-kaolinite	0	17.15	17.15 + 7.9Z
Gibbsite	0	16.65	16.65 + 7.9Z
Pseudoboehmite	0	16.95	16.95 + 7.9Z

The relatively small effect of temperature on K_2^{II} in region II indicates that the process is largely governed by a positive entropy change having a value of about 17 e.u. for kaolinite, gibbsite and pseudoboehmite respectively (Table 28), using a standard state of 1 g mole/l in the bulk when the surface is half covered.

The lack of a significant heat of adsorption (Table 28) is commonly observed for ion exchange phenomenon (Boyd, Schubert and Adamson, 1947; Helfferich, 1962) and is attributed to the fact that the ions are located in an energetically similar environment after exchange. The driving force for exchange reaction is therefore due to some gain in entropy. This increase of entropy arises mainly from the entropy of mixing. In addition it will include a configurational entropy change of the matrix, together with contributions from changes in the degree of ordering of solvent molecules resulting from the formation and degradation of solvation shells.

A positive entropy change is also commonly observed in complex formation where a ligand displaces several water molecules from around a central ion, whereas adsorption processes are usually associated with a loss of entropy due to ordering.

The positive entropy change observed for the phosphate adsorption in region II may be attributed to a disordering of the water around the adsorbing site and the adsorbate. This process was not specifically taken into account in the formulation of the adsorption reaction. Such suggestion would be reasonable since the hydroxyl is displaced by the larger phosphate ion. However, detailed calculation

of the entropy change expected for the present model would be difficult. Assuming that the basic entropy changes due to the liberation of a water molecule and adsorption of H^+ from H_3O^+ (Step 1) cancel out and similarly, those due to the exchange between OH^- and phosphate ion (Step 2), then the observed unitary entropy gain of $(17 + 7.9Z)$ e.u. (Table 28) is equal to $Z \times 16.7$ e.u. for the release of Z moles of water (16.7 e.u. for one mole of water - Rossotti, 1960). Therefore Z is 2 corresponding to the liberation of about two moles of water which may result from the adsorption of one mole of phosphate.

The effect of temperature in increasing the number of sites in region II for adsorption may be to break some of the internal bonds near the edge of the crystal with the same energy as region II.

It should be noted from Table 28 that the values of unitary entropy change ($\Delta S_{\text{unitary}}$) for different adsorbents (kaolinite, gibbsite and pseudoboehmite) are about equal, indicating that the phosphate adsorption in region II for different adsorbents is essentially the same.

3.2.3. Region III.

Temperature has a marked positive effect in region III (Figures 41, 42, 43), however, phosphate adsorption within this region is reversible with respect to temperature. Thus the slope K , i.e. the equilibrium constant, for this linear isotherm is a function of temperature.

The heat of adsorption in region III can be calculated from the change in slope (K) as function of temperature, as follows:

$$\Delta G = \Delta H - T\Delta S \quad \dots \dots \dots (67a)$$

$$\frac{d(\Delta G)}{dT} = -\Delta S$$

Substituting $-\Delta S$ into (67a), gives

$$\Delta G = \Delta H + T \frac{d(\Delta G)}{dT} \quad \dots \dots \dots (67b)$$

$$\Delta G = -RT \ln K \quad \dots \dots \dots (68a)$$

differentiating equation (68a) with respect to T, gives

$$\frac{d(\Delta G)}{dT} = -R \ln K - RT \frac{d \ln K}{dT} \quad \dots \dots \dots (68b)$$

Substituting equation (68b) into equation (67b), gives

$$\Delta H = RT^2 \frac{d \ln K}{dT}$$

or

$$\frac{d \ln K}{dT} = \frac{\Delta H}{RT^2} \quad \dots \dots \dots (69a)$$

Equation (69a) can also be written as

$$\frac{T^2 d \ln K}{dT} = \frac{\Delta H}{R}$$

or

$$\frac{d \ln K}{d(1/T)} = -\frac{\Delta H}{R} \quad \dots \dots \dots (69b)$$

By plotting $\log K$ against $\frac{1}{T}$, (equation 69b) for K-kaolinite API-9, a straight line was obtained (Figure 48), with the slope = $-\frac{\Delta H}{2.303 R}$ (Table 29).

The ΔH is found to be about + 5.3 Kcal/mole. The process is thus endothermic and probably involves bond breaking, possibly hydrogen bonding, in order to gain entry into the amorphous material of region III.

For gibbsite and pseudoboehmite the heat of adsorption in region III can only be determined approximately because the adsorption for these materials have been carried out at only two temperatures i.e. 20° and 40°C. The calculated ΔH is about 3 kcal./mole for gibbsite and 4 kcal./mole for pseudoboehmite (Table 30), which is the same order of magnitude to that of K-kaolinite.

The heat of adsorption* of potassium phosphate from 200 mls. of 0.1 M solution at pH 5, onto 20 g. of K-kaolinite API-9 at 30°C, was measured calorimetrically. The temperature change was found to be less than the sensitivity of the calorimeter, indicating that the integral heat of adsorption for these conditions is less than 0.2 kcal./mole of phosphate.

The adsorption isotherms indicated that the heat should be slightly positive. The failure to indicate a heat of adsorption suggests that the actual heat may vary with temperature, being approximately zero at 30°C.

* This was measured by Dr. W.W. Forrest of the C.S.I.R.O., Division of Biochemistry and General Nutrition, University of Adelaide, South Australia, using apparatus described by him (1961).

RELATION BETWEEN LOG.K (SLOPE OF REGION III) AND $\frac{1}{T}$

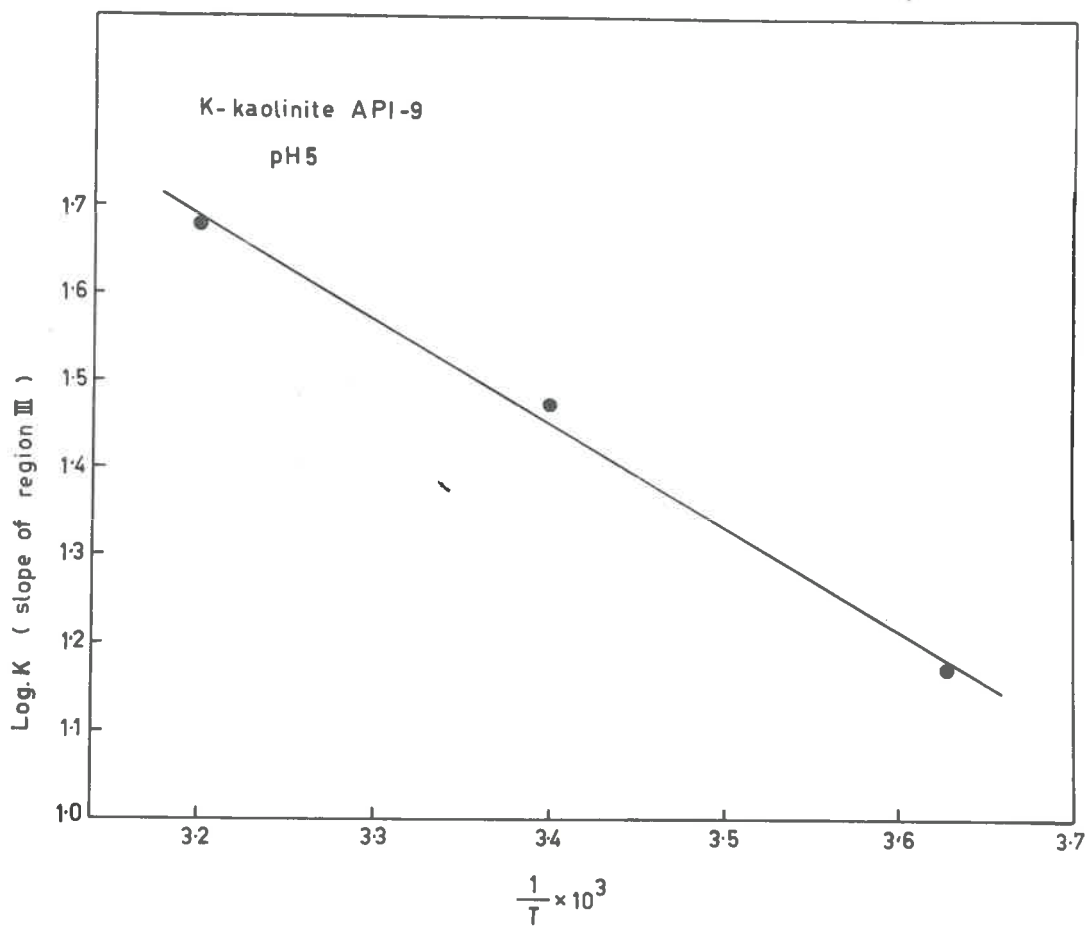


FIGURE 48

TABLE 29

HEAT OF ADSORPTION IN REGION III FOR K-KAOLINITE API-9

Temp. °C	$\frac{1}{T} \times 10^3$	K (ml/100 g.)	Log K	Slope $\times 10^{-3}$	ΔH Kcal./mole
2°	3.63	14.7	1.170		
20°	3.40	29.4	1.468		
40°	3.19	48.0	1.681		
				-1.16	+5.3

TABLE 30

HEAT OF ADSORPTION IN REGION III FOR GIBBSITE AND PSEUDOBOEHMITE

(i) Gibbsite

Temp. °C	$\frac{1}{T} \times 10^3$	K (ml/100g)	log K	Slope $\times 10^{-3}$	ΔH Kcal./mole
20°	3.40	550	2.740		
40°	3.19	744	2.872		
				-0.63	+2.90

(ii) Pseudoboehmite

Temp. °C	$\frac{1}{T} \times 10^3$	K (ml/100g)	log K	Slope $\times 10^{-3}$	ΔH Kcal./mole
20°	3.40	899	2.954		
40°	3.19	1395	3.145		
				-0.95	+4.15

The calorimetric measurements confirm the suggestion that the driving force of the reaction is largely entropic.

CHAPTER IVGENERAL DISCUSSION

The adsorption isotherms of phosphate on K-kaolinite, gibbsite and pseudoboehmite at a constant pH value, are very similar in shape and differ only in the amount of phosphate adsorbed. The order was pseudoboehmite > gibbsite > K-kaolinite (Figure 11). This was also the order of their surface area, as measured by using low temperature N₂ adsorption, although there was no simple relationship. However, there was a more direct relationship between the extent of phosphate adsorption of these materials and their respective edge face areas as estimated by using shadowed electron micrographs of the particles. This suggests that the adsorption sites on the adsorbent surface might be associated with the edge face groupings of the crystals.

Over the concentration range used in this study the isotherms could not be described by a single equation. However, it was possible to divide all the adsorption isotherms into three distinct regions, designated as regions I, II and III (Figures 7, 8, 9 and 10). These are related to the affinity of phosphate ion for three energetically different types of reactive sites. Depending on the experimental conditions the three regions have been shown to behave independently of one another, particularly in the case of the kaolinite system. The regions were described as follows:

- Region I. At low phosphate concentrations ($< 1 \times 10^{-4} \text{M}$) the isotherm rises steeply and remains close to the y-axis. This region represents sites with very high affinity for phosphate.
- Region II. The second region commences approximately at 10^{-4}M when the isotherm becomes convex to the y-axis. The experimental results in this region conform to a Langmuir isotherm. Both regions I and II increase to a maximum with decreasing pH value.
- Region III. The third part of the isotherm is linear and occurs at medium to high concentration of phosphate (10^{-3} to 10^{-1}M). The slope for region III passed through a maximum at about neutrality.

From considerations of the structure of the kaolinite and gibbsite crystals, and the origin of their positive charges, it has been suggested that the most likely site responsible for adsorption in regions I and II is an aluminium atom situated on the edge face of the crystal. Edge faces of the crystals are formed either by the termination of crystal growth or by the fracture of crystals along the plane perpendicular to the (001) plane, giving rise to unsatisfied valency bonds. This will lead to the formation of aluminium atoms on the edge face in the form of $>\text{Al-OH}$ or $-\text{Al}(\text{OH})_2$, depending on the direction of the plane of termination of crystal growth or the plane of fracture.

—Al(OH)₂ groupings are also present on exchange sites of kaolinite, and are also considered as possible sites for adsorption.

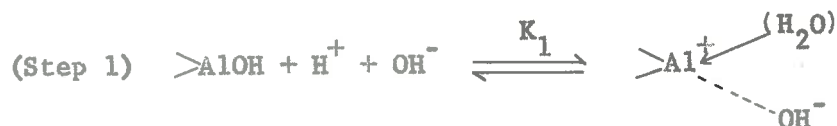
Several workers (Kolthoff, 1936; Hsu and Rennie, 1962) have suggested a simple exchange reaction for phosphate adsorption, which can be represented as follows:

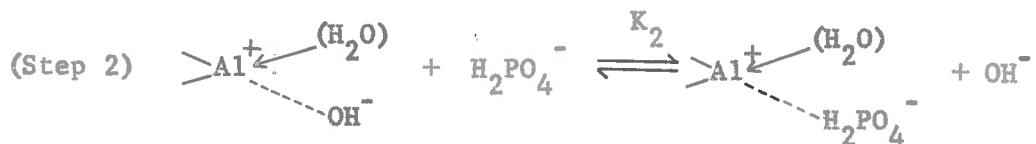


The reaction suggests that the adsorbed phosphate would be reversible with respect to concentration. The fact that phosphate adsorbed in region I was reversible with pH and irreversible with respect to phosphate concentration showed that the mechanism of adsorption does not involve a simple exchange phenomenon. Furthermore, a simple exchange such as this would lead to a maximum number of adsorption sites which would be independent of pH value; however, the results showed that this was not the case (Figure 20; Table 3).

It has been suggested (Schofield, 1949) that the positively charged aluminium atoms on the edge face of a crystal are the result of proton uptake from a water molecule. The results in regions I and II were consistent with a mechanism involving ion exchange of a phosphate ion for the OH⁻ counter ion of a positively charged edge aluminium atom.

To simplify the derivation of the adsorption equation, the aluminium atoms on the edge faces are denoted by >AlOH. It is envisaged that the reaction consists of two steps,





where K_1 and K_2 are the equilibria constants of the appropriate step. It is considered that reaction 1 is independent of reaction 2 in so far as the uptake of phosphate in reaction 2 does not promote the formation of further positively charged adsorption sites. This situation was thought to arise because the positively charged sites maintained their identity after exchange with phosphate and retained their role in determining the uptake of a proton, as would be the case for an ion-exchange reaction. If this were not so, then provided sufficient phosphate is present, the number of sites available for adsorption in regions I and II would not show the observed dependency on the pH value (Table 3; Figures 23, 25, 26, 27 and 28).

The scheme proposed above can account for the observed variations in phosphate adsorption with pH value for all the adsorbents.

The values of K_1 for regions I and II of the isotherms were similar for all adsorbents suggesting that the energies of proton uptake is the same for kaolinites and the hydrated aluminium oxides. The K_2^{II} values for region II were also similar for the various adsorbents, but because K_2^{I} was immeasurably large for region I no comparison could be made.

The biggest difference between the adsorbents thus appears to lie in the number of sites per unit weight, although even this difference can be reduced if the results are expressed on the basis of

the edge face area (see Part III,1.2.2.)

The value of K_2^{II} should be a constant and independent of pH if the adsorption in region II is species independent. While K_2^{II} was not absolutely constant, it showed none of the trends required by any phosphate species dependency.

The value of pK_1 for the uptake of a proton (Step 1) is about -10 (Table 23), which is similar in magnitude to the value expected from the second hydrolysis constant of aluminium salts (Jackson, 1962).

It is of significance that for the 20°C isotherms, the extent of phosphate adsorption in region I is approximately equal to that of region II for the different adsorbents (Table 16; Figure 35). This would be so if the sites for regions I and II are associated with the first and second hydroxyls of an $—Al(OH)_2$, situated on the edge face of the crystal. This grouping would be common to both kaolinites and hydrated aluminium oxides and is likely to be the most reactive. Furthermore, the maximum positive charges of the different adsorbents at pH 3 (Table 5), as measured by chloride adsorption, is approximately equal to the extent of phosphate adsorption in region I. Thus the same sites, responsible for the positive adsorption of chloride, seem to be also responsible for the adsorption of phosphate in region I.

The fact that the extent of phosphate adsorption in regions I and II for an Al-kaolinite system was increased considerably to similar values (Table 19), whereas region III was unchanged, supports the idea that the aluminium on the exchange site of the clay might have the form or grouping of regions I and II. Several workers (Hsu and

Rich, 1960; Thomas, 1960; Shen and Rich, 1962) have shown that when aluminium occupies an exchange site either on a resin or clay mineral, some of the exchangeable aluminium may undergo further hydrolysis to give a hydroxy aluminium compound having a formula of $—Al(OH)_2$. The hydroxy aluminium compound associated with the exchange site therefore can act as the adsorption site for a phosphate ion, in the same way as a similar group that forms part of the edge face. It is noteworthy that K_2^{II} is substantially the same for the adsorption on the Al-kaolinite as for the K-kaolinite.

Because $Al(OH)_2^+$ on the exchange site of the clay is held by Coulombic forces, it would be expected that most of it would be removed by treatment at pH 1, whereas the $—Al(OH)_2$ grouping at the edge face, being part of the crystal lattice has a partly covalent bond, and hence will not be affected to the same extent by acid treatment. Acid treatment only reduced region I of K-kaolinite by a small amount suggesting that the number of aluminium atoms associated with the exchange site of the K-kaolinite may be small in the present case (Table 17).

It appears that the reactive sites for regions I and II can be located on $—Al \begin{matrix} / OH \\ \backslash OH \end{matrix}$ groupings situated on the exchange sites. However, as the hydrated aluminium oxides possess no negative charge, the edge face of these minerals is also implicated and, by analogy, the edge faces of kaolinite crystals.

The constancy of the value of K_2^{II} , for the derived kaolinite systems [such as K-kaolinite, in the presence or absence of KCl, Al-kaolinite, Na-kaolinite, acid treated K-kaolinite in the presence of

KCl, and K-halloysite (Table 24)] further supports the suggestion that the adsorption of phosphate by -Al(OH)_2 on an exchange site involves essentially the same basic mechanism as adsorption onto a positively charged aluminium atom associated with the edge face of the crystal.

The linear isotherm (region III) can be formulated as a simple partition phenomenon in which the solute effectively distributes itself between the bulk and the surface phase.

The linearity of the isotherm in region III indicates that either the number of adsorption sites remains constant even though the amount of solute adsorbed increases or the number of sites is large compared with the amount adsorbed. If the former is the case, the solute may swell the substrate structure exposing a fresh site on which the next molecule can be adsorbed. Giles et al (1960) have suggested that this swelling process takes place most readily in the less ordered or amorphous regions of the adsorbent, the crystalline material being impenetrable.

Only in region III was potassium uptake a necessity for phosphate adsorption (Figure 18), which supports the idea that the adsorption mechanism in this region was distinct from those of regions I and II.

Limited entry of a phosphate ion pair, i.e. $(\text{K}^+\text{H}_2\text{PO}_4^-)$, might be possible into the crystal lattice itself or between crystal lamellae through the steps on the crystal edges.

If interlamellar penetration was an important factor, then a very steep slope would be expected for region III of the hydrated K-halloysite isotherm. The results obtained for K-halloysite (Figure 39) at concentration < 0.1 M, suggest that region III was not associated with the entry between crystal lamellae but was presumably associated with some amorphous material present on the clay surface. This poorly crystallized region on the clay crystal surfaces was readily removed by acid pretreatment at pH 1.

The slope of region III for kaolinites and hydrated aluminium oxides passed through a maximum at about neutrality. The effect of pH on the slope of region III might be due to some dissolution or destruction of this region at the lower pH values, while the OH^- ions were able to compete with phosphate for sites at the higher pH values. An aluminium oxide might be implicated, because region III also exists for gibbsite and pseudoboehmite.

An increase in ionic strength had a pronounced effect on increasing the slope of region III (Figure 38), suggesting that part of the barrier preventing entry might be electrostatic. An alternative explanation is that the material responsible for region III has an amphoteric character and hence there would be a pH value at which the electrostatic barrier preventing the entry into the poorly crystallized region would be at a minimum.

Considerations of the area available for adsorption of phosphate in regions I, II and III on kaolinites, have shown that the adsorption of phosphate in regions I and II could always be accommodated

as a monolayer on the available edge face area. However, the amount of phosphate adsorbed in region III could not be accommodated on the edge face, supporting the idea that in region III penetration of phosphate occurs into some region of the crystal surface. This suggestion is further supported by the results of phosphate adsorption in sodium systems, which showed that there was a marked difference for region III when adsorption took place from sodium and potassium phosphates (Figure 39).

The complete absence of region III for the sodium phosphate, while regions I and II are hardly affected, suggests that the penetration into some less crystalline region of the kaolinite surface is limited by the greater size of the more highly hydrated sodium ion that would have to accompany the phosphate ion.

It is not possible to decide with certainty what type of phosphorus compounds exist in regions I, II and III. However, it may be that these phosphate species exist only as surface complexes having no three dimensional counterpart.

It is of interest to note that the only known phosphate compound with the nearest chemical composition to the adsorbed phase in regions I, and II is variscite, $\text{Al}(\text{OH})_2\text{H}_2\text{PO}_4$. Crystalline aluminium phosphate has been shown (Haseman, Brown and Whitt, 1950; Kittrick and Jackson, 1956) to occur when kaolinite or an aluminium oxide is treated with a strong phosphate concentration ($> 1 \text{ M}$). However, under the experimental conditions in the present study it has been concluded that at concentrations $< 10^{-2} \text{ M}$ (regions I and II), dissolution and precipita-

tion reactions with the formation of separate phases is not occurring. Furthermore, for the pseudoboehmite system at pH 3, the calculated ionic activity product (K_{sp}) of variscite for the observed data in regions I and II was very variable and too high for the pure variscite system (Bache, 1962). For the gibbsite system at pH 5 the equilibrium concentrations of Al^{3+} in regions I and II were effectively zero. (Appendix 15, thus a reaction which leads to the formation of a discrete solid phase i.e. variscite in regions I and II is not acceptable.

It may be argued that the uptake of phosphate in region III is due to the formation of a new crystalline phase such as variscite ($Al(OH)_2H_2PO_4$) or potassium taranakite (potassium aluminium phosphate) or brazilianite (sodium taranakite: $NaAl_3(PO_4)_2OH_4$). However, this idea can be dismissed because.

- (i) The linear isotherm in region III was continuous. It did not show any sudden break to form an isotherm parallel to the y-axis, as would be expected from the solubility product principle governing the dissolution-precipitation of a separate solid phase.
- (ii) The formation of a separate crystalline phase such as variscite or potassium taranakite should lead to the result that these compounds would be most stable under acid conditions, becoming more soluble in the alkaline region. However, the observed results for all the adsorbents have shown that this is not the case, since the slope of region III passes through a maximum at about neutrality.

(iii) Under the experimental conditions used it is most unlikely that at concentrations of 0.1 M phosphate or less, kaolinite would dissolve to give sufficient aluminium for the formation of a new solid phase. In fact no appreciable amount of Al^{3+} could be detected in the phosphate solution at pH 3 in equilibrium with the K-kaolinite. The values of K_{sp} of variscite from the observed data in region III for the gibbsite and pseudoboehmite systems at pH 5 and 3 respectively were very variable (appendix 15), with values which were far too high for the pure variscite system.

Desorption experiments in which the concentration is lowered drastically are not necessarily good criteria of thermodynamic reversibility. Such a procedure could induce a phase change or re-orientation of the adsorbed phase. Adsorption hysteresis is particularly evident for the hydrated aluminium oxides. For infinitesimal changes in concentration, phosphate adsorption in these systems is considered to be thermodynamically reversible.

Adsorption is usually exothermic and hence the extent of adsorption decreases with increasing temperature if the number of sites on which adsorption can occur remain constant.

A very significant feature of the adsorption of phosphate on K-kaolinite, gibbsite and pseudoboehmite was the increase in adsorption as the temperature was raised (Figures 41, 42 and 43).

It has been shown in preliminary kinetic experiments (Appendix 4) that the isotherms at 2° , 20° and 40°C reported in this thesis show no

change with time, and are therefore equilibrium measurements. Hunter and Alexander (1963) have suggested that the increase in phosphate adsorption with temperature reported by Low and Black (1950) is an experimental artefact due to the lack of equilibrium. This criticism can not be applied to the present results especially as the increased adsorption of phosphate remains when the temperature is lowered.

An increase in temperatures affects the three regions in different ways (Figure 41, 42 and 43). The extent of region I reached a maximum at about 20°C, presumably because of the large value of K_2^I and the fact that the experiment was carried out at pH 5, where the number of sites available was at a maximum. In region II there was a definite increase in the number of sites available for adsorption of phosphate. These new sites were presumably formed at 40°C by breaking some bonds with the same energy as region II. However, the increase in the sites at 40°C was irreversible, since the adsorption was not substantially decreased by lowering the temperature to 2°C, the isotherm tending to maintain the shape present at the higher temperature (Figure 47). It is of interest to note that cooling from 20°C does appear to reverse some of the adsorption (Figure 41), suggesting that bond re-formation might be able to occur if the system is not heated to too high a temperature.

The values of K_2^{II} of region II are very similar at 40°C and 2°C (40→2°C). This indicates that the reaction of phosphate with the reactive site in region II involves basically the same mechanism at different temperatures but the number of sites increases (Tables 25, 26).

The heat of adsorption may be divided into two parts.

- (i) due to the irreversible increase in the number of sites, i.e. an endothermic process, and
- (ii) due to the effect of temperature on the exchange process represented by K_2^{II} .

For adsorption to take place the free energy of adsorption must be negative (i.e. Table 16a), and since ΔH is apparently positive $T \Delta S$ should be positive and greater than ΔH , in accordance with $\Delta G = \Delta H - T \Delta S$. This is not unreasonable in solid-solution systems, since the adsorption of one adsorbate molecule on an adsorption site might release several solvent molecules into the solution with a net heat change of zero. Consequently the number of translational degrees of freedom is increased due to the liberation of solvent molecules, with a positive entropy change.

The relatively small effect of temperature on K_2^{II} in region II indicates that the process in this region is largely governed by a positive entropy change ($\Delta S_{1/2}$) having a value of about 17 e.u. for kaolinite, gibbsite and pseudoboehmite (Table 28).

The lack of a significant heat of adsorption, i.e. $\overline{\Delta H}_{1/2} = 0$ (Table 28), is commonly observed for ion-exchange phenomena (Boyd et al, 1947; Helfferich, 1962) and is attributed to the fact that the ions are located in an energetically similar environment after exchange. Thus the driving force for the exchange reaction is due to some gain in entropy. A positive entropy change is also commonly observed in complex formation where a ligand displaces several water

molecules from around a central ion. However, adsorption processes are usually associated with a loss of entropy due to the ordering of the adsorbate species.

The positive entropy change observed for phosphate adsorption in region II may be attributed to a disordering of the water molecules around the adsorption site and adsorbate. This process was not specifically taken into account in formulating the adsorption reaction. Such a suggestion would not be unreasonable since the hydroxyl is displaced by the larger phosphate ion. Detailed calculation of the entropy change expected for the present model would be difficult. However, assuming that the basic entropy change due to the liberation of a water molecule and adsorption of H^+ (i.e. step 1) cancel out, and similarly those due to the exchange between OH^- and phosphate ion (i.e. step 2), then the observed unitary entropy gain is equal to the release of two moles of water, resulting from the adsorption of one mole of phosphate.

Temperature has a marked positive effect in region III (Figures 41, 42 and 43). However, the adsorption within this region is reversible with respect to temperature. The heat of adsorption has been calculated from the change in slope of region III (Figure 48) and is found to be about +5 kcal/mole for kaolinite, +3 kcal/mole for gibbsite, and +4 kcal/mole for pseudoboehmite. This process is thus endothermic and conceivably involves bond breaking, possibly hydrogen bonds, for phosphate to gain entry into the less crystalline region of the crystal surface.

The absence of any heat of adsorption that can be detected calorimetrically, supports the suggestion that the driving force may be largely entropic.

From the results described in this thesis the following conclusions can be drawn:

- (i) The adsorption isotherms of phosphate at constant pH for K-kaolinite, gibbsite and pseudoboehmite are very similar in shape and differ only in the amount of phosphate adsorbed. The order being pseudoboehmite > gibbsite > kaolinite. A slightly better correlation is obtained with the edge face area.
- (ii) The isotherm can be divided by inspection into three distinct regions, designated as regions I, II and III, and it has been suggested that these are related to the affinity of phosphate for three energetically different types of reactive sites.
- (iii) It has been suggested that the adsorption sites of region I and II are located on the first and second hydroxyl of
- $$\begin{array}{l} \text{—Al} \begin{array}{l} \nearrow \text{OH} \\ \searrow \text{OH} \end{array} \end{array}$$
- situated at the edge face of the crystals and on the exchange sites of kaolinite. Adsorption mechanisms for regions I and II have been proposed. The basic difference between the reactions in these regions is that the affinity of the phosphate ion for the positively charged adsorption site in region II is no longer large.

The sites for phosphate adsorption in regions I and II are thus depicted as



These will be common to the edge faces of kaolinite and hydrated aluminium oxides, and the aluminium associated with the exchange sites of kaolinite. The apparent 1:1 correlation between the extent of regions I and II would tend to rule out $>\text{AlOH}$ as the reactive sites. Furthermore this grouping is unlikely to be present on the exchange site of the clay, as an intermediate hydrolysis product of exchangeable aluminium (Hsu and Rich, 1960; Thomas, 1960; Shen and Rich, 1962).

- (iv) Region III is associated with the occlusion or absorption of potassium phosphate ($\text{K}^+\text{H}_2\text{PO}_4^-$) into an amorphous or semi-crystalline region of the clay surface.
- (v) The affinity constants of the various processes proposed to describe phosphate adsorption in regions I and II are very similar for all the adsorbents examined, indicating the essential similarity of the processes for these materials.
- (vi) The adsorption isotherms of phosphate on kaolinite are reversible with respect to pH in all regions and with respect to concentration in regions II and III. The isotherms for the hydrated oxides are largely irreversible with respect to concentration and hence it appears that a phase change occurs under the conditions of the desorption experiments.
- (vii) Apart from increasing the number of adsorption sites in region II, increasing the temperature has little effect on regions I and II.

Thus the driving force for phosphate adsorption was considered to be a positive entropy change associated with a desorption or rearrangement of perhaps two water molecules around the phosphate ion and at the adsorption site.

There was a small positive heat of adsorption (ΔH) in region III of the order of 3 to 5 kcal/mole, which probably arises from the need to break some hydrogen bonds before occlusion can occur.

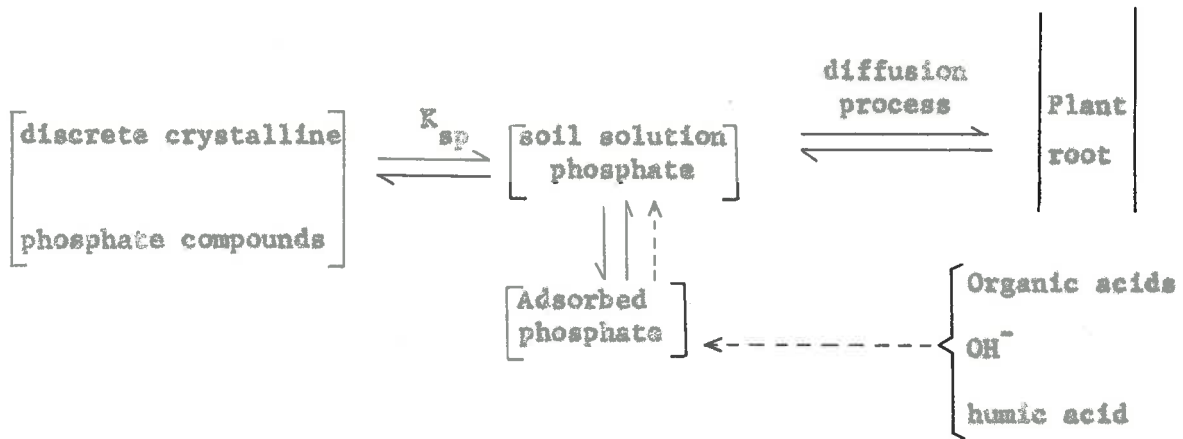
The work described in this thesis may have the following implications.

1. The proposed model and the mechanism of adsorption of phosphate onto kaolinite could be applicable to other aluminosilicate minerals such as montmorillonite and illite. The amount of phosphate adsorbed will depend on the number of aluminium atoms per unit edge face area. It would be expected that the amount of phosphate adsorbed/unit weight would be in the following order gibbsite > K-kaolinite > K-montmorillonite, because of the dilution effect of the silicate layers. However, for an Al-montmorillonite system the amount of phosphate adsorbed will be greater than Al-kaolinite.
2. The reversibility of the adsorbed phosphate may be used as a measure of the availability of phosphate to the plant. For K-kaolinite systems, most of the adsorbed phase in regions II and III is readily released into solution, at least until the end of the steep rise (region I). Thus in a kaolinitic soil the adsorbed phosphate would be expected to be readily available to the plant (i.e. more than 60%).

In some highly weathered tropical soils containing high amounts of hydrated aluminium oxides, i.e. gibbsite and pseudoboehmite the availability of the adsorbed phosphate would be much less than in the kaolinitic soil, since the adsorbed phosphate on these oxides seems to undergo a phase change, becoming less reversible when there is a drastic change in the equilibrium concentration. Thus under high rainfall conditions the adsorbed phosphate may very readily become less available. Plant roots may however have some mechanism for releasing adsorbed phosphate by exuding organic compounds which can displace phosphate making it available to the plant. Plant roots may also release OH^- and this would cause a desorption of phosphate.

3. It must be realized that phosphate ions in the soil solution may have to move from the bulk soil solution through the pore space toward the root surface. The movement of an ion in solution is known to be governed by diffusion processes. The magnitude of the diffusion coefficient of the phosphate ion is partly governed by side reactions taking place with soil colloids during the diffusion process. The low values of the diffusion coefficient for the phosphate ion in soils has been attributed to adsorption by soil colloids (Graham - Bryce, 1963).

The following diagram may be used to illustrate the relation between the soil phosphate system and plant roots.



In view of the results presented in this thesis it is suggested that future investigations may be carried out on the following aspects of phosphate adsorption.

1. Valuable information may be obtained from the direct study of the adsorption of phosphate with synthetic hydrated iron oxide $\text{FeO}(\text{OH})$ (goethite) and the unhydrated iron oxide (Fe_2O_3). It has been generally agreed that unhydrated iron oxides do not react with phosphate, although the evidence is not conclusive. Most of the work on iron oxide - phosphate systems has been carried out by indirect methods, such as the removal of iron oxides by chemical (Mitchell and Mackenzie, 1954) or biological methods (Bromfield, 1964). This indirect method however, does not differentiate between the relative roles of the hydrated and unhydrated iron oxides, in the adsorption of phosphate. It is predicted that the reactive group on the hydrated iron oxide would be $>\text{FeOH}$ and thus, other considerations apart, the reactions of $\text{FeO}(\text{OH})$ would be very different from gibbsite.
2. Adsorption studies such as the present one are only indirect in

locating the adsorption sites. Auto-radiography on a large crystal, such as a dickite crystal, may give direct information about the location of the adsorbed phosphate (P^{32}).

3. Infra-red studies on the adsorbed phase may also give some further information regarding the state of the adsorbed phosphate, particularly after washing the hydrated aluminium oxide systems with water.

4. Detailed studies on the desorption of phosphate, particularly from an aluminium - clay system, will provide further information about the availability of adsorbed phosphate in this system.

5. Detailed kinetic studies on phosphate adsorption will increase our understanding of the mechanisms of phosphate adsorption. However, this will require special techniques for studying fast reactions in solid-solution systems i.e. clay - phosphate system. Preliminary kinetic experiments carried out by the author have shown that most of the phosphate is adsorbed by kaolinite within a very short period of time.

APPENDIX 1Preparation of K-kaolinite API-9

I. Saturation with 1M KCl pH 3 (100 g. clay/l.)

No. of washing	Equilibration time	pH	Al ³⁺ concentration μg/ml.
1	12 hour	4.52	11.2
2	1 "	4.46	7.3
3	0.5 "	4.25	6.7
4	0.5 "	4.07	6.9
5	0.5 "	3.77	6.6
6	0.5 "	3.40	6.0
7	standing overnight	3.96	8.8
8	0.5 hour	3.23	4.5
9	0.5 "	3.22	3.8
10	0.5 "	3.20	3.5
11	0.5 "	3.12	3.0
12	0.5 "	3.20	3.6
14	0.5 "	3.16	3.0

II. Re-saturation with 1M KCl solution

1	0.5 hour	4.4	2.1
2	0.5 "	4.62	2.2
3	0.5 "	4.78	2.0
4	12 "	4.94	2.0

III Removing excess salt with distilled water

1	0.5 hour	4.74	0.5
2	"	5.14	0
3	"	5.76	0
4	"	6.18	0
5	"	6.34	0
6	"	6.34	0
7	"	6.34	0
8	"	6.40	0
9	"	6.50	0
10	"	6.48	0
11	"	6.50	0
12	"	6.48	0
13	"	6.42	0
14	"	6.58	0

APPENDIX 2

Aluminium and Silicon released in the acid washing (0.1 N HCl) of
K-kaolinite API-9

Washing	Equilibration time	Al ³⁺ µg./g	Si ⁴⁺ µg./g
1	12 hour	661.0	600.0
2	0.5 "	80.0	40.0
3	0.5 "	50.0	60.0
4	Standing over- night	160.6	247.0
5	0.5 hour	56.0	86.0
6	0.5 "	16.0	20.0
7	0.5 "	12.8	20.0
		Total = 1023.9	1074.0
		= 1.023mg/g	1.074 mg/g

$$\text{Ratio of } \frac{\text{Si}}{\text{Al}} = \frac{1.074}{1.023} = 1$$

$$\frac{\text{SiO}_2}{\text{Al}_2\text{O}_3} = \frac{2.37}{1.90} = 1.2$$

APPENDIX 3Determination of electric charges

Positive and negative charges carried by the clay at different pH values were determined by the method of Schofield (1949). A sample of 0.50 g clay was placed in a tared 40 ml polypropylene centrifuge tube, and 25 ml of 0.2 N NH_4Cl solution at a desired pH value was added. The tube was well shaken, centrifuged and the clear supernatant was decanted to avoid any loss of clay. The pH of the supernatant was then determined. This procedure was repeated until the pH of the supernatant approached closely that of the added solution, when equilibrium was considered to have been attained. This procedure required about 16 washings.

When washing with the NH_4Cl solution at a given pH was judged to have been sufficient, the centrifuge tube and moist sample was weighed to determine the weight of the entrained NH_4Cl solution. The sample was then washed five times with 25 ml portions of 0.2N KNO_3 . These five washings were bulked into a 200 ml volumetric flask, and finally made up to 200 ml volume with 0.2 N KNO_3 solution; this solution was then analysed for NH_4^+ and Cl^- .

A series of experiments at different pH values (ranging from pH 3 to 9) was carried out, in each of which the pH of the 0.2 N NH_4Cl solution was adjusted to a required value by the addition of suitable amounts of HCl or NH_4OH solution. Thus the dependence of the electric charges on pH could be determined.

Determination of NH_4^+

A suitable aliquot of the KNO_3 washings was distilled with NaOH solution in a Markham still and the ammonia displaced was collected in 4% boric acid solution with methyl red-bromo-cresol green indicator. The ammonia was then titrated with standard 0.001 N hydrochloric acid solution.

Determination of chloride

The chloride contents were determined potentiometrically by AgNO_3 titration, using a modified method of Best (1929), and Kolthoff and Kuroda (1951), as given in Appendix 8.

Calculation of NH_4^+ and Cl^- adsorption

To determine the amount of NH_4^+ and Cl^- adsorbed by the clay from the 0.2 N NH_4Cl solution at different pH values, the empty centrifuge tubes were weighed. The tube and the moist sample with the entrained liquid was also weighed just before washing with the KNO_3 solution. Since the weight of the oven-dry sample is known, the weight of the entrained NH_4Cl solution could be determined.

From the amount of NH_4^+ and Cl^- present in the original solution at the particular pH, the amount of NH_4^+ and Cl^- in the entrained solution were calculated, and these were used as a correction factor. Therefore the amount of NH_4^+ and Cl^- adsorbed were determined and expressed as meq. per 100 g clay (meq.%).

APPENDIX 4Kinetic adsorption data at different temperatures for
various adsorbents (pH 5)1. The amount of phosphate adsorbed (meq. %) by K-kaolinite API-9 (2°C)

Time (hour)	Equilibrium concentration mgP/ml			
	1.6	91.0	950	3100
12	0.40	0.97	1.44	2.40
24	0.43	0.98	1.45	2.41
48	0.42	1.0	1.45	2.40

2. The amount of phosphate adsorbed (meq. %) by K-kaolinite API-9 (20°C)

Time (hour)	Equilibrium concentration mgP/ml			
	1.6	91.0	920	3100
12	0.80	1.50	2.27	4.40
24	0.88	1.58	2.34	4.45
48	0.89	1.57	2.36	4.42
96	0.87	1.57	2.32	4.44

3. The amount of phosphate adsorbed (meq. %) by K-kaolinite API-9 (40°C)

Time (hour)	Equilibrium concentration mgP/ml			
	1.7	91.0	920	3100
12	0.85	1.87	3.20	6.30
24	0.90	1.95	3.30	6.55
48	0.92	1.96	3.33	6.60
96	0.90	1.90	3.31	6.64
168	-	1.93	-	6.65

Appendix 4 (cont.)4. The amount of phosphate adsorbed (meq. %) by Gibbsite (20°C)

Time (hour)	Equilibrium concentration mgP/ml.			
	1.8	92.0	940	3100
12	18.5	30.0	54.0	97.9
24	19.0	81.5	54.6	98.5
48	19.5	32.0	55.0	99.0
96	19.2	32.5	54.0	98.6
168	-	30.0		98.3

5. The amount of phosphate adsorbed (meq. %) by Gibbsite (40°C)

Time (hour)	Equilibrium concentration mgP/ml			
	1.5	90.0	920	3100
12	20.0	41.0	90.0	142.0
24	21.2	43.0	92.5	145.0
48	21.6	43.8	92.3	145.5
96	21.0	44.0	92.8	146.0
168	-	43.5	-	145.7

Appendix 4 (cont.)6. The amount of phosphate adsorbed (meq. %) by Pseudoboehmite (20°C)

Time (hour)	Equilibrium concentration mgP/ml.			
	1.4	86.0	920	3080
12	-	167.0	-	258.0
24	40.0	169.9	209.0	262.0
48	40.2	170.8	209.7	264.6
96	40.5	171.0	210.0	268.0
168	-	170.0	-	265.0

7. The amount of phosphate adsorbed (meq. %) by Pseudoboehmite (40°C)

Time (hour)	Equilibrium concentration mgP/ml			
	1.3	85	910	3070
12	-	178.0	-	307.0
24	40.0	184.0	240.9	314.7
48	39.7	185.0	241.8	315.5
96	39.9	186.0	242.0	315.7
168	-	185.2	-	315.0

APPENDIX 5

Determination of Phosphorus using the heteropoly blue method
(Boltz and Mellon, 1947)

Apparatus: Optical density measurements were made in 2 cm cells using a "Unicam S.P. 600" Spectrophotometer at a wavelength of 820 m μ with a red sensitive photocell.

- Solution
1. Standard phosphate solution (1 μ g/ml.)
 2. Acid ammonium molybdate (1% Ammonium molybdate in 5 N H₂SO₄)
 3. Hydrazine sulphate (0.125%)
 4. Reductant. (4 volumes of Acid ammonium molybdate and 1 volume Hydrazine sulphate).

Procedure:

Pipette an appropriate volume into a 100 ml volumetric flask and dilute with distilled water to about 60 ml. Then add 25 ml of reductant, adjust the final volume to the 100 ml mark with distilled water and mix the contents of the flask thoroughly. Using the same procedure prepare a set of standards containing 0, 2, 5, 10, 20, and 40 μ g phosphorus. Immerse the flasks in a boiling waterbath for 15 minutes, remove and cool rapidly.

Measure the optical density of all solutions. Construct a standard calibration curve. The phosphorus concentration of the unknown samples can be read from the standard calibration curve.

APPENDIX 6

Determination of Silicon using the method of Mullin and Riley (1955)

Apparatus: Optical density measurements were made in 2 cm cells using a "Unicam S.P. 600" Spectrophotometer at a wavelength of 812 m μ with a red sensitive photocell.

- Solution 1. Acid ammonium molybdate (2% Ammonium molybdate in 0.69 N HCl)
2. Oxalic acid (10%)
 3. Sulphuric acid (25% v/v)
 4. Metol-sulphite solution (2% Metol and 1.2% anhydrous sodium sulphite).
 5. Reductant (5 volumes of Metol-sulphite, 3 volumes of Oxalic acid, 6 volumes of sulphuric acid solution and 1 volume of distilled water.)
 6. Standard sodium silicate solution (2 μ g Si/ml).

Procedure:

Pipette 20 ml of the sample (up to 60 μ g Si) into a 50 ml volumetric flask containing 3 ml of the acid molybdate reagent and mix thoroughly. After standing for 10 minutes, add 15 ml of the reducing agent using dip pipette, and dilute to 50 ml with distilled water. Mix the solution and allow to stand for 3 hours. Using the same procedure prepare a series of standard silicon solutions. Measure the optical density of the solution at 812 m μ .

APPENDIX 7

Determination of aluminium using the Alizarin red-S method

(Modified method as suggested by Bond (1957))

Apparatus: Optical density measurements were made in 1 cm cells using a "Unicam S.P. 600" Spectrophotometer at wavelength of 495 m μ with a blue sensitive photocell.

- Solutions:
1. CaCl₂ solution (1.4%)
 2. Sodium acetate-acetic acid buffer (70 g hydrated sodium acetate, 30 ml. glacial acetic acid in 500 ml distilled water).
 3. Alizarin red-S solution (0.10% of purified reagent).
 4. Thioglycollic acid solution (2% v/v).
 5. Potassium aluminium sulphate standard solution (4 μ g. Al/ml)

Procedure:

Pipette a suitable aliquot of solution containing less than 75 μ g of Al into a 100 ml volumetric flask, and dilute to about 60 ml with distilled water. Add sufficient standardised HCl solution to give a total of 0.5 meq. of excess acid. Add 2 ml. of thioglycollic acid, 1 ml of CaCl₂ and 10 ml of sodium acetate buffer. Allow to stand 10 minutes before further addition of 5 ml of alizarin red-S solution and make up to 100 ml. Using the same procedure prepare a set of standards containing 0-75 μ g of Al. Invert several times and then allow to stand for 3 hours.

Measure the optical density of all solutions in a spectrophotometer at 495 m μ .

APPENDIX 8

Determination of chloride using potentiometric titration techniques
(Modified methods of Best (1929), and Kolthoff and Kuroda (1951)).

Apparatus: The potential difference was measured using a modified electrode which was



coupled with a "Cambridge pH meter".

- Solutions:
1. Standard silver nitrate solution (0.001 N)
 2. Supporting electrolyte (202 g KNO_3 , 25 ml concentrated HNO_3 , made up to 2 litres volume with distilled water).
 3. Buffer solution pH 3.2 (10.21 g Potassium hydrogen phthalate, 148 ml 0.1 N H_2SO_4 , made up to 1 litre volume with distilled water.).

Procedure:

Pipette a suitable aliquot (10 ml) of the solution into a titrating flask, and add twice this amount of supporting electrolyte into the flask. Lower the electrodes into the flask so that the electrodes are below the liquid at all times. Titrate with standard AgNO_3 (0.001 N) until the end point is reached, i.e. zero e.m.f.

APPENDIX 9

Calculation of the results for K-kaolinite API-9 (pH 5, 20°C)

	Equilibrium conc. µgP/ml.	Total P in acid digest µgP.	C.F.* µgP.	Corrected total P		Amount adsorbed	
				µgP/wt of clay	µgP/g	µgP/g**	meq. %
1	0.74	49.69	0.14	49.55/0.18560	267.0	217.0	0.70
2	1.88	60.0	0.36	59.64/0.18530	321.85	271.85	0.88
3	5.86	69.39	1.13	68.26/0.17740	384.81	334.81	1.08
4	7.90	74.73	1.51	73.22/0.18150	403.46	353.46	1.14
5	9.16	74.70	1.90	73.88/0.17750	415.79	365.79	1.18
6	9.10	78.27	2.03	76.24/0.18202	418.90	368.90	1.19
7	12.2	68.55	1.64	69.91/0.15741	425.10	375.10	1.21
8	20.8	91.20	4.24	86.96/0.18440	471.62	421.62	1.36
9	21.0	89.62	4.10	85.53/0.17904	477.80	427.80	1.38
10	36.6	102.28	7.11	95.17/0.18820	505.73	455.73	1.47
11	91.6	123.32	17.53	105.78/0.18840	561.48	511.48	1.65
12	92.0	120.24	17.20	103.04/0.18555	555.30	505.30	1.63
13	154.0	138.48	28.20	110.28/0.18810	586.30	536.30	1.73
14	154.0	138.86	27.90	110.96/0.18630	595.61	545.61	1.76
15	218.0	156.72	40.18	116.55/0.18883	617.30	567.30	1.83
16	219.0	154.84	41.60	113.24/0.18530	611.10	561.10	1.81
17	310.0	174.59	54.00	120.59/0.18690	645.20	595.20	1.92
18	312.0	177.20	53.70	123.50/0.19054	648.32	598.32	1.93
19	481.0	218.50	87.20	131.30/0.18814	697.90	647.90	2.09
20	481.0	216.37	85.40	130.97/0.18520	707.21	657.21	2.12
21	627.5	244.38	105.90	138.48/0.18603	744.40	694.4	2.24
22	912.5	306.10	162.20	143.90/0.18560	775.43	725.43	2.34
23	913.0	300.70	159.30	141.47/0.18100	781.59	731.59	2.36
24	1550	447.30	259.20	188.10/0.18440	1020.30	970.30	3.13
25	1550	450.0	262.0	188.0/0.18660	1007.50	957.50	3.09
26	3070	753.3	484.0	269.32/0.18840	1429.53	1379.53	4.45
27	3070	770.23	496.0	274.23/0.19062	1438.80	1388.80	4.48

* C.F. is the correction factor = equilibrium concentration x the entrained solution.

** Blank correction P = 50 µg. was made for calculating the amount adsorbed (µgP/g) from the corrected total P (µgP/g.).

APPENDIX 10Regression analysis of region I

For $\frac{1}{V_0}$ against $\frac{1}{[H^+]}$, according to equation (55):

$$\frac{1}{V_0} = \frac{1}{K_1^I V_1} \frac{1}{[H^+]} + \frac{1}{V_1}$$

1. K-kaolinite API-9

$\frac{1}{V_0}$	$\frac{1}{[H^+]}$	V_1 (meq.%)	K_1^I (ml/meq.)
1.18	10^3		
1.18	10^4		
1.18	10^5		
1.67	10^7		
2.22	10^9		
6.66	10^{10}		
		0.72	0.26×10^{10}

regression coefficient $r = 0.99$

Standard error: $SE(V_1) = 0.065$

$SE(K_1^I) = 0.03 \times 10^{10}$

2. K-kaolinite KG:

$\frac{1}{V_0}$	$\frac{1}{[H^+]}$	V_1 (meq. %)	K_1^I (ml/meq.)
1.0	10^3		
1.0	10^5		
1.25	10^8		
1.54	10^9		
3.30	10^{10}		
		0.86	0.54×10^{10}

regression coefficient $r = 0.96$

$$SE(V_1) = 0.06$$

$$SE(K_1^I) = 0.16 \times 10^{10}$$

3. Gibbsite

$\frac{1}{V_0}$	$\frac{1}{[H^+]}$	V_1 (meq. %)	K_1^I (ml/meq.)
4.55×10^{-2}	10^3		
4.55×10^{-2}	10^5		
11.7×10^{-2}	10^9		
22.5×10^{-2}	10^{10}		
		15.9	0.38×10^{10}

regression coefficient $r = 0.94$

$$SE(V_1) = 5.2$$

$$SE(K_1^I) = 0.2 \times 10^{10}$$

4. Pseudoboehmite

$\frac{1}{V_0}$	$\frac{1}{[H^+]}$	V_1 (meq. %)	K_1^I (ml/meq.)
0.87×10^{-2}	10^3		
0.87×10^{-2}	10^5		
1.51×10^{-2}	10^9		
2.23×10^{-2}	10^{10}		
		98.0	0.85×10^{10}

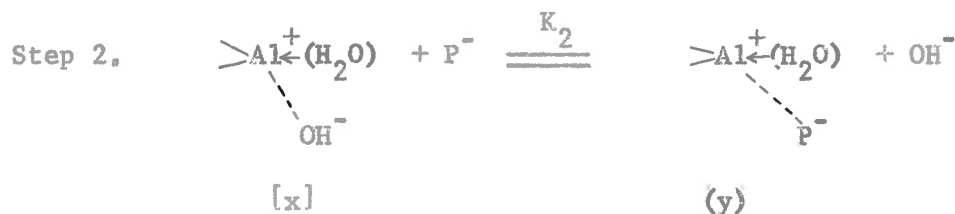
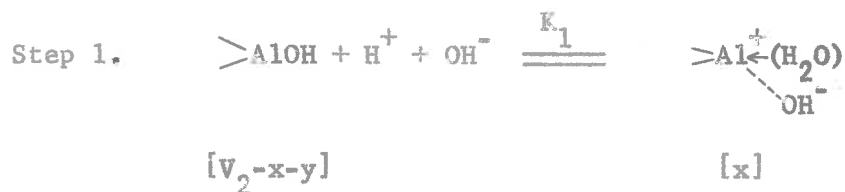
regression coefficient $r = 0.96$

$$SE(V_1) = 13.2$$

$$SE(K_1^I) = 0.29 \times 10^{10}$$

APPENDIX 11

Derivation of adsorption isotherm for region II, if Step 1 is dependent on Step 2, and the theoretical value of adsorption.



where V_2 is the total number of sites in region II (meq. %)

$$K_1 = \frac{[x]}{[V_2 - x - y][\text{H}^+]}$$

$$K_2 = \frac{(y)}{[x][\text{P}]} \quad [x] = \frac{(y)}{K_2[\text{P}]}$$

Substituting $[x]$ and rearranging, gives

$$\begin{aligned} K_1 &= \frac{(y)}{K_2[\text{P}](V_2 - \frac{(y)}{K_2[\text{P}]} - (y))[\text{H}^+]} \\ (y) &= \frac{K_1 K_2 V_2 [\text{P}][\text{H}^+]}{K_1[\text{H}^+] + K_1 K_2 [\text{H}^+][\text{P}] + 1} \\ (y) &= \frac{K_1 K_2 V_2 [\text{P}]}{K_1 + K_1 K_2 [\text{P}] + \frac{[\text{OH}^-]}{K_w}} \end{aligned}$$

Assuming hypothetical value for

$$K_1 = 1$$

$$K_2 = 2$$

$$V_2 = 10$$

$$K_w = 1$$

gives

$$(y) = \frac{20[P]}{1 + 2[P] + [OH^-]}$$

Theoretical values of adsorption in region II at
different values of $[OH^-]$ (Figure 23)

[P]	$[OH^-]=1$	$[OH^-]=10$	$[OH^-]=50$	$[OH^-]=100$
0	0	0	0	0
1	4.0	1.43	0.37	0.19
2	5.70	2.50	0.71	0.37
3	6.70	3.34	1.30	0.55
5	7.70	4.55	1.61	0.90
10	8.70	6.25	2.78	1.64
20	9.30	7.70	4.35	2.82
50	9.70	8.90	6.55	4.95
100	10.0	9.95	8.0	6.65
500	10.0	10.0	9.5	9.1
1000	10.0	10.0	9.8	9.5

APPENDIX 12

Regression analysis of the Langmuir plots (region II) (equation 60c)
for K-kaolinite API-9 (20°C) (Figure 29).

(1) pH 3

$\frac{[P]}{A} \times 10^3$	$[P] \times 10^3$	Slope S	Intercept I $\times 10^3$	$K_2^{II} \times 10^{-3}$ (ml/meq.)
1.58	0.55			
2.07	1.24			
3.63	2.31			
4.87	3.43			
13.24	10.52			
		1.18	0.81	1.46

regression coefficient $r = 0.999$

$$SE(K_2^{II}) = 0.18 \times 10^3$$

(2) pH 4

$\frac{[P]}{A} \times 10^3$	$[P] \times 10^3$	Slope S	Intercept I $\times 10^3$	$K_2^{II} \times 10^{-3}$ (ml/meq.)
1.85	0.57			
2.58	1.05			
2.88	2.03			
2.90	2.08			
5.06	3.10			
8.16	4.97			
14.30	9.74			
		1.36	1.10	1.23

$r = 0.999$

$$SE(K_2^{II}) = 0.14 \times 10^3$$

(3) pH 5

$\frac{[P]}{A} \times 10^3$	$[P] \times 10^3$	Slope S	Intercept I $\times 10^3$	$K_2^{II} \times 10^{-3}$ (ml/meq.)
1.13	0.39			
1.37	0.67			
2.02	1.18			
4.20	2.96			
6.58	4.97			
9.06	6.94			
12.75	10.0			
		1.21	0.62	1.95

$$r = 0.999$$

$$SE(K_2^{II}) = 0.10 \times 10^3$$

(4) pH 7

$\frac{[P]}{A} \times 10^3$	$[P] \times 10^3$	Slope S	Intercept I $\times 10^3$	$K_2^{II} \times 10^{-3}$ (ml/meq.)
3.13	1.02			
4.62	2.03			
6.37	3.19			
9.60	5.09			
7.16	9.68			
		1.63	1.33	1.23

$$r = 0.999$$

$$SE(K_2^{II}) = 0.10 \times 10^3$$

(5) pH 9

$\frac{[P]}{A} \times 10^3$	$[P] \times 10^3$	Slope S	Intercept I $\times 10^3$	$K_2^{II} \times 10^{-3}$ (ml/meq.)
1.74	0.17			
2.40	0.61			
2.68	1.06			
5.82	2.01			
6.90	3.06			
8.86	4.83			
11.95	6.94			
		2.06	1.38	1.49

$$r = 0.999$$

$$SE(K_2^{II}) = 0.20 \times 10^3$$

(6) pH 10

$\frac{[P]}{A} \times 10^3$	$[P] \times 10^3$	Slope S	Intercept I $\times 10^3$	$K_2^{II} \times 10^{-3}$ (ml/meq.)
2.28	0.12			
3.10	0.46			
4.75	0.93			
6.86	1.88			
9.20	2.91			
13.50	4.81			
		2.38	2.20	1.08

$$r = 0.998$$

$$SE(K_2^{II}) = 0.09 \times 10^3$$

APPENDIX 13

Confidence limit for K_2^{II} , K-kaolinite API-9 (20°C)

pH	$K_2^{II} \times 10^{-3}$ (ml/meq.)
3	1.46
4	1.23
5	1.95
7	1.23
9	1.49
10	1.08

Average value = 1.40

Variance $\sigma^2 = 0.095$

Standard error of individual = $\sqrt{0.095} = 0.33$

Standard error of mean = $\sqrt{\frac{\sigma^2}{n}} = 0.14$

t-test

$t_{5\%}$ (at 5% level) = 2.57

$$\text{L.S.D.} = \pm t_{5\%} \times \sqrt{\frac{\sigma^2}{n}}$$

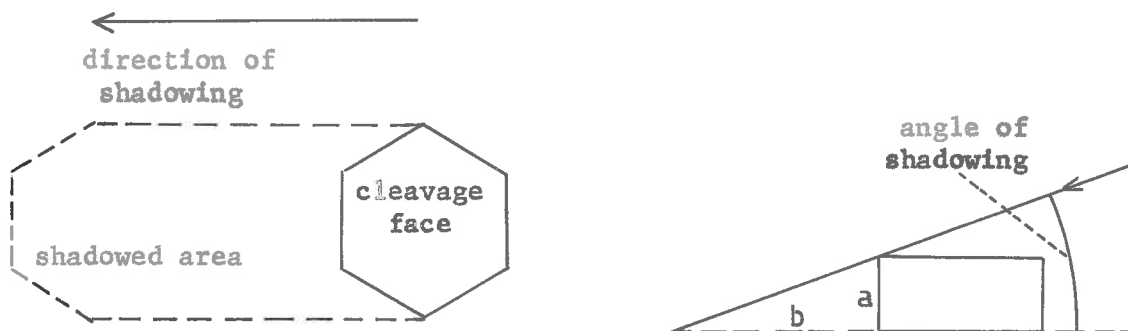
$$= \pm 0.36$$

The true value of K_2^{II} lies between (1.05 to 1.76) $\times 10^3$

It is concluded that even at the 5% level the value of K_2^{II} at different pH values is not significantly different from the mean value.

APPENDIX 14Estimation of edge face area from the shadowed electron micrograph

For surface area measurements, only those particles in the shadowed electron micrograph which were lying flat and were well defined, were used. The cleavage area of the particle (mostly hexagonal) was measured using a planimeter. Since there are two cleavage faces for each particle, the measured cleavage area was multiplied by 2.



The perimeter of the cleavage surface and the apparent thickness of the particle from the shadowed photograph were measured. Since the angle of shadowing, hence the ratio of $\frac{b}{a}$ (the value of cotangent) was known, the true thickness of the particle (a) could be calculated. Thus the total area of edge face, regarded as rectangular, was calculated (thickness (a) x total perimeter of the cleavage area). The percentage of the edge face area for individual particles was then computed.

1. K-kaolinite API-9 (magnification 20,000x; ratio $\frac{b}{a} = 5$)

Calculated cleavage area (cm ²)	Calculated Edge area (cm ²)	Edge area of individual particle as percentage of total area (%)
1.60	0.38	19.2
0.20	0.20	50.0
0.60	0.32	34.8
1.20	0.90	43.0
1.40	0.60	30.0
0.80	0.29	26.6
0.40	0.14	26.0
0.40	0.19	32.2
0.40	0.21	34.4
1.60	0.48	23.0
0.25	0.25	50.0
0.80	0.45	36.0

Average = 34%

Total surface area of K-kaolinite API-9 as measured using low temperature nitrogen adsorption = 12 m²/g.

$$\text{Edge face area} = \frac{34}{100} \times 12 = 4.1 \text{ m}^2/\text{g}.$$

2. K-kaolinite RG. (magnification 100,000x; ratio $\frac{b}{a} = 5$)

Calculated cleavage area (cm ²)	Calculated Edge area (cm ²)	Edge area of individual particle as percentage of total area (%)
6.0	0.85	12.4
6.1	0.71	10.6
3.0	0.50	14.3
5.4	0.78	12.6
5.9	0.92	13.5
4.5	0.75	14.3
6.4	0.79	11.0
5.2	0.92	15.0
		Average = 13.0%

Total surface area of K-kaolinite RG as measured using low
temperature nitrogen adsorption = 40 m²/g.

$$\text{Edge area} = \frac{13}{100} \times 40 = 5.2 \text{ m}^2/\text{g}.$$

3. Gibbsite (magnification 40,000x; ratio $\frac{b}{a} = 4$).

Calculated cleavage area (cm ²)	Calculated edge area (cm ²)	Edge face area of individual particle as percentage of total area (%)
0.68	0.48	41.4
0.96	0.46	32.4
0.64	0.32	33.0
0.88	0.50	36.3
0.40	0.30	42.8
0.40	0.32	44.0
0.44	0.29	37.0
0.48	0.39	44.0
		Average = 38.8%

Total surface area of gibbsite as measured using low
temperature nitrogen adsorption = 48 m²/g.

$$\begin{aligned} \text{Edge face area} &= \frac{38.8}{100} \times 48 = \\ &= \underline{\underline{18.6 \text{ m}^2/\text{g}}}. \end{aligned}$$

APPENDIX 15

Calculation of the solubility product, K_{sp} , of variscite

$$\text{(Equation (1)) : } K_{sp} = a_{Al} \times a_{OH}^2 \times a_{H_2PO_4}.$$

The activity of a phosphate solution is the molar concentration multiplied by the activity coefficient γ . Since the concentration of aluminium was very low, the activity coefficient of aluminium was assumed to be unity. The activity coefficient for the phosphate ion was calculated from the Debye and Hückel first approximation (1923).

$$-\log \gamma = Z^2 A \sqrt{\mu}$$

where the ionic strength $\mu = 0.5 \sum cZ^2$

A is constant and equal to 0.5 at room temperature (Bjerrum and Unmack, 1929).

Z is the valency of the ions.

c is the molar concentration.

I. Gibbsite (pH 5, 20°C)

Region	Phosphate conc. mole/l. $\times 10^3$	Activity conc. [P] $\times 10^3$	[Al ³⁺] mole/l. $\times 10^6$	[OH ⁻] ² mole/l. $\times 10^{18}$	ionic activity product $K_{sp} \times 10^{25}$
I	0.029	-	0	1.58	0
	0.082	-	0	1.32	0
II	0.985	-	0	1.23	0
	1.93	-	0	1.00	0
	4.94	-	0	1.32	0
III	10.20	9.10	3.70	1.38	0.465
	20.20	17.10	4.45	1.32	1.00
	50.10	38.80	7.40	1.00	2.87
	100.0	69.50	11.80	1.00	8.2

II. Pseudoboehmite (pH 3, 20°C)

Region	Phosphate conc. mole/l. $\times 10^3$	Activity conc. [P] $\times 10^3$	[Al ³⁺] mole/l. $\times 10^4$	[OH ⁻] ² mole/l. $\times 10^{22}$	Ionic activity product K _{sp} $\times 10^{29}$
I	0.052	0.052	2.82	1.51	0.22
	0.0970	0.097	3.55	1.30	0.45
II	0.532	0.532	3.52	1.53	2.87
	1.05	1.05	3.52	1.50	5.54
	3.12	2.94	3.09	1.58	14.4
	4.93	4.55	3.15	1.58	22.7
III	10.30	9.26	4.02	1.44	53.6
	20.90	17.70	5.37	1.32	125.0
	50.10	38.80	7.76	1.32	397.0
	100.0	69.50	8.98	1.30	821.0

REFERENCES

- Adamson, A.W. (1960).- "Physical Chemistry of Surfaces". p. 531.
Interscience, N.Y.
- Agronomy Monograph (1953).- Vol. IV. "Soil and Fertilizer Phosphorus
in Crop Nutrition". Ed. Pierre, W.H. and Norman, A.G.
Academic Press Inc. N.Y.
- Arnon, D.I. (1953).- Agronomy Monograph Vol. IV, 1.
Ed. Pierre W.H. and Norman, A.G. Academic Press Inc. N.Y.
- Aslyng, H.C. (1954).- Denmark Roy. Vet. Ag. Coll. Yearbook, 1.
- Bache, B.W. (1963).- J. Soil Sci. 14, 113.
- Best, R.J. (1929).- J. agric. Sci. 19, 533.
- Bernal, J.D. and Megaw, H.D. (1935).- Proc. roy. Soc. Ser. A, 151, 384.
- Birch, H.F. (1958).- Plant and Soil 10, 9.
- Birch, H.F. (1959).- Plant and Soil 11, 263.
- Birch, H.F. (1960).- Plant and Soil 12, 81.
- Bjerrum, N. and Ummack, A. (1929).- Kgl. danske Vidensk. Selsk. Math.-
fys. Medd. IX. 1, 115.
- Boltz, D.F. and Mellon, M.G. (1947).- Analyt. Chem. 19, 873.
- Bond, R.D. (1957).- Tech. Memo. 1/57. C.S.I.R.O. Division of Soils.
- Boyd, C.E., Schubert, J. and Adamson, A.W. (1947).- J. Amer. chem.
Soc. 69, 2818.
- Brindley, G.W. (1961).- "The X-ray Identification and Crystal
Structures of Clay Minerals", p. 51.
Ed. Brown, G., Miner. Soc. Lond.
- Brindley, G.W. and Robinson, K. (1946).- Miner. Mag. 27, 242.
- Brindley, G.W. and Nakahira, M. (1958).- Miner. Mag. 31, 781.

- Bromfield, S.M. (1964).- Nature, 201, 321.
- Brown, W.E. and Lehr, J.R. (1959).- Proc. Soil Sci. Soc. Amer. 23, 7.
- Brunauer, S. (1943).- "The Adsorption of Gases and Vapours", p. 27, 53. Oxford. Univ. Press, London.
- Cashen, G.H. (1959).- Trans. Faraday Soc. 55, 477.
- Clark, J.S. and Peech, M. (1955).- Proc. Soil Sci. Soc. Amer. 19, 171.
- Cole, C.V. and Jackson, M.L. (1950a).- J. phys. Chem. 54, 128.
- Cole, C.V. and Jackson, M.L. (1950b).- Proc. Soil Sci. Soc. Amer. 15, 84.
- Coleman, R. (1944).- Proc. Soil Sci. Soc. Amer. 9, 72.
- de Boer, J.H. (1950).- "Advances in Colloid Science", Interscience, N.Y. 3, 1.
- De, S.K. (1961a).- Kolloidzshr. 179, 134.
- De, S.K. (1961b).- Kolloidzshr. 179, 140.
- Debye, P. and Hückel, E. (1923).- Phys. Z. 24, 185, 305.
- Drosdoff, M. and Truog, E. (1935).- J. Amer. Soc. Agron. 27, 312.
- Everett, D.H. (1950).- Trans. Faraday Soc. 46, 942.
- Everett, D.H. (1954).- Trans. Faraday Soc. 50, 1077.
- Everett, D.H. (1955).- Trans. Faraday Soc. 51, 1551.
- Everett, D.H. (1957).- Proc. chem. Soc. Lond. 38.
- Everett, D.H. and Whitton, W.I. (1952).- Trans. Faraday Soc. 48, 749.
- Everett, D.H. and Smith, F.W. (1954).- Trans. Faraday Soc. 50, 187.
- Ewing, F.J. (1935).- J. chem. Phys. 3, 203.
- Farr, T.D. (1950).- Chem. Eng. Report No. 8, T.V.A., Wilson Dam, Alabama.
- Fieldes, M. and Schofield, R.K. (1960).- N.Z. J. Sci. 3, 563.
- Forrest, W.W. (1961).- J. sci. Instrum. 38, 143.
- Fowler, R.H. (1935).- Proc. Camb. phil. Soc. 31, 260.

- Frederickson Jr., L.D. (1954).- *Analyt. Chem.* 26, 1883.
- Fried, M. and Shapiro, R.E. (1956).- *Proc. Soil Sci. Soc. Amer.* 20, 471.
- Fried, M. and Shapiro, R.E. (1960).- *Soil Sci.* 90, 69.
- Fripiat, J.J. (1960a).- *Trans. Seventh Int. Congr. Soil Sci. Madison, Wisc. U.S.A., IV*, 502.
- Fripiat, J.J. (1960b).- *Bull. Gr. Fr. Argiles*, XII, 7, 25.
- Gastuche, M.C. and Herbillon, A. (1962).- *Bull. Soc. chim. Fr.* 1404.
- Ghani, M.C. (1943).- *Indian J. agric. Sci.* 13, 562.
- Giles, C.H. and MacEwan, T.H. (1957).- *Second Int. Congr. Surface Activity*, III, 457.
- Giles, C.H., MacEwan, T.H., Nakhwa, S.N. and Smith, D. (1960).- *J. chem. Soc.* 3973.
- Graham-Brice, I.J. (1963).- *J. Soil Sci.* 14, 195.
- Greenland, D.J., Laby, R.H. and Quirk, J.P. (1962).- *Trans. Faraday Soc.* 58, 829.
- Gregg, S.J. (1961).- "The Surface Chemistry of Solids" p. 4. Second ed., Chapman & Hall Ltd.
- Gruner, J.W. (1932).- *Z. Kristallogr.* 83, 75.
- Gurney, R.W. (1953).- "Ionic Processes in Solution", p. 90, 96. *Int. Chemical Series*, McGraw-Hill Inc.
- Harward, M.E. and Coleman, N.T. (1954).- *Soil Sci.* 78, 181.
- Haseman, J.F., Lehr, J.R. and Smith, J.P. (1950).- *Proc. Soil Sci. Soc. Amer.* 15, 76.
- Haseman, J.F., Brown, E.H. and Whitt, C.D. (1950).- *Soil Sci.* 70, 257.
- Heath, N.S. and Culver, R.V. (1955).- *Trans. Faraday Soc.* 51, 1575.
- Helfferich, F. (1962).- "Ion Exchange," (McGraw-Hill Series in Advanced Chemistry), p. 95. 166, 176, McGraw-Hill, N.Y.
- Hemwall, J.B. (1957).- *Advanc. Agron.* IX, 95. Ed. Norman, A.G., Acad Press, N.Y.
- Hendricks, S.B. (1936).- *Z. Kristallogr.* 95, 247.

- Hendricks, S.B. (1945).- *Industr. Engng. Chem. (Industr.)* 37, 625.
- Hirst, W. (1948).- *Disc. Faraday Soc.* 3, 22.
- Hsu, P.H. and Rich, C.I. (1960).- *Proc. Soil Sci. Soc. Amer.* 24, 21.
- Hsu, P.H. and Rennie, D.A. (1962).- *Canad. J. Soil Sci.* 42, 197.
- Jackson, M.L. (1962).- *Proc. Soil Sci. Soc. Amer.* 27, 1.
- Johansen, P.G. and Buchanan, A.S. (1947).- *Aust. J. Chem.* 10, 392.
- Kelly, J.B. and Midgley, A.R. (1943).- *Soil Sci.* 55, 167.
- Kemball, C. (1950).- *Advanc. Catalys. II*, 233. Acad. Press.
- Kittrick, J.A. and Jackson, M.L. (1954).- *Science* 120, 508.
- Kittrick, J.A. and Jackson, M.L. (1955a).- *Proc. Soil Sci. Soc. Amer.* 19, 292.
- Kittrick, J.A. and Jackson, M.L. (1955b).- *Proc. Soil Sci. Soc. Amer.* 19, 455.
- Kittrick, J.A. and Jackson, M.L. (1955c).- *Soil Sci.* 79, 415.
- Kittrick, J.A. and Jackson, M.L. (1956).- *J. Soil Sci.* 7, 81.
- Koch, L.F. (1956).- *Aust. J. Sci.* 18, 200.
- Kolthoff, I.M. (1936).- *J. phys. Chem.* 40, 1027.
- Kolthoff, I.M. and Kuroda, P.K. (1951).- *Analyt. Chem.* 23, 1304.
- Koral, J., Ullman, R. and Eirich, F.R. (1958).- *J. phys. Chem.* 62, 541.
- Kukhareenko, N.I. and Nosouska, O.I. (1953).- *Dopovidi Akad. Nauk. Ukr. R.S.R.* 1, 41.
- Kurtz, L.T. (1953).- *Agronomy Monograph IV*, 59.
Ed. Pierre, W.H. and Norman, A.G. Acad. Press.
- Langmuir, I. (1918).- *J. Amer. chem. Soc.* 40, 1361.
- Leaver, J.P. and Russell, E.W. (1957).- *J. Soil Sci.* 8, 113.
- Lin, C. and Coleman, N.T. (1960).- *Prcc. Soil Sci. Soc. Amer.* 24, 444.

- Lindsay, W.L. and Stephenson, H.F. (1959a).- Proc. Soil Sci. Soc. Amer. 23, 12.
- Lindsay, W.L. and Stephenson, H.F. (1959b).- Proc. Soil Sci. Soc. Amer. 23, 18.
- Low, P.F. (1955).- Proc. Soil Sci. Soc. Amer. 19, 135.
- Low, P.F. and Black, C.A. (1947).- Proc. Soil Sci. Soc. Amer. 12, 180.
- Low, P.F. and Black, C.A. (1950).- Soil Sci. 70, 273.
- Martin, R.T. (1960).- Proc. Ninth Nat. Conf. Clays and Clay minerals, Lavayette, 28.
- Mitchell, B.D. and Mackenzie, R.C. (1954).- Soil Sci. 77, 173.
- Muljadi, D. (1961).- Honours Thesis, University of Adelaide.
- Mullin, J.B. and Riley, J.P. (1955).- Analyt. chem. acta 12, 162.
- Newham, R.E. (1956).- Ph.D. Thesis, The Pennsylvania State University, quoted by Brindley, G.W. (1961). "The X-ray Identification and Crystal Structures of Clay minerals", p. 51.
- Norrish, K. (1957).- Proc. Second Aust. Conf. in Soil Sci. (Melbourne) paper No. 17.
- Norrish, K. and Sweatman, T.R. (1962).- Proc. Third Aust. Conf. in Soil Sci. (Canberra), paper no. 66.
- Olsen, S.R. (1952).- J. phys. Chem. 56, 630.
- Olsen, S.R. and Watanabe, F.S. (1957).- Proc. Soil Sci. Soc. Amer. 21, 144.
- Papée, D., Terian, R. and Biaïis, R. (1958).- Bull. Soc. chim. Fr. 1301.
- Pauling, L. (1930).- Proc. nat. Acad. Sci. Wash. 16, 578.
- Pauling, L. (1960).- "The Nature of the Chemical Bond," Third ed., p. 5. Oxford Univ. Press. Lond.
- Posner, A.M. and Quirk, J.P. (1964).- Proc. roy. Soc. Ser. A. 278, 35.
- Quirk, J.P. (1960).- Nature, 188, 253.
- Reichertz, P.P. and Yost, W.J. (1946).- J. chem. Phys. 14, 495.

- Rooksby, H.P. (1961).- "The X-ray Identification and Crystal Structures of Clay Minerals", p. 354. Ed. Brown, G., Miner. Soc. Lond.
- Ross, C.S. and Kerr, P.F. (1934).- Prof. Pap. U.S. geol. Surv. 185G, 135.
- Rossotti, F.J.C. (1960).- "Modern Co-ordination Chemistry", p. 21. Ed. Lewis, J. and Wilkins, R.G., Interscience.
- Russell, E.W. (1961).- "Soil Conditions and Plant Growth", Ninth Ed., p.476. Longmans.
- Russell, G.C. and Low, P.F. (1954).- Proc. Soil Sci. Soc. Amer. 18, 22.
- Samson, H.R. (1953).- Ph.D. Thesis, University of London.
- Schofield, R.K. (1946).- Soils & Fert. 9, 265.
- Schofield, R.K. (1948).- Clay Min. Bull. 1-2, 18.
- Schofield, R.K. (1949).- J. Soil Sci. 1, 1.
- Schofield, R.K. (1955).- Soils & Fert. 18, 373.
- Schofield, R.K. and Samson, H.R. (1953).- Clay Min. Bull. 2, 45.
- Schofield, R.K. and Samson, H.R. (1954).- Disc. Faraday Soc. 18, 135.
- Schofield, R.K. and Taylor, A.W. (1954).- J. chem. Soc. 4445.
- Schwertmann, U. and Jackson, M.L. (1963).- Science, 139, 1052.
- Shen, M.J. and Rich, C.I. (1962).- Proc. Soil Sci. Soc. Amer. 26, 33.
- Stout, P.R. (1939).- Proc. Soil Sci. Soc. Amer. 4, 177.
- Sumner, M.E. (1962).- Agrochemica 6, 183.
- Swenson, R.M., Cole, C.V. and Sieling, D.H. (1949).- Soil Sci. 67, 3.
- Teakle, L.J.H. (1928).- Soil Sci. 25, 143.
- Thomas, G.W. (1960).- Proc. Seventh Int. Congr. Soil Sci, Madison, Wisc. U.S.A. II, 364.
- Toth, S.J. (1937).- Soil Sci. 44, 299.
- Toth, S.J. (1942).- Soil Sci. 53, 265.

- van Olphen, H. (1951).- Disc. Faraday Soc. 11, 82.
- Vanselow, A.P. (1932).- Soil Sci. 33, 95.
- Vogel, A.I. (1951).- "Quantitative Inorganic Analysis, p. 64.
Longmans.
- Wada, K. (1959).- Soil Sci. 87, 325.
- Weir, C.C. and Soper, R.J. (1963).- J. Soil Sci. 14, 256.
- Weiser, H.B. (1935).- "Inorganic Colloid Chemistry", Vol. II, p. 90.
John Wiley & Sons, N.Y.
- Wells, A.F. (1950).- "Structural Inorganic Chemistry", second ed., p. 408.
Oxford Univ. Press.
- Wild, A. (1950).- J. Soil Sci. 1, 221.
- Woodroffe, K. and Williams, C.H. (1953).- Aust. J. agric. Res. 4, 127.
- Young, D.M. and Crowell, A.D. (1962).- "Physical Adsorption of Gases,
p. 1, 70. Butterworths, London.

- - -